

University of Bath



PHD

Lewis Acids for the Activation of Pyridines for Further Functionalisation

Abou-Shehada, Sarah

Award date:
2015

Awarding institution:
University of Bath

[Link to publication](#)

General rights

Copyright and moral rights for the publications made accessible in the public portal are retained by the authors and/or other copyright owners and it is a condition of accessing publications that users recognise and abide by the legal requirements associated with these rights.

- Users may download and print one copy of any publication from the public portal for the purpose of private study or research.
- You may not further distribute the material or use it for any profit-making activity or commercial gain
- You may freely distribute the URL identifying the publication in the public portal ?

Take down policy

If you believe that this document breaches copyright please contact us providing details, and we will remove access to the work immediately and investigate your claim.

Download date: 22. May. 2019

University of Bath

LEWIS ACIDS FOR THE ACTIVATION OF PYRIDINES FOR FURTHER FUNCTIONALISATION

Sarah Abou-Shehada

A thesis submitted for the degree of Doctor of Philosophy

University of Bath

Department of Chemistry

May 2015

COPYRIGHT

Attention is drawn to the fact that copyright of this thesis rests with its author. A copy of this thesis has been supplied on the condition that anyone who consults it is understood to recognise that its copyright rests with its author and they must not copy it or use material from it except as permitted by law or with the consent of the author. This thesis may be made available for consultation within the University Library and may be photocopied or lent to other libraries for the purposes of consultation effective from.....

Signed on behalf of the Faculty of Science.....

ACKNOWLEDGMENTS	VII
ABSTRACT.....	VIII
DECLARATION OF MATERIAL FROM A PREVIOUSLY SUBMITTED THESIS AND WORK DONE IN CONJUNCTION WITH OTHERS.....	IX
ABBREVIATIONS.....	X
CHAPTER 1: INTRODUCTION.....	3
1.1.INDUSTRIAL RELEVANCE OF PYRIDINES AND PYRIDINE FUNCTIONALISATION¹	5
1.2. FUNCTIONALISING PYRIDINES.....	11
1.3. ROUTES TO FUNCTIONALISED PYRIDINES (OVERVIEW)	12
1.3.1 RING SYNTHESIS	12
1.3.2. DIRECT INTRODUCTION OF FUNCTIONALITY	14
1.3.2.1. AROMATIC SUBSTITUTION REACTIONS OF PYRIDINES	14
1.3.2.2. BUCHWALD–HARTWIG AND ULLMANN REACTIONS	21
1.3.3. TRANSITION METAL CATALYSED C-H FUNCTIONALISATION	25
1.3.3.1. SELECTIVE FUNCTIONALISATION AT THE 2-POSITION IN PYRIDINE⁵	25
1.3.3.2. SELECTIVE FUNCTIONALISATION AT THE 3-POSITION OF PYRIDINE⁵	30
1.3.3.3. SELECTIVE FUNCTIONALISATION AT THE 4-POSITION⁵	32
1.4. CONJUGATE ADDITION REACTIONS OF VINYL PYRIDINES.....	34
1.4.1 CONJUGATE ADDITION REACTIONS OF CARBON NUCLEOPHILES WITH VINYL PYRIDINES.....	40
1.4.2. CONJUGATE ADDITION REACTIONS OF NITROGEN BASED NUCLEOPHILES WITH VINYL PYRIDINES ...	46
1.4.3. CONJUGATE ADDITION REACTIONS OF OXYGEN AND SULFUR BASED NUCLEOPHILES WITH VINYL PYRIDINES	50
1.4.4. TRANSITION METAL CATALYSED CONJUGATE ADDITION REACTIONS OF VINYL PYRIDINES.....	53
1.5. DIELS–ALDER CYCLISATION REACTIONS OF VINYL PYRIDINES.....	56

1.6. GREEN CHEMISTRY AND OUTLOOK ON PYRIDINE FUNCTIONALISATION	64
1.7. AIMS	65
CHAPTER 2: LEWIS ACIDS FOR THE ACTIVATION OF PYRIDINES TOWARDS NUCLEOPHILIC AROMATIC SUBSTITUTION	
67	
2. INTRODUCTION	69
2.1. AIM.....	72
2.2. RESULTS AND DISCUSSION.....	74
2.2.1. SOLVENT SCREEN FOR CONTROL REACTION	75
2.2.2. TEMPERATURE SCREEN FOR CONTROL REACTION	76
2.2.3. LEWIS ACID SCREEN.....	77
2.2.3.1. ZIRCONIUM AND ZINC BASED LEWIS ACID SCREEN	79
2.2.4. OPTIMISATION	82
2.2.4.1. OPTIMISING CONVERSION	82
2.2.4.2. OPTIMISING CATALYST LOADING	84
2.2.5. REACTION KINETICS	87
2.2.5.1. REACTION ORDER WITH RESPECT TO 4-CHLOROPYRIDINE	88
2.2.5.2. REACTION ORDER WITH RESPECT TO <i>N</i> -METHYLANILINE	91
2.2.5.3. REACTION ORDER WITH RESPECT TO ZINC NITRATE	93
2.2.5.4. RATE LAW	96
2.2.6. NUCLEOPHILE SCREEN.....	99
2.2.6.1. AMINES	99
2.2.6.3. ALCOHOLS.....	103
2.2.6.4. MISCELLANEOUS NUCLEOPHILES.....	107
2.2.7. SCOPE OF NUCLEOPHILE - SUMMARY.....	109
2.2.8. SUBSTRATE SCREEN.....	113
2.2.8.1 2-CHLOROPYRIDINE	118
2.3. CONCLUSIONS	122

2.4. FUTURE WORK	123
2.4.1. BROADER SCOPE OF NUCLEOPHILE	123
2.4.3. OXYGEN TRANSFER CATALYSIS IN PYRIDINES.....	124
 CHAPTER 3: LEWIS ACIDS FOR THE ACTIVATION OF VINYL PYRIDINES TOWARDS	
CONJUGATE ADDITION AND CYCLISATION REACTIONS.....	
3.1. AIMS.....	129
3.2. RESULTS AND DISCUSSION.....	130
3.2.1. LEWIS ACID CATALYST SCREEN	130
3.2.2. SOLVENT SCREEN	132
3.2.3. ALTERNATIVE LEWIS ACID CATALYST SCREEN	134
3.2.4. REACTION OPTIMISATION.....	135
3.2.4.1. REACTION OPTIMISATION FOR 2-VINYLPYRIDINE	140
3.2.5. SCOPE IN INCOMING GROUP FOR CONJUGATE ADDITION	143
3.2.5.1. 4-VINYLPYRIDINE	143
3.2.5.1.1. Piperidine	144
3.2.5.1.2. <i>N</i> -Methylaniline	146
3.2.5.1.3. Thiophenol	147
3.2.5.2. 2-VINYLPYRIDINE	149
3.2.5.2.1. Piperidine	151
3.2.5.2.2. <i>N</i> -Methylaniline	154
3.2.5.2.3. Thiophenol	155
3.2.5.3 OXYGEN AND CARBON BASED NUCLEOPHILES	156
 3.3. LEWIS ACID CATALYSED DIELS–ALDER REACTIONS OF VINYL PYRIDINES.....	160
 3.3.1. 4-VINYLPYRIDINE.....	162
3.3.2. 2-VINYLPYRIDINE.....	170
 3.4. SCOPE IN NUCLEOPHILE – SUMMARY.....	176

3.5. CONCLUSIONS	177
3.6. FUTURE WORK	178
3.5.1. OXYGEN NUCLEOPHILES	178
3.5.2. BROADER SUBSTRATE SCOPE	178
CHAPTER 4: EXPERIMENTAL	181
4.1. MATERIALS AND METHODS	183
4.2. CHAPTER 2 EXPERIMENTAL PROCEDURES.....	184
PROCEDURE I: 4-HALOPYRIDINE FREEBASE.....	184
GENERAL NOTE ON HANDLING 4-CHLOROPYRIDINE FREEBASE:	184
SOLVENT SCREEN: CONTROL REACTION.....	185
TEMPERATURE SCREEN: CONTROL REACTION	186
LEWIS ACID CATALYST SCREEN.....	186
TEMPERATURE SCREEN	187
CATALYST LOADING AND TEMPERATURE SCREEN	187
PROCEDURE FOR KINETIC STUDY.....	188
AMINE NUCLEOPHILE SCREEN	194
REACTION ON <i>N</i> -METHYLANILINE WITH 4-CHLOROPYRIDINE IN THE PRESENCE OF BENZYLAMINE.....	194
REACTION OF 4-CHLOROPYRIDINE WITH PIPERIDINE IN THE PRESENCE OF DIETHYLAMINE	195
SOLVENT SCREEN FOR REACTION OF 4-CHLOROPYRIDINE WITH 4-CHLOROANILINE.....	195
SOLVENT SCREEN FOR REACTION OF 4-CHLOROPYRIDINE WITH 4-CHLOROANILINE.....	196
INITIAL ALCOHOL SCREEN.....	196
BASE SCREEN FOR ALCOHOL NUCLEOPHILES	197
BASE SCREEN FOR INCOMING ALCOHOL GROUPS- 1:1 4-CHLOROPYRIDINE TO ETHANOL	197
OPTIMISED METHODOLOGY FOR REACTION OF 4-CHLORPYRIDINE WITH ALCOHOL NUCLEOPHILES	198
MISCELLANEOUS NUCLEOPHILE SCREEN	198
PROCEDURE II: NITROGEN-BASED NUCLEOPHILES	199
PROCEDURE III: ALCOHOL INCOMING GROUP	199
REPRESENTATIVE PROCEDURE IV: SUBSTRATE SCREEN.....	200
PROCEDURE V: SCOPE IN NUCLEOPHILE FOR 2-CHLOROPYRIMIDINE	200

LEWIS ACID CATALYST SCREEN FOR S _N AR REACTION OF 2-CHLOROPYRIDINE WITH PIPERIDINE	201
REACTION OF 2-CHLOROPYRIDINE WITH PIPERIDINE IN DMSO	201
REACTION OF 2-CHLOROPYRIDINE WITH PIPERIDINE IN XYLENES	202
SOLVENT SCREEN FOR REACTION OF 2-CHLOROPYRIDINE WITH PIPERIDINE CATALYSED BY ZN(NO ₃) ₂ •6H ₂ O	202
LEWIS ACID SCREEN FOR THE REACTION OF 4-CHLOROPYRIDINE WITH BENZYLAMINE	203
OXYGEN TRANSFER BETWEEN 4-(3-PHENYLPROPYL)PYRIDINE AND PYRIDINE N-OXIDE	203

4.2.3. CHARACTERISATION OF STARTING MATERIALS..... 204

4-Chloropyridine ⁷⁷	204
4-Bromopyridine freebase ⁷⁸	204

4.2.1. CHARACTERISATION OF NUCLEOPHILIC AROMATIC SUBSTITUTION PRODUCTS .. 205

N-Methyl-N-phenylpyridin-4-amine ¹¹¹	205
N-Phenylpyridin-4-amine ¹¹²	205
N-(4-Chlorophenyl)pyridin-4-amine ¹¹³	206
N-(3-Chlorophenyl)pyridin-4-amine ¹¹⁴	206
N-(2-Chlorophenyl)pyridin-4-amine ¹¹⁵	207
N-Benzyl-N-phenylpyridin-4-amine	207
4-(Pyrrolidin-1-yl)pyridine ¹¹⁶	208
4-(Piperidin-1-yl)pyridine ¹¹⁸	208
4-(Pyridin-4-yl)morpholine ¹²⁰	209
4-(3-Methylpiperidin-1-yl)pyridine	209
1-(Pyridin-4-yl)indoline ¹²¹	210
2-(Pyridin-4-yl)decahydroisoquinoline	210
4-(1H-Imidazol-1-yl)pyridine ¹²²	211
4-Methoxypyridine ¹²³	211
4-Ethoxypyridine ¹²⁴	212
4-Propoxypyridine.....	212

4.2.2. CHARACTERISATION OF SUBSTRATE SCREEN FOR NUCLEOPHILIC AROMATIC SUBSTITUTION..... 213

N-Methyl-N-phenylquinolin-4-amine ¹²⁵	213
N-Methyl-N-phenylpyrimidin-2-amine ¹⁰⁴	213
2-(Piperidin-1-yl)pyrimidine ¹²⁶	214
2-(1H-Imidazol-1-yl)pyrimidine ¹²⁷	214

4.3. CHAPTER 3 EXPERIMENTAL PROCEDURES..... 215

GENERAL NOTE ON HANDLING 2- AND 4-VINYLPYRIDINE:	215
LEWIS ACID CATALYST SCREEN.....	215
SOLVENT SCREEN.....	216
SECOND LEWIS ACID CATALYST SCREEN- MORPOLINE NUCLEOPHILE	217
CATALYST LOADING SCREEN FOR THE BEST PERFORMING LEWIS ACIDS.....	218
TEMPERATURE AND CATALYST LOADING SCREEN- 8 H	218
REPRESENTATIVE PROCEDURE FOR DEGRADATION OF CONJUGATE ADDITION PRODUCT AT 80 °C IN THE PRESENCE OF 20 MOL% ZN(NO₃)₂•6H₂O.....	219
TEMPERATURE, TIME AND CATALYST LOADING SCREEN.....	219
REACTION OPTIMISATION FOR 2-VINYLPYRIDINE	220
INITIAL NUCLEOPHILE SCREEN FOR 2- AND 4-VINYLPYRIDINE	220
OPTIMISING REACTION CONDITIONS FOR PIPERIDINE INCOMING GROUP	221
4-VINYLPYRIDINE - TEMPERATURE AND CATALYST LOADING SCREEN (25-40 °C, 2.5 AND 5 MOL% CATALYST LOADING).....	221
2-VINYLPYRIDINE - TEMPERATURE AND CATALYST LOADING SCREEN (25-40 °C, 2.5 AND 5 MOL% CATALYST LOADING).....	221
OPTIMISING REACTION CONDITIONS FOR N-METHYLANILINE INCOMING GROUP	222
4-VINYLPYRIDINE - TEMPERATURE AND CATALYST LOADING SCREEN (25-90 °C, 5-20 MOL% CATALYST LOADING).....	222
2-VINYLPYRIDINE - TEMPERATURE AND CATALYST LOADING SCREEN (25-90 °C, 5-20 MOL% CATALYST LOADING).....	223
OPTIMISING REACTION CONDITIONS FOR THIOPHENOL INCOMING GROUP.....	223
4-VINYLPYRIDINE - TEMPERATURE AND CATALYST LOADING SCREEN (25 °C, 2.5 AND 5 MOL% CATALYST LOADING).....	223
2-VINYLPYRIDINE - TEMPERATURE AND CATALYST LOADING SCREEN (25-40 °C, 2.5 AND 5 MOL% CATALYST LOADING).....	224
REACTION OF METHOXYACETONITRILE WITH 4-VINYLPYRIDINE	224
REACTION OF METHOXYACETONITRILE WITH 4-VINYLPYRIDINE	225

OPTIMISING REACTION CONDITIONS FOR DIELS–ALDER CYCLISATION OF 1,2,3,4,5-PENTAMETHYLCYCLOPENTADIENE WITH 2-/4-VINYLPYRIDINE	226
4-VINYLPYRIDINE - TEMPERATURE AND CATALYST LOADING SCREEN (25-40 °C, 2.5 AND 5 MOL% CATALYST LOADING).....	226
2-VINYLPYRIDINE - TEMPERATURE AND CATALYST LOADING SCREEN (25-40 °C, 2.5 AND 5 MOL% CATALYST LOADING).....	227
<u>4.3.1. CHARACTERISATION OF CONJUGATE ADDITION PRODUCTS</u>	<u>228</u>
4-(2-(Pyridin-4-yl)ethyl)morpholine ¹²⁸	228
N-Methyl-N-(2-(pyridin-4-yl)ethyl)aniline.....	229
4-(2-(Piperidin-1-yl)ethyl)pyridine ¹²⁸	230
4-(2-(Phenylthio)ethyl)pyridine ¹²⁹	231
N-Methyl-N-(2-(pyridin-2-yl)ethyl)aniline ¹³⁰	233
2-(2-(Piperidin-1-yl)ethyl)pyridine ¹²⁸	234
2-(2-(Phenylthio)ethyl)pyridine ¹³¹	235
<u>4.3.2. CHARACTERISATION OF DIELS–ALDER CYCLISATION PRODUCTS</u>	<u>236</u>
4-(1,4,5,6,7-Pentamethylbicyclo[2.2.1]hept-5-en-2-yl)pyridine.....	236
2-(1,4,5,6,7-Pentamethylbicyclo[2.2.1]hept-5-en-2-yl)pyridine)	237
<u>REFERENCES</u>	<u>238</u>

Acknowledgments

First and foremost, I would like to thank my supervisors Steve Bull and Jonathon Williams, for the opportunity to carry out my PhD in their groups. Specifically I would like to thank Jonathan Williams for his support, guidance, patience and belief in me, which were pivotal to seeing me through this PhD, and I am deeply grateful.

I must thank Benjamin “Benny boo boo” Atkinson and Ruth “Twinny” Lawrence for your friendship as well as your unvarying willingness to brainstorm chemistry ideas with me, it has been a pleasure starting my PhD adventures with you. I would also like to thank members of the Bull and Williams groups: Rosie Chhatwal, Dr. “Party” James Walton, Richard Blackburn, Helen Lomax, Dave Tickell, Rob Chapman, Caroline Jones and Dr. Marc Hutchby for patiently sitting through numerous cat videos, as well as patiently putting up with many episodes of hyperactivity after I had guzzled a bag of sweets and a litre of diet coke- which was nearly every day.

To my DTC cohort, I’d like to thank you for laughs over the past four years, being part of a cohort not only made my PhD bearable, but dare I say, sometimes actually enjoyable! Specifically I would like to thank Jessica Sharpe my housemate and thesis writing buddy, who helped maintain my sanity whilst writing up, as well as Lisa Sargeant and Anyela Ramirez Canon. I would mention Lee Burton, but he abstained from including me in his own acknowledgements even though I know I was clearly the only reason he got through and enjoyed his PhD, hence I’m acknowledging myself in mine, on his behalf.

To Catherine Lyall and Christopher Roche, you have been good friends and a source of great comfort and support throughout my PhD- especially through the more trying times.

To my Mum and Dad, thank you for your constant support and unwavering belief in me. To my sister Miriam “Pipsqueak” Abou-Shehada, thank you for your friendship and support.

Abstract

This thesis outlines work carried out over the past three years concerning the development of an experimentally simple, sustainable catalytic method for the functionalisation of pyridines by means of a zinc nitrate based Lewis acid. It encompasses reaction discovery and optimisation, determination of the scope of the method through nucleophile and substrate screens as well as investigations into the mechanism by which the reaction takes place.

Chapter 1 gives a general overview of the industrial relevance of pyridine functionalisation as well as the synthetic methods for the synthesis of ring functionalised pyridines, covering traditional stoichiometric aromatic substitution methods, transition metal catalysed cyclisations, standard catalytic methods for the functionalisation of pyridines: Buchwald-Hartwig and Ullmann reactions, as well as a précis of some recent transition metal catalysed methods for C-H functionalisation of pyridines. It also reviews classical and transition metal catalysed methods for conjugate addition and Diels–Alder reactions of vinylpyridines.

Chapter 2 involves reaction discovery for the use of Lewis acids for the activation of pyridines towards nucleophilic aromatic substitutions, reaction optimisations, kinetic investigations and an examination of the scope in substrates and incoming groups.

Chapter 3 investigates the use of Lewis acids for the activation of vinylpyridines toward conjugate addition, reaction optimisations, investigations into scope of incoming groups and subsequent optimisation studies for each. The method is also extended to Diels–Alder cyclisations, for which the reaction is also optimised.

Declaration of Material from a Previously Submitted Thesis and Work Done in Conjunction with Others

Chapter 3: Initial Lewis acid catalyst screens and optimisation work concerning magnesium nitrite catalysis of the conjugate addition reactions of 4-vinylpyridine (Tables 26-29, Chapter 3) were carried out by Matthew C Teasdale (MChem student, October 2012-March 2013). Other contributions include the reaction in Scheme 98.

Abbreviations

acac	Acetoacetate
AcOH	Acetic acid
API	Active pharmaceutical ingredient
b.p.	boiling point
BINAP	2,2'-bis(diphenylphosphino)-1,1'-binaphthyl
bpy	Bipyridyl
Bu	Butyl; <i>t</i> -, <i>sec</i> -, or <i>n</i> - denote tertiary, secondary or linear
BuLi	Butyllithium; <i>t</i> -, <i>sec</i> -, or <i>n</i> - denote tertiary, secondary or linear
CA	Conjugate addition
cod	Cyclooctadiene
coe	<i>cis</i> -Cyclooctene
cp	Cyclopentadienyl
Cp*	1,2,3,4,5 pentamethyl cyclopentadienyl
Cp*H	1,2,3,4,5 pentamethyl cyclopentadiene
Cy	Cyclohexyl
4-Cl-pyr	4-Chloropyridine
DA	Diels–Alder
dba	Dibenzylideneacetone
DCM	Dichloromethane
DMF	Dimethyl formamide
DPPP	1,3-Bis(diphenylphosphino)propane
EI	electrophile
Et	Ethyl
HMPA	Hexamethylphosphoramide
HOMO	Highest occupied molecular orbital

Hz	Hertz
ind	Indenyl
IPA	Isopropyl alcohol
LUMO	Lowest unoccupied molecular orbital
MAD	bis(2,6-di- <i>tert</i> -butyl-4-methylphenoxide)
Me	Methyl
MeCN	Acetonitrile
MHz	Megahertz
mmol	millimole
NADPH	Nicotinamide adenine dinucleotide phosphate
NaHMDS	Hexamethyldisilazane sodium salt
NHC	N-heterocyclic carbene
NMA	<i>N</i> -methylaniline
NMR	Nuclear Magnetic Resonance
Nuc	Nucleophile
OAc	Acetate
Ph	Phenyl
phen	phenanthroline
pin	Pinacol ester
ppy	2-phenyl pyridine
pr	Propyl
pyr	Pyridine
pyrim	Pyrimidine
pyzl	Pyrazole
q	8-hydroxyquinolinato
r.d.s.	Rate determining step
rt	Room temperature
S_NAr	Substitution Nucleophilic Aromatic
S_NEA	Substitution Nucleophilic Elimination Addition

TFA	Trifluoroacetic acid
THF	Tetrahydrofuran
TMS	Trimethylsilane
Tol	Tolyl
Ts₂O	<i>p</i> -toluenesulfonic anhydride
α	Alpha
β	Beta
γ	Gamma
π	Pi
σ	Sigma

Chapter 1: Introduction

*“I’m writing a book. I’ve got the
page numbers done” - Steven
Wright*

1.1.Industrial relevance of pyridines and pyridine functionalisation¹

Pyridines are considered one of the most important classes of heterocycles and are ubiquitous in nature. The significance of pyridine emerged in the 1930s with the identification of the use of niacin (**1**, Figure 1) in the prevention of dermatitis and dementia.¹ A decade later a large application for 2-vinylpyridine was discovered (**2**, Figure 1) as a constituent of latex that promoted the binding of rubber to tyre cord.¹ By this point the demand for the 2-picoline (**3**, Figure 1), also used in latex production, had superseded its availability from the production methods of time (coal tar sources) and thus Reilly industries developed an industrial synthesis for the production of 2- and 4-picoline (**3** and **4**, Figure 1) by vapour phase catalytic reactions. The demand for pyridine derivatives had only increased from that point with the discovery of many biologically active pyridine-containing compounds.¹

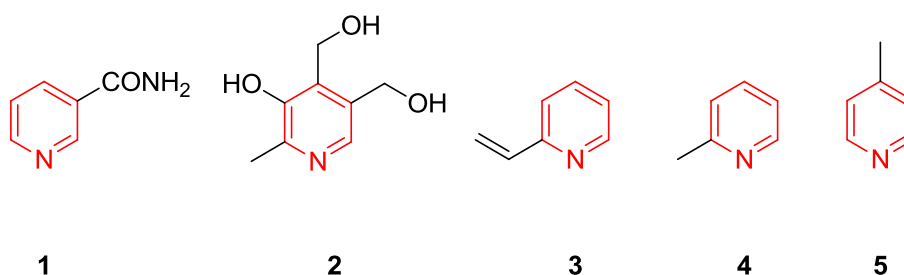
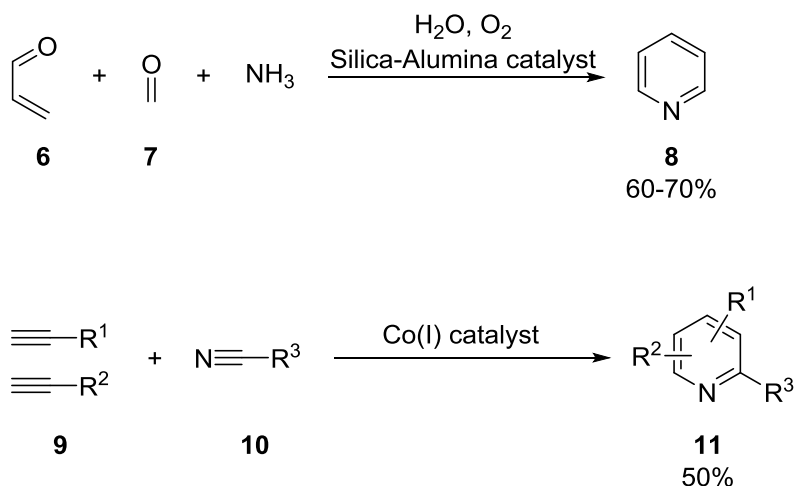


Figure 1: Variety of important pyridine derivatives

Current commercial methods for the production of pyridine (**8**, Scheme 1) rely on gas-phase, high-temperature, condensation reactions similar to those developed by Reilly industries. Air, ammonia, crotonaldehyde (**6**, Scheme 1), formaldehyde (**7**, Scheme 1) and steam passed over a silica-alumina catalyst react to give pyridine in a 60-70% yield (Scheme 1).¹ A variety of alkyipyridines are produced through use of acetylenes (**9**, Scheme 2) and nitriles (**10**, Scheme 1) over a cobalt catalyst in ~50% yield (Scheme 1, this method is discussed further in **section 1.3.1**).



Scheme 1: Commercial production of pyridines and alkylpyridines[1]

Pyridine has assumed an important role in the development of our understanding of the chemistry of biological systems; it plays an integral role in catalysing both biological and chemical processes. Nicotinamide adenine dinucleotide phosphate (NADP, **12**, Figure 2) is a pyridine nucleotide that is involved in a variety of oxidation-reduction processes in enzymes. Further evidence of the biological activity of pyridine is its presence in the important vitamins niacin and pyridoxine (**1** and **2**, Figure 1) and in biologically active alkaloids such as nicotine (**13**, Figure 2).¹

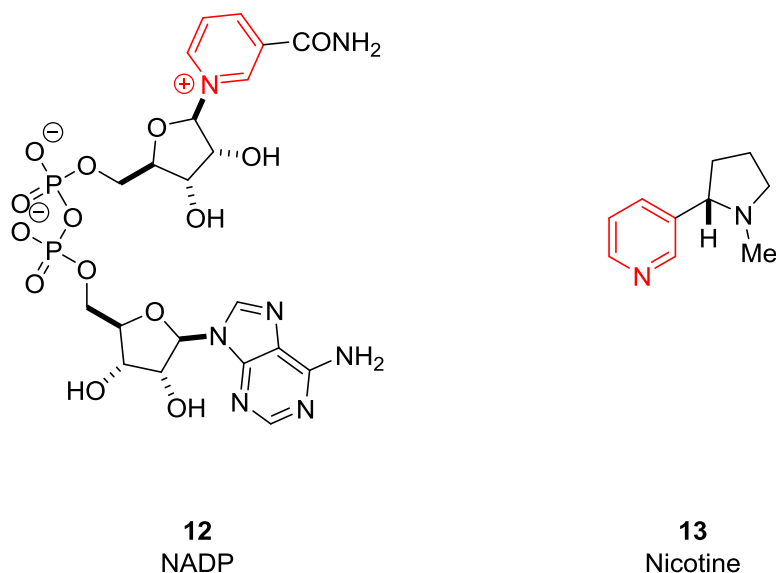
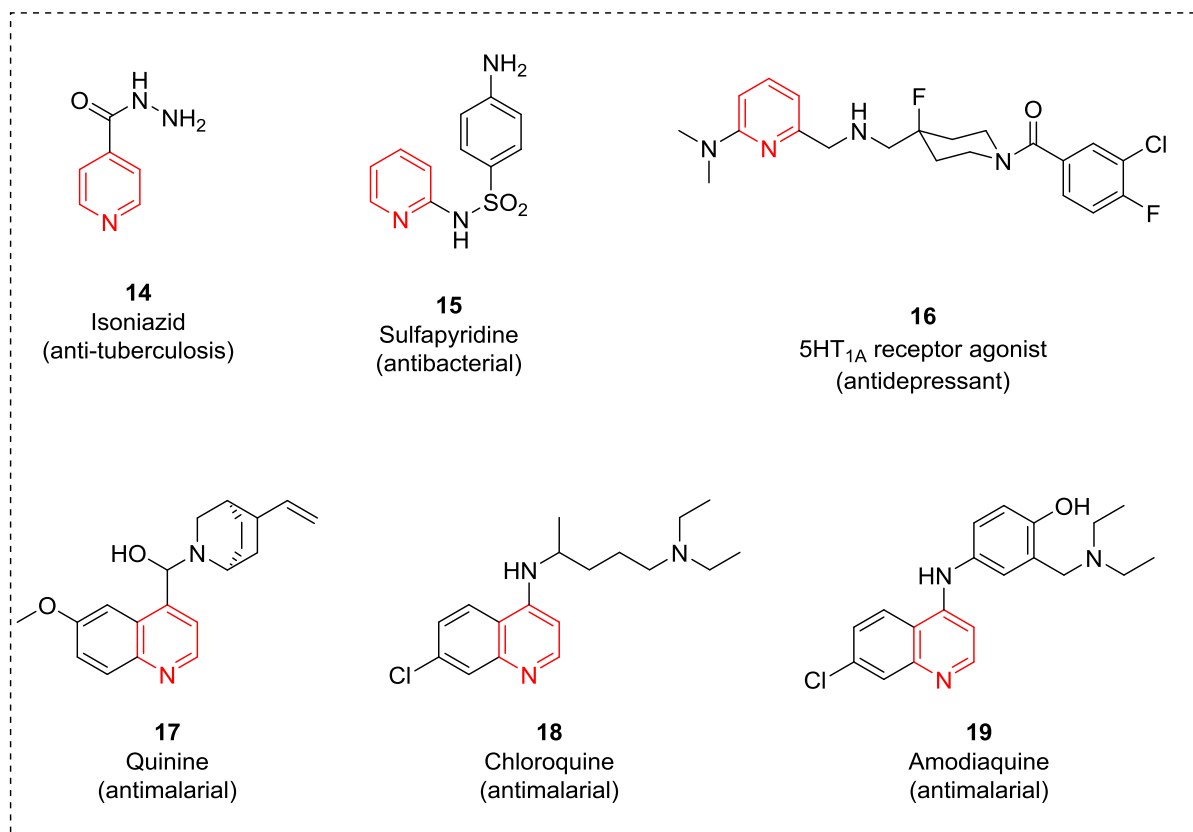


Figure 2: Naturally occurring pyridine-containing molecules

Within the pharmaceutical industry, the pyridine motif is present in over 7000 existing drugs; some of which are shown in Figure 3. It is also present in a variety of agrochemical molecules (**20-23**, Figure 3).¹

Pharmaceutical molecules



Agrochemical molecules

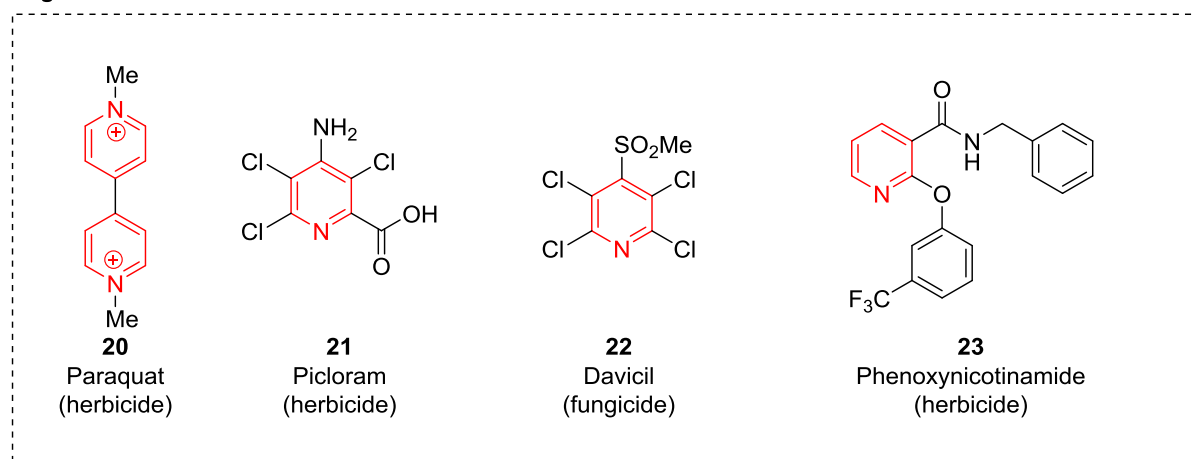
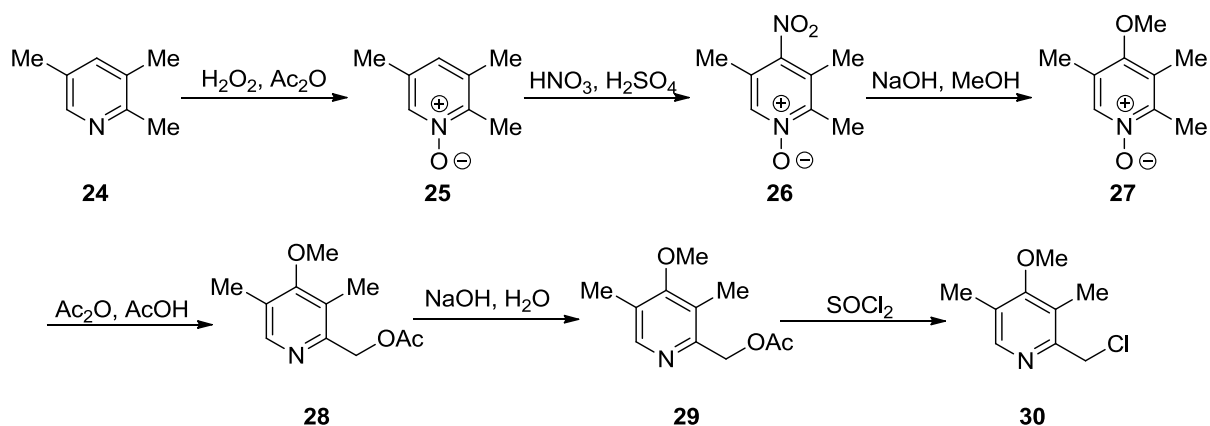


Figure 3: A variety of pyridine-containing pharmaceutical and agrochemical molecules

Carey *et al.*² and Roughley *et al.*³ investigated the most commonly used transformations in industrial processes and medicinal chemistry Research and Development (R&D) departments respectively at Astra Zeneca, GlaxoSmithKline and Pfizer. Both included heterocycle formation (and functionalisation) in the top ten transformations employed in these fields.

Of the 128 drug candidate molecule syntheses investigated by Carey *et al.*² there were 131 occurrences of heterocycle manipulation/synthesis; 41% of these involved the purchase of *N*-containing heterocycle starting materials and 40% involved direct synthesis of the *N*-heterocyclic aromatic. The most commonly occurring aromatic heterocycle was pyridine with 88% (23 instances out of 26) of the manipulations involving the purchase of a pyridine derivative and subsequent manipulation. The authors state that although pyridine chemistry is well understood some substitution patterns are difficult to prepare, for example **30** (Scheme 2), which is a starting material for the synthesis of omeprazole. In order to introduce two extra functionalities to starting material **24**, the synthetic route required initial activation of the pyridine ring by forming its *N*-oxide analogue (**25**); by treating **24** with hydrogen peroxide in acetic anhydride. Intermediate **25**, now a lot more activated towards electrophilic aromatic substitution, undergoes nitration to give **26**; from here the route relied on the substitution of the nitro group to give the methoxy derivative **27**. Using the *N*-oxide handle, reaction of **27** with acetic anhydride in acetic acid introduced an acetate moiety to the 2-methyl group (**28**). This was subsequently reduced (**29**) and treated with thionyl chloride to give **30**.



Scheme 2: Synthetic route to API for the synthesis of Omeprazole [4]

In the analysis of reactions used in medicinal chemistry research laboratories in industry, carried out by Roughley *et al.*³ the number of heterocyclic starting materials and their subsequent functionalisation far outstrips the frequency of the heterocycle-forming reactions. As with Carey's analysis, pyridines are the most common heterocycle accounting for 25% of all heteroaromatics, with pyrimidine and pyrazole closely following at 15% for each.

Further to its applications in biological systems, pyridine derivatives are widely used in synthetic organic chemistry, examples include dimethylaminopyridine (DMAP, **31**, Figure 4), which is used in process-scale acylations and in the activation of carboxylic acids. Furthermore, an axially chiral DMAP analogue (**32**, Figure 4) has been developed to achieve enantioselective acylation - a method that was previously dependant on enzymatic transformations.¹

Pyridine analogues such as vinylpyridine polymers have found use industrially as acid scavengers, supports for oxidising and reducing agents as well as materials for chemical separations. *N*-alkylpyridinium salts such as **35** (Figure 4) have been used as ionic liquids with the ability to dissolve organic and inorganic compounds, are highly polar with the added benefit of being non-coordinating.¹

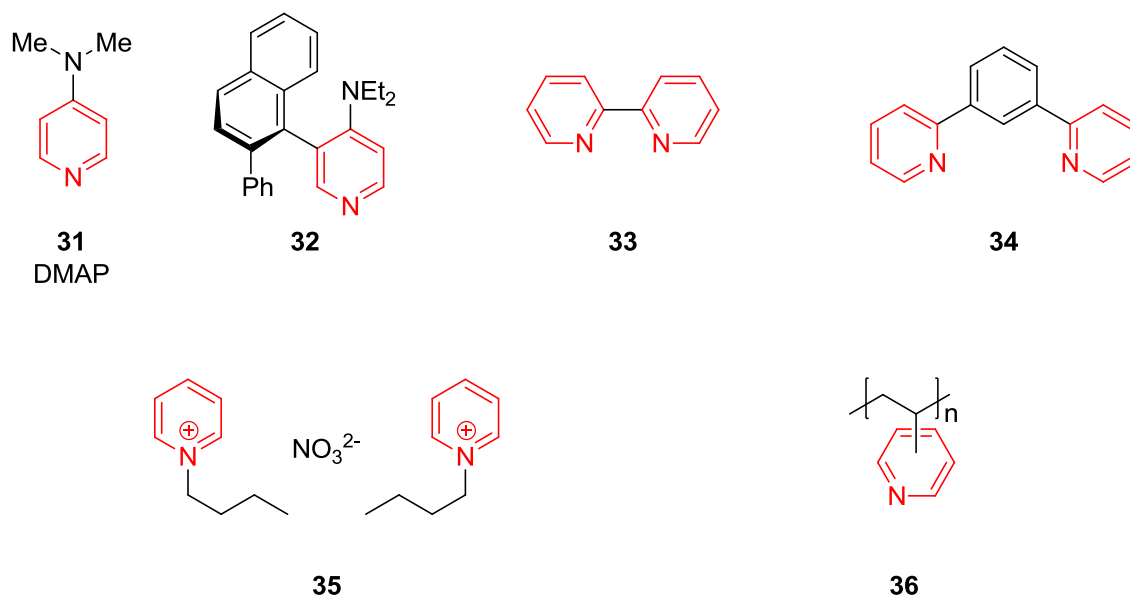
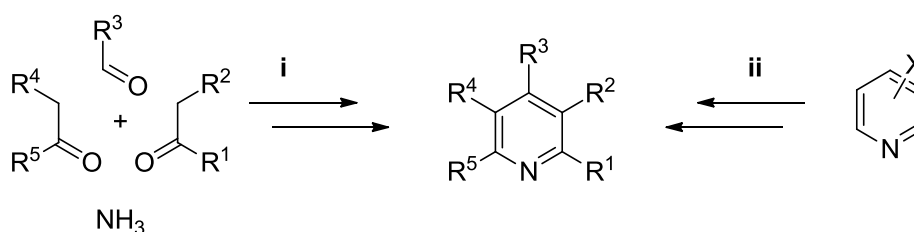


Figure 4: Pyridine-containing compounds used in preparative organic chemistry

Given their high applicability, it comes as no surprise that the development of an efficient synthetic methodology for the production of functionalised pyridines has generated a large interest within the synthetic organic community. Furthermore, with the production of a wide variety of pyridine analogues on industrial scale, there is an impetus to develop such methods that are also sustainable coupled with a minimised environmental impact.

1.2. Functionalising pyridines

Chiefly, there are two primary approaches for the synthesis of functionalised pyridines. The first and oldest methods involve a series of inter- and intramolecular polycondensation reactions between reactive species carrying carbonyl and amine functionalities (i, Scheme 3), the most notable being the Hantzsch synthesis of pyridines. The second and more efficient route involves the direct introduction of functionality to an unsubstituted, or partially substituted pyridine ring (ii, Scheme 3).⁵



Scheme 3: Synthetic pathways to functionalised pyridines

There are various methods in the literature that employ either synthetic route; however they are not without their individual drawbacks. The first approach is often a long, multistep process and in some instances the starting materials are not readily available. The second method is more direct and can be employed through aromatic substitution reactions, however this route is mitigated by the low reactivity of the pyridine ring to both electrophilic and nucleophilic aromatic substitution. Although some electrophilic substitution reactions have been achieved with pyridines, such as nitration, halogenations and sulfonation, the protocols occur under forcing reaction conditions.⁵

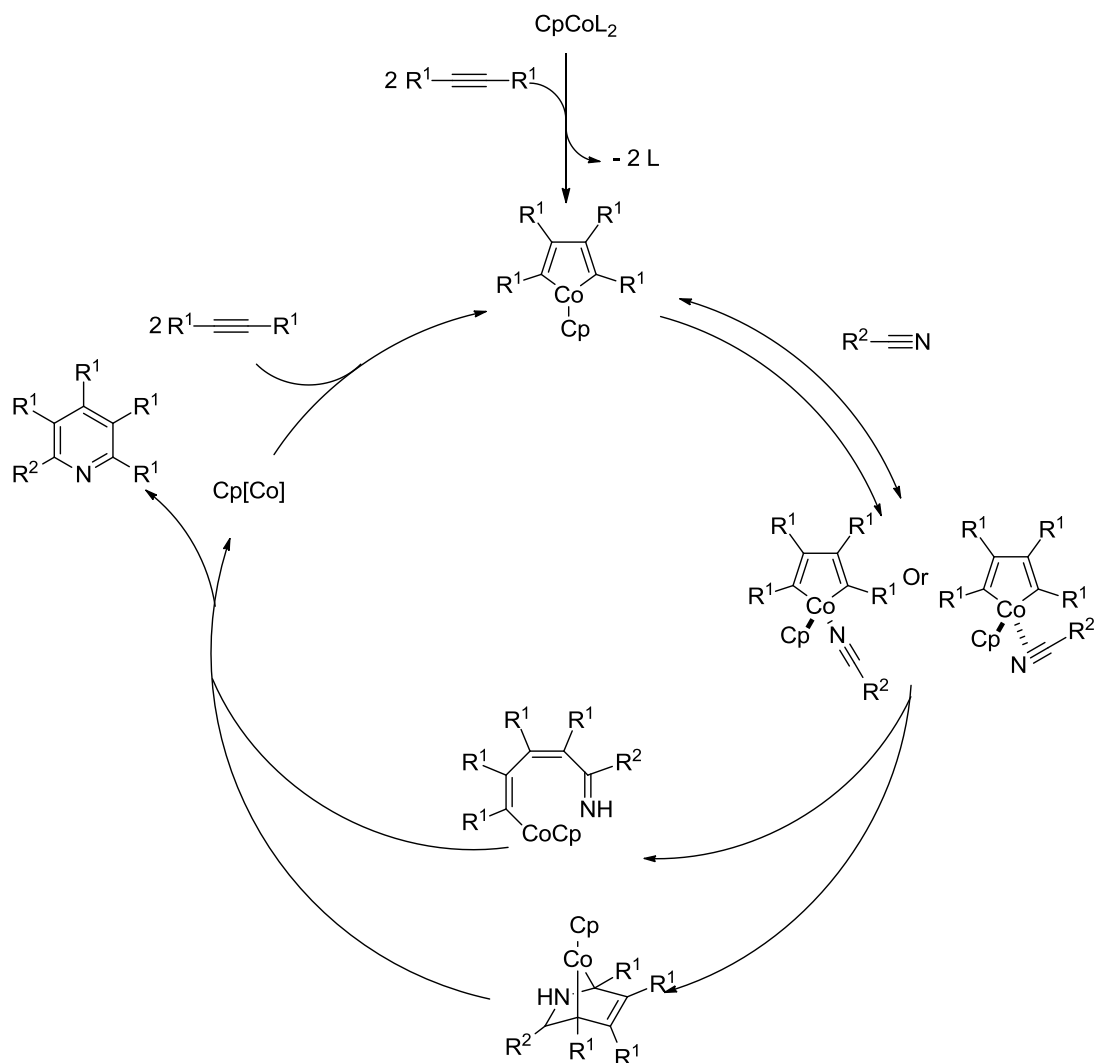
1.3. Routes to functionalised pyridines (overview)

This section aims to give an overview of methods used to functionalise pyridines that fall under the two classical approaches; it will give an overview of ring synthesis methods, but will not address it in great detail, given that industrially, pyridine ring synthesis is not adopted as frequently as direct ring functionalisation. Therefore, the focus will be on the area of direct functionalisation of the pyridine ring; looking into classical aromatic substitution reactions and how its challenges can be overcome by use of pyridine *N*-oxides. Moving onto classical transition metal catalysed methods of functionalising pyridines, to more recent advances in the area of transition metal catalysed direct pyridine ring functionalisation.

1.3.1 Ring synthesis

Classic condensation methods for the synthesis of functionalised pyridine rings rely on aldol and Michael-type reaction steps; the identity of the substituents as well as their position is dictated by the activating groups required for the reaction to proceed, a comprehensive review of standard polycondensation reactions has been published by Henry.¹ Alternatives that offer broader scope in position and functionality on the pyridine ring are cycloaddition reactions, which form a selective and efficient route to the formation of multiple bonds, rings and stereocentres; however, thermal [2+2+2] cycloadditions are rarely seen as they are disfavoured by enthalpy barriers associated with bringing three reactants together.⁶ However, this barrier can be overcome through the use of a transition metal catalyst, which can act as a site for stepwise addition of the reactants, and presents an efficient approach to the synthesis of functionalised pyridines.⁶ A number of transition metal complexes can be used as catalysts for these cycloaddition reactions, with varying reactivities and functional group tolerances. Most of the commonly used metals for mediating the cycloaddition reactions (cobalt, rhodium, zinc and ruthenium among others) have similar features.⁶ The most

commonly used example in the literature is that of the cobalt catalysed cycloaddition of acetylene and functionalised nitriles (Scheme 4).



Scheme 4: [2+2+2] cycloaddition [3]

The first step involves formation of the reactive species from the precursor, which involves coordination of the incoming acetylene groups, followed by oxidative coupling to yield a metallocyclopentadiene. The subsequent step involves the reaction of the metallocycle with a third triple bond (in this case a nitrile) *via* an insertion or cycloaddition reaction, followed by elimination from the metal centre to give the final functionalised pyridine.⁶

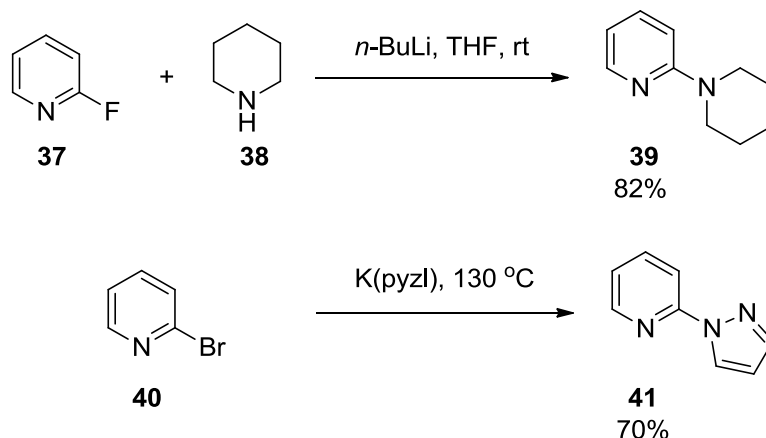
Comprehensive literature reviews have been carried out by Henry,² Heller,⁴ Saà³ and Yamamoto⁵ in this area, which cover commonly used polycondensation reactions as well as transition metal catalysed cyclisation reactions for the formation of functionalised pyridines.

1.3.2. Direct introduction of functionality

1.3.2.1. Aromatic substitution reactions of pyridines

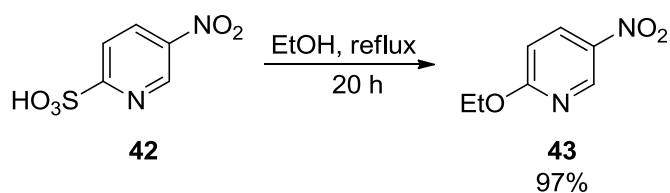
The formal displacement of a CH unit in benzene for a nitrogen atom in pyridine leads to a large difference in reactivity. Pyridines are far less susceptible to electrophilic substitution and more so to nucleophilic attack than benzene. Nonetheless, pyridine does undergo a variety of simple electrophilic addition reactions involving the formation of pyridinium salts, which have no counterpart in benzene chemistry.⁷ Another key aspect of pyridine chemistry is the electron deficiency of the pyridine ring, specifically at the α - and γ -carbons, which allows for nucleophilic addition at those carbons as well as formal displacement of electron withdrawing groups such as halides.⁸

Fluoropyridines are more reactive than their other halopyridine counterparts,⁹ for example 2-fluoropyridine readily undergoes nucleophilic substitution with deprotonated dialkylamines at room temperature (Scheme 5).⁸ This is far more reactive than in the case of the corresponding 2-bromopyridine with the potassium salt of pyrazole (Scheme 5).⁹



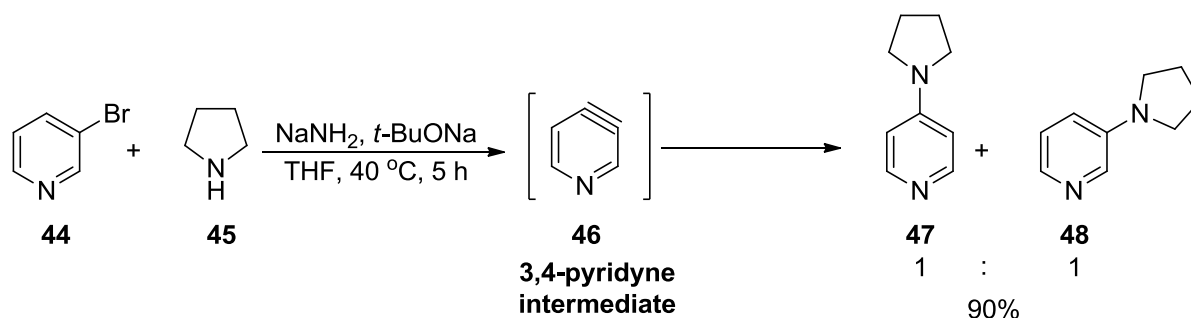
Scheme 5: Substitution of fluorine and bromine at the 2-position on pyridine by anionic nitrogen nucleophiles [7,10]

Sulfonic acids such as that in 5-nitropyridine-2-sulfonic acid,¹¹ can be displaced by alcohols, amines or chlorides (Scheme 6).¹² However the system does rely on the combined effect of a *para*-directing nitro group as well as the electron deficient nature of the α -position of the pyridine.



Scheme 6: Displacement of sulfonic acid substituent by an ethoxy group under reflux conditions [12]

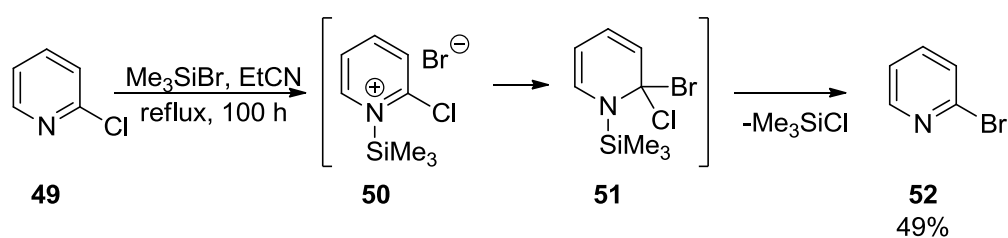
Although the above mechanism operates *via* the expected two-step process for nucleophilic aromatic substitution, some displacements occur by means of a different mechanism. The reaction of 3-bromopyridine with secondary amines in the presence of sodium amide/sodium *t*-butoxide produces a mixture of 3- and 4-dialkylaminopyridines, as this reaction occurs *via* an elimination process, S_NEA (Substitution Nucleophilic Elimination Addition) with the generation of a 3,4-pyridyne intermediate (Scheme 7).¹³



Scheme 7: Substitution of bromine in 3-bromopyridine by means of an S_NEA reaction mechanism via a 3,4-pyridyne intermediate [13]

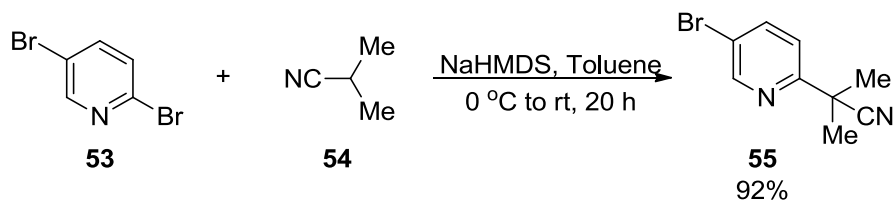
The fact that no 2-amino pyridine is produced in the reaction indicates the difficulty of generating a 2,3-pyridyne. 2-Substituted products can be obtained from the 2,3-pyridyne intermediate on reaction of 3-bromo-2-chloropyridines with *n*-butyllithium¹³ or by the reaction of 3-trimethylsilyl-2-trifluoromethanesulfonyloxy pyridine with fluoride.¹⁴ Interestingly, a 4-aryloxy or 4-phenylthio substituent has been shown to afford a 2,3-pyridyne intermediate selectively.¹⁵

α -Chlorines can be displaced by bromine or iodine using a halotrimethylsilane donor; this process involves an intermediate pyridinium salt formed by complexation of the silyl cation to the nitrogen lone pair on the pyridine, further enhancing the electron deficient nature of the α -position, enabling the substitution reaction to proceed (Scheme 8).¹⁶



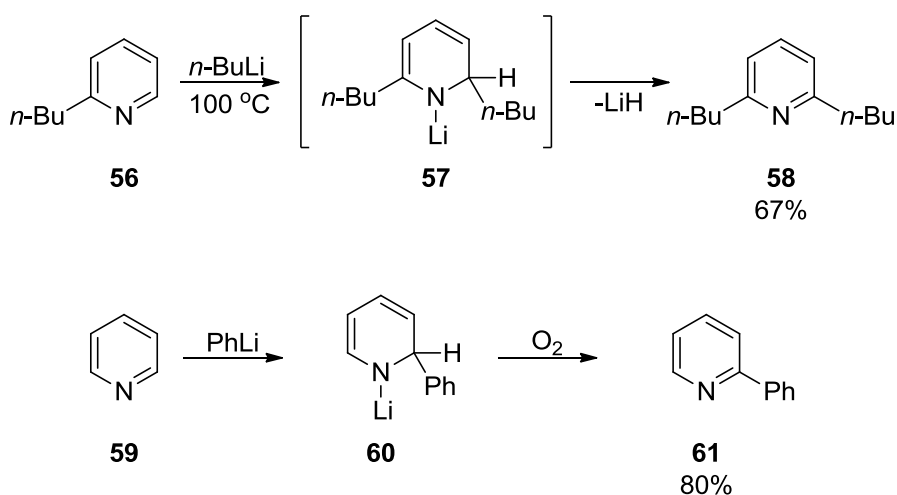
Scheme 8: Displacement of chlorine in 2-chloropyridine by reaction with trimethylsilyl bromide, reaction proceeds via an *N*-silyl pyridinium salt intermediate [16]

Carbon-carbon bond formation can be facilitated through nucleophilic substitution of halopyridines, with deprotonated nitriles readily displacing a halogen group in the α -position (Scheme 9).¹⁷ The generation of a strong nucleophile, through use of the NaHMDS base, allows the reaction to proceed at low temperatures.



Scheme 9: Formation of carbon-carbon bonds through nucleophilic aromatic substitution of pyridines using carbon nucleophiles [17]

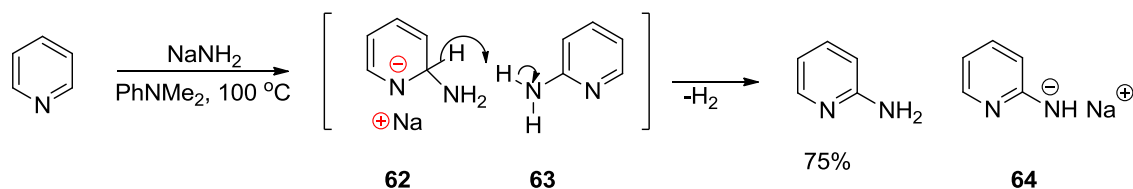
In the absence of an α - or γ -leaving group, pyridines are less reactive; they can however undergo nucleophilic additions that proceed *via* dihydropyridine adducts with the loss of a hydride to achieve the overall substitution.⁷ Reactions such as these are selective for the α -position as the nucleophile is delivered by complexation of the pyridine to a metal cation or hydride associated with the nucleophile.⁷ For example, the reaction of pyridines with aryl or alkyl lithiums proceeds *via* a two-step process: first involving addition of the alkyl lithium to generate a dihydropyridine-*N*-lithio-salt that is subsequently converted into the aromatic pyridine by means of oxidation, disproportionation or elimination of lithium hydride (Scheme 10).¹⁸ Generally, attack is at the α -position, reactions involving 3-substituted pyridines take place at both α -positions but will predominantly occur in the 2-position relative to the 3-substituent.⁷



Scheme 10: Alkylation and arylation of pyridines through reaction with alkyl/aryl-lithiums [7,18]

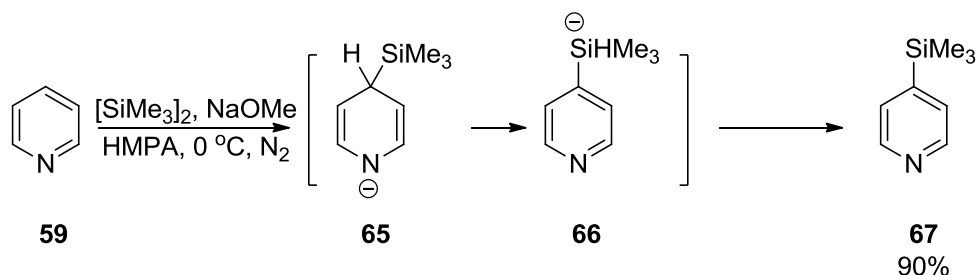
Amination of pyridines at the α -position is known as the Chichibabin reaction (Scheme 11), which involves the reaction of pyridine with sodium amide. The hydride transfer step is thought to involve the interaction of the aminopyridine

product (**63**) as an acid donor with an anionic intermediate (**62**). The bias towards the α -position is due to the intramolecular delivery of the nucleophile guided by the complexation of the pyridine nitrogen to the metal cation.¹⁹



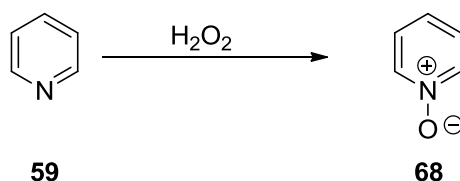
Scheme 11: Chichibabin reaction [19]

Interestingly, 4-trimethylsilylpyridine is generated by reaction of pyridine with trimethylsiliconide anion; the transformation proceeds *via* a 1,4-dihydro-adduct in which the pyridine is rearomatised through hydride shift to the silicon (Scheme 12).



Scheme 12: Silylation of pyridine [7]

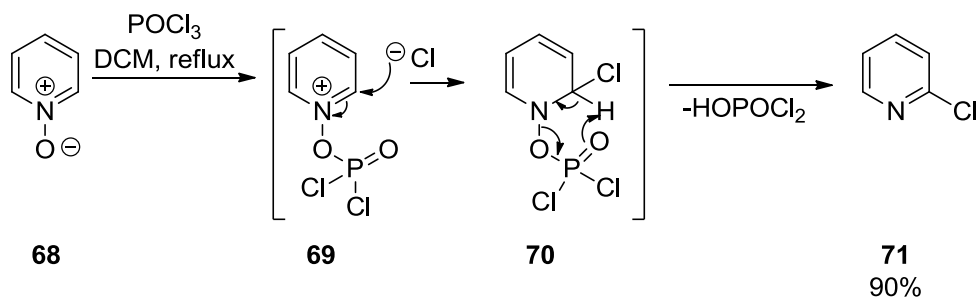
The majority of these methods take advantage of the availability of the lone pair on the pyridine ring nitrogen through coordination of a metal or proton, which activates the pyridine ring towards aromatic substitution reactions. Indeed there is extensive literature around stoichiometric methods for the aromatic substitution of halopyridines by virtue of their hydrochloride salts. This effect can be further enhanced by coordination of an oxygen atom to the pyridine ring nitrogen to form the *N*-oxide. Pyridine *N*-oxides are generated through the reaction of pyridines with peroxides (Scheme 13), which have a very rich chemistry differing from that of neutral pyridines and pyridinium salts.



Scheme 13: Synthesis of pyridine *N*-oxides

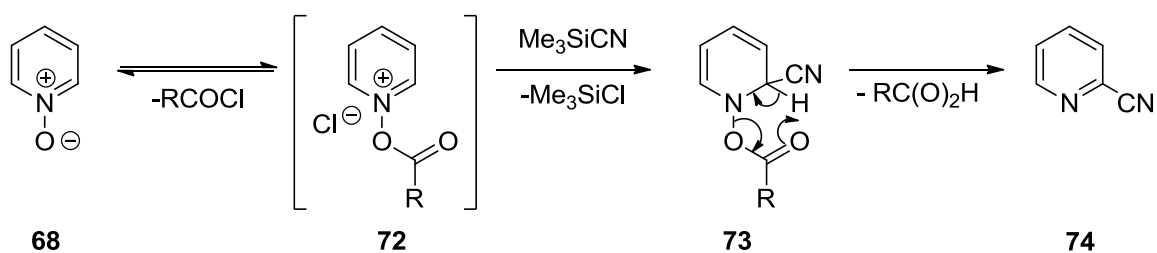
A prominent difference between pyridines and their *N*-oxide counterparts is the susceptibility of the *N*-oxides to electrophilic nitration. This is due to the mesomeric electron release from the oxygen, which can be compared with the electron release by the oxygen in phenols and phenoxides, which activates them towards electrophilic substitution. As a result of their enhanced reactivity towards both electrophiles and nucleophiles relative to neutral pyridines, *N*-oxides offer a synthetic avenue to substituted pyridines whose α - and γ -substituents have been modified.

Reactions of *N*-oxides with phosphoryl chloride or acetic anhydride lead to the formation of 2-chloro and 2-acetoxypyridines respectively; phosphorylation of the *N*-oxide is followed by nucleophilic addition of chloride at the α - or γ -position with the intermediate regaining aromaticity by proton elimination (Scheme 14).²⁰



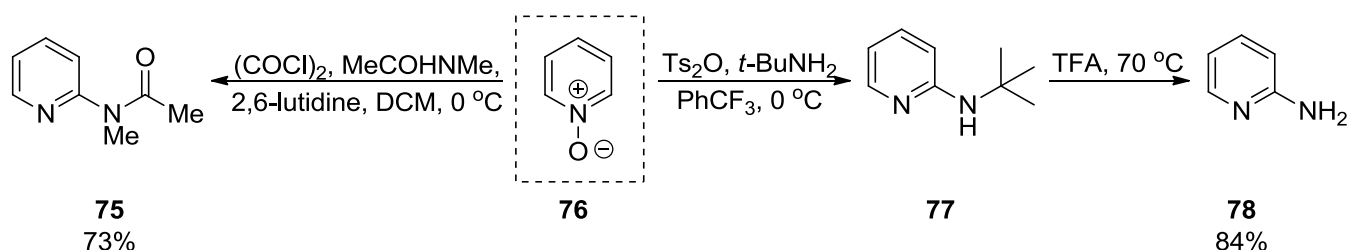
Scheme 14: Nucleophilic substitution in *N*-oxides by reaction with phosphoryl chloride to give 2-chloropyridine [20]

In parallel, the conversion of *N*-oxides into 2-cyanopyridines requires a prior conversion of the *N*-oxide into a *N*-acetoxy or siloxy functionality (Scheme 15).²¹



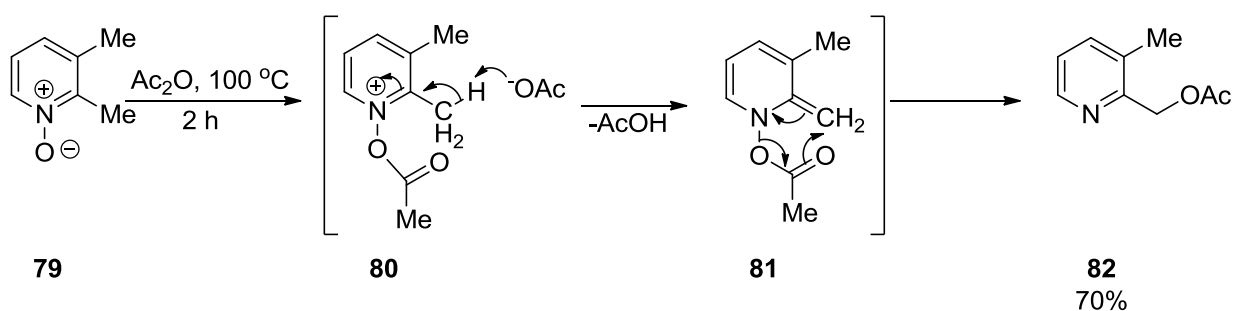
Scheme 15: Introduction of a nitrile to *N*-oxides proceeds with conversion of the oxide functionality into an *N*-acetoxy group [21]

Nitrogen functionality can be introduced in a variety of ways; either *via* *O*-tosylation followed by reaction with *t*-butylamine leading to 2-aminopyridines²² or by use of oxalyl chloride with a secondary amide to give 2-aminopyridine amides (Scheme 16).²³



Scheme 16: Introduction of nitrogen functionality to pyridines through pyridine *N*-oxides [22, 23]

Reaction of 2-methylpyridine *N*-oxides with hot acetic anhydride gives 2-acetoxymethylpyridines, whilst the use of trifluoroacetic anhydride at room temperature gives the same result with fewer by-products. It is thought that the rearrangement proceeds *via* the electrocyclic mechanism shown in Scheme 17.²⁴

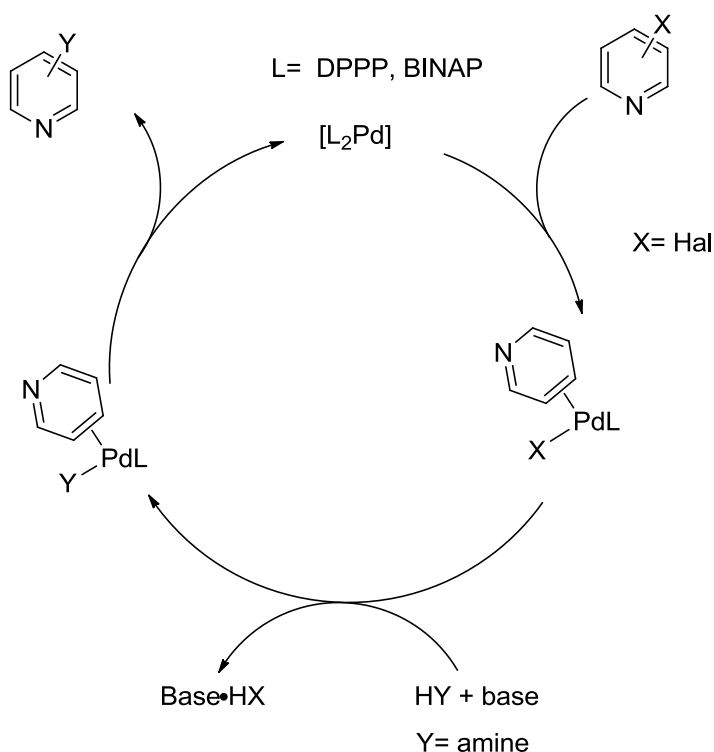


Scheme 17: Synthesis of 2-acetoxymethylpyridines by reaction of 2-methylpyridine *N*-oxides with acetic anhydride [24]

1.3.2.2. Buchwald–Hartwig and Ullmann reactions

In the field of transition metal-catalysed cross-coupling reactions, the amination of aromatic compounds independently developed by the Buchwald and Hartwig labs is now considered a standard tool in the formation of C(sp²)-N bonds. Better known as the “Buchwald-Hartwig” reaction, this method relies on a Pd⁰-Pd^{II} catalytic cycle in conjunction with bulky phosphine ligands and a base. The method can convert aromatic and vinyl C(sp²)-X bonds into C(sp²)-N bonds for a wide variety of amines.

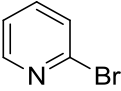
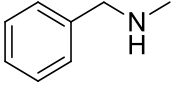
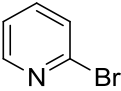
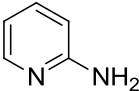
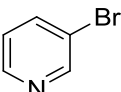
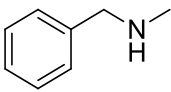
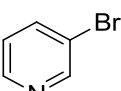
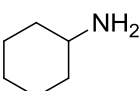
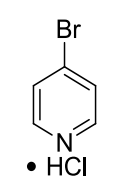
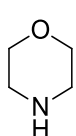
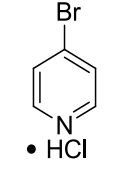
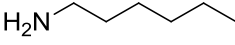
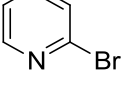

Given the deviation in reactivity of pyridines from benzene chemistry, achieving ring functionalisations in pyridines had initially proved challenging. The Lewis basicity of the nitrogen lone pair of the pyridines results in strong binding affinities to late transition metals, which tend to displace weakly bound ligands such as P(*o*-tol)₃; rendering such systems ineffective for amination of pyridines. However, the Buchwald-Hartwig reaction has been adapted for application to pyridines by use of chelating phosphine ligands, affording a better system for pyridine amination (Scheme 18).²⁵



Scheme 18: Buchwald–Hartwig cross-coupling with pyridines [26]

The most general system uses palladium acetate as a catalyst precursor with BINAP as the most effective ligand for amination with either primary or secondary amines. Linear primary amines however, proceed with lower yields than branched amines. The use of the cheaper 1,3-bis(diphenylphosphino)propane (DPPP) ligand in combination with $[\text{Pd}_2(\text{dba})_3]$ was found to be an effective catalytic system for the amination of bromopyridines with secondary amines, or amines lacking a proton in the α -position to the nitrogen atom, as summarised in Table 1.²⁶

Table 1 Buchwald–Hartwig amination of halopyridines [26]

Entry	Pyridine	Amine	Catalyst	Ligand	Yield (%)
1			$\text{Pd}(\text{dba})_3$	DPPP	86
2			$\text{Pd}(\text{dba})_3$	DPPP	87
3			$\text{Pd}(\text{dba})_3$	(\pm)BINAP	77
4			$\text{Pd}(\text{dba})_3$	(\pm)BINAP	82
5			$[\text{Pd}(\text{OAc})_2]$	DPPP	91
6			$[\text{Pd}(\text{OAc})_2]$	(\pm)BINAP	67
7			$[\text{Pd}(\text{OAc})_2]$	(\pm)BINAP	71

This system has since been further developed to improve the yields with linear primary amines by using Josiphos ligands (Figure 5). The increased steric bulk of the catalyst yields an improvement in monoarylation of primary amines, as a result of the robust chelation of the Josiphos ligand which

prevents pyridines and amines from binding to and deactivating the catalyst.²⁷

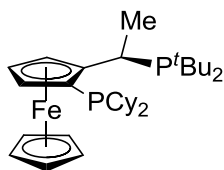
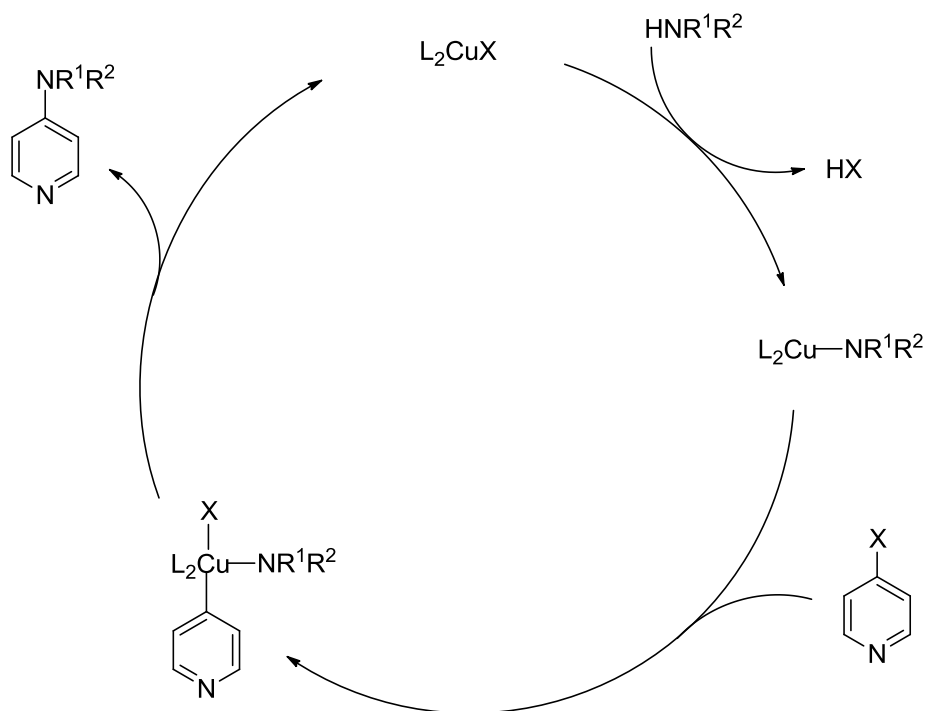


Figure 5: Fourth generation Josiphos ligand used in aryl amination

This system has all the benefits of its predecessor but also displays significant improvements for the amination of chloropyridines with acyclic primary amines, affording yields of 93% and 83% for the amination of 2- and 4-chloropyridine with octylamine respectively.²⁷

Other methods developed for the amination of pyridines include the Ullmann condensation,^{28, 29} a variation of the widely known Ullmann aryl coupling reaction, whereby anilines can be coupled to aryl halides to generate biaryl amines using a copper catalyst in the presence of a base under reflux conditions (Scheme 19).



Scheme 19: Proposed mechanism of the Ullmann amination of pyridines [30]

A notable aspect of both the Buchwald–Hartwig and Ullmann reactions is that they can take place at any position on the pyridine ring, making them better alternatives to the stoichiometric S_NAr reactions of pyridines. However, the Ullmann reactions are carried out under forcing conditions ($\sim 200\text{ }^\circ\text{C}$), albeit using a cheap and naturally abundant metal to generate a catalytic species. In comparison, the Buchwald–Hartwig reactions of pyridines are carried out under relatively milder conditions. However, this method uses expensive transition metals and requires a stoichiometric amount of base and ligand; aspects that could be addressed to improve the green credentials of pyridine functionalisation.

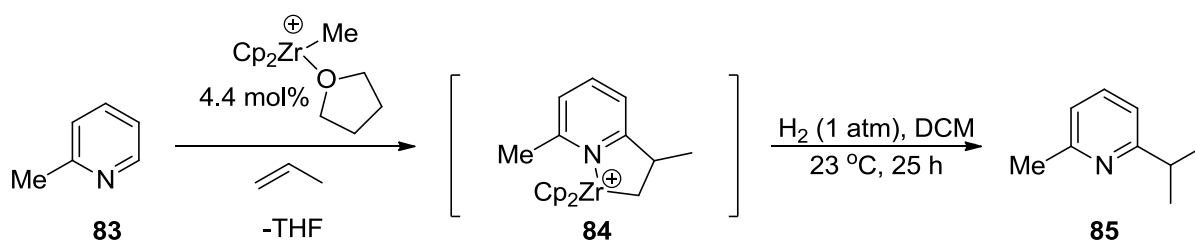
It is beyond the scope of this review to address exhaustively the various synthetic methods in the literature for functionalising pyridines; a review of a variety of methodologies that utilise transition metals for the C-H functionalisation of pyridines has been published by Nakao¹ and a comprehensive study of methodologies for (hetero)arylation of pyridines has also been reviewed by Rossi.³¹

1.3.3. Transition metal catalysed C-H functionalisation

This section aims to give a synopsis of recent developments in the area of pyridine functionalisation; the sections are subcategorised into functionalisation methods at the 2/6-, 3/5- and 4-positions on the pyridine ring to demonstrate the challenges in developing a single method that can be applied to the functionalisation of pyridines at any position on the ring.

1.3.3.1. Selective functionalisation at the 2-position in pyridine⁵

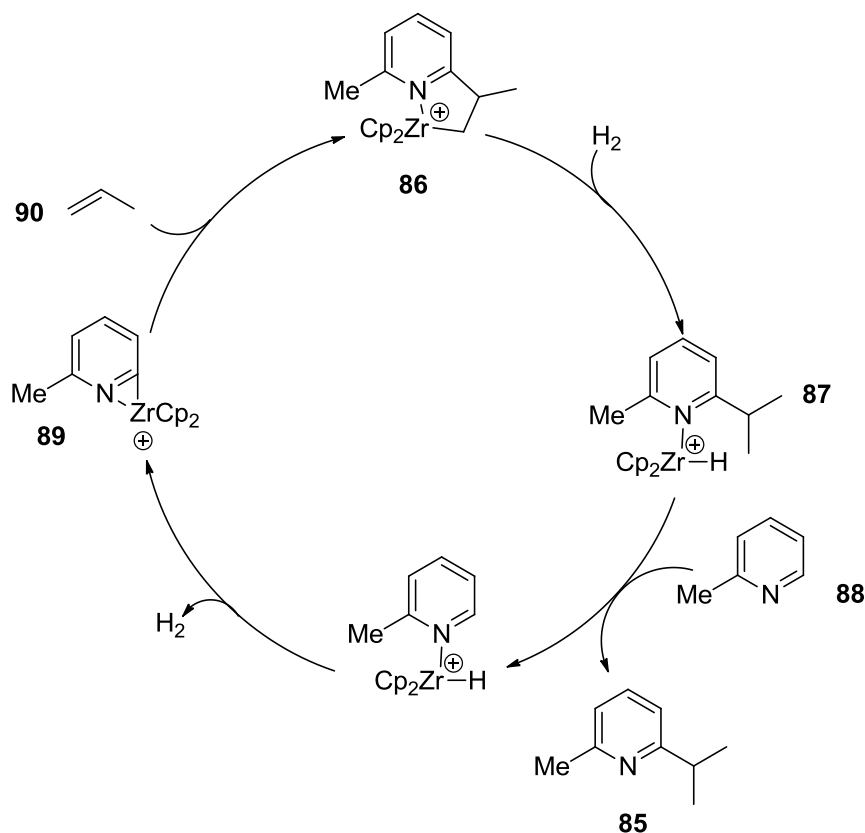
The nitrogen lone pair of the pyridine provides a site at which it can coordinate to a metal, the resultant proximity of the metal complex leads to C-2 metalation on the pyridine. Subsequent processes lead to carbon-carbon bond formation by means of functionalisation of the C-H bond at the α -position in pyridine, as a result, the majority of transition metal catalysed methodologies developed tend to be selective to the 2-position. A very early report by Jordan *et al.*³² described a method in which an alkyl zirconium complex catalysed C-2 alkylation of 2-picoline (**83**) with propene under an atmospheric pressure of hydrogen, Scheme 20.



Scheme 20: Alkylation of 2-picoline using a zirconium catalyst [32]

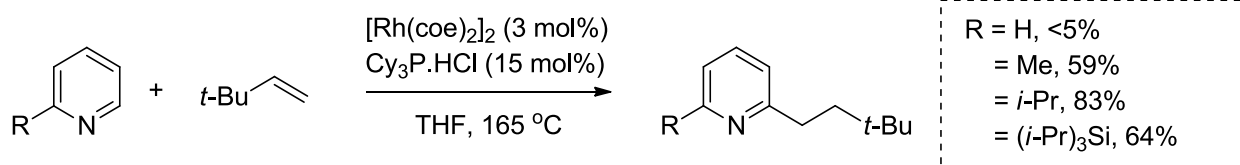
The catalytic cycle is thought to proceed *via* hydrogenolysis of the alkyl zirconium complex (**86**), with the coordinating 2,6-functionalised pyridine (**87**) exchanging with a free 2-picoline. This is followed by metalation at the C-2 position (**89**) with liberation of H₂ and insertion of the metallocycle across the double bond of propene to regenerate the original cationic zirconium complex, **86** (Scheme 21). The use of chiral zirconium catalysts with a

bis(trihydroindenyl) ligand gave the methodology an enantioselective dimension.³³



Scheme 21: Proposed mechanism of alkylation of 2-picoline catalysed by a zirconium complex [33]

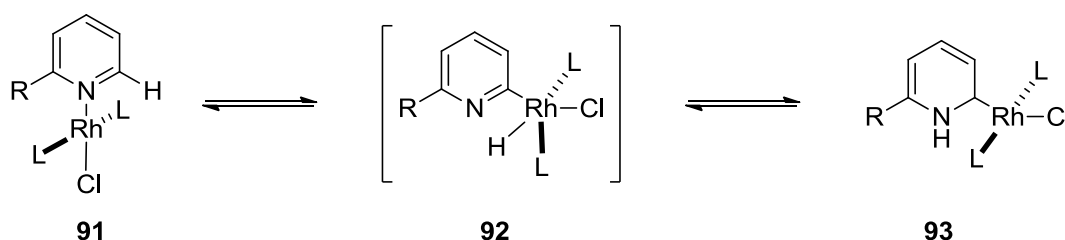
More recently, Lewis *et al.*³⁴ reported the alkylation of pyridine using a rhodium based catalyst. The reaction was effective for a wide variety of substituted pyridines and quinolines with a diverse range of functionalised alkenes (Scheme 22).



Scheme 22: Alkylation of C-2 functionalised pyridines catalysed by a rhodium complex [34]

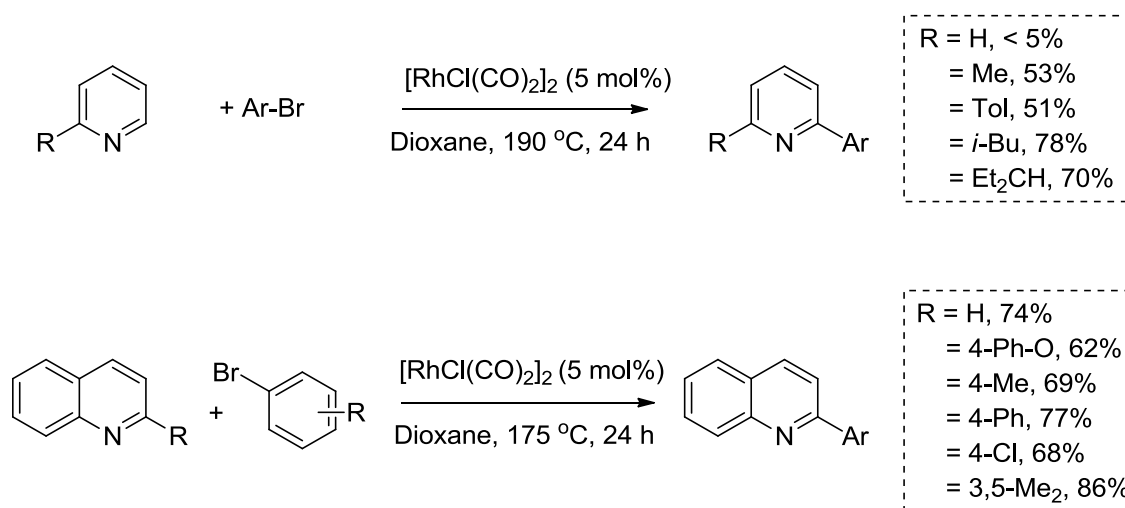
Good to excellent yields were reported for the reaction of linear alkenes with 2-substituted pyridines. When the alkylation reaction was carried out on an

unsubstituted pyridine, the product was achieved in less than 5% yield (Scheme 23). The observed substituent effect is a direct result of the reaction proceeding *via* the nitrogen bound complex (**91**), which is in equilibrium with a carbon-bound rhodium intermediate, **92** (Scheme 23); the C-2 substituent drives the equilibrium from the nitrogen-bound intermediate towards the carbene intermediate (**93**). The presence of a catalytic amount of acidic species, such as a phosphonium salt, is considered intrinsic to the reaction through promotion of the formation of the carbene complex.³⁵



Scheme 23: 2-Substituent effect on the rhodium catalysed alkylation of pyridines [35]

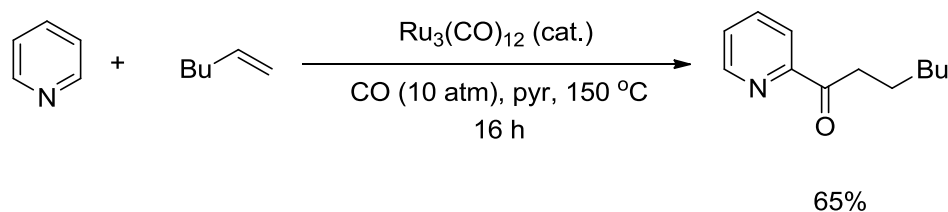
Berman *et al.*³⁶ illustrated the use of rhodium for the C-6 arylation of C-2 substituted pyridines and quinolines using aryl bromides; the process follows a similar mechanism to that outlined in Scheme 23.



Scheme 24: Reaction of 2-substituted pyridines and quinolines with aryl bromides catalysed by a rhodium complex [36]

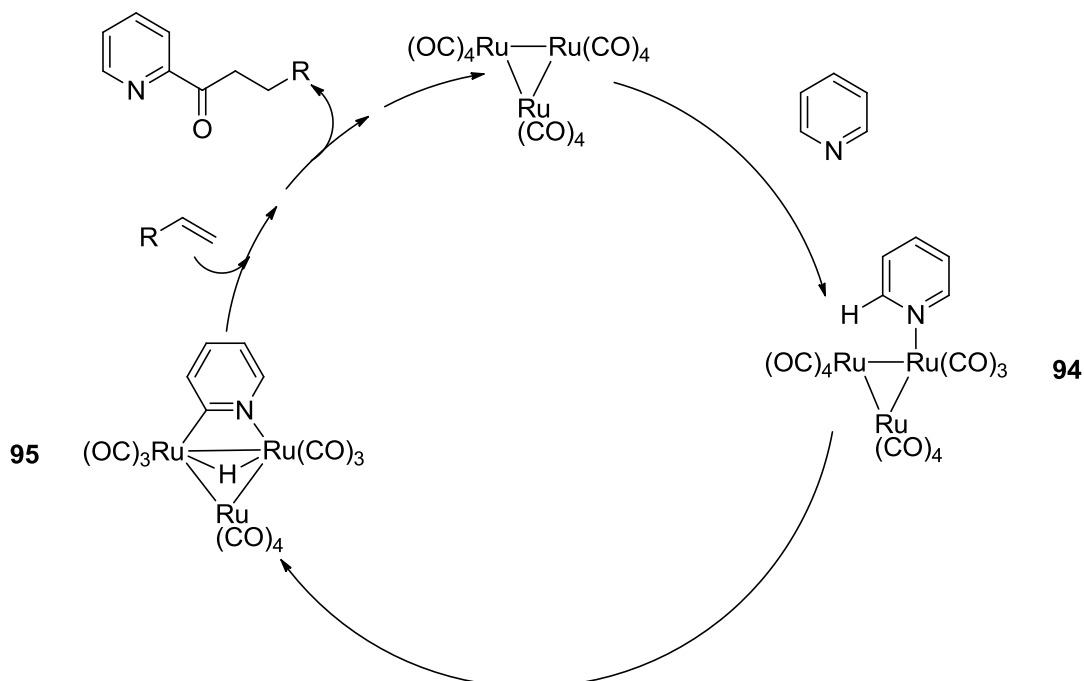
Ruthenium has also been shown to catalyse the C-2 functionalisation of unsubstituted pyridines, as exemplified by the work of Moore *et al.*³⁷ who

showcased the use of ruthenium dodecacarbonyl as a catalyst for the selective acylation of pyridines by reaction with alkenes under a carbon monoxide atmosphere (Scheme 25).



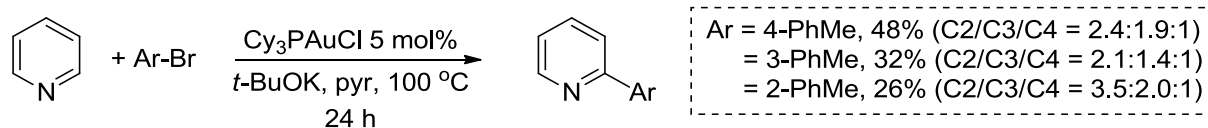
Scheme 25: Selective acylation of pyridines at the 2-position catalysed by ruthenium dodecacarbonyl [37]

The catalytic cycle for this process begins with coordination of pyridine to one of the ruthenium centres of the cluster (**94**), which is followed by oxidative addition of an adjacent ruthenium atom into the C2-H bond of the bound pyridine, **95** (Scheme 26). The alkene then partakes in migratory insertion into the ruthenium hydrogen bond followed by carbonylation of the resultant ligand; reductive elimination at this stage produces the 2-acylpyridine product and regenerates the catalytic species (Scheme 26).



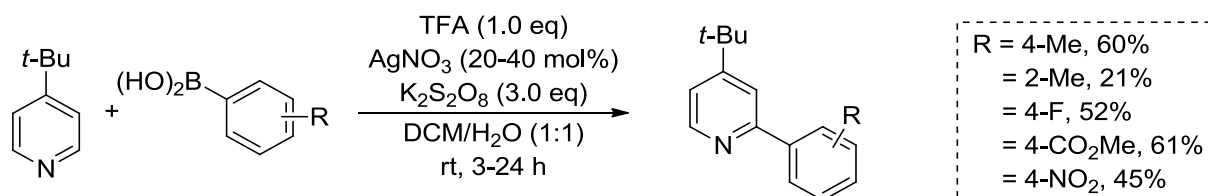
Scheme 26: Catalytic cycle for the 2-acylation of pyridine catalysed by a ruthenium cluster [37]

Other metals that have been shown to catalyse C-2 selective functionalisation of pyridines include gold, which has been reported to mediate the 2-arylation of pyridines with aryl bromides to give a mixture of arylated products with a preference for the C-2 position (Scheme 27).³⁸



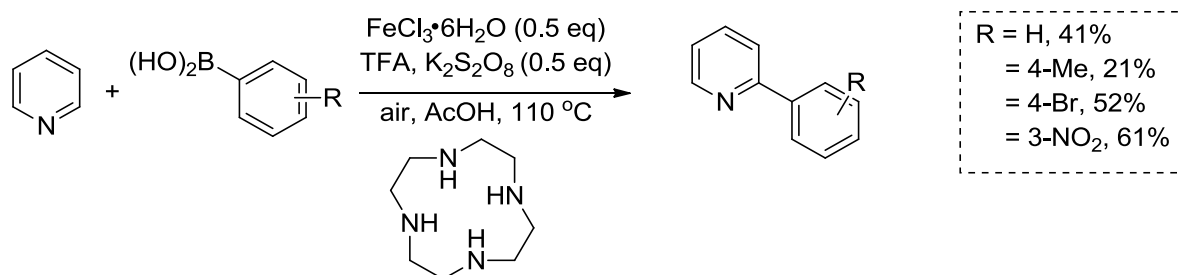
Scheme 27: C-2 arylation of pyridines catalysed by a gold based complex [38]

Arylation has also been reported using silver nitrate as the catalyst, in conjunction with arylboronic acids, as demonstrated by Seiple *et al.* (Scheme 28).³⁹



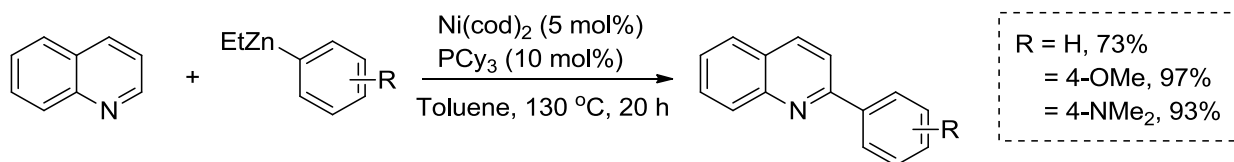
Scheme 28: C-2 aryl functionalisation of 4-substituted pyridines catalysed by silver nitrate [39]

The previous examples show the use of rare earth metal based catalysts, in contrast Wen *et al.*⁴⁰ made use of iron(III)chloride in combination with a cyclic amine for the arylation of pyridines. As with the gold catalysis the regioselectivity was modest and resulted in a mixture of 2- and 4-aryl pyridines (Scheme 29).



Scheme 29: Iron trichloride catalysed arylation of pyridines [40]

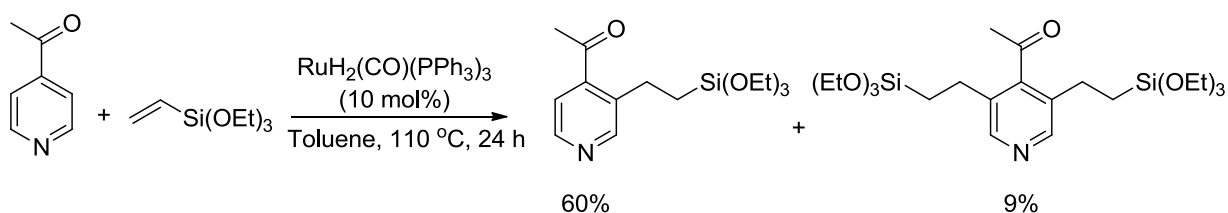
Superior regioselectivities and a broad substrate scope were observed for the 2-pyridine arylation method developed by Tobisu *et al.*, in which the pyridine analogues were reacted with an aryl zinc species in the presence of a nickel catalyst (Scheme 30).⁴¹



Scheme 30: Nickel catalysed arylation of quinoline [41]

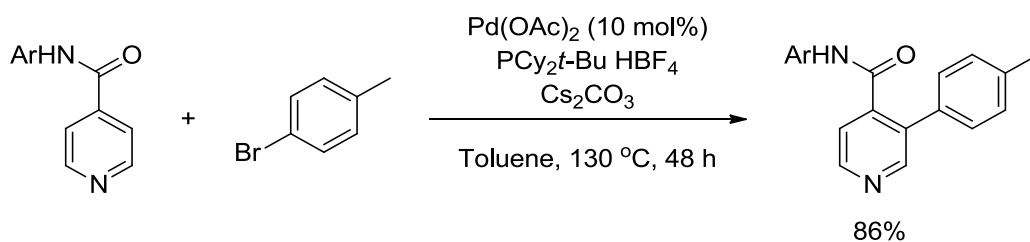
1.3.3.2. Selective functionalisation at the 3-position of pyridine⁵

The functionalisation of pyridines at the 3-position is very challenging; the selectivity observed for C-2 functionalisations of pyridine are a result of their proximity to the metal in the complex. However, direct functionalisations at the C-3 position have been shown to occur in pyridines that carry directing groups at the C-4 position, which aid in directing metalation to the C-3 position. For example, Grigg *et al.*⁴² demonstrated C-3 functionalisation in the reaction of 4-acetylpyridine with triethoxy(vinyl)silane in the presence of a ruthenium based catalyst (Scheme 31).



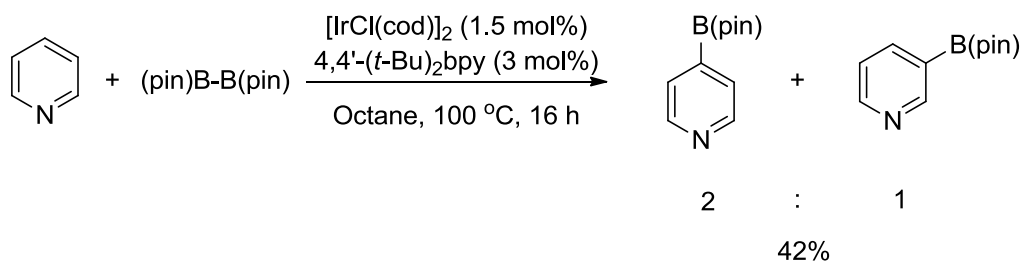
Scheme 31: Functional groups at the 4-position in pyridine direct metalation at the C-3 position using a ruthenium based catalyst [42]

Similarly, Wasa *et al.*⁴³ reported a method for directing the arylation of 4-aminocarbonylpyridines to the 3-position catalysed by palladium acetate (Scheme 32).



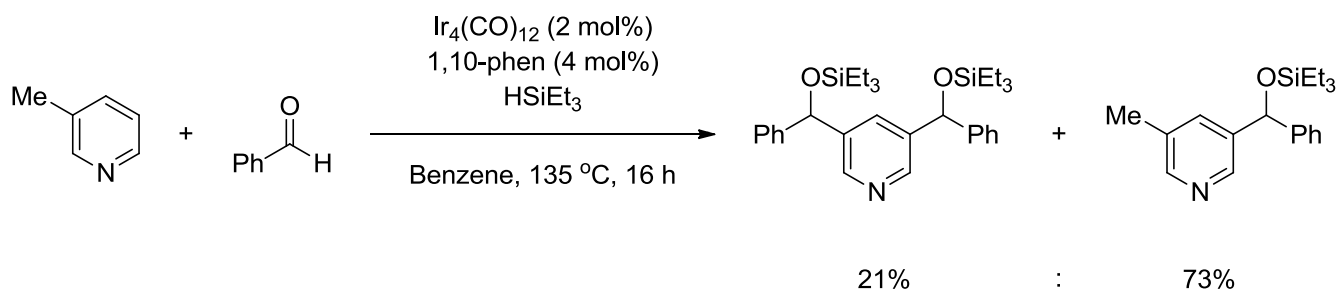
Scheme 32: Palladium-catalysed C-3 directed arylation in 4-aminocarbonylpyridines [43]

In pyridines that lack a directing group at the 4-position, functionalisation at the 3-position is problematic. This is exemplified in the iridium catalysed borylation of pyridine, which yields a mixture of 3- and 4-borylated pyridines (Scheme 33).⁴⁴



Scheme 33: C-3 Borylation of pyridine mediated by an iridium based catalyst [44]

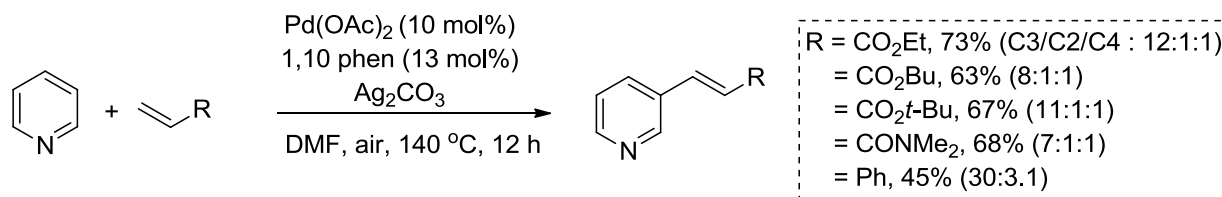
Recent efforts by Fischer *et al.*⁴⁵ used a pyridine carrying a substituent at the 3-position to direct iridium-catalysed borylation at the C-5 position in a 75% yield. Li and co-workers⁴⁶ reported a highly selective C-3 iridium-catalysed addition of pyridine with aromatic aldehydes in the presence of trimethylsilane (Scheme 34).



Scheme 34: Iridium catalysed C-3 addition reaction of aryl aldehydes to pyridine [46]

A noteworthy C-3 selective oxidative alkenylation of pyridine catalysed by palladium has been reported by Yu *et al.*,⁴⁷ the mechanism of the overall process has not yet been elucidated (Scheme 35). However, the report

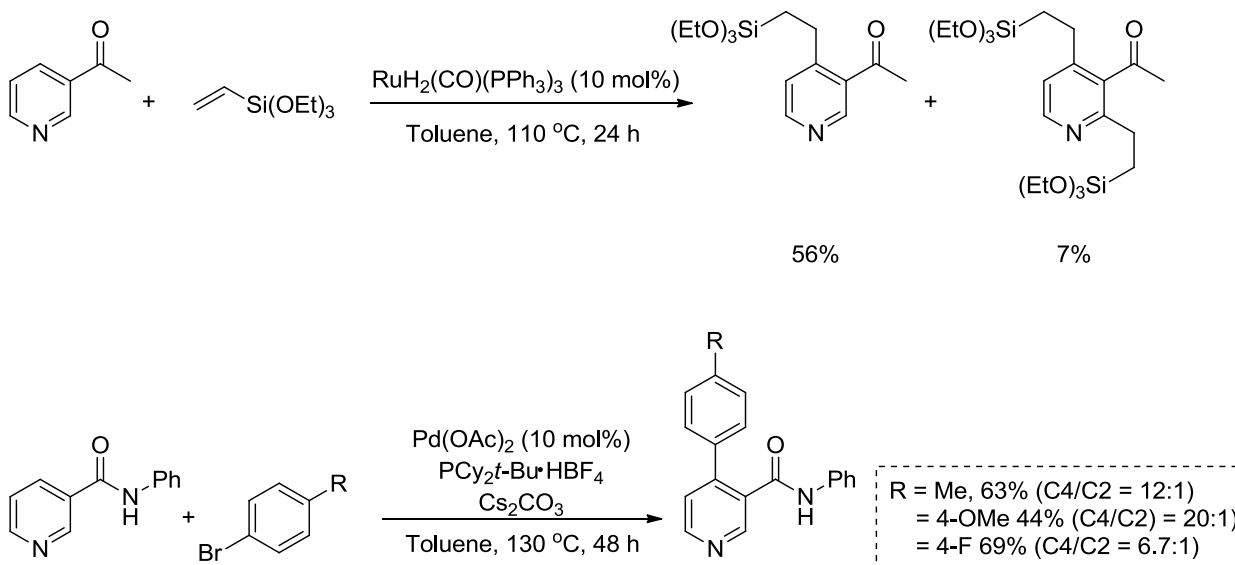
indicates that a carbon-hydrogen bond cleavage step by the palladium operates based on the large observed kinetic isotope effect ($k_H/k_D = 4.0$).⁴⁷



Scheme 35: Ligand-promoted C-3 selective olefination of pyridines facilitated by a palladium catalyst [47]

1.3.3.3. Selective functionalisation at the 4-position⁵

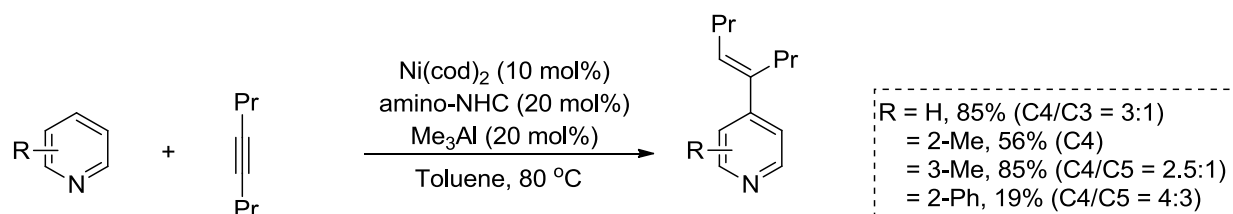
As with the 3-position in pyridines, C-4 functionalisation is limited to transformations in which pyridines contain a directing group, in this case at the 3-position. Both ruthenium and palladium catalysed alkylations and arylations have been shown to proceed at the C-4 position over the C-2 position for pyridines carrying a substituent at a β -carbon (Scheme 36).^{42,43}



Scheme 36: Ruthenium catalysed alkylation and palladium catalysed arylation of 3-substituted pyridines to afford C-4 functionalised pyridine products [42,43]

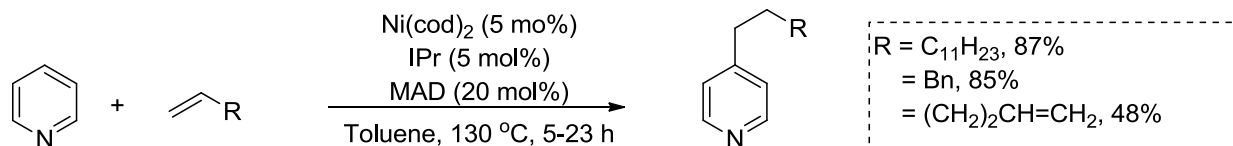
A more sustainable alternative developed by Tsai *et al.*⁴⁸ for the C-4 selective alkenylation of pyridines is mediated by a nickel catalyst in the presence of trimethylaluminium, which proceeds in the absence of a directing group (Scheme 37). The method uses *N*-heterocyclic carbene (NHC) ligands

to achieve the observed high C-4 selectivity. The pyridine coordinates to trimethylaluminium and subsequently binds to the nickel in an η^2 -fashion. This binding was found to take place exclusively at the C3-C4 double bond and is responsible for the observed C-4 regioselectivity.⁴⁸



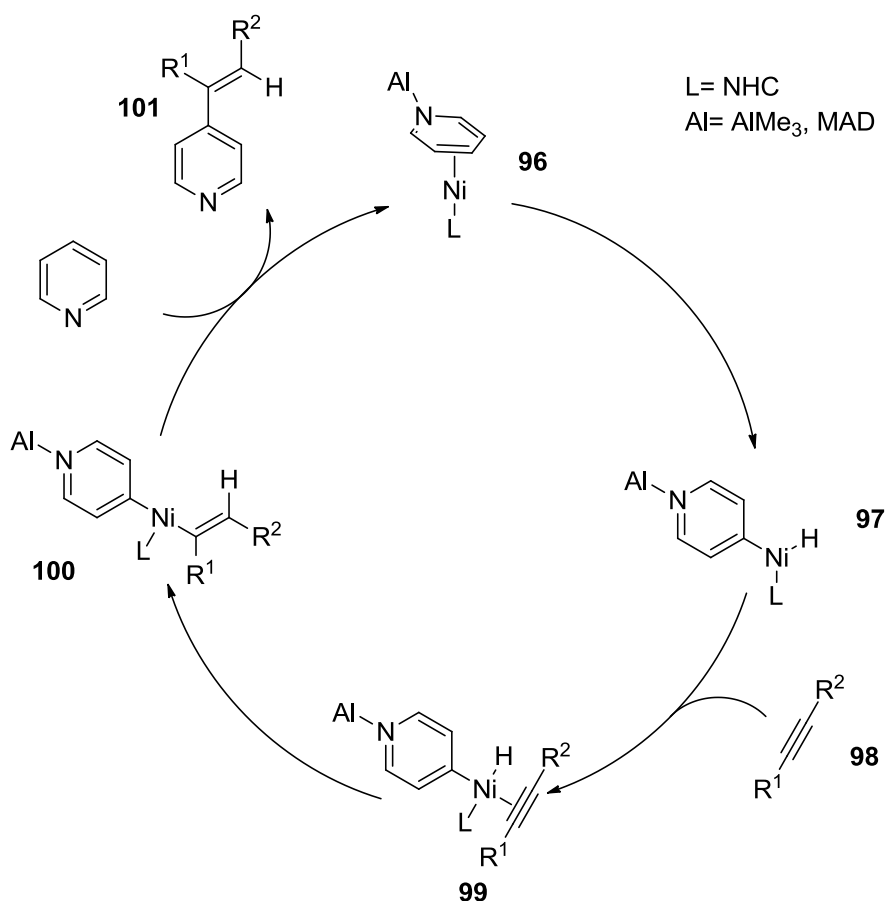
Scheme 37: C-4 selective alkenylation of pyridines catalysed by nickel [48]

This method was further developed by Nakao *et al.*⁴⁹ using the same nickel catalyst but with methyl aluminium bis(2,6-di-*tert*-butyl-4-methylphenoxide) (MAD); excellent regioselectivities were reported for the alkylation of pyridines, which were attributed to the use of the bulky aluminium Lewis acid. The steric bulk of the Lewis acid directs the metalation step exclusively to the C-4 position (Scheme 38).



Scheme 38: Nickel catalysed 4-alkylation of pyridine with use of an aluminium Lewis acid as a co-catalyst [49]

Both nickel catalysed processes proceed *via* oxidative addition of the C4-H bond of the pyridine that is coordinated to the nickel at its C3-C4 bond, followed by coordination and successive migratory insertion of the unsaturated compound into the Ni-H bond. Reductive elimination of the C4-functionalised pyridine and ligand exchange then occurs to regenerate the catalytic species (Scheme 39).⁴⁹

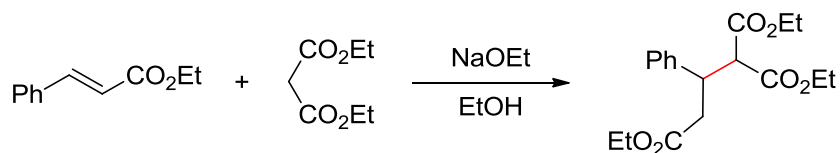


Scheme 39: Catalytic cycle for C-4 selective alkenylation of pyridines mediated by nickel/Lewis acid catalysis [49]

1.4. Conjugate addition reactions of vinylpyridines

Conjugate addition (CA) reactions or 1,4-addition reactions are classically known for the nucleophilic attack at the β -position in an α,β -unsaturated carbonyl moiety. The reaction can also take place with unsaturated systems in conjugation with electron withdrawing groups.⁵⁰

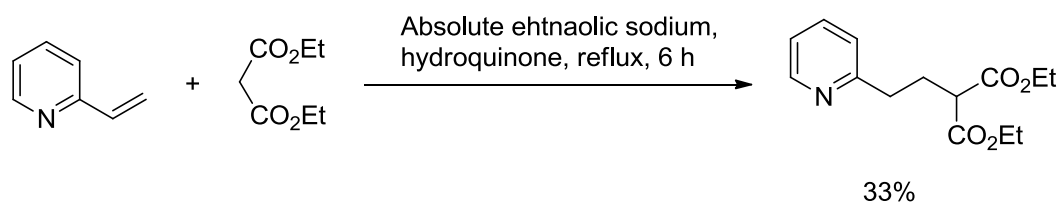
Komnenos studied the first example of a 1,4-addition involving the facile addition of the anion of diethyl malonate to ethylidene malonate.⁵¹ Seminal work in this area was carried out by Michael, who systematically investigated the reaction of stabilised anions with α,β -unsaturated systems. As a consequence of this study, it was found that diethyl malonate added across the double bond of ethyl cinnamate in the presence of sodium ethoxide to afford the substituted pentanedioic ester (Scheme 40).⁵²



Scheme 40: Addition of diethyl malonate to ethyl cinnamate: seminal work carried out by Michael in 1887 [52]

Following on from this work, Michael further demonstrated that as well as electron-deficient double bonds, triple bonds could be used as the reaction partner for carbon nucleophiles. This method of forming new carbon-carbon bonds became the reaction known today as the Michael addition. The conjugate addition reaction is now an effective tool for introducing new carbon-carbon bonds, new functionality as well as achieving ring-forming reactions.

Doering and Wiel were the first to recognise the potential for the use of vinylpyridine in conjugate addition reactions, using base-promoted conjugate addition reactions of diethylmalonate with 2- and 4-vinylpyridines (Scheme 41).⁵³ Although their investigations showed that a conjugate addition reaction is feasible with vinylpyridines, the conjugate addition product was only achieved in 33% yield.

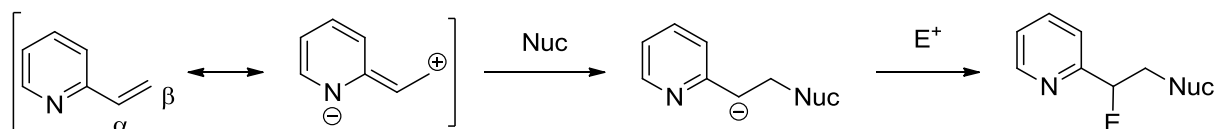


Scheme 41: Base-promoted conjugate addition reaction of 2-vinylpyridine with diethylmalonate [53]

As a result of this work, conjugate addition reactions have been demonstrated for a wide variety of vinyl-substituted-*N*-heteroaromatics, though pyridine remains the most extensively studied system. Equally, a variety of different nucleophiles have been investigated for conjugate addition to these systems.⁵⁴

Conjugate addition with vinylpyridines can be explained by the polarised nature of the vinyl system and by stabilisation of the anionic intermediates. Pyridines, being electron deficient systems, act as electron withdrawing

groups on the vinyl functionality, leading to decreased electron density at the β -carbon of the vinyl group (Scheme 42). Nucleophilic attack leads to formation of a negative charge on the vinyl- α -carbon and reaction with an electrophile (usually a liberated proton) completes the reaction.⁵⁴



Scheme 42: Conjugate addition reaction of 2-vinylpyridine with a nucleophile [67]

Due to the electron-deficiency of the α - and γ -carbons on the pyridine ring imposed by the nitrogen, only a vinyl group at these positions would be sufficiently activated towards conjugate addition ((**2**) and (**3**), Figure 6). Conjugate addition to a vinyl group at the β -position on pyridine does not occur, this can be rationalised by considering the interaction between the intermediate carbanion with the pyridine ring nitrogen. The carbanion cannot be stabilised, as the pyridine β -carbon is essentially electron rich and does not allow for accommodation of the negative charge on the nitrogen ((**1**), Figure 6).

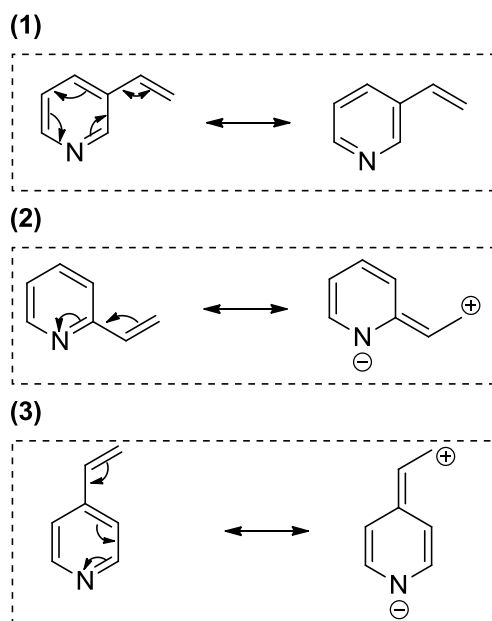
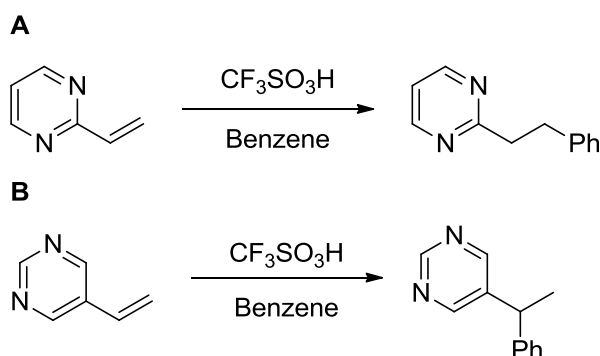


Figure 6: Polarisation of the vinyl group in vinylpyridines at the α -, β - and γ -positions in pyridine

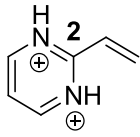
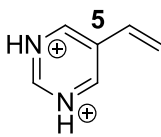
Regioelectronics can have an effect on conjugate addition to *N*-heteroaromatic vinyl-groups. In work carried out by Klumpp and co-workers,^{55, 56} they observed that 2-vinylpyrimidine will react with benzene in triflic acid to give the conjugate addition product (**A**, Scheme 43). However, when 5-vinylpyrimidine was reacted with benzene under the same conditions, the Markovnikov addition product was achieved (**B**, Scheme 43).



Scheme 43: Reactions of 2- and 5-vinylpyrimidine with benzene in triflic acid [56]

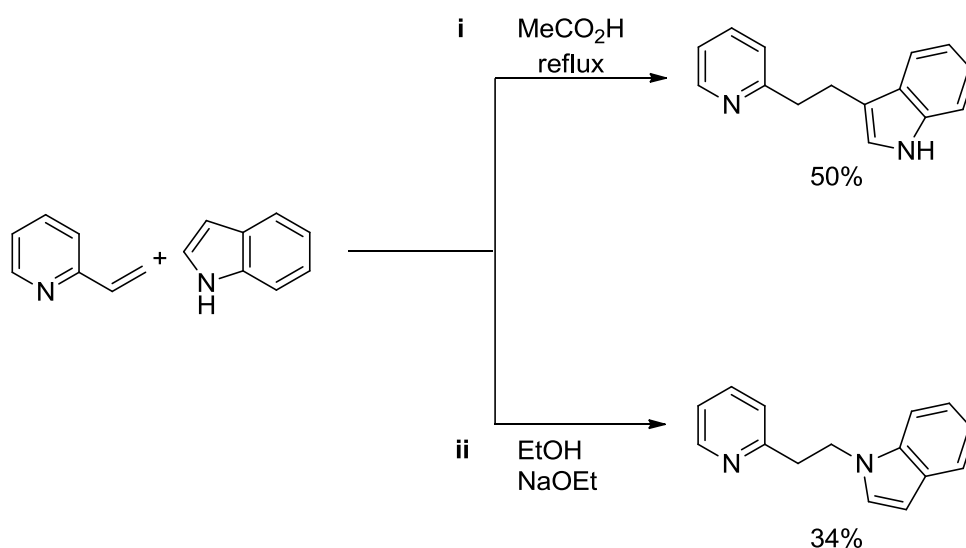
The group ran theoretical calculations on both systems and found that different natural bonding orbital (NBO)ⁱ charges were observed for the ring carbon bound to the vinyl groups in the two systems; protonation of the ring nitrogens led to cations and NBO charges of +0.7 and -0.08 for the 2- and 5-vinylpyrimidines respectively (Table 2). This indicated that the 2-vinylpyrimidine favoured the conjugate addition product due to the large positive charge on the ring carbon, whereas the 5-vinylpyrimidine favoured the Markovnikov addition product as protonation of the vinyl group gives rise to formation of a carbocation adjacent to a site of relatively high electron density.⁵⁶

Table 2 Calculated NBO charges of carbon atoms on diprotonated vinylpyrimidines [56]

		
Carbon	C2	C5
NBO Charge	+0.70	-0.08
Addition type	Conjugate	Markovnikov

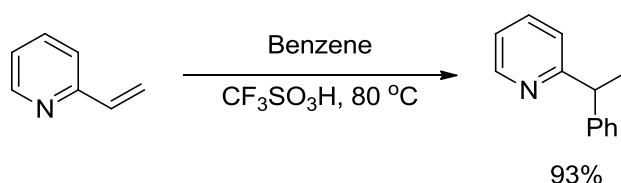
ⁱ Natural bonding orbitals are calculated bonding orbitals with maximum electron density

The outcome of conjugate addition reactions can also be a result of the conditions under which the reaction proceeds. 2-Vinylpyridine reacts with indole under acidic conditions at reflux to give the conjugate addition product resulting from nucleophilic attack by the 3-position on the indole (i, Scheme 44). When the same reaction was run under basic conditions, the product achieved was a result of the conjugate addition of the indole nitrogen to the vinyl group (ii, Scheme 44).⁵⁷



Scheme 44: Reaction of 2-vinylpyridine with indole under acidic conditions (i) and basic conditions (ii) [57]

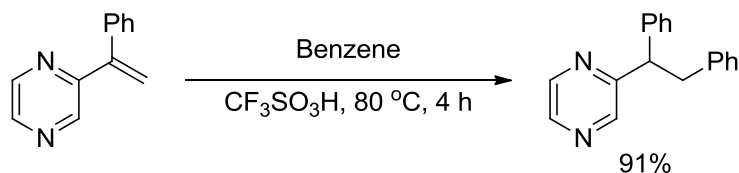
Acid catalysed conjugate addition to vinylpyridines also occur using weaker nucleophiles such as benzene. Reaction of vinylpyridines with benzene using superacids leads to the Markovnikov addition products (Scheme 45).⁵⁸



Scheme 45: Reactions of vinylpyridines with weak nucleophiles using a superacid leads to the Markovnikov addition product [58]

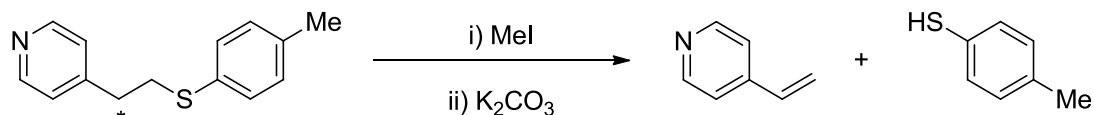
Given the previous example, it is clear that there is some competition for the reactions of vinylpyridine and its analogues to undergo conjugate versus Markovnikov addition. The tendency for these substrates to undergo

conjugate addition over Markovnikov addition is quite high.⁵⁵ Such examples include the reaction of benzene with styryl-substituted pyrazine in superacid, which proceeds exclusively *via* conjugate addition (Scheme 46).⁴⁶



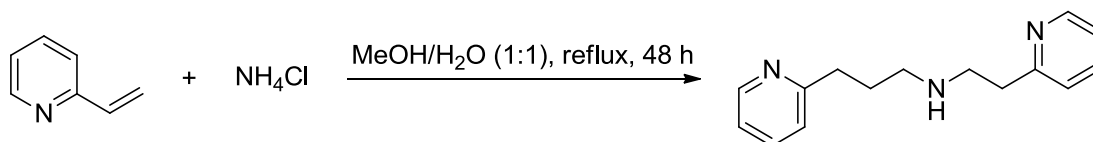
Scheme 46: Reaction of styrylpyrazine with benzene in superacid proceeds exclusively *via* conjugate addition [46]

Certain conjugate addition reactions have shown to be reversible. Katritzky *et al.*^{59, 60} used methyl thiophenol as a protecting group for vinylpyridines. They demonstrated that thioethers can be treated with a methylating agent and a base to yield the conjugate addition starting materials in an elimination reaction (Scheme 47). The nitrogen of the pyridine ring is methylated, which draws electrons away from the starred methylene carbon (Scheme 47), making it more susceptible to deprotonation by the base.



Scheme 47: Conjugate addition products can be cleaved to form the original reactants [60]

Double conjugate additions of 2-vinylpyridines to primary amines under acidic conditions have also been reported to achieve tridentate metal ligands (Scheme 48).^{61, 62}

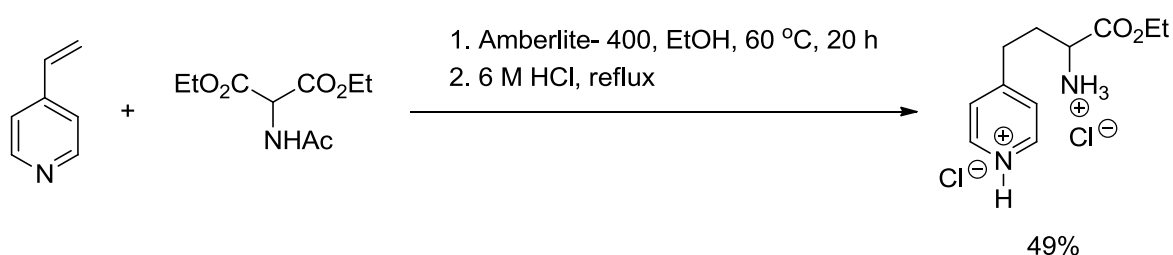


Scheme 48: Double addition of 2-vinylpyridine to primary amines[61,62]

The following subsections look into the classical conjugate addition reactions of vinylpyridines with carbon, nitrogen, oxygen and sulfur centred nucleophiles, as well as those mediated by transition metal catalysts.

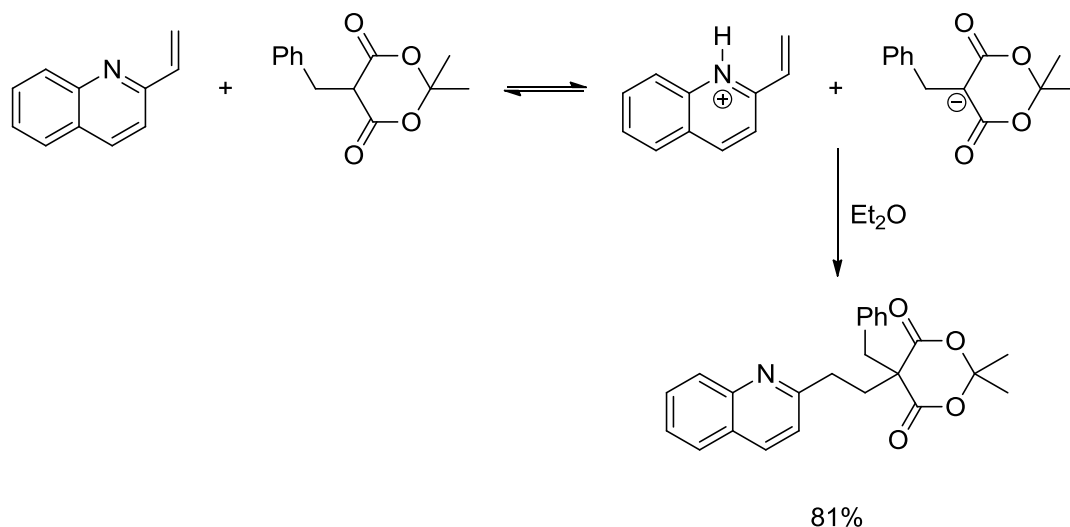
1.4.1 Conjugate addition reactions of carbon nucleophiles with vinylpyridines

Since the work carried out by Doering and Wiel, a plethora of methodologies have been applied to the conjugate addition of activated esters to vinylpyridine, the majority of which rely on the activating effect of a Brønsted acid on the pyridine ring by virtue of the pyridinium ion. For example, the reaction of diethyl acetamidomalonate with 4-vinylpyridine in the presence of a solid acid catalyst, followed by subsequent addition of HCl achieved the conjugate addition product amino acid in 49% yield (Scheme 49)



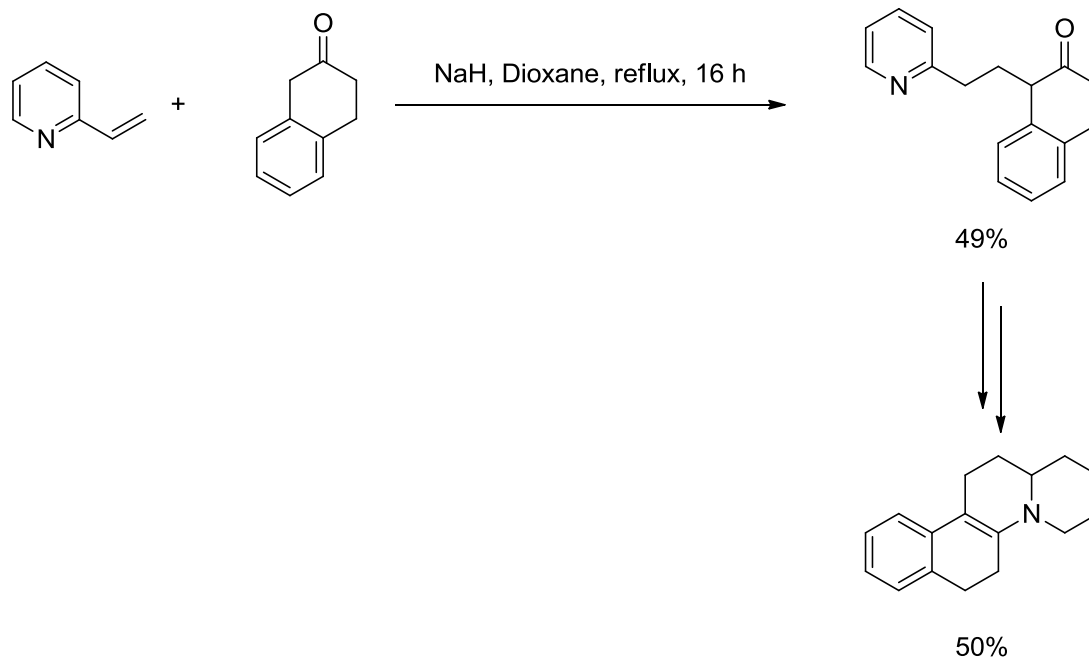
Scheme 49: Conjugate addition reaction of diethyl acetamidomalonate with 4-vinylpyridine mediated by a solid acid catalyst

In the case of more activated systems such as vinylquinolines, the use of mildly acidic nucleophiles is sufficient to activate the substrate towards conjugate addition. For example, the reaction of 2-vinylquinoline with isopropylidene esters of malonic acid (Scheme 50); the nucleophile reacts spontaneously with the vinyl group of the system, similar reactivity with these nucleophiles was observed with 2- and 4-vinylpyridines.



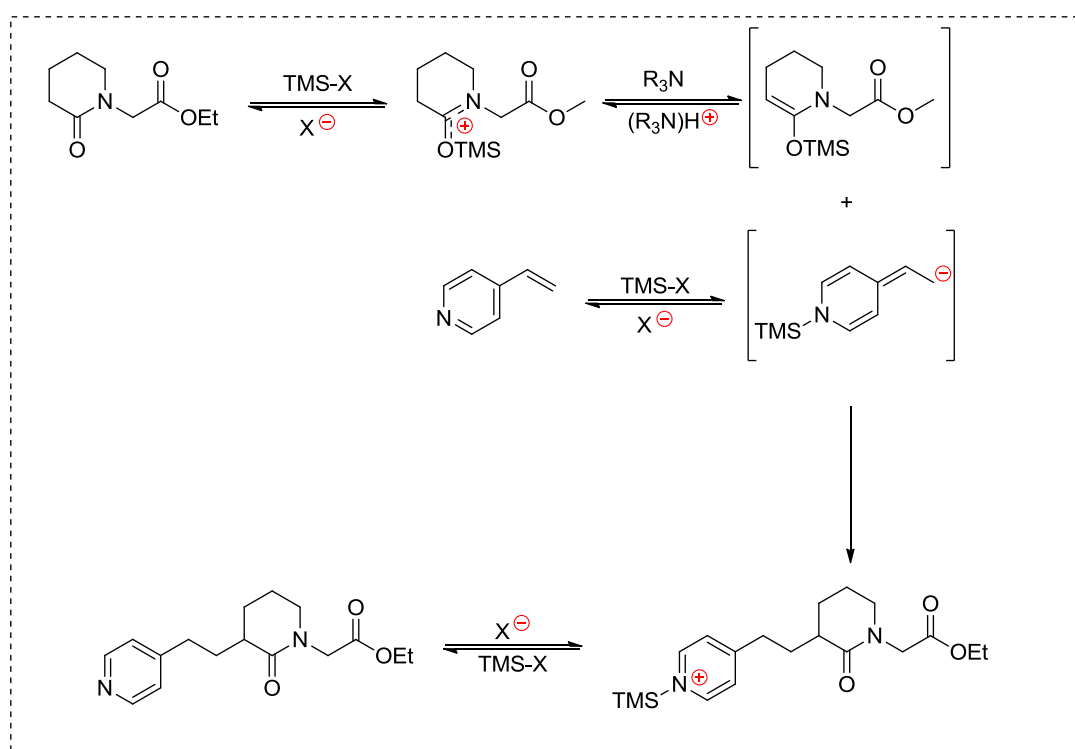
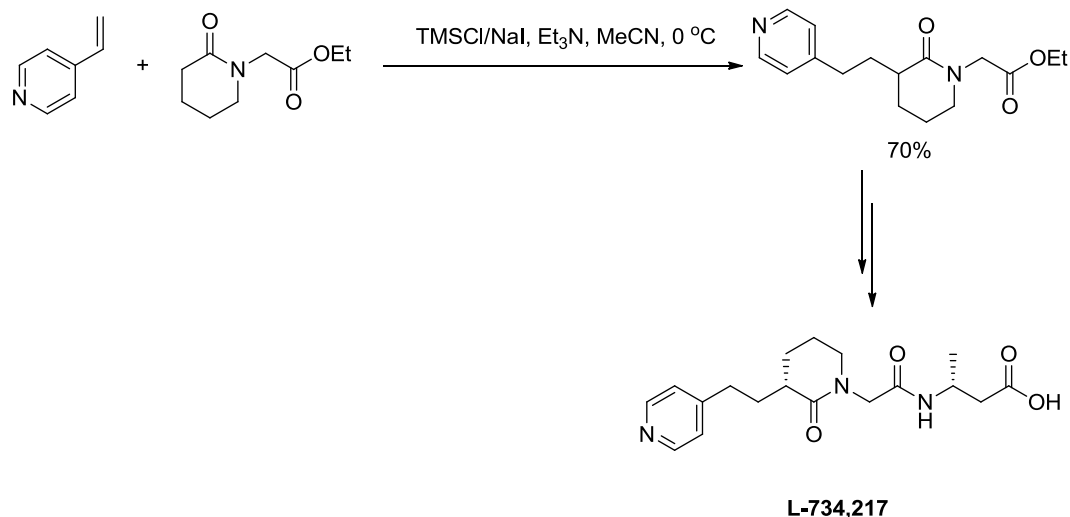
Scheme 50: Conjugate addition reaction of 2-vinylquinoline with mildly acidic nucleophile

Enolate ions and their equivalents have also been used as nucleophiles in conjugate addition reactions to vinylpyridines, one such example was used in the synthesis of an aza-steroid molecule (Scheme 51). The reaction was base-promoted to give the conjugate addition product in 49% yield, from which the final aza-steroid molecule was synthesised.⁶³



Scheme 51: The use of enolate ions as nucleophiles in a conjugate addition reaction to 2-vinylpyridine

A synthetic approach to a fibrinogen receptor antagonist (L-734,217) developed by Merck researchers, used conjugate addition of a δ -lactam to 4-vinylpyridine in a key synthetic step to the target molecule (Scheme 52).⁶⁴ The methodology proceeded in an analogous manner to the acid catalysed conjugate addition reaction of vinylpyridines. The transformation is mediated by coordination of a trimethylsilyl group to the pyridine nitrogen, activating the vinyl group towards a conjugate addition reaction with the TMS protected ethyl 2-(2-oxopiperidin-1-yl)acetate. Subsequent loss of the TMS group occurs due to the increased acidity of the reaction mixture, thus generating the final conjugate addition product (Scheme 52).

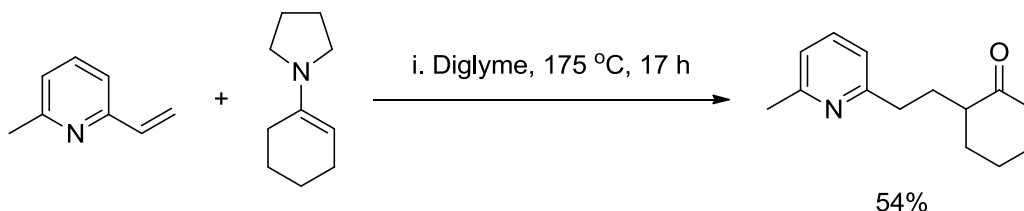


Proposed mechanism for formation of conjugate addition product

Scheme 52: Use of a conjugate addition reaction to 4-vinylpyridine in the synthetic route to the fibrinogen receptor antagonist L-734,214[64]

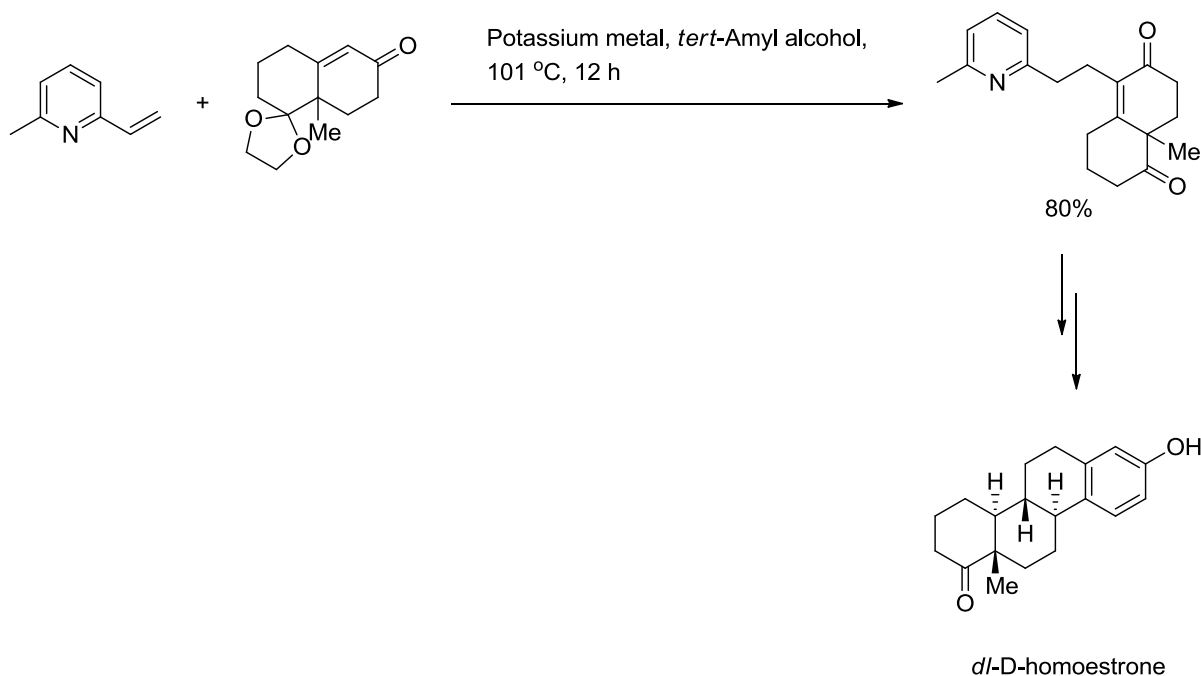
Alternative methods for conjugate addition of carbon based nucleophiles with vinylpyridines use enamines; Danishefsky *et al.*⁶⁵ carried out a conjugate addition reaction between 2-vinyl-6-picoline and 1-pyrrolidino-1-cyclohexene. The contrast in reaction conditions between reacting a vinylpyridine in the presence of an activating agent such as TMS chloride (as in the previous example) and with a more reactive nucleophile is clearly evident. Whilst the reaction with the enolate required a low reaction temperature (0 °C),

indicating that the reaction was facile and perhaps lead to over alkylation at rt, the reaction of 2-vinyl-6-picoline with the enamine in diglyme, necessitated a forcing reaction temperature of 175 °C to give the product in 54% yield (Scheme 53).



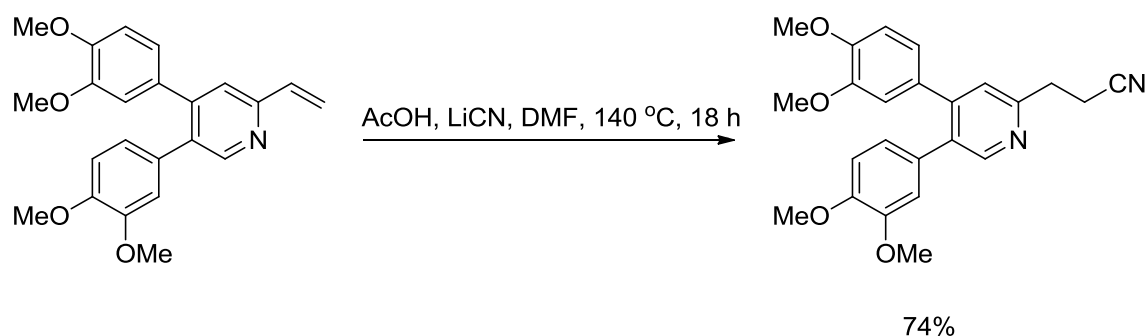
Scheme 53: Enamines used as nucleophiles in conjugate addition reactions to vinylpyridines [65]

Danishefsky and co-workers improved upon this transformation in their synthetic route to *dl*-D-homoestrone, by reacting 2-vinyl-6-picoline with a Wieland–Mischer ketone derivative, the reaction occurs *via* the potassium enolate anion of the ketone and subsequent nucleophilic attack on the vinylpyridine (Scheme 54).⁶⁶ The reaction though proceeding at a lower temperature to the enamine method, still requires the generation and use of the highly hazardous potassium 2-methyl-2-butoxide.



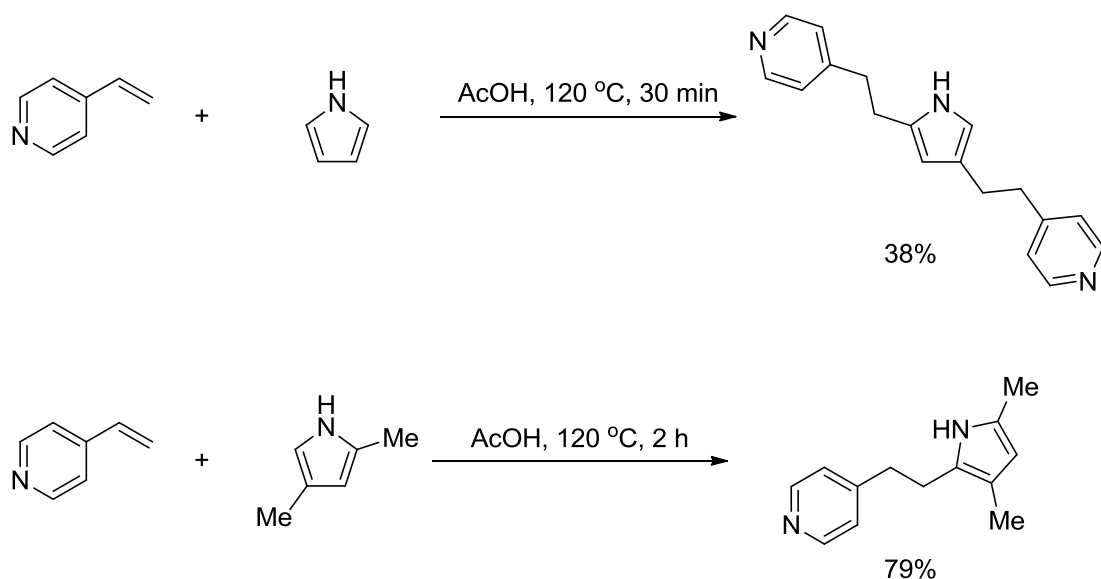
Scheme 54: Vinylogous aldol reaction step between a vinylpyridine and a Wieland-Mischer ketone analogue in the synthesis *dl*-D-homoesterone [66]

The introduction of a nitrile functionality to vinylpyridines was also been developed, in a synthetic route to phenanthroizidine alkaloids, a nitrile group was introduced to a vinylpyridine moiety through reaction with lithium cyanide (LiCN), in the presence of acetic acid, to give the conjugate addition product in good yield.⁶⁷ Overlooking the use of the highly toxic LiCN, the reaction still has drawbacks with respect to the reaction temperature and use of a reprotoxic solvent (Scheme 55). A familiar pattern is beginning to emerge, noting the use of acidic media, which aids in activating the vinylpyridine.



Scheme 55: Introduction of a nitrile group through conjugate addition reaction of vinylpyridine moiety with lithium cyanide [67]

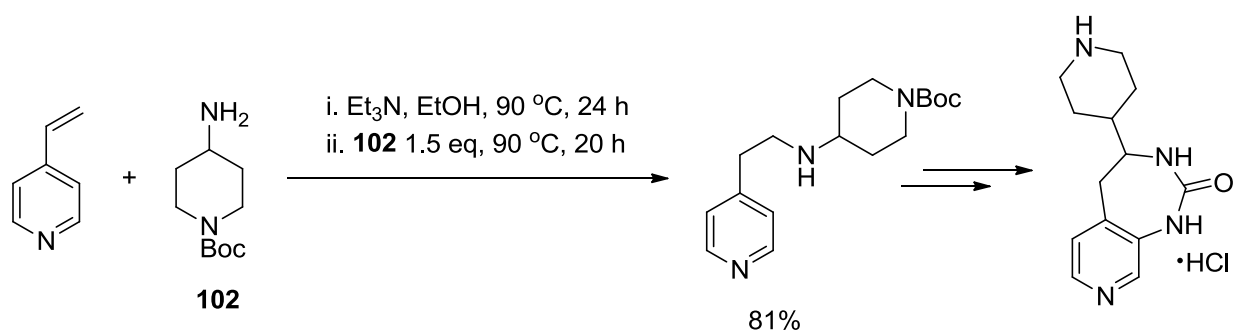
As detailed in section 1.3 (Scheme 44), indoles have been shown to act as good carbon nucleophiles in conjugate addition reactions to vinylpyridines. In a similar manner pyrroles have also been shown to undergo conjugate addition reactions with these substrates. Pyrrole reacts with vinylpyridine in an acidic medium to give the dialkylation product, in low yield (38%), blocking the 2- and 5-positions of the pyrrole allows for monoalkylation under similar conditions and give the product in good yield (Scheme 56).⁶⁸



Scheme 56: Conjugate addition reactions of 4-vinylpyridine with pyrrole and 2,5-dimethylpyrrole [68]

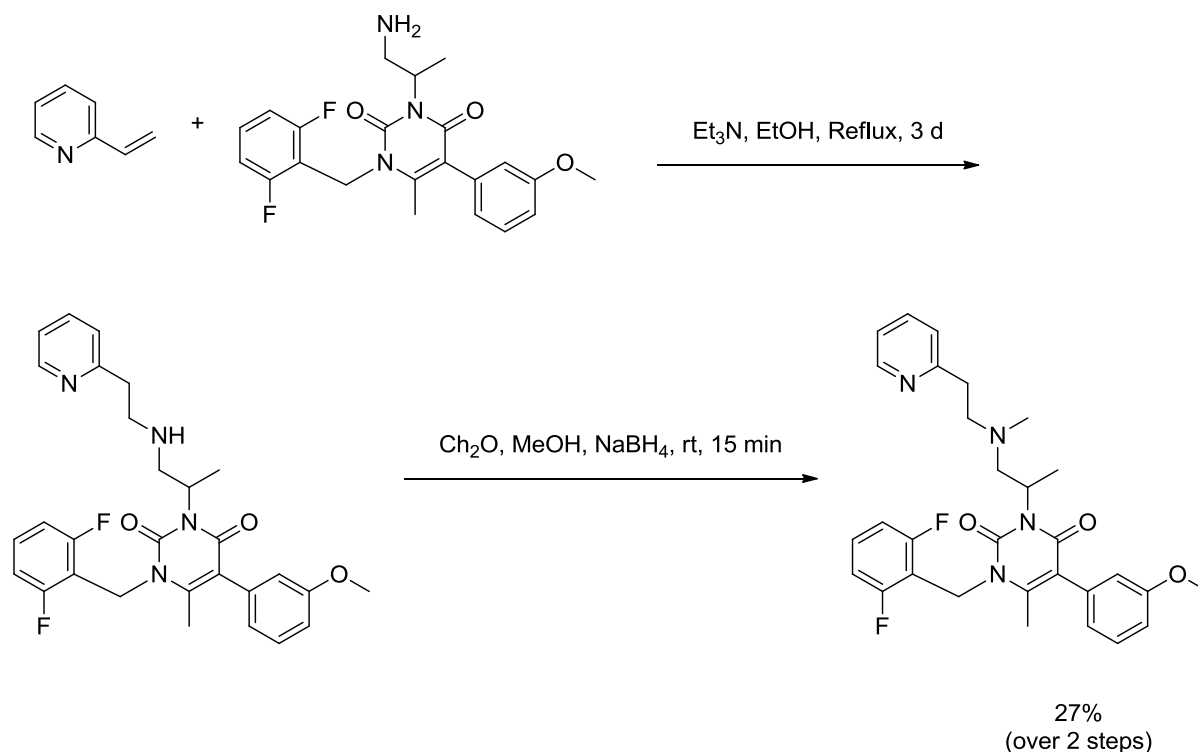
1.4.2. Conjugate addition reactions of nitrogen based nucleophiles with vinylpyridines

Conjugate addition reactions of nitrogen centred nucleophiles such as amines with vinylpyridines are well known, and have been widely used in the synthesis of biologically active molecules. Aza analogues of benzodiazapines, synthesised to improve upon the bioavailability and solubility properties of benzodiazapenes, were prepared using a conjugate addition step of a boc-protected 4-aminopiperidine to 4-vinylpyridine, to give the target intermediate in good yield (Scheme 57).⁶⁹ The reaction conditions are far less forcing than those seen for carbon-centred nucleophiles, however this methodology did require a large excess in the incoming amine nucleophile and long reaction times (44 h in total).



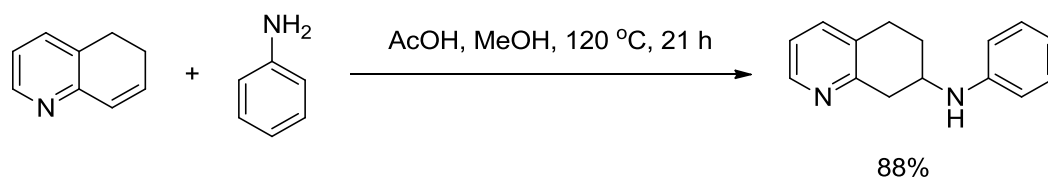
Scheme 57: Conjugate addition of primary amine to 4-vinylpyridine in a synthetic route to aza-analogues of benzodiazapenes[69]

Pyridylethylation of amine functionalities has been used in the synthetic route to the human gonadotropin-releasing hormone (GnRH) receptor antagonists.⁷⁰ The transformation also required a long reaction time (3 d) to achieve the final product in modest yield, after a subsequent methylation step (Scheme 58).



Scheme 58: Conjugate addition of amine to vinylpyridine in synthetic route for the production of human GnRH receptor antagonists [70]

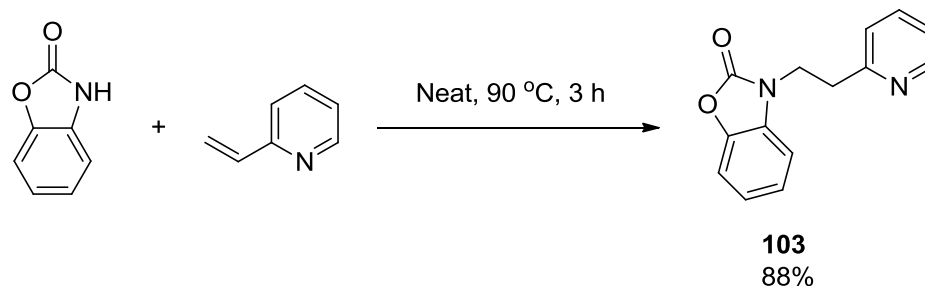
Furthermore, conjugate addition of amines to 5,6-dihydroquinoline has been used in the synthesis 7-amino-5,6,7,8-tetrahydroquinolines, a class of compounds considered as potential $\text{HT}_{1\text{A}}$ receptor ligands. Aniline was reacted with 5,6-dihydroquinoline in the presence of acetic acid in methanol at reflux to furnish the conjugate addition product in 88% yield (Scheme 59). The transformation proceeded under much shorter reaction times with a small increase in temperature ($120\text{ }^\circ\text{C}$).⁷¹



Scheme 59: Conjugate addition reaction of aniline with 5,6-dihydroquinoline [71]

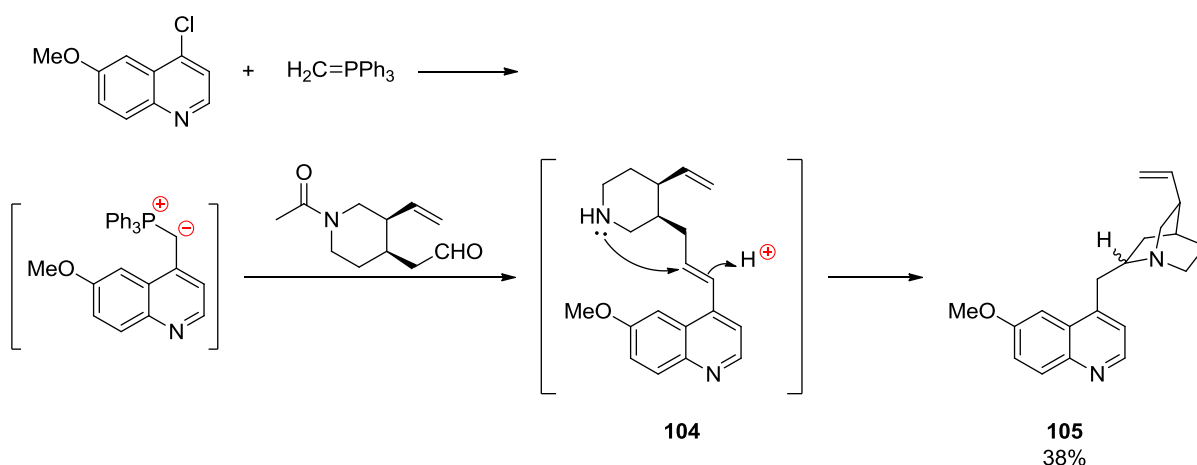
Derivatives of benzaoxazinone are recognised for their properties as analgesics and anti-inflammatories.⁵⁴ Conjugate addition reactions to vinylpyridines have been used in the preparation of such derivatives as potential drug candidates, such as compound **103** (Scheme 60), which was

prepared by reaction of 2-vinylpyridine with benzoxazolinone in the absence of a reaction solvent, at 90 °C for 3 h, to give the product in good yield (80%).⁷²



Scheme 60: Conjugate addition of benzoxazolinone to 2-vinylpyridine [72]

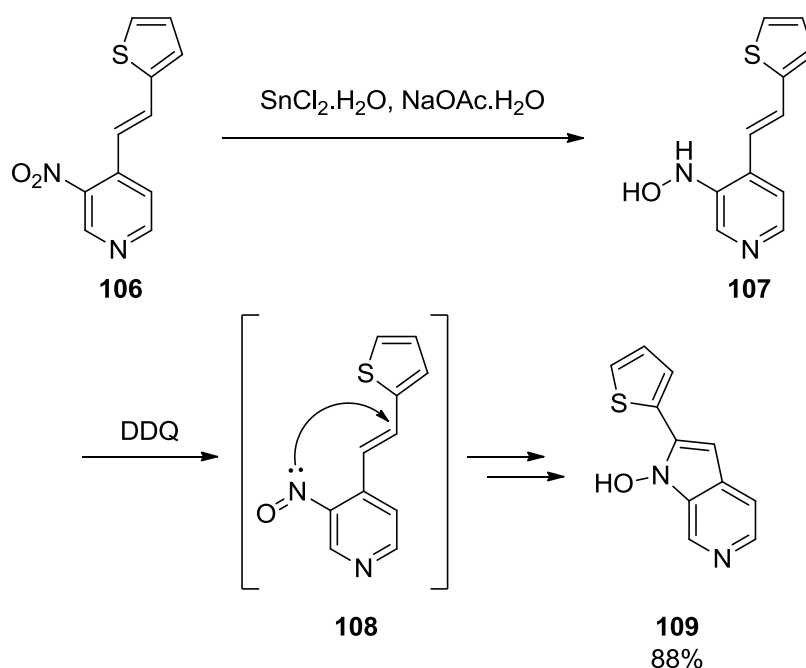
Reactions of nitrogen centred nucleophiles residing on the same molecule as a vinylogous pyridine have shown to undergo ring forming reactions. In a particular example (Scheme 61), this strategy allowed for the development of a route to Cinchona alkaloids, which included quinine.⁷³ After formation of the ylide, *N*-acetyl-3(R)-vinyl-4(S)-piperidineacetaldehyde was introduced to give **104** as an intermediate (Scheme 61), the amine functionality of **104** underwent conjugate addition with the vinyl group to give the quinuclidine product (**105**) in 38% yield.⁷³ The exact experimental procedures were not included in the publication for this methodology.



Scheme 61: Conjugate addition reaction step in the synthesis of a Cinchona alkaloid [73]

In a similar manner, these conjugate addition reactions have been used for the preparation of azaindoles; Macor *et al.*⁷⁴ demonstrated that a nitroso group can cyclise with a vinyl functionality of a pyridine *via* a reduction of the

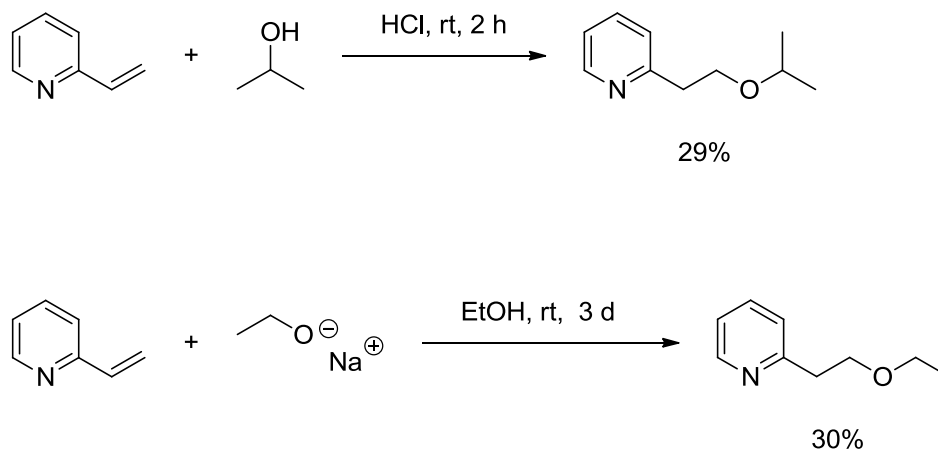
nitro group of the same pyridine. Compound **106** (Scheme 62) is selectively reduced to the hydroxylamine (**107**), subsequently reoxidised to the nitroso intermediate (**108**), which undergoes facile cyclisation with the vinyl group to give the final azaindole (**109**) in 88% yield.



Scheme 62: Intramolecular conjugate addition reaction of nitroso groups with vinylpyridine groups furnish azaindoles[74]

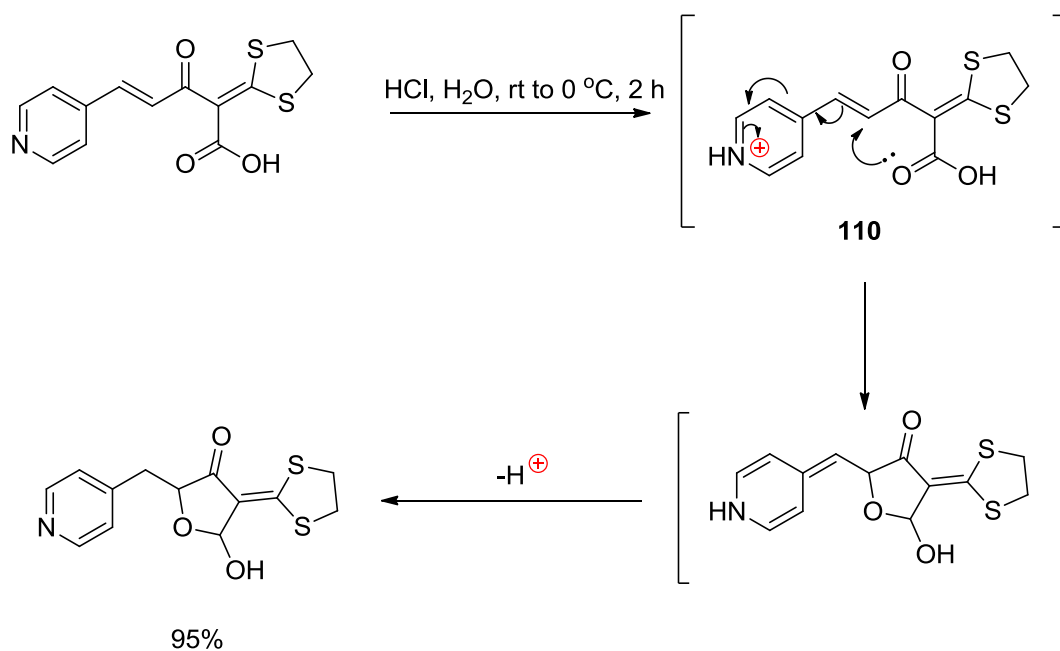
1.4.3. Conjugate addition reactions of oxygen and sulfur based nucleophiles with vinylpyridines

Alcohols and alkoxides have been shown to react with vinylpyridines, for example 2-vinylpyridine reacts with isopropyl alcohol in acidic media at room temperature to give the product in a modest yield.⁷⁵ Reaction of 2-vinylpyridine with alkoxides such as sodium ethoxide in ethanol, also yields the product in similar yields, at room temperature for 3 days.⁷⁶



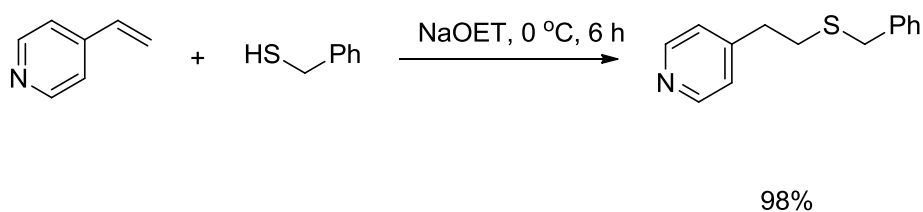
Scheme 63: Reaction of vinylpyridines with alcohols and alkoxides [75,76]

On reaction of an α -oxo ketene-*S,S*-acetal with heterocyclic acetals, Liu and co-workers found that the intermolecular oxa-pyridylethiation took place. The intermediate **110** (Scheme 64) forms as an initial aldol condensation product, through activation of the pyridine ring by virtue of the acidic reaction conditions, the compound undergoes intramolecular conjugate addition between the oxygen of the carboxylic acid and the vinyl group to yield the furan dione product in 90% yield. The reaction does not require forcing conditions and proceeds at 0 °C in 2 hours (Scheme 64).⁷⁷



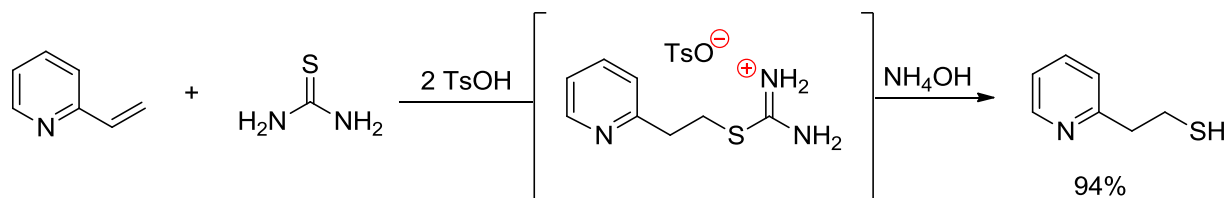
Scheme 64: Acid-promoted intramolecular oxa-pyridylethlation[77]

In a similar manner to alcohols and amines, basic and acidic media help to promote conjugate addition reactions of thiols; the reaction of benzyl mercaptan with 4-vinylpyridine proceeds in 6 h at 0 °C to give the product in near quantitative yield (Scheme 65).⁵⁴



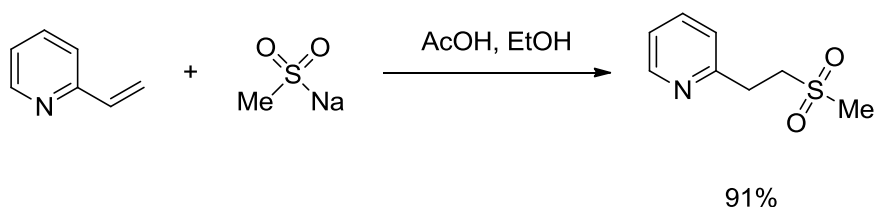
Scheme 65: Reaction of mercaptan with 4-vinylpyridine [54]

Pyridine thiols can be prepared indirectly *via* S-isothiurium salts; acid mediated reactions of 2- and 4-vinylpyridine with thiourea, followed by treating the reaction with aqueous ammonia yields the product in excellent yield (Scheme 66).⁷⁸



Scheme 66: Reaction of thiourea with 2-vinylpyridine [78]

In the preparation of alkylsulfones as possible kinase inhibitors, Schaaf *et al.*⁷⁹ developed a method for the conjugate addition of sodium methane sulfonate to vinylpyridine, the method involved running the reaction in the presence of acetic acid to give the product alkylsulfone in excellent yield. Other acids such as boric, hydrochloric, trifluoroacetic and borontrifluoric acid also gave the product in good yield.⁷⁹

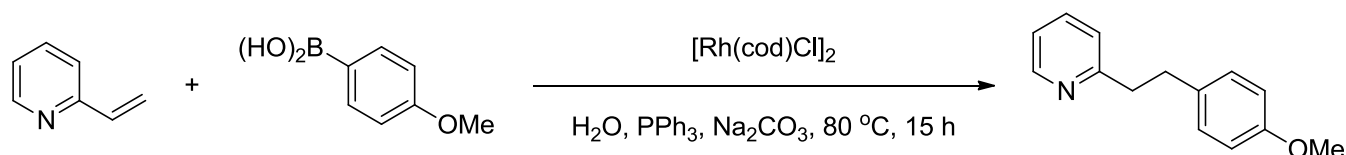


Scheme 67: Conjugate addition reaction of sodium methane sulfonate to vinylpyridine in the synthesis of alkylsulfones[79]

1.4.4. Transition metal catalysed conjugate addition reactions of vinylpyridines

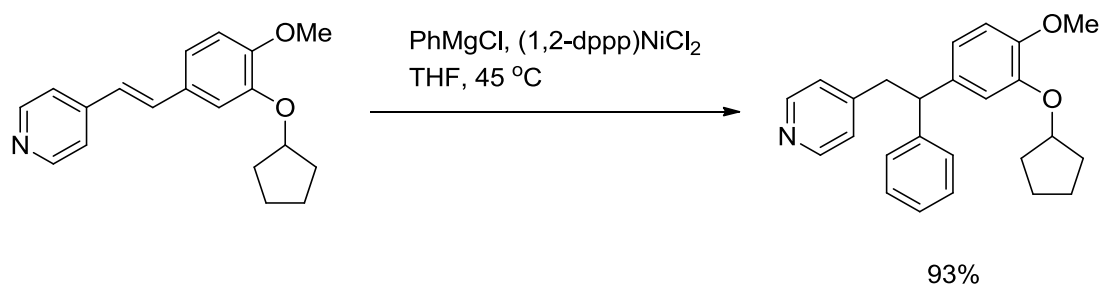
Transition metal catalysts have been found to mediate conjugate addition reactions of vinylpyridines. Though the mechanisms do not proceed in the same manner as that of classical conjugate addition reactions, there are some similarities between the two types. A rhodium catalysed addition reaction developed by Lautens *et al.*⁸⁰ using arylboronic acids in water was applied to vinylogous pyridines and yielded the conjugate addition products. The authors proposed that the mechanism proceeded *via* a conjugate

addition reaction of the arylboronic acid, followed by isomerisation of the C-bound rhodium species to the *N*-bound form, which undergoes hydrolysis in the aqueous medium thus regenerating the active catalytic species.⁸⁰ Their preliminary kinetic investigations supported this hypothesis; running this reaction in D₂O showed quantitative incorporation of deuterium at the benzylic position of the product.



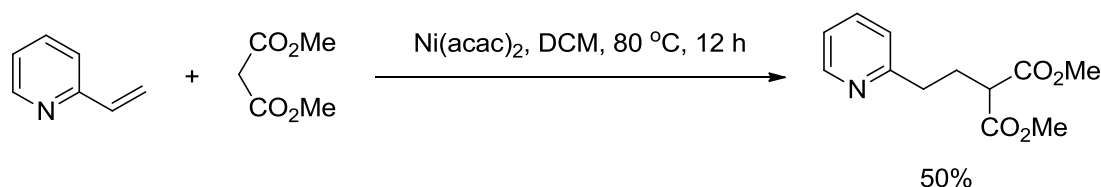
Scheme 68: Rhodium catalysed conjugate addition reaction of arylboronic acids to vinylpyridines [80]

An alternative method uses a nickel based catalyst in conjunction with an aryl Grignard to give the product in good yield. The methodology was used in a synthetic route to triarylethane-based phosphodiesterase inhibitors (antiasthmatic drugs, Scheme 69). The authors reported that no reaction proceeded in the absence of the nickel catalyst, with good conversions also reported for [Ni(acac)₂] and [NiCl₂(PPh₃)₂]. Benzyl and vinyl Grignards as well as phenyl zinc reagents were shown to successfully yield the conjugate addition products in the presence of nickel catalysts.⁸¹



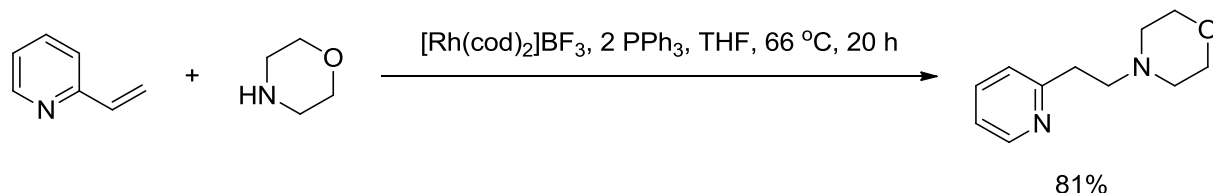
Scheme 69: Conjugate addition reaction of vinylpyridines with Grignard reagents mediated by nickel catalysts [81]

Nickel catalysts have been used in the absence of these metal alkyl reagents, such as the reaction shown in Scheme 70. Malonic esters react with 2-vinylpyridine at comparatively milder reaction conditions to classical conjugate addition reactions, however the product was achieved in modest yields.⁸²



Scheme 70: Conjugate addition reaction of malonic ester with 2-vinylpyridine mediated by a nickel catalyst [82]

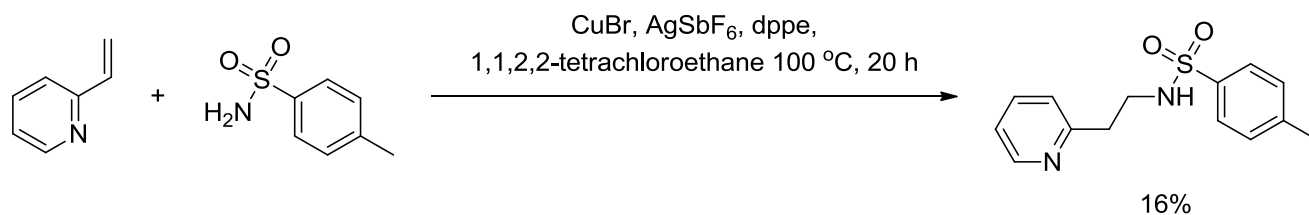
Hydroaminations catalysed by transition metal complexes have also been reported with vinylpyridines. The cationic complex shown in Scheme 71, has been demonstrated to facilitate the addition of amines to vinylpyridines by Beller *et al.*⁸³ Subject to reaction conditions, oxidative amination could also occur, giving the imine product rather than that of the conjugate addition. The mechanistic investigations carried out by the authors indicated that the system was activated by coordination of the pyridine nitrogen to the rhodium complex, which resulted in remote activation of the vinyl group. In fact, isolation of the reaction intermediate showed coordination of the rhodium to both the incoming amine and the vinylpyridine.⁸³



Scheme 71: Hydroamination reactions of vinylpyridines mediated by rhodium catalysts [83]

Hartwig and coworkers similarly used a rhodium catalyst with the DPEphos ligand in THF at 70 °C for 48 h, to mediate vinylpyridine hydroaminations to give the products in good yield and high selectivity for the anti-Markovnikov product.⁸⁴

A copper and silver catalytic system was developed for the hydramination reaction between vinylpyridines and tosylamines, which yielded the product in modest yields. Interestingly, mechanistic investigation into the transformation indicated that it was a proton transfer step that was key to mediating the conjugate addition reaction.⁸⁵



Scheme 72: Hydroamination reaction of vinylpyridines with tosylamines mediated by Brønsted acid catalysis [85]

Notably, from examining these transformations, it is clear that transition metal catalysts allow the conjugate addition product to be attained under much milder reaction conditions than those of classical conjugate addition reactions. The reaction temperatures for these examples range from 45 °C to 100 °C, with the highest temperature being reported for a reaction that would have probably proceeded with lower temperatures in the presence of a Brønsted acid alone (Scheme 72). However, the methodologies tend to be complex requiring air and moisture exclusion, complex ligand systems and other reaction auxiliaries; and the most successful catalytic system is based on the use of a rare earth metal based catalyst.

1.5. Diels–Alder cyclisation reactions of vinylpyridines

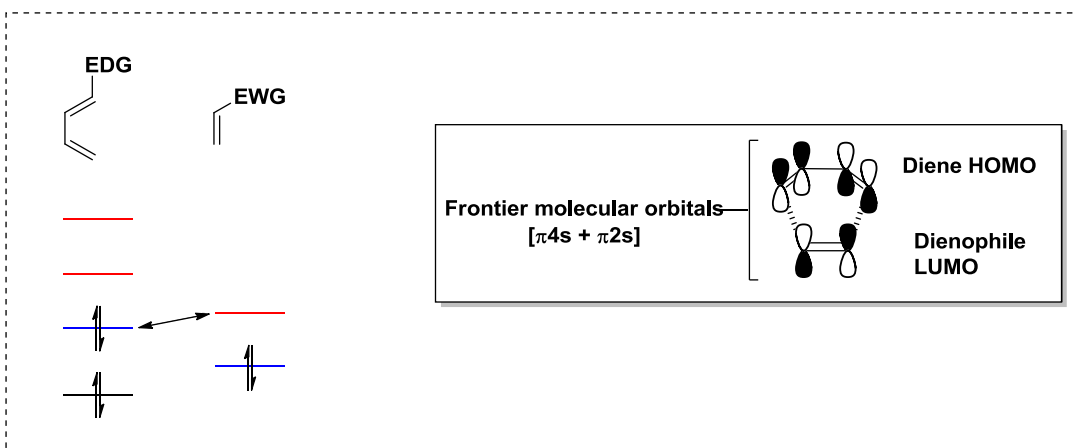
Pericyclic reactions have had a fundamental impact in the field of synthetic organic chemistry. Such reactions have been used to build a variety of complex structures with an exceptional level of control. Moreover, the theory around the subject of pericyclic reactions has allowed for a high degree of predictability for these transformations.⁷⁵ Intermolecular pericyclic reactions combine two components in a convergent synthetic sequence; they are highly atom economic and proceed with no overall change in redox state. By far the most widely used pericyclic reaction is the Diels–Alder (DA) reaction. This is a [4+2] reaction between a conjugated diene and a dienophile (usually a substituted alkene); to produce a substituted cyclohexene system.⁷⁵

In a Diels–Alder reaction two new bonds are formed simultaneously between the reactants in a [$\pi 4_s + \pi 2_s$] manner. The process kinetics are governed by the difference in energy between one reactant's HOMO and the other's

LUMO; the smaller the energy gap between the frontier orbitals the more quickly the reaction proceeds. There are several classes of DA reaction; normal, neutral or inverse electron-demand. In order to determine which reaction is operating, the reactant that contains the interacting HOMO and which contains the interacting LUMO needs to be established.⁷⁵

If the frontier orbital on the diene (π_{4s} system) is the HOMO, then the reaction is classed as a normal-electron demand DA reaction. Conversely, if it is the LUMO of the π_{4s} system that is the interacting frontier orbital, then the reaction is said to be proceeding through inverse-electron demand (Figure 7). Inverse electron-demand DA reactions arise from the nature of the functional groups on either the diene or the dienophile; electron withdrawing groups (EWG) on either reactant will lower the energy of the HOMO and LUMO whilst the opposite effect is observed for electron donating groups (EDG), Figure 7. Accordingly, inverse electron-demand DA reactions involve electron poor dienes and electron rich dienophiles.⁷⁵

Normal Electron-Demand Diels-Alder



Inverse Electron-Demand Diels-Alder

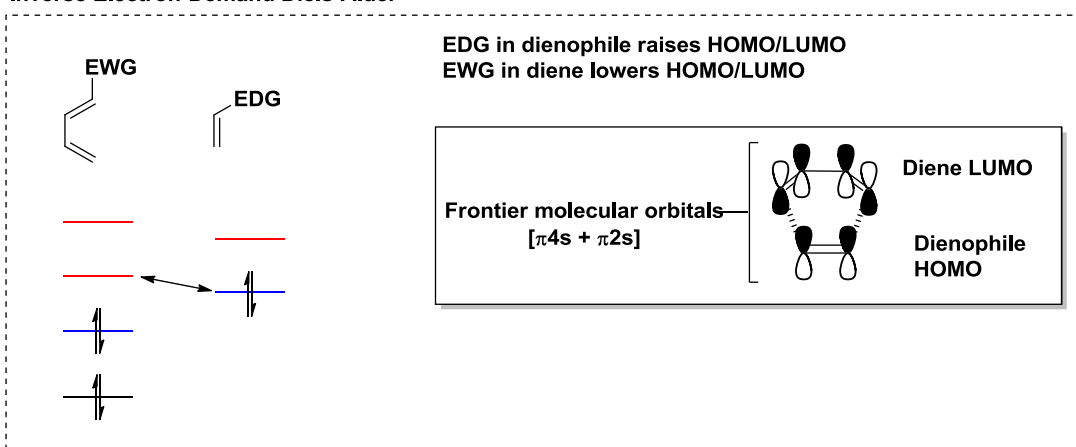
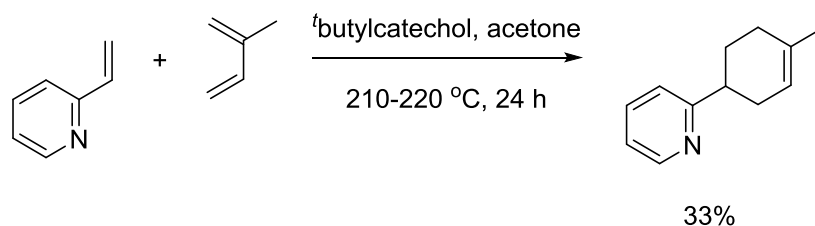


Figure 7: Frontier orbitals in diene and dienophile for normal- and inverse-electron demand Diels-Alder cyclisations [75]

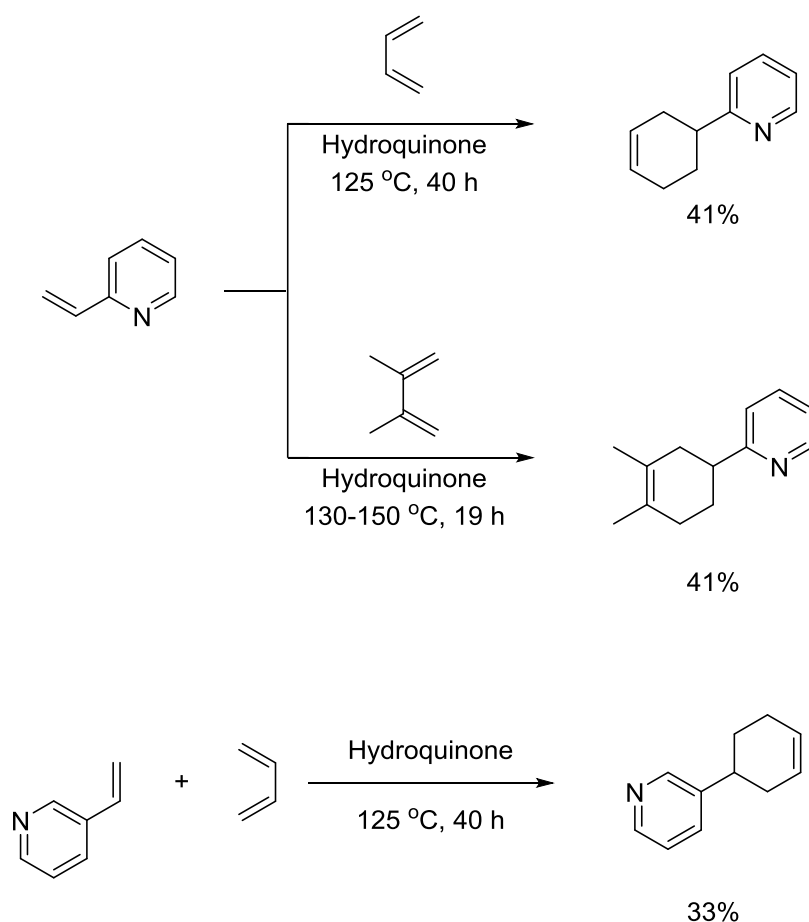
Neutral-demand DA reactions are rare as they fall into neither category of the aforementioned reactions; their reactivity is not enhanced by modifying the electronics of the DA reactants, so it is not clear which frontier orbitals are interacting.⁷⁵

The earliest example of the use of vinylpyridines in DA reactions was carried out by Meek *et al.*⁸⁶ in which 2-vinylpyridine was reacted with isoprene in the presence of *t*-butylcatechol, to give the DA product in 33% yield (Scheme 73).



Scheme 73: Diels-Alder reaction of 2-vinylpyridine with isoprene carried out by Meek *et al.*[86]

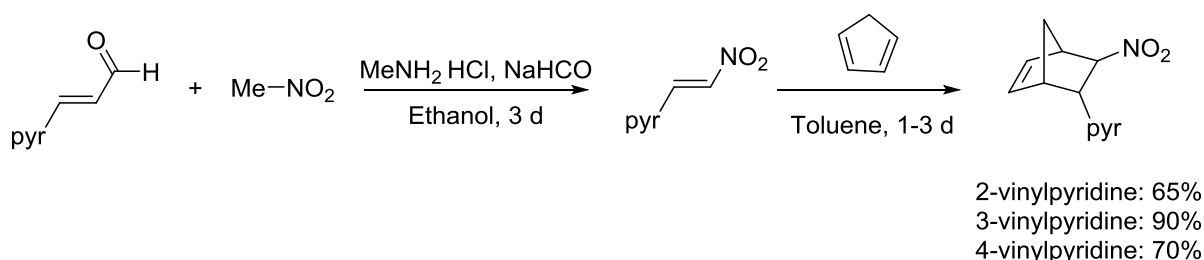
This was closely followed by a publication by Doering *et al.*,⁸⁷ who built further on his work with conjugate addition reactions of vinylpyridines (Scheme 74), through the use of hydroquinone to facilitate DA reactions of 2- and 3-vinylpyridines with butadiene and 2,3-dimethylbutadiene. The reactions yielded the DA products in modest yields of 33-47% (Scheme 74).



Scheme 74: Diels-Alder reaction of 2- and 3-vinylpyridine with butadiene and 2,3-dimethylbutadiene mediated by hydroquinone [87]

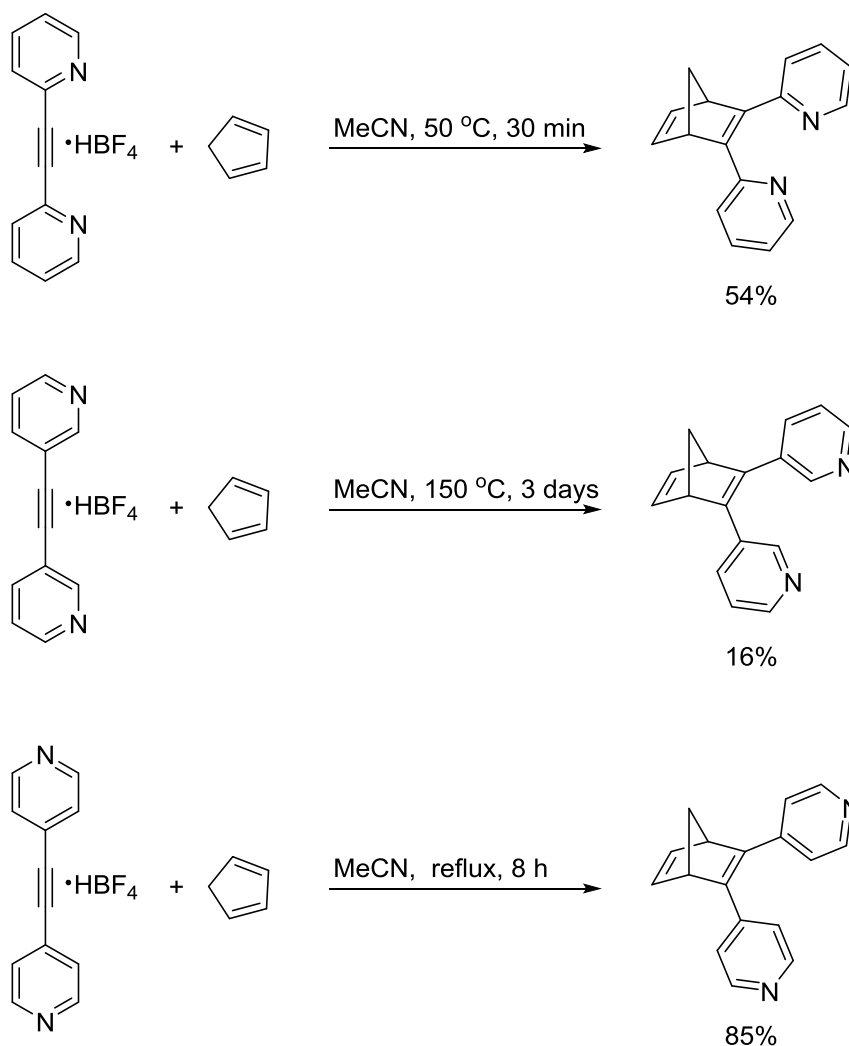
Queguiner and co-workers used the activating effect of a nitro group bound to the vinyl group of a vinylpyridine to achieve a DA reaction.⁸⁸ The methodology involves the initial synthesis of the nitrostyrene analogues,

followed by reaction of the substrates with cyclopentadiene at room temperature for 1-3 days (Scheme 75). The reverse reactivity is observed for this reaction and the 3-vinylpyridine analogue gives the highest yield of 90%; the methodology works on the direct activating effect of the nitro group on the vinyl-system.⁸⁸ The reason the 3-vinyl analogue shows highest reactivity, is again due to the electron rich nature of the β -carbon of the pyridine, allowing the vinyl group to be sufficiently polarised to react with the cyclopentadiene system.



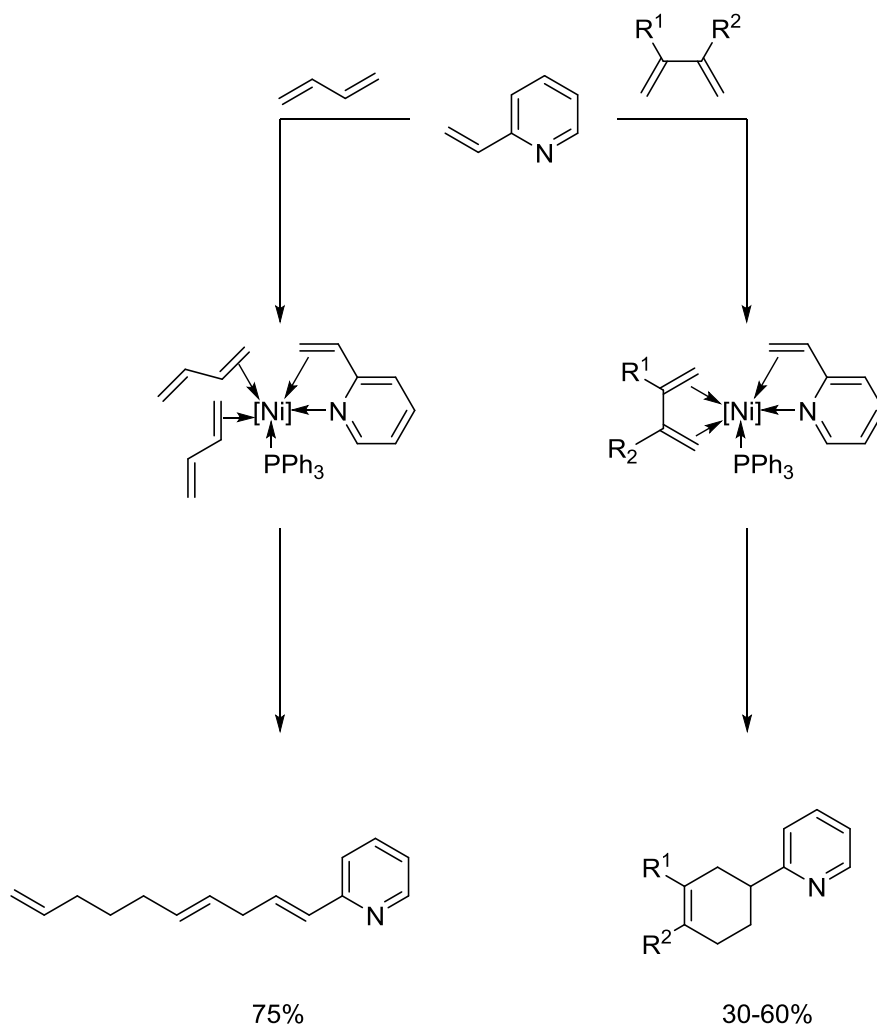
Scheme 75: Diels–Alder reaction of nitrovinylpyridines with cyclopentadiene [88]

Yamashita *et al.*⁸⁹ investigated the synthesis of dipyridylnorbornadienes by reacting the tetrafluoroborate salts of 2-, 3- and 4-dipyridylacetylenes with cyclopentadiene, yielding the 2,3-dipyridylnorbornadienes in 54, 16 and 85% yield for each of the 2-, 3- and 4-dipyridyl acetylenes (Scheme 76). Unsurprisingly, the 3-dipyridylacetylenes required the most forcing conditions, being heated to 160 °C for three days. The authors argued the reaction could not proceed without the activating effect of the tetrafluoroborate ion; the *trans*-5,6-di-4-pyridylnorbornene product was reported for the 4-dipyridylacetylene HBF_4 salt starting material, in contrast to the reaction run in the absence of the tetrafluoroborate ion which yielded the 1,2-di(4-pyridyl)ethylene.⁸⁹



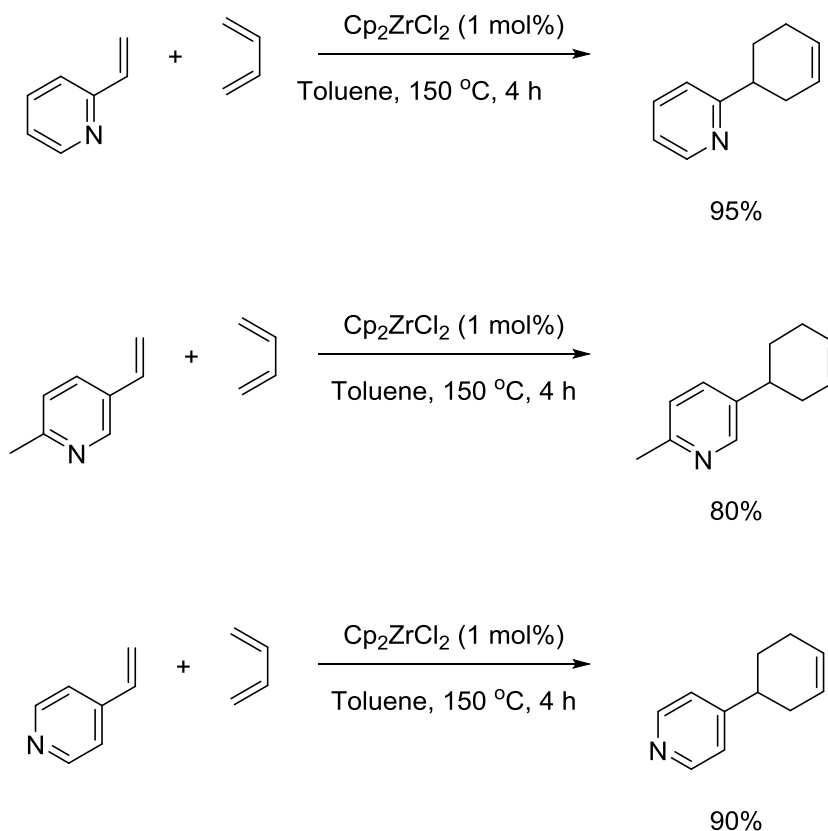
Scheme 76: Reaction of tetrafluoroborate salts of dipyriddyacetylene with cyclopentadiene [89]

Selimov *et al.*⁹⁰ investigated the reaction of 2-, 3- and 4-vinylpyridines with 1,3-dienes catalysed by a variety of transition metal complexes and found that nickel acetylacetonate complexes in conjunction with a triphenylphosphorous ligand to be the optimum catalytic pair. In the study, they found that 2,3-substituted dienes always yielded the DA reaction product, with unsubstituted dienes such as butadiene yielding the cooligomeration product. They hypothesised that the mechanism for each reaction was proceeding according to Scheme 77.



Scheme 77: Reaction of 2-vinylpyridine with butadiene and a 2,3-disubstituted diene catalyzed by a nickel/phosphine complex [90]

The study went further to investigate the use of Cp_2ZrCl_2 as a catalyst which exclusively gave the DA reaction product, through which an optimised system was developed for 2-vinylpyridine, 2-methyl-5-vinylpyridine and 4-vinylpyridine, which yielded the products in good to excellent yields (Scheme 78).



Scheme 78: Reaction of 2-, 3- and 4-vinylpyridines with butadiene mediated by a zirconium based catalyst [90]

Nelson carried out a body of work in the area of diastereoselective DA reactions mediated by a variety of transition metal complexes, which include the use of $[\text{CpRu}(\text{DMPP})_{3-n}(\text{dienophile})_n]\text{PF}_6$ catalyse for intramolecular DA reaction within the coordination sphere of the metal complex, between the incoming dienophile and the DMPP ligand. This chemistry was developed further with complexes based on iron, platinum and palladium.⁹¹⁻⁹⁶ However given that the final product is achieved as part of a metal complex, this work is not considered relevant to this discussion.

1.6. Green chemistry and outlook on pyridine functionalisation

The term “Green Chemistry” was devised by Anastas as “*chemistry that utilises (preferably renewable) raw materials, eliminates waste and solids and avoids the use of toxic and/or hazardous reagents and solvents in the manufacture and application of chemical products*”.⁹⁷ The primary principle of green chemistry is the concept of designing environmentally friendly products and processes.⁹⁸

The concept is represented by the twelve principles of green chemistry that determine that the “perfect” synthesis is one that utilises environmentally benign solvents, low hazard and low toxicity reagents, draws on efficient methodologies and avoids waste and derivatisation.⁹⁸ Such a process would also need to be energy efficient, use catalytic rather than stoichiometric reagents and use renewable raw materials.⁹⁸

Given high relevance of pyridines in synthetic chemistry; the development of greener, more efficient methods for their functionalisation is of great interest. Stoichiometric methods, either through polycondensation reactions or aromatic substitutions suffer from forcing reaction conditions, limited scope, excessive waste generation and derivatisation steps.

From the brief précis of direct pyridine ring functionalisation methods, it is evident that the area of pyridine functionalisation does not suffer from a lack of catalytic transformations, indeed there is a wide variety of standard and novel catalytic methodologies for the functionalisation of pyridine in the literature, the most prominent being the Buchwald–Hartwig reaction. This methodology boasts of excellent yields and functional group tolerance; it is not limited to a particular position on the pyridine ring and has become an important tool for the synthetic organic chemist. However, the main area that is lacking in terms of pyridine functionalisation is the use of cheap and earth abundant metals as catalysts for these transformations. Recently developed methodologies in this area still exploit the use of expensive metals and/or

require air and moisture exclusion, complex ligand systems as well as stoichiometric use of additives.

A key aspect of all the transformations covered is that the presence of the nitrogen in the pyridine ring offers an enhanced reactivity for pyridine systems relative to their benzenoid counterparts. Moreover, by virtue of binding to the nitrogen by a Brønsted or Lewis acidic species, a leaving group such as a halogen or vinyl group bound to the pyridine ring can be activated towards aromatic substitution and conjugate addition reactions respectively. Classical systems require forcing reaction conditions to proceed in good yield, transition metal catalysed processes allow for the reaction to proceed under milder conditions, however the procedures tend to be complex, requiring air and moisture exclusions and are not resource efficient, requiring ligands and other reaction auxiliaries.

When considering the development of greener alternatives for methodologies, especially for areas so well investigated such as pyridine functionalisation, considerations to applicability on a large scale need to be taken into account. There is a distinct lack in simple and efficient catalytic methodologies that operate under mild reaction conditions, avoid waste, and exploit naturally abundant resources. Building on the work carried out thus far, it is clear that there is an opportunity to develop a Lewis acid catalysed system that should allow nucleophilic aromatic substitution and classical conjugate addition reactions to proceed under such desirable conditions.

1.7. Aims

The research presented herein aims to address the deficiency in the area of pyridine functionalisation highlighted in the previous section. Specifically, the exploration of the innate chemistry of pyridines with respect to activation of the pyridine ring itself towards aromatic substitution, conjugate addition and Diels–Alder reactions through catalytic means.

Chapter 2: Lewis acids for the activation of pyridines towards nucleophilic aromatic substitution

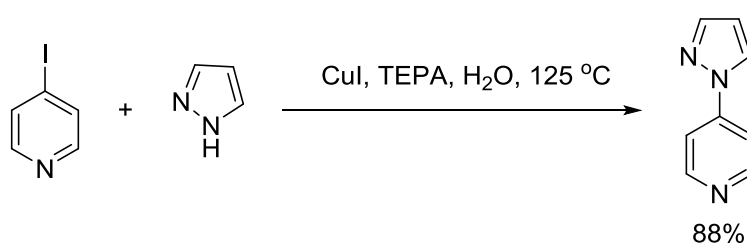
*“What's another word for
Thesaurus?”*

- Steven Wright

2. Introduction

As discussed in Chapter 1, traditional methods for the functionalisation of pyridines include nucleophilic aromatic substitutions (S_NAr) on substrates that are appropriately activated. However, the substrate scope is limited and the reactions tend to require forcing conditions. The Buchwald–Hartwig reaction using palladium-catalysed *N*-arylations has facilitated a wide range of aryl functionalisation which can be readily applied to the elaboration of halopyridines and their derivatives.⁹⁹ However, the application of these reactions can have limitations due to the high cost of the catalysts and their associated air and moisture-sensitive ligands.¹⁰⁰

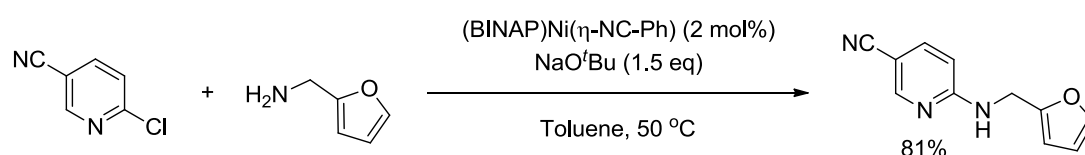
As a result, Ullmann-type reactions modified for use with copper catalysts have become the favoured alternative on an industrial scale, in the case of the most successful adaptations, ligands are still required.¹⁰¹ In some cases, the methodology may require stoichiometric amounts of the copper catalyst and base as well as high reaction temperatures. A recent noteworthy development in Ullmann-type reactions is the work by Zhang *et al.*, which involves the use of tetraethylenepentamine in conjunction with the copper catalyst in water; the coupling is reported to proceed cleanly with good yields for a broad scope of functional groups.¹⁰²



Scheme 79: Ullmann-type reaction developed by Zhang *et al.* using a copper catalyst in water [102]

Avoiding the use of precious metal catalysts in the functionalisation of pyridines and its analogues has been reported in the recent work by Hartwig *et al.* using a nickel based complex to achieve a methodology of varied scope in incoming nucleophile, and has been used on a wide variety of aryl and pyridine analogues. However this methodology still suffers from the need

for an air and moisture-free environment and use of a stoichiometric amount of base.¹⁰³

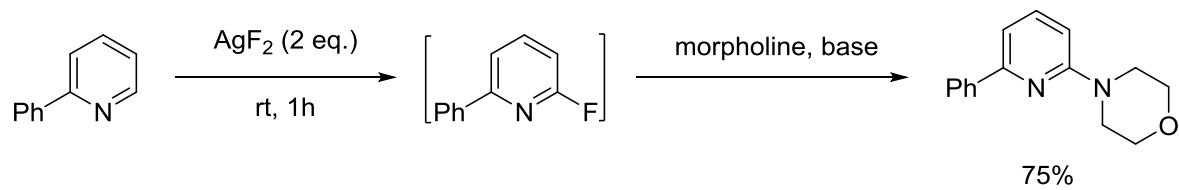


Scheme 80: Nickel catalysed amination of pyridines [103]

Methodologies that use cheap transition metals include a zinc-catalysed, base-assisted amination of chloropyrimidines,¹⁰⁴ or copper catalysed amination of heteroaryl halides which depending on the nature of the amine, may require microwave assistance.^{105, 106} The development of an efficient methodology using cheaper and more abundant metals as catalysts is a valuable approach from an environmental standpoint.

In a recent publication by Moody *et al.*, they argue that pyridine analogues which are activated enough to undergo standard S_NAr reactions such as pyrimidinyl halides are still being subjected to the more costly transformations, although greener alternatives that harness the substrate's innate reactivity could be developed and used.¹⁰⁷ In this work we wanted to consider approaches to arene coupling reactions which did not involve direct metal catalysed activation of the aryl halide bond, and specifically to apply this to the functionalisation of pyridines *via* remote catalytic activation of the halide.

With this in mind we considered pyridine *N*-oxides, which are orders of magnitude more reactive towards nucleophilic substitution than pyridines.⁷ We anticipated that the use of a Lewis acid in a similar manner to that of the oxygen in pyridine *N*-oxides would activate the pyridine ring towards S_NAr catalytically. An approach that was also recognised by the Hartwig lab in their recent publication on late stage functionalisation of pyridine through initial fluorination of the pyridine followed by aromatic substitution of the halide functionality (Scheme 81). However this methodology is not catalytic and requires the use of two equivalents of silver fluoride.¹⁰⁸



Scheme 81: C-H Fluorination of pyridines followed by nucleophilic aromatic substitution [108]

2.1. Aim

Given the reactivity of pyridines towards nucleophilic substitution as highlighted in Chapter 1, halopyridines are good substrates for nucleophilic substitution, specifically when the halogen is situated at the α - and γ -positions. Furthermore the *N*-oxide analogues of these halopyridines offer a more reactive species capable of carrying out substitution reactions under less forcing conditions. Figure 8 highlights the differences in the rates of substitution of various chlorobenzenes, chloropyridines and their equivalent *N*-oxides with methanol at 50 °C.

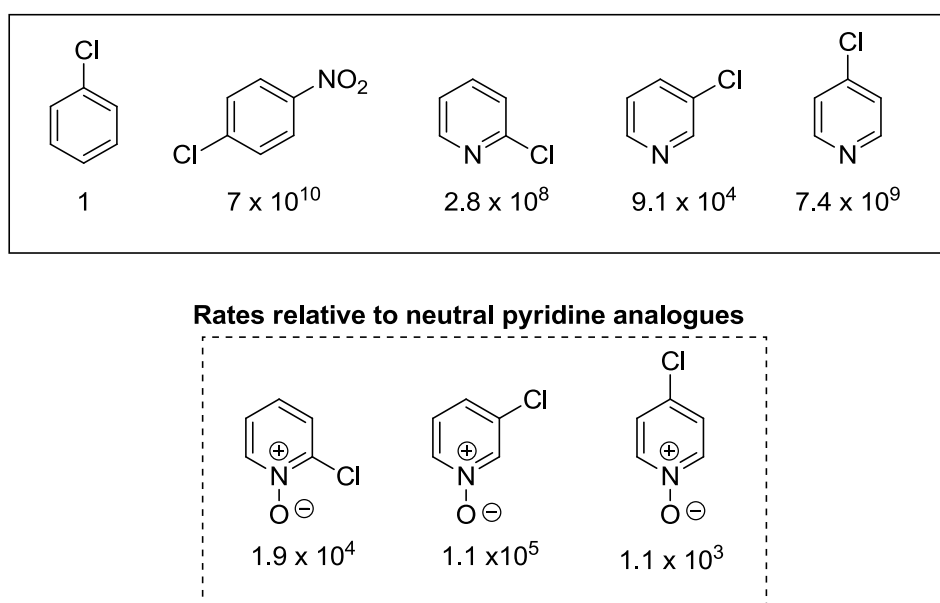
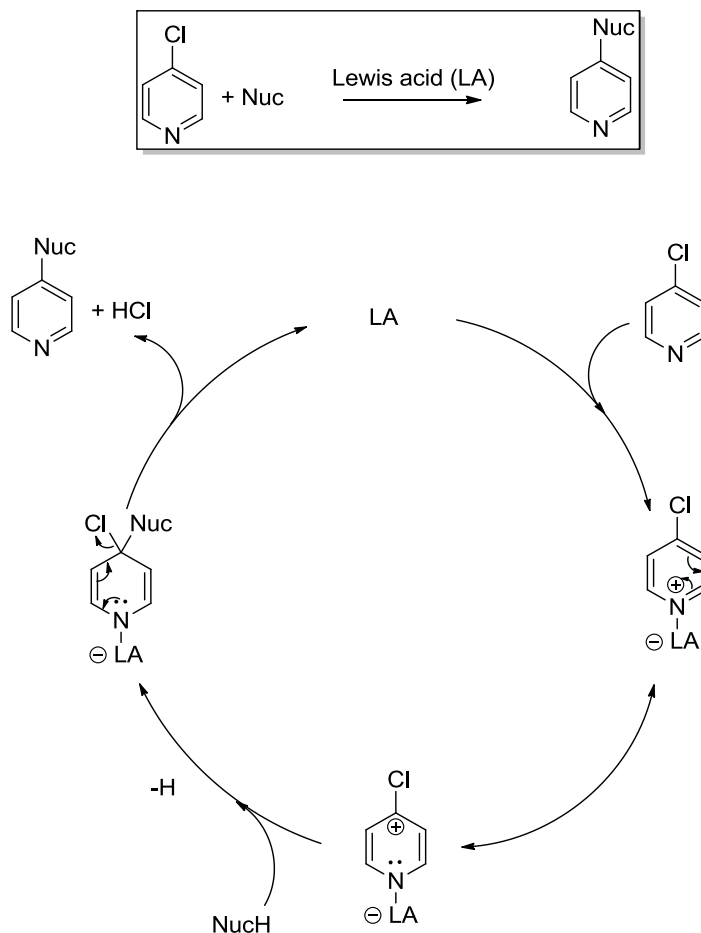


Figure 8: Rates of substitution of chloride with methoxide at 50 °C [8]; neutral pyridine rates given relative to chlorobenzene, pyridine *N*-oxide rates given relative to their neutral pyridine analogues

Indeed many synthetic routes do utilise the *N*-oxides' ease of chemistry to prepare functionalised pyridines. However, this requires the addition of two extra steps to the synthetic route; involving the oxidation of the pyridine (to the *N*-oxide) and the reduction of the functionalised *N*-oxide product. These additional steps render the process inefficient and inapplicable on large scale, especially when considering the complications involved in carrying out industrial scale oxidations.

We propose the use of metal based Lewis acids as catalysts for activating pyridine, in a manner that parallels pyridine ring activation through the

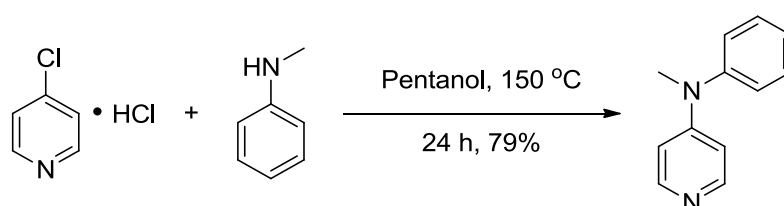
oxygen of the *N*-oxide. This methodology would benefit from *N*-oxide like reactivity whilst avoiding the associated extra oxidation/reduction steps (Scheme 82).



Scheme 82: Proposed methodology to be investigated for activating pyridines with Lewis acid based catalysis

2.2. Results and Discussion

To explore the utility of Lewis acids as catalysts for the activation of pyridines, we considered substitution reactions of pyridines that have been carried out without the use of catalysts. The reaction presented by Campos *et al.*⁶¹ for the functionalisation of pyridine to afford *N*-methyl-*N*-phenylpyridine-4-amine was carried out through a nucleophilic aromatic substitution reaction of *N*-methylaniline (NMA) with the hydrochloride salt of 4-chloropyridine (4-Cl-pyr), shown in Scheme 83.



Scheme 83: Functionalisation of pyridine to *N*-methyl-*N*-phenylpyridine-4-amine through the substitution reaction between *N*-methylaniline and 4-chloropyridine [109]

The above reaction is an S_NAr , carried out at 150 °C and is mediated through formation of the pyridinium ion from the liberated HCl. This transformation presents an ideal reaction on which our methodology can be developed. With the aim that a Lewis acid catalysed process should achieve the product in high conversion at much lower reaction temperatures and/or times.

To achieve the transformation only through the catalytic means of Lewis acids and avoid Brønsted acid catalysis of the substitution, the use of the 4-Cl-pyr freebase was favoured over the hydrochloride salt.

2.2.1. Solvent screen for control reaction

In developing catalytic processes, it is necessary to ascertain the reaction conditions under which the control does not proceed and screen for catalytic activity under these conditions. With this in mind a small solvent screen was carried out for the control reaction at 80 °C, the results of which are given in Table 3.

Table 3 Solvent screen for the control reaction of 4-chloropyridine and *N*-methylaniline at 80 °C for 24 h

The reaction scheme shows 4-chloropyridine (a pyridine ring with a chlorine atom at the 4-position) reacting with *N*-methylaniline (a benzene ring with an -NHCH₃ group). The reaction arrow is labeled 'Solvent' above and '80 °C, 24 h' below. The product is *N*-methyl-4-(pyridin-2-yl)aniline, where the chlorine atom has been replaced by the *N*-methylphenyl group.

Entry	Solvent	Conversion (%) ^[a]
1	Toluene	0
2	Acetonitrile	26
3	Isopropyl alcohol	10
4	Cyclohexane	0

^[a]Conversions were determined through analysis of the ¹H NMR spectra of the crude reaction mixture (the integral for the protons at the α-position on the pyridine in the product were compared to the integral of the protons at the α-position on the pyridine in 4-chloropyridine (dd, 8.36 ppm)).

From this small solvent screen, it is reasonable to deduce that the reaction is favoured in more polar solvents, with conversions of 26% and 10% observed for acetonitrile and isopropyl alcohol (IPA) respectively. Complete recovery of starting materials for the apolar solvents toluene and cyclohexane was observed under the same conditions.

2.2.2. Temperature screen for control reaction

In order to eliminate any background transformation when screening for a potential Lewis acid catalyst, a temperature screen for the control reaction was run and the reaction time limited to 6 h. The results of this investigation are given in Table 4.

Table 4 Temperature screen for the control reaction of 4-chloropyridine with *N*-methylaniline in acetonitrile (MeCN) for 6 h

The reaction scheme shows 4-chloropyridine (a pyridine ring with a chlorine atom at the 4-position) reacting with *N*-methylaniline (a benzene ring with an -NHCH₃ group). The reaction conditions are MeCN and 6 h. The product is *N*-methyl-4-(phenylamino)pyridine, where the chlorine atom has been replaced by the *N*-methylphenylamino group.

Entry	Temperature (°C)	Conversion (%) ^[a]
1	40	0
2	60	0
3	80	6
4	100	29

^[a] Conversions were determined through analysis of the ¹H NMR spectra of the crude reaction mixture (the integral for the protons at the α-position on the pyridine in the product were compared to the integral of the protons at the α-position on the pyridine in 4-chloropyridine (dd, 8.36 ppm)).

From Table 4 it is evident that a background reaction would begin to take place at a temperature between 60-80 °C. Consequently the Lewis acid screens would be run at 60 °C, to eliminate this possibility.

2.2.3. Lewis acid screen

When considering which Lewis acids to screen for this transformations it seemed apt to not only screen metals with a known affinity to the nitrogen of the pyridine ring (late transition metals), but to screen as wide a range of metal based Lewis acids as possible, specifically non-toxic earth abundant metals such as iron, copper and nickel. The Lewis acid screen shown in Table 5 is a selection of some of the metals screened for this reaction.

Table 5 Catalyst screen for the Lewis acid mediated reaction of 4-chloropyridine with N-methylaniline at 60 °C in MeCN for 6 h

Reaction scheme: 4-chloropyridine + N-methylaniline $\xrightarrow[\text{MeCN, 60 } ^\circ\text{C, 6 h}]{\text{Lewis acid (20 mol\%)}}$ N-methyl-4-(pyridin-2-yl)aniline

Entry	Lewis acid	Conversion (%) ^[a]
1	LiBF ₄	0
2	Li(OTf)	0
3	MgCl ₂	18
4	Al(O ⁱ Pr) ₃	6
5	AlCl ₃	40
6	KPF ₆	15
7	Sc(OTf) ₃	39
8	Ti(Cp) ₂ Cl ₂	4
9	FeSO ₄	32
10	FeCl ₂	0
11	Zr(Cp) ₂ Cl ₂	49
12	ZnI ₂	36
13	Zn(OTf) ₂	41
14	RhCl ₃	36
15 ^[b]	[Rh(nbd)Cl] ₂	52
16	Rh ₂ (OAc) ₄	0
17 ^[c]	Pd(acac) ₂	32
18	PdCl ₂	0
19	Pd ₂ (dba) ₃	0
20 ^[c]	Pd(OAc) ₂	0
21	Pd(PPh ₃) ₄	0
22	InCl ₃	22
23	Hf(Cp) ₂ Cl ₂	27
24	Control	0

^[a] Conversions were determined through analysis of the ¹H NMR spectra of the crude reaction mixture (the integral for the protons at the α-position on the pyridine in the product were compared to the integral of the protons at the α-position on the pyridine in 4-chloropyridine (dd, 8.36 ppm)). ^[b] 10 mol% in Rh; ^[c] Run for 24 h

From the results given in Table 5, it is evident that borderline or hard Lewis acids such as Mg^{2+} , Al^{3+} , Sc^{3+} , Fe^{2+} , Zr^{2+} , Zn^{2+} (Entries 3, 5, 7, 9, 11 and 13 respectively, Table 5) are the most suited for mediating this transformation. The 2,5-norbornadiene-rhodium(I) chloride dimer (Entry 15, Table 5) and palladium diacetate (Entry 17, Table 5) do not follow the same trend observed with the other metals that show good initial catalytic activity for this reaction. It is thought the formation of the product with these Lewis acids is mechanistically distinct from the transformation mediated by hard metals.

Despite the promise displayed by a number of Lewis acids in Table 5, it is evident that Lewis acids based on scandium (Entry 7), zirconium (Entry 11), zinc (Entry 13) and rhodium (Entry 15) are potentially the best at mediating this reaction, which provided the highest conversions of 49%, 39%, 41% and 52% respectively.

2.2.3.1. Zirconium and zinc based Lewis acid screen

Although Lewis acids based on rhodium and scandium would be of academic interest, the overarching aim of developing this method was to avoid the use of expensive and scarce metals, with both of these metals falling into this category. Thus zinc and zirconium, being the cheaper and more earth abundant metals, were chosen as suitable candidates for further investigation. A screen of a variety of zinc and zirconium based Lewis acids was run, the results of which are given in Table 6.

Table 6 Zinc and zirconium based Lewis acid screen for the reaction of 4-chloropyridine with *N*-methylaniline with a catalyst loading of 20 mol%, at 60 °C, in MeCN for 6 h

Reaction scheme: 4-chloropyridine + *N*-methylaniline $\xrightarrow[\text{MeCN, 60 } ^\circ\text{C, 6 h}]{\text{Lewis Acid (20 mol\%)}}$ *N*-methyl-4-phenylpyridine

Entry	Lewis acid	Conversion (%) ^[a]
1	[rac-ethylenebis(indenyl)]ZrCl ₂	27
2	Zr(ind) ₂ Cl ₂	20
3	Zr(Cp) ₂ Cl ₂	0
4	ZrCpCl ₃	51
5	ZrF ₄	43
6	ZrCl ₄	58
7	ZnI ₂	43
8	ZnBr ₂	22
9	ZnCl ₂	15
10	Zn(NO ₃) ₂ •6H ₂ O	71
11	Zn(OAc) ₂	0
12	Zn(OTf) ₂	0
13	Zr(O ^{<i>n</i>} Bu) ₄	5
14	Zr(acac) ₄	81
15	Control	0

^[a] Conversions were determined through analysis of the ¹H NMR spectra of the crude reaction mixture (the integral for the protons at the α-position on the pyridine in the product were compared to the integral of the protons at the α-position on the pyridine in 4-chloropyridine (dd, 8.36 ppm)).

From Table 6 it is evident that the most successful catalyst was zirconium(IV) acetylacetonate (Zr(acac)₄, Entry 14), giving the product in 81% conversion, closely followed by zinc nitrate (Zn(NO₃)₂•6H₂O, Entry 10) providing a conversion of 71%.

However, when one considers the relative price per mole of either Lewis acid, it is clear that the zinc nitrate is significantly cheaper than the zirconium(IV)acetylacetonate, as shown in Table 7.

Table 7 Comparison of price (£/mol) of zinc nitrate hexahydrate, zirconium(IV)acetylacetonate and Hydrochloric acid

Lewis Acid	Price (£/mol)
Zn(NO₃)₂·6H₂O	19.20 ^[a]
Zr(acac)₄	332.60 ^[a]
HCl	6.74 ^[b]

^[a]prices based on 100 g of each, purchased from Sigma-Aldrich® (correct on 27/08/2014); ^[b] price based on 500 mL (37% solution) HCl from Sigma-Aldrich® (correct on 13/02/2015)

Given the large difference in price and relatively small difference in conversion, a disadvantage that could be corrected with optimisation studies, we elected to focus our efforts on the use of zinc nitrate as the Lewis acid catalyst for the activation of 4-chloropyridine towards nucleophilic aromatic substitution.

Clearly use of a Brønsted acid such as HCl is cheaper than the use of either metal Lewis acid (Table 7), however the energy and environmental savings in using a catalytic amount of the Lewis acid at lower temperatures and better yields should outweigh the initial cost of purchase of the catalyst. Furthermore, metal catalysts can be supported or heterogenised, meaning further use out of 1 mole of the catalyst can be achieved compared to 1 mole of a Brønsted acid catalysed system.

2.2.4. Optimisation

The primary aim for optimising this reaction was to achieve the substitution product in 100% conversion. Added to this, the catalyst loading used thus far was rather high (20 mol%), and although the zinc catalyst is cheap, reducing the amount used for the reaction would benefit both the economy of the process and limit loss of the catalyst into the product during purification.

2.2.4.1. Optimising conversion

Initially the effect of temperature on the reaction was explored. Given that a 71% conversion was achieved using zinc nitrate at 60 °C, the temperature at which the reaction took effect was investigated (under catalytic conditions). The results are given in Table 8.

Table 8 Optimisation of conversion for the reaction of 4-chloropyridine with *N*-methylaniline catalysed by zinc nitrate (20 mol%) in MeCN for 6 h

Reaction scheme: 4-chloropyridine + *N*-methylaniline $\xrightarrow[\text{MeCN, 6 h}]{\text{Zn(NO}_3)_2 \cdot 6\text{H}_2\text{O (20 mol\%)}}$ *N*-methyl-4-(pyridin-2-yl)aniline

Entry	Temperature (°C)	Catalysed/control	Conversion (%) ^[a]
1	40	Catalysed	15
2	40	Control	0
3	50	Catalysed	35
4	50	Control	0
5	60	Catalysed	69
6	60	Control	0
7	70	Catalysed	85
8	70	Control	0
9	80	Catalysed	100
10	80	Control	9
11	75	Catalysed	95
12	75	Control	2
13 ^[b]	75	Catalysed	100
14 ^[b]	75	Control	2

^[a]Conversions were determined through analysis of the ¹H NMR spectra of the crude reaction mixture (the integral for the protons at the α-position on the pyridine in the product were compared to the integral of the protons at the α-position on the pyridine in 4-chloropyridine (dd, 8.36 ppm)); ^[b]Reaction run for 8 h

From the results shown in Table 8, it is clear that high conversions cannot be achieved below 60 °C (Entries 1 and 3, Table 6). Conversions improved above 60 °C, with 85% being obtained at 70 °C (control - nil) (Entry 7, Table 8) and a 100% conversion at 80 °C (Entry 9, Table 8). However the control gave 9% conversion into the product at 80 °C indicating that the 100% conversion obtained is not entirely the result of the catalytic activity of the zinc nitrate.

We investigated the reaction at 75 °C for 6 h (Entry 11, Table 8), which gave a 95% conversion, the control did show some formation of the product, although at trace levels (2%). At this point the reaction time was extended by 2 h in order to achieve a 100% conversion at this temperature. This is seen in Entry 13 (Table 8), and indeed 100% conversion was achieved in 8 h, at 75 °C, with the control reaction showing little conversion (2%).

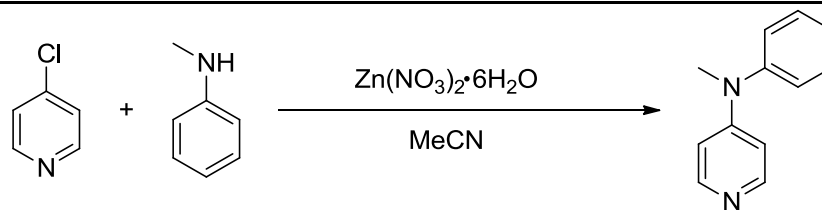
As a result, 75 °C was selected as the reaction temperature: a 100% conversion was achieved with the control showing minimal product formation.

2.2.4.2. Optimising catalyst loading

Having achieved a 100% conversion into the product under the conditions outlined in the previous section, we investigated the effect of catalyst loading on conversion under various reaction temperatures and reaction times, starting with 75 °C for 8 h, the results of which are given in Table 9.

From entries 1-3 (Table 9) it is evident that there is very little difference in the effect of catalyst loading between 5 and 15 mol%.

Table 9 Catalyst loading optimisation for the reaction of 4-chloropyridine with *N*-methylaniline catalysed by zinc nitrate, in MeCN



Entry	Temperature (°C)	Time (h)	Mol%	Conversion (%) ^[a]
1	75	8	5	83
2	75	8	10	90
3	75	8	15	93
4	75	8	0	2
5	60	18	5	82
6	60	18	10	85
7	60	18	15	86
8	60	18	0	0
9	75	18	5	100
10	75	18	10	100
11	75	18	15	100
12	75	18	0	5
13	60	24	5	83
14	60	24	0	0
15	75	24	2.5	100
16	75	24	0	6

^[a] Conversions were determined through analysis of the ¹H NMR spectra of the crude reaction mixture (the integral for the protons at the α -position on the pyridine in the product were compared to the integral of the protons at the α -position on the pyridine in 4-chloropyridine (dd, 8.36 ppm)).

The reaction time was extended to 18 h, at both 60 °C and 75 °C for various catalyst loadings with the aim of realising both a lower catalyst loading and a lower reaction temperature (Entries 5-11, Table 9). From this study we found that at 60 °C, the catalyst loading also had very little effect between 5 and 15 mol% (Entries 5-7, Table 9). Similarly, carrying out the reaction at 75 °C also demonstrated little effect when increasing the catalyst loading from 5 to

15 mol%, with all three catalyst loadings giving quantitative conversion into the product (Entries 9-11, Table 9).

We hypothesised that an extension of the reaction time to 24 h using 5 mol% catalyst loading at 60 °C could yield the desired product in 100% conversion (Entry 13, Table 9). A further investigation was carried out by increasing the reaction time to 24 h and lowering the catalyst loading to 2.5 mol% at 75 °C (Entry 15, Table 9), with a view that the methodology could either be carried out at a lower temperature of 60 °C and a catalyst loading of 5 mol%, or to retain the reaction temperature at 75 °C with a lower catalyst loading of 2.5 mol%.

As can be seen from Entry 13 (Table 9), despite the increase in time the conversion did not reach 100% for the reaction at 60 °C with a 5 mol% catalyst loading. However, the decrease in catalyst loading to 2.5 mol% for the reaction at 75 °C coupled with the extension in reaction time did yield the product in 100% conversion, as shown in Entry 15 (Table 9).

As a result of these investigations, the optimal reaction conditions are as follows: acetonitrile, at 75 °C, for 24 h using only 2.5 mol% zinc nitrate.

2.2.5. Reaction kinetics

Initially we sought to determine the rate law of our reaction to confirm our hypothesis that the zinc was indeed activating the pyridine ring towards nucleophilic substitution. We elected to use the initial rates method to determine the rate law of the reaction, by investigating the reaction order of the reactants up to and including the rate limiting step.

The rate law for a given reaction has the form given in Equation 1:

$$\text{Rate} = k [A]^a [B]^b [C]^c$$

Equation 1

Substituting in the reagents for the reaction of 4-Cl-pyr with NMA, gives the rate law as follows:

$$\text{Rate} = k [N\text{-methylaniline}]^a [4\text{-chloropyridine}]^b [\text{zinc nitrate}]^c$$

Equation 2

Where k is the overall rate constant for the reaction, at a specific temperature.

The initial rates method involves measuring the initial rate of a series of reactions in which the initial concentration of one reactant is varied whilst the concentration of all other reactants is kept constant. The initial rate of the reaction can be calculated by plotting the conversion to the product versus elapsed reaction time. The rate is determined by measuring the gradient of the graph produced.

Using 4-Cl-pyr as the variable reagent; and keeping the initial concentrations of NMA and zinc nitrate constant, Equation 2 can be simplified thus:

$$\begin{aligned} \text{Rate} &= k [N\text{-methylaniline}]^a [4\text{-chloropyridine}]^b [\text{zinc nitrate}]^c \\ &= k_{\text{obs}} [4\text{-chloropyridine}]^a \end{aligned}$$

Equation 3

To determine the order of the reaction with respect to pyridine, taking the natural log of Equation 3 gives:

$$\ln(\text{Rate}) = \ln k_{\text{obs}} + a [\text{4-chloropyridine}]$$

Equation 4

Once the rates at the various concentrations have been determined, their natural logs can be plotted versus the natural log of the concentrations, to give a straight line plot, the gradient of which would give “a” (Equation 4), which is the order of the reaction with respect to 4-Cl-pyr. The method is thus repeated for NMA (4-Cl-pyr and zinc nitrate concentrations are kept constant) and zinc nitrate (4-Cl-pyr and NMA concentrations are kept constant).

2.2.5.1. Reaction order with respect to 4-chloropyridine

A series of reactions outlined in Table 10 was run for 4 hours and monitored through ^1H NMR spectroscopy at 10 minute intervals. The results for which are shown in Figure 9.

Table 10 Initial rate experiments varying initial 4-chloropyridine concentration

Entry	Temp. (°C)	[4-Cl-pyr] (mmol)	[NMA] (mmol)	[zinc nitrate] (mmol)
1	75	0.5	1	0.025
2	75	0.7	1	0.025
3	75	0.9	1	0.025
4	75	1.1	1	0.025

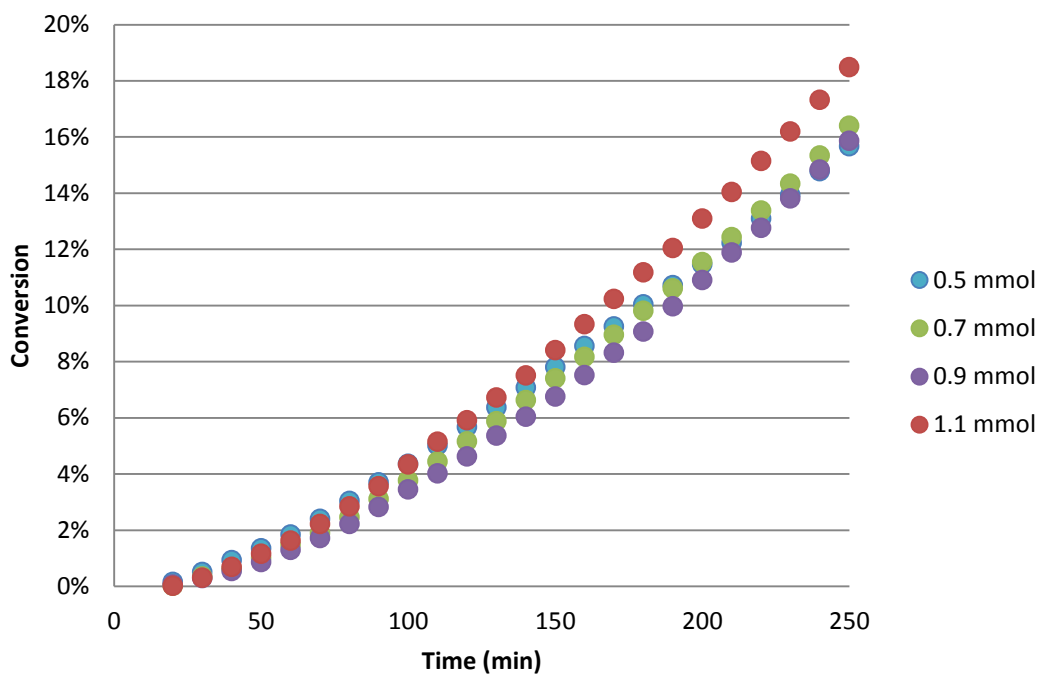


Figure 9: Conversion into product versus time (min) for various initial concentrations of 4-chloropyridine over 250 minutes

The conversions over the first 100 minutes were selected to measure the initial rate of the various reactions, for which the gradients (and therefore the reaction rates) were measured (Figure 10).

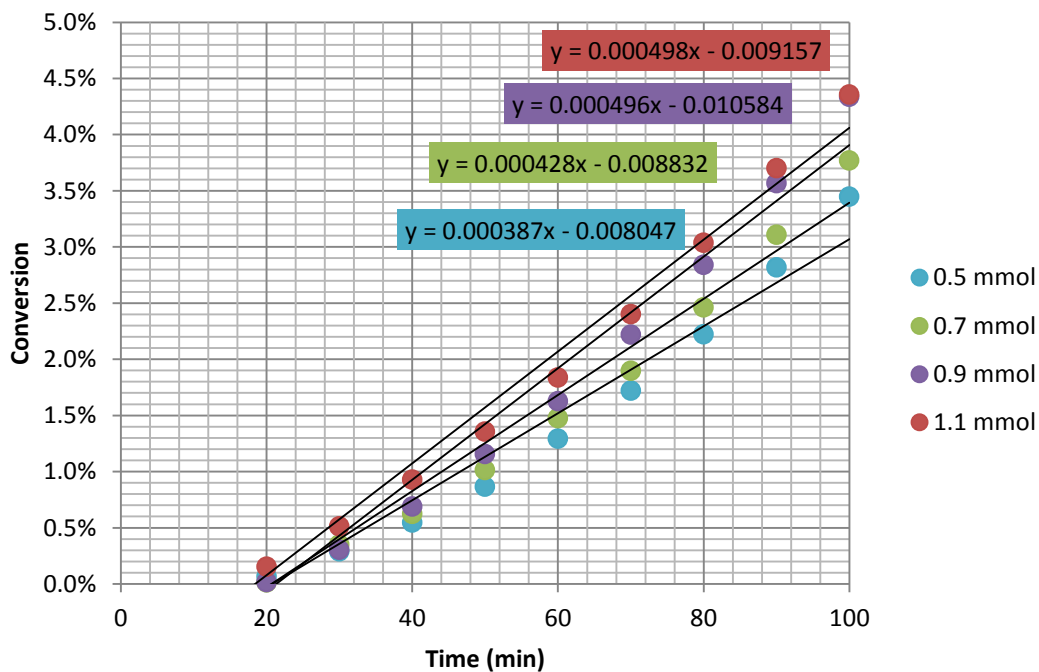


Figure 10: Conversion into product versus time (min) for various concentrations of 4-chloropyridine – initial rates shown in coloured boxes as the gradient of each trend line

The natural logs of the rates and their respective concentrations were calculated and plotted against each other as shown in Figure 11.

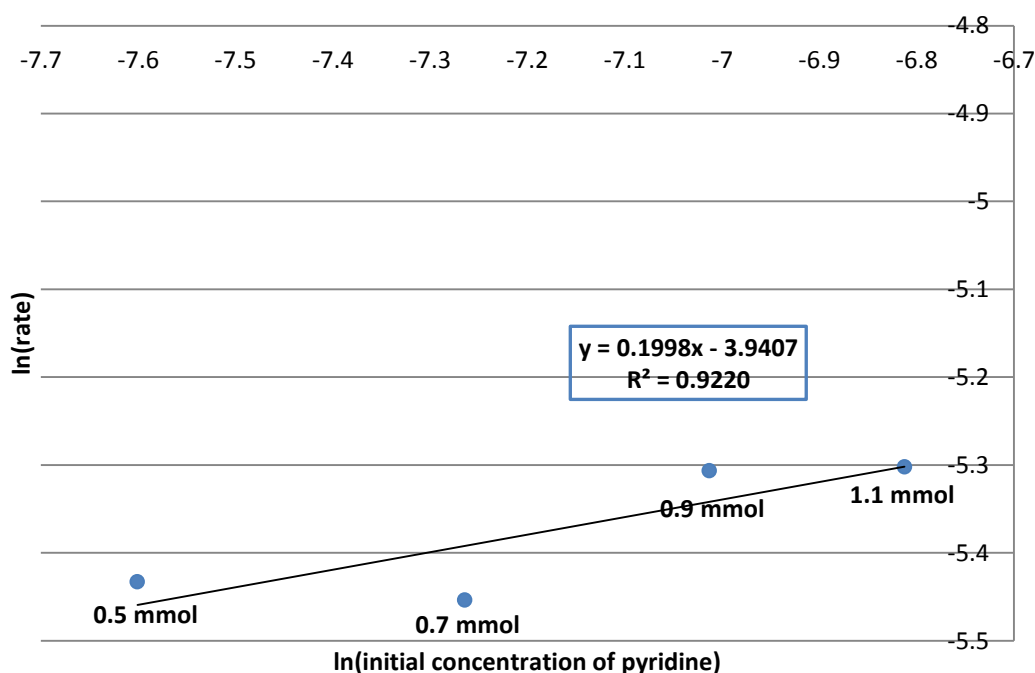


Figure 11: Plot of $\ln(\text{rate})$ vs $\ln(\text{concentration})$ for various initial concentrations of 4-chloropyridine based on the formation of aromatic substitution product

The gradient for the graph shown in Figure 11, is 0.19 (0.2), thus the reaction order with respect to 4-Cl-pyr is 0.2. However, given the margin of error that could be introduced when measuring out milligram quantities, and the R^2 value (measure of how well the line of best fit follows the trend, best fit is where $R^2=1$); a more apt description of the order of pyridine is pseudo-zero order reaction kinetics with respect to the rate determining step. The reaction order of all the reactants will be discussed in section **2.2.5.4**.

2.2.5.2. Reaction order with respect to *N*-methylaniline

A series of reactions outlined in Table 11 was run for 4 hours and monitored through ^1H NMR spectroscopy at 10 minute intervals. The results for which are shown in Figure 12.

Table 11 Initial rates experiments varying initial *N*-methylaniline concentration

Entry	Temp. ($^{\circ}\text{C}$)	[pyridine] (mmol)	[aniline] (mmol)	[zinc nitrate] (mmol)
1	75	1	0.5	0.025
2	75	1	0.7	0.025
3	75	1	0.9	0.025
4	75	1	1.1	0.025

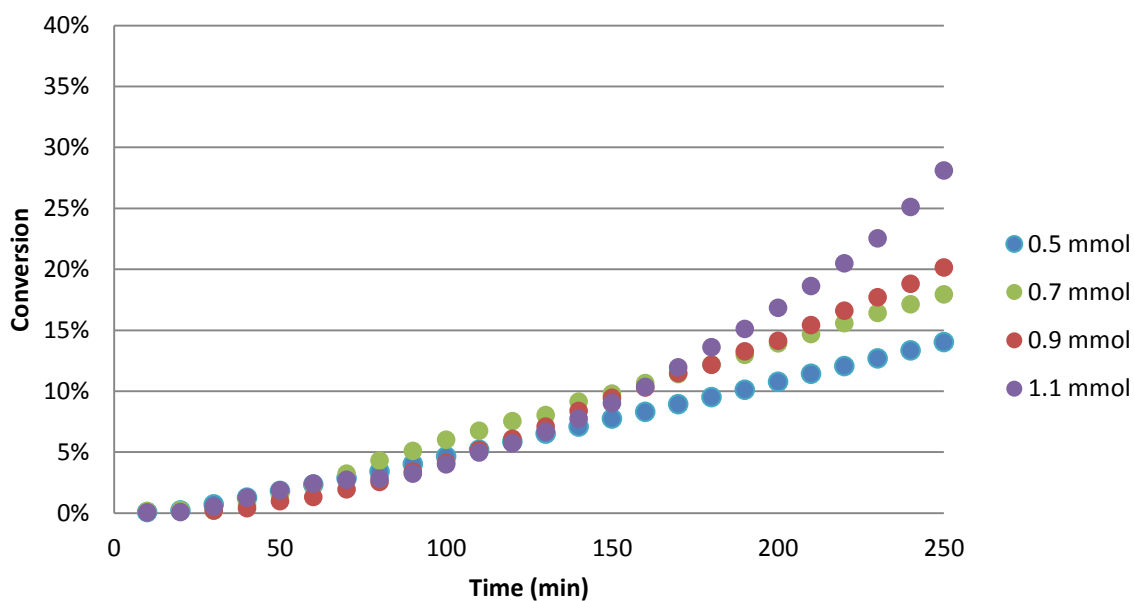


Figure 12: Conversion into product versus time (min) for various initial concentrations of *N*-methylaniline over 250 minutes

The conversions over the first 70 minutes were chosen to measure the initial rate of the various reactions, for which the gradients were calculated (Figure 13).

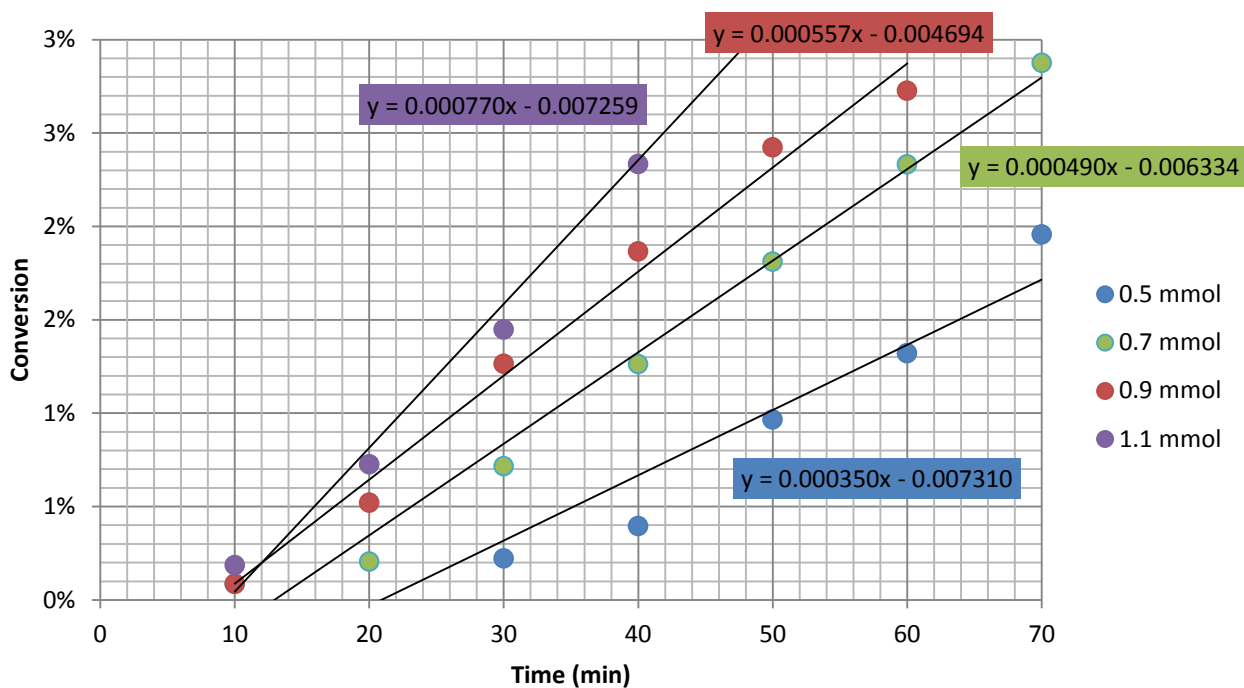


Figure 13: Conversion into product versus time (min) for various concentrations of *N*-methylaniline – initial rates shown in coloured boxes as the gradient of each trend line

The natural logs of the rates and their respective concentrations were calculated and plotted against each other as shown in Figure 14.

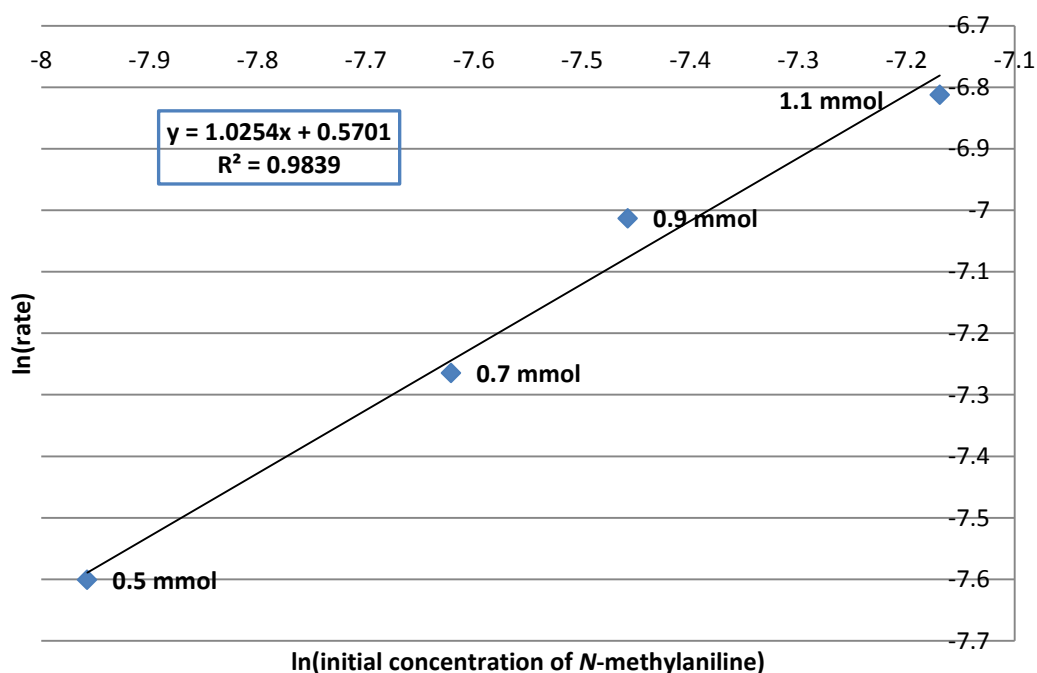


Figure 14: Plot of $\ln(\text{rate})$ vs $\ln(\text{concentration})$ for various initial concentrations of *N*-methylaniline based on the formation of aromatic substitution product

The gradient for the graph shown in Figure 14, is 1.025 or 1, thus the reaction is first order with respect to NMA.

2.2.5.3. Reaction order with respect to zinc nitrate

A series of reactions outlined in Table 12 was run for 4 hours and monitored through ^1H NMR spectroscopy at 10 minute intervals. The results for which are shown in Figure 15.

Table 12 Initial rates experiments varying initial zinc nitrate concentration

Entry	Temp. (°C)	[pyridine] (mmol)	[aniline] (mmol)	[zinc nitrate] (mmol)
1	75	0.5	0.5	0.014
2	75	0.5	0.5	0.025
3	75	0.5	0.5	0.042
4	75	0.5	0.5	0.051

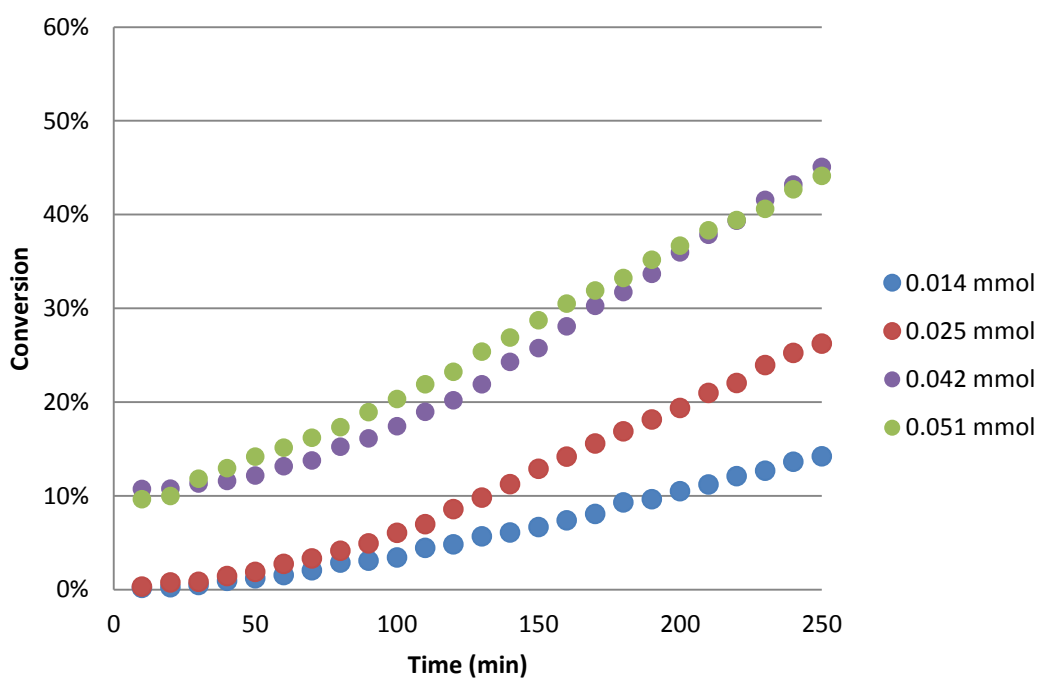


Figure 15: Conversion into product versus time (min) for various initial concentrations of zinc nitrate over 250 minutes

Trend lines can be drawn for the data points of the first 140 minutes. From which the initial rates were determined (Figure 16).

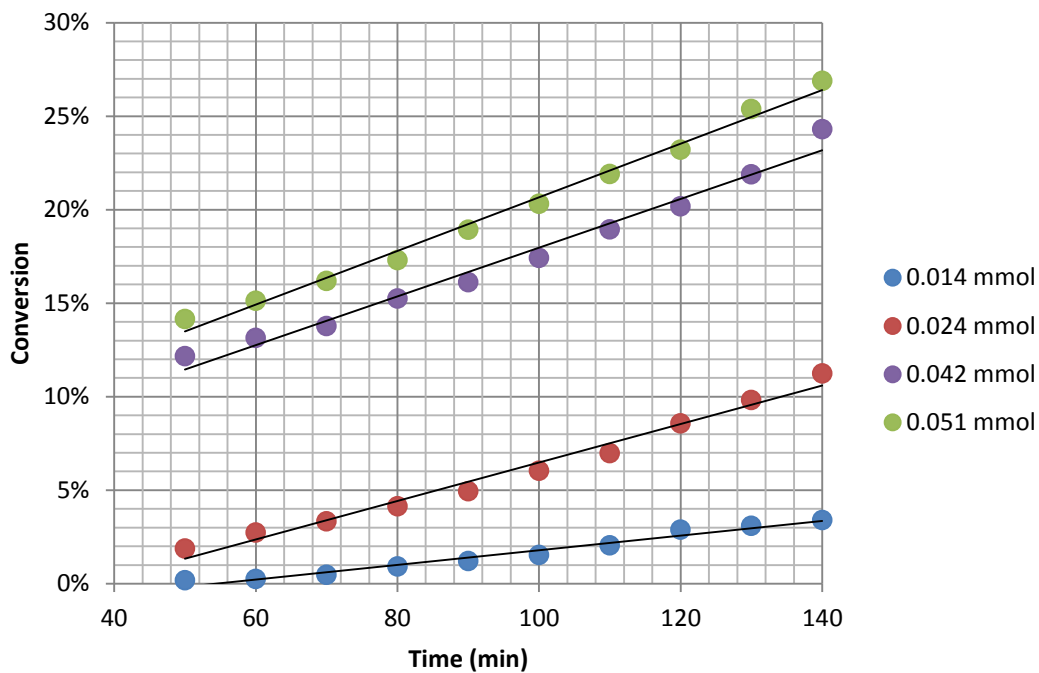


Figure 16: Initial rates of reaction by varying initial concentration of zinc nitrate – initial rates shown in coloured boxes as the gradient of each trend line

The natural logs of the rates and their respective concentrations were calculated and plotted against each other as shown in Figure 17.

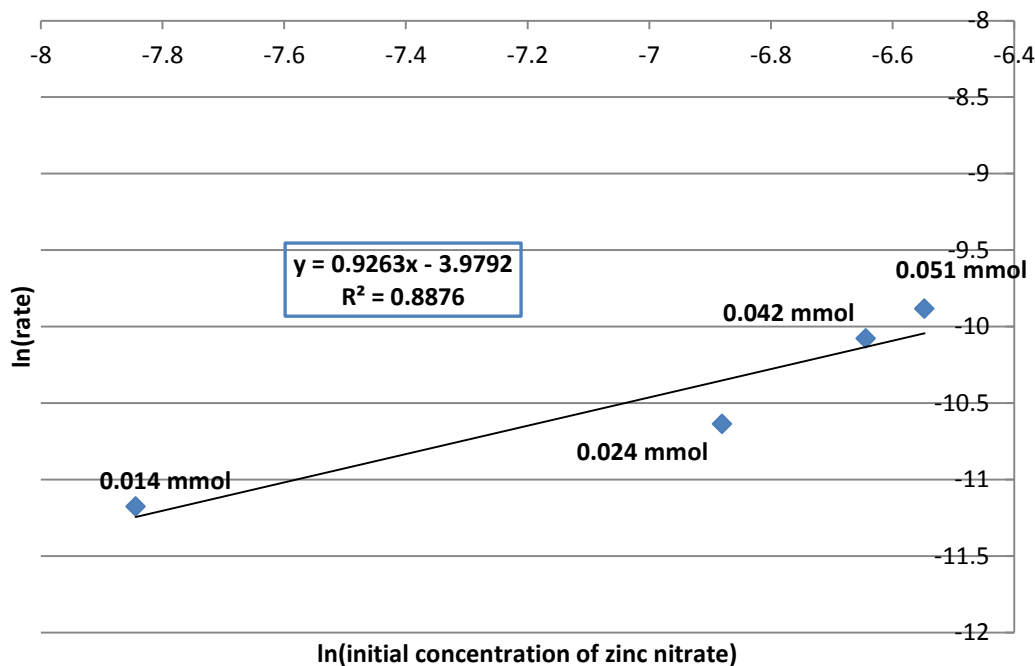


Figure 17: Plot of $\ln(\text{rate})$ vs $\ln(\text{concentration})$ for various initial concentrations of zinc nitrate based on the formation of aromatic substitution product

The gradient for the graph shown in Figure 17, is 0.92 or 1, thus the reaction is first order with respect to zinc nitrate.

2.2.5.4. Rate law

Given the results from the initial rates investigation are a result of one iteration per concentration for each reagent, the resultant rate law from this investigation cannot be considered as absolute and so no certain conclusions can be drawn. However, from the data collected, an approximate rate law for the reaction of 4-Cl-pyr with NMA mediated by zinc nitrate can be reached:

$$\begin{aligned} \text{Rate} &= k[N\text{-methylaniline}]^1[4\text{-chloropyridine}]^0[\text{zinc nitrate}]^1 \\ &= k[N\text{-methylaniline}][\text{zinc nitrate}] \end{aligned}$$

Equation 5

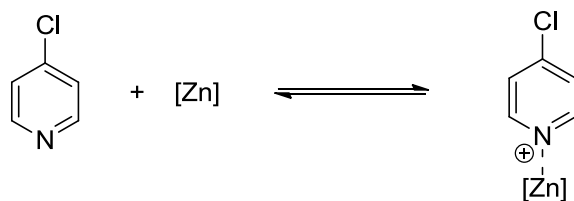
On first inspection, the conclusion to draw from this rate law would be that 4-Cl-pyr is indeed not involved in the rate limiting step and thus the reaction in fact does not proceed through the activation mechanism first hypothesised. The reaction as mentioned in section **2.2.5.1** is in fact pseudo-zero order with respect to 4-Cl-pyr. Zero order kinetics can arise under two circumstances:⁶²

1. Only a small fraction of a reactant is in a state or a location in which it can react, which is being replenished from a larger pool
2. Two or more reactants are involved and the concentration of one is in much greater excess than the others

The reaction under investigation can be described by either situation; if we consider that the concentration of the zinc nitrate in the reaction mixture is 0.025 mmol, then only 0.025 mmol of the 4-Cl-pyr substrate can bind to the zinc at any one time (assuming absolute binding). At the lowest initial concentration of pyridine (0.5 mmol, Entry 1, Table 10), there are 20 molecules of 4-Cl-pyr molecules to every 1 molecule of zinc nitrate. Assuming that the hypothesised mode of activation of zinc to 4-Cl-pyr is in fact in operation, only when the 4-Cl-pyr is bound to the zinc is it able to react with NMA. In short, only a small fraction (5%) of the 4-Cl-pyr molecules is in a state in which it can react and is being subsequently replenished by a larger pool (circumstance 1).

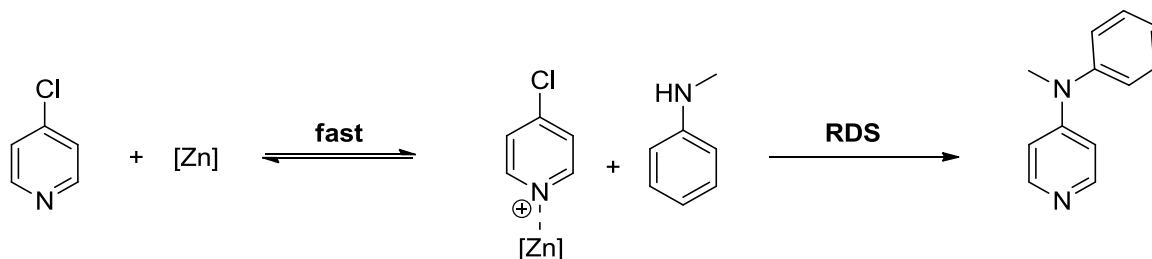
Equally, the reaction of 4-Cl-pyr with NMA is dependent on the binding of 4-Cl-pyr with the zinc nitrate and in this instance the 4-Cl-pyr is in great excess compared to the zinc nitrate (circumstance 2).

From this result, we can infer that the free 4-Cl-pyr is indeed uninvolved in the rate limiting step, but is in rapid equilibrium with the zinc-bound 4-Cl-pyr complex (Scheme 84). The vast excess of the 4-Cl-pyr substrate to the zinc nitrate generates the pseudo-zero order kinetics with respect to 4-Cl-pyr. Therefore the impediment to the formation of the active 4-Cl-pyr species is the small amount of zinc relative to the 4-Cl-pyr in solution.



Scheme 84: Rapid exchange between 4-chloropyridine and zinc-bound 4-chloropyridine complex prior to rate determining step

From this we can propose that the 4-Cl-pyr/zinc complex is involved in the rate determining step. The zinc displays first order reaction kinetics that would be expected; as the concentration of zinc nitrate increases relative to the 4-Cl-pyr, a larger amount of active 4-Cl-pyr/zinc complex is available in solution to react with the NMA. The first order reaction kinetics with respect to NMA can also be explained in terms of generating the more reactive 4-Cl-pyr/zinc complex species, once some of this complex has formed, the 4-Cl-pyr moiety is activated towards aromatic substitution with the NMA. As the product is formed and disassociates from the zinc nitrate, more zinc nitrate is freed to bind to the 4-Cl-pyr, pushing the equilibrium towards formation of more 4-Cl-pyr/zinc complex (Scheme 85).



Scheme 85: Hypothesised reaction mechanism based on reaction order experiment results

As result to this exploratory study, we can suggest that the zinc nitrate could be activating the 4-Cl-pyr towards reaction with the NMA, albeit we cannot confirm through these studies whether it is activating the pyridine ring in the manner we hypothesised. Given that the two possibilities for the mode of “activation” in this case would be either a coupling reaction, which would require air and moisture free conditions (neither condition is met under our reaction conditions) or activation through binding of the zinc to the pyridine nitrogen, we can confidently state that the reaction is proceeding *via*

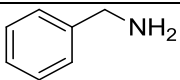
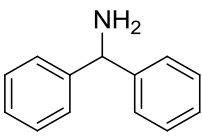
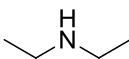
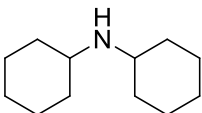
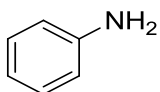
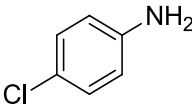
activation of the pyridine ring through the coordination of the 4-Cl-pyr to the zinc through the nitrogen lone pair.

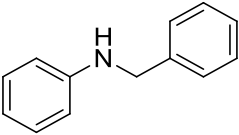
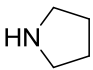
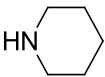
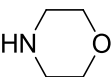
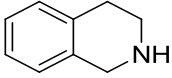
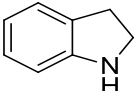
2.2.6. Nucleophile screen

2.2.6.1. Amines

As the parent reaction involved amination of 4-Cl-pyr, we set out to explore the scope of the reaction with respect to the incoming amine. A screen of aliphatic, aromatic and cyclic amines was performed, the results for which are shown in Table 13.

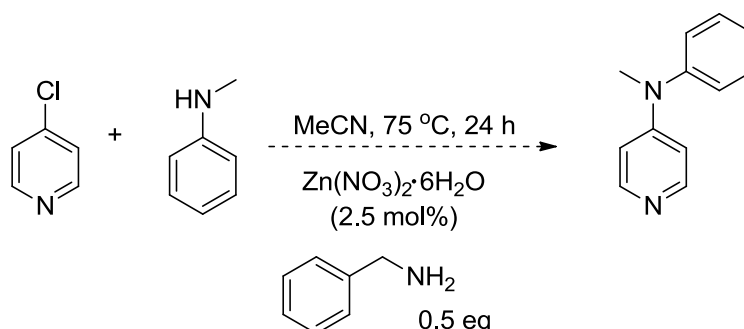
Table 13 Amine screen for the substitution of chlorine in 4-chloropyridine using zinc nitrate as a catalyst in MeCN, 75 °C, 24 h

Entry	Nucleophile	Conversion (%) ^[a]
1		0
2		0
3		0
4		0
5		80
6		58

7		45
8		100
9		92
10		100
11		95
12		100

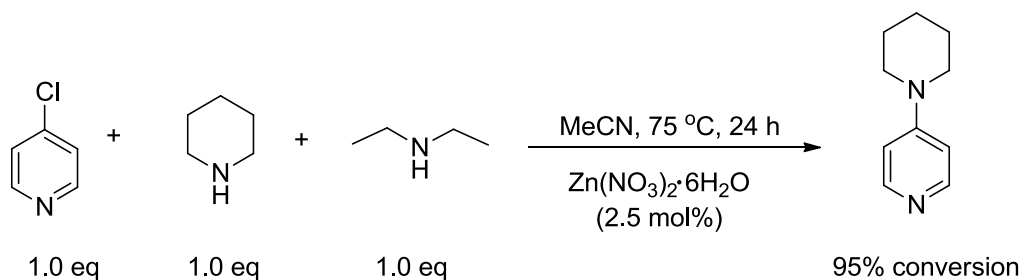
^[a] Conversions were determined through analysis of the ¹H NMR spectra of the crude reaction mixture (the integral for the protons at the α -position on the pyridine in the product were compared to the integral of the protons at the α -position on the pyridine in 4-chloropyridine (dd, 8.36 ppm)).

A series of primary amines were screened, two of which have been included in the table as a representative sample (Entries 1-2, Table 13) did not yield a substitution product. We hypothesised that this lack of reactivity is a result of a higher binding affinity of primary amines to the zinc catalyst. This effectively results in a competition for binding to the zinc between the 4-Cl-pyr and the incoming amine and prevents the substitution reaction from taking place. Indeed, when the parent reaction was run in the presence of 0.5 equivalents of benzylamine, no product was formed, indicating that the benzylamine bound strongly to the zinc Lewis acid, effectively poisoning it and preventing its approach to the pyridine to mediate the substitution reaction (Scheme 86).



Scheme 86: Parent reaction of 4-chloropyridine with *N*-methylaniline mediated by zinc nitrate, poisoned with half an equivalent of benzylamine yields no product

When the reaction is run with cyclic amines (Entries 8-12, Table 13) good to excellent conversions are observed. However when secondary acyclic systems were investigated no reaction occurred (again, the entries shown in the table are a representative sample of a wide range of acyclic secondary amines screened), even with increased steric bulk around the nitrogen (Entries 3-4, Table 13); given that the chemical environment of the nitrogen in piperidine and diethylamine should be similar, one cannot make the competitive binding argument observed with the primary amines. To rule this option out, we ran a similar test experiment: 4-Cl-pyr in the presence of the zinc Lewis acid was reacted with one equivalent of each of piperidine and diethylamine in the same reaction vessel. Assuming a competitive binding event, the reaction would shut down, yielding return of starting materials; however the reaction proceeded to the piperidine substitution product, with complete return of diethylamine (Scheme 87).



Scheme 87: Test reaction for competitive binding of diethylamine with zinc Lewis acid

The success of the cyclic amines over their acyclic counterparts, is more likely associated with the favourable steric situation around the nitrogen atom where the aliphatic chains are pinned back and away from the nucleophilic

lone pair making them more available for the nucleophilic aromatic substitution reaction.

Running the reaction in MeCN yielded good conversions for the anilinic amines (Entries 5-7, Table 13), which makes this methodology attractive given that these amines have relatively low nucleophilicities. On observation of the reaction, it was clear that 4-chloroaniline and *N*-benzylaniline were sparingly soluble in MeCN, thus a small solvent screen was run for the reaction with 4-chloroaniline (Table 14). Given that that parent reaction proceeded well in MeCN a polar aprotic solvent, thus the solvents selected for the screen were THF, EtOAc and DMF (Entries 1-3, Table 14). From the results shown in Table 14, it is clear that the reaction run in THF gave the best conversion to the product (91%, Entry 1, Table 14). The reaction of *N*-benzylaniline with 4-chloropyridine was also run in THF (Entry 5, Table 14) and showed a vast improvement in conversion to the product, indicating that the system can tolerate substituents that are more bulky than a methyl group on the aniline nitrogen.

Table 14 Solvent screen for the reaction of 4-chloroaniline and 4-chloropyridine mediated by zinc nitrate at 75 °C, for 24 h

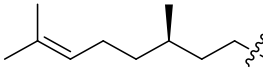
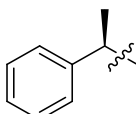
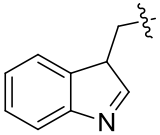
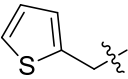
Entry	R ¹ =	R ² =	Solvent	Conversion(%) ^[a]
1	Cl	H	THF	91
2	Cl	H	EtOAc	75
3	Cl	H	DMF	0
4	Cl	H	MeCN	58
5	H	Bn	THF	89

^[a]Conversions were determined through analysis of the ¹H NMR spectra of the crude reaction mixture (the integral for the protons at the α-position on the pyridine in the product were compared to the integral of the protons at the α-position on the pyridine in 4-chloropyridine (dd, 8.36 ppm)).

2.2.6.3. Alcohols

There was a considerable difference observed in the reaction profile when the incoming nucleophile was not a strong enough base or nucleophile. When the reaction was run with incoming alcohol groups we noticed degradation of the 4-Cl-pyr starting material as a result of the high temperature, and release of HCl that was not sequestered by a strong base, as in the case of the amine substitution products. The first screen of alcohol incoming groups, when run at a 1:1 stoichiometric ratio to the pyridine showed little if any conversion and predominant degradation of the halopyridine starting material (Table 15).

Table 15 Sample of alcohol nucleophiles screen for S_NAr reaction with 4-chloropyridine catalysed by zinc nitrate

Entry	R=	Conversion (%) ^[a]
1		0
2		2
3		1
4		1

^[a] Conversions were determined through analysis of the ¹H NMR spectra of the crude reaction mixture (the integral for the protons at the α-position on the pyridine in the product were compared to the integral of the protons at the α-position on the pyridine in 4-chloropyridine)

With this in mind and the relative low nucleophilicities of alcohols, we investigated the use of the incoming alcohol as the reaction solvent in the presence of a base. The goal being that once we were able to overcome the

degradation of the starting material over the course of the reaction, we could work on optimising the stoichiometry to a near 1:1 ratio.

We screened the reaction of 4-Cl-pyr, catalysed by $\text{Zn}(\text{NO}_3)_2 \cdot 6\text{H}_2\text{O}$ in ethanol, with a variety of bases (Table 16).

Table 16 Screen of bases for the reaction of ethanol with 4-chloropyridine under Lewis acid catalysed conditions

Entry	Base	Equivalents	Conversion (%) ^[a]
1	LiOH	2	2
2	KOH	2	0
3	K ₂ CO ₃	2	84
4	NaHCO ₃	2	30
5	Cs ₂ CO ₃	2	36
6	Na ₂ S ₂ O ₃	2	23
7	NaH ₂ PO ₄	2	22
8	Na ₂ HPO ₄	2	40
9	NEt ₃	2	0
10	Control	0	0

^[a]Conversions were determined through analysis of the ¹H NMR spectra of the crude reaction mixture (the integral for the protons at the α-position on the pyridine in the product were compared to the integral of the protons at the α-position on the pyridine in 4-chloropyridine (dd, 8.36 ppm)).

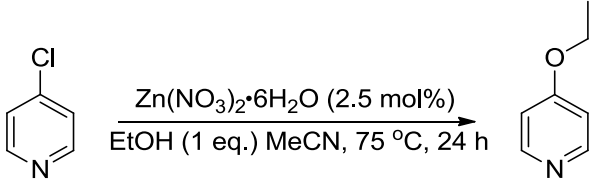
From the screen shown in Table 16, the bases that assisted in providing the best conversions were potassium carbonate, sodium hydrogencarbonate, caesium carbonate and disodium phosphate (Entries 3-5 and 8 respectively, Table 16). However, a large amount of degradation was observed in the ¹H NMR spectrum of the crude reaction mixture when the disodium phosphate was used, while the other bases provided an enhanced stability for the 4-Cl-pyr starting material under these conditions, with no degradation observed in the ¹H NMR spectra of the crude reaction mixtures.

Homogeneous bases did not offer an effective alternative; any nitrogen centred base was required to be less nucleophilic than the incoming alcohol group to prevent competition for reaction with the pyridine. In the case of triethylamine (Entry 9, Table 16), the ^1H NMR spectrum of the recovered material showed no degradation of 4-Cl-pyr, however, given the lack of formation to the substitution product, it is thought that this system suffered from similar competitive binding issues to those associated with benzylamine.

Given the success of the four bases in Table 16, the reaction was run using a 1:1 ratio of ethanol to 4-Cl-pyr, the results for which are shown in Table 17.

Table 17 Screen of bases for the nucleophilic substitution reaction of ethanol with 4-chloropyridine catalysed by zinc nitrate

Entry	Base	Equivalents	Conversion (%) ^[a]
1	NaHCO_3	2	1
2	Na_2HPO_4	2	10
3	K_2CO_3	2	4
4	Cs_2CO_3	2	0



^[a]Conversions were determined through analysis of the ^1H NMR spectra of the crude reaction mixture (the integral for the protons at the α -position on the pyridine in the product were compared to the integral of the protons at the α -position on the pyridine in 4-chloropyridine (dd, 8.36 ppm)).

The results in Table 17 show that the system developed thus far is unable to proceed without a vast excess of alcohol incoming group, with sodium hydrogen carbonate and potassium carbonate (Entries 1 and 3 respectively, Table 17) giving the product in 1% and 4% conversion and the system with caesium carbonate showing no conversion at all to the product (Entry 4, Table 17). However, all three bases exhibited no degradation of the 4-Cl-pyr starting material.

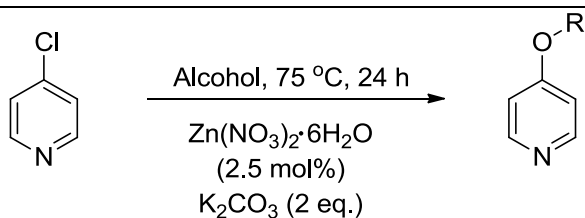
Despite the higher conversion achieved with the use of disodium phosphate as the base, its presence in excess to the ethanol incoming group gave rise to further degradation of the 4-Cl-pyr, by virtue of the formation of phosphoric acid *in situ*, as the base neutralised the HCl liberated from the reaction of 4-Cl-pyr with ethanol.

Given the results for the alcohols thus far, the system remained effective with use of the incoming O-nucleophile as the reaction solvent. A screen of three alcohols was run as a proof of concept, shown in Table 18.

Table 18 Reaction of a variety of common alcohols for nucleophilic aromatic substitution with 4-chloropyridine

Entry	Alcohol	Conversion (%) ^[a]
1	Methanol	76
2	Ethanol	84
3	Propanol	85

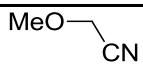
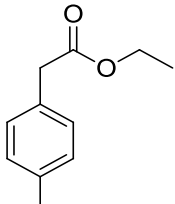
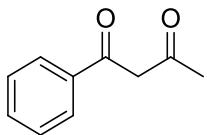
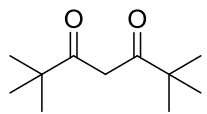
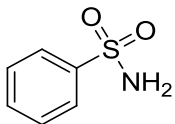
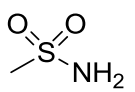
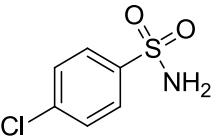
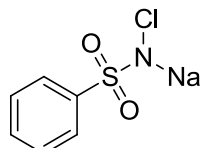
^[a]Conversions were determined through analysis of the ¹H NMR spectra of the crude reaction mixture (the integral for the protons at the α-position on the pyridine in the product were compared to the integral of the protons at the α-position on the pyridine in 4-chloropyridine (dd, 8.36 ppm)).

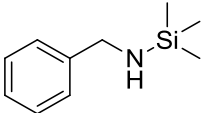
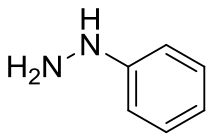


2.2.6.4. Miscellaneous nucleophiles

Other nucleophiles that were investigated include activated esters, sulfonamides and silyl amines (the latter as a means for achieving the substitution product for primary amines), results of which are given in Table 19.

Table 19 Miscellaneous nucleophiles screened for substitution reaction with 4-chloropyridine catalysed by zinc nitrate (2.5 mol%), in MeCN, 75 °C, 24 h (in the case of the activated esters and sulfonamides, 2 equivalents of potassium *t*-butoxide were also used)

Entry	Substrate	Conversion (%) ^[a]
1		6
2		13
3		0
4		0
5		0
6		0
7		0
8		0

9		0
10		70

^[a]Conversions were determined through analysis of the ¹H NMR spectra of the crude reaction mixture (the integral for the protons at the α-position on the pyridine in the product were compared to the integral of the protons at the α-position on the pyridine in 4-chloropyridine (dd, 8.36 ppm)).

The results of this screen demonstrate the scope and limitations this methodology offers. In the case of the activated methylenes, two rationales can be extended to explain their lack of activity. The first is that steric bulk on the esters prevent the approach of the nucleophile to the 4-Cl-pyr and thus no substitution product was observed, or alternatively chelation of the carbonyl oxygen to the zinc could prevent it from catalysing the reaction through coordination to the 4-Cl-pyr (Entries 3 and 4, Table 19), Figure 18. Equally, sulfonamides did not serve as good nucleophiles for this process even when using their sodium chloride salts (Entries 5-9, Table 19).

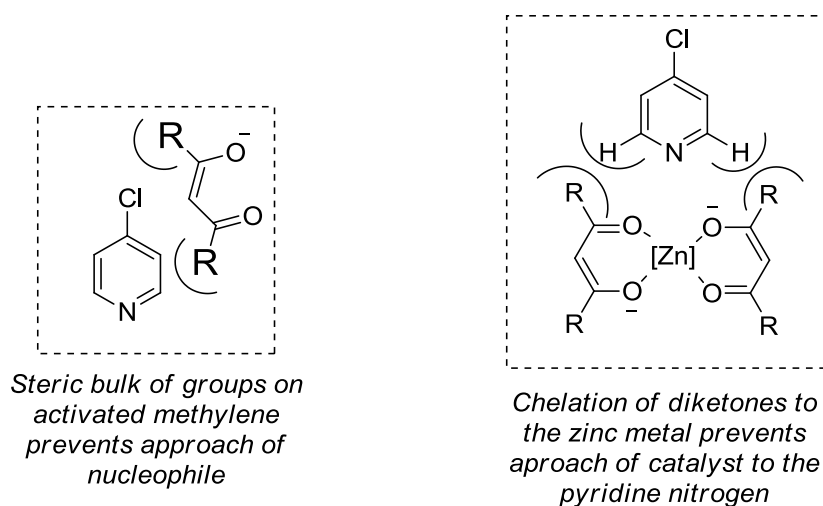


Figure 18: Lack of reactivity of diketones in S_NAr reaction catalysed by zinc nitrate

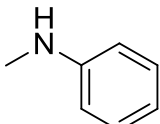
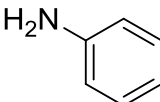
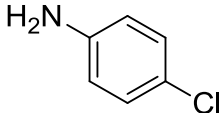
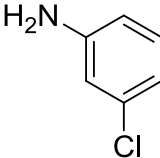
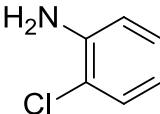
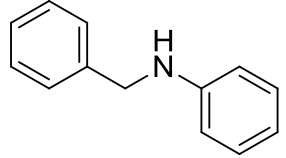
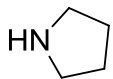
The silyl amine was used as an alternative to benzylamine, with the aim of lowering the nucleophilicity and its binding affinity to the zinc, to realise a process that would achieve the benzylamine substituted product, *via* loss of the silyl group on workup. However the system yielded no conversion into

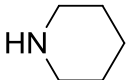
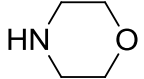
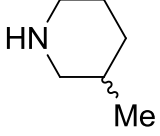
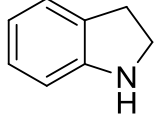
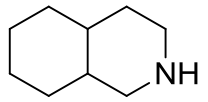
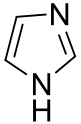
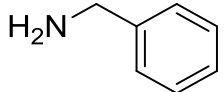
the product (Entry 9, Table 19). Intriguingly, hydrazines such as phenyl hydrazine (Entry 10, Table 19), showed good promise as nucleophiles for this methodology.

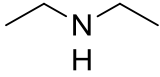
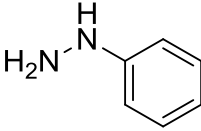
2.2.7. Scope of nucleophile - Summary

Having investigated a wide variety of incoming groups tolerated by this system; a screen of the successful nucleophiles was run, and the system optimised for each nucleophile and the products were isolated. The results for which are shown in Table 20.

Table 20 Optimised conditions and isolated yields for the substitution reaction of successful nucleophiles with chlorine in 4-chloropyridine using zinc nitrate as the Lewis acid catalyst

Entry	Nucleophile	Solvent	Conversion(%) ^[a]	Yield (%)
1		MeCN	100	99
	Control		2	--
2		MeCN	80	65
	Control		0	--
3		THF	100	91
	Control		6	--
4		THF	100	95
	Control		13	--
5		THF	93	87
	Control		7	--
6		THF	89	75
	Control		20	--
7		MeCN	100	89

	Control		8	--
8		MeCN	80	71
	Control		7	--
9^[b]		MeCN	69	56
	Control		3	--
10^[b]		MeCN	100	89
	Control		7	--
11^[b]		MeCN	100	95
	Control		23	--
12^[b]		MeCN	100	95
	Control		5	--
13		MeCN	69	56
	Control		0	--
14		MeCN	0	--
	Control		0	--

15		MeCN	0	--
	Control		0	--
16		MeCN	71	--*
	Control		21	--
17 ^[c]	Methanol	MeOH	76	75
	Control		0	--
18 ^[c]	Ethanol	EtOH	84	81
	Control		0	--
19 ^[c]	Propanol	PrOH	85	84
	Control		0	--

^[a]Conversions were determined through analysis of the ¹H NMR spectra of the crude reaction mixture (the integral for the protons at the α -position on the pyridine in the product were compared to the integral of the protons at the α -position on the pyridine in 4-chloropyridine (dd, 8.36 ppm));

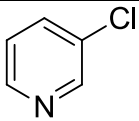
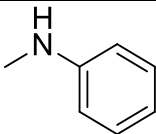
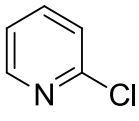
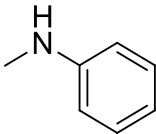
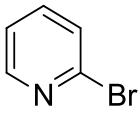
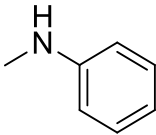
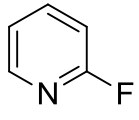
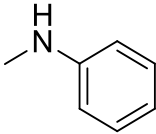
^[b]Reactions run for 4 h; ^[c]Reaction run with 2 eq. of K₂CO₃

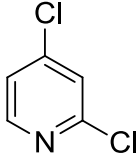
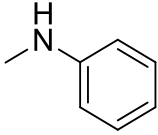
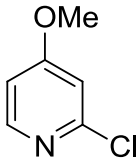
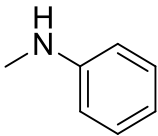
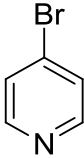
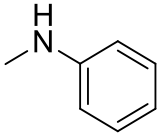
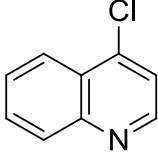
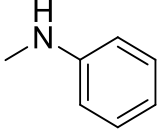
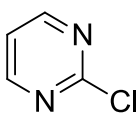
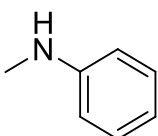
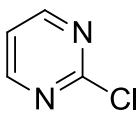
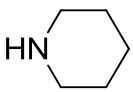
*Could not be isolated

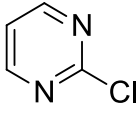
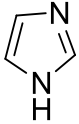
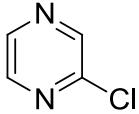
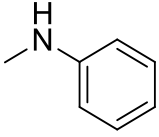
2.2.8. Substrate screen

With the nucleophilic reactants thoroughly investigated, the scope of pyridine substrates was examined next. The substrates investigated were pyridines carrying a variety of good leaving groups, such as different halogens at various positions, and 113quinolone. We also considered halodiazenes as their chemistry is exaggerated relative to pyridine for nucleophilic aromatic substitution. Results of this investigation are found in Table 21.

Table 21 Substrate screen for zinc nitrate activation of various pyridine analogues

Entry	Substrate	Nucleophile	Time (h)	Conv. (%) ^[a]	Yield (%)
1			24	0	--
	Control		24	0	--
2			24	0	--
	Control		24	0	--
3			24	0	--
	Control		24	0	--
4			24	0	--
	Control		24	0	--

5			24	0	--
	Control		24	0	--
6			24	0	--
	Control		24	0	--
7			2	100 ^[b]	89
	Control		2	17 ^[b]	--
8			1	100 ^[c]	93
	Control		1	36 ^[c]	--
9			8	80 ^[d]	71
	Control		8	10 ^[d]	--
10			4	70 ^[d]	63
	Control		4	6 ^[d]	0

11			8	74 ^[d]	61
	Control		8	9 ^[d]	0
12			8	0	0
	Control		8	0	0

^[a]Conversions were determined by analysis of the ¹H Spectra of the crude reaction mixtures (the integral for the protons at the α -position on the pyridine in the product were compared to the integral of the protons at the α -position on the pyridine in 4-chloropyridine (dd, 8.36 ppm)).

These results give a good insight into the general mechanism of the process. Reactions of chloropyridines, in which the chlorine is in the 4-position proceed successfully however, those in the 2-position did not react (Entries 2-4, Table 21). This is likely to be due to the steric bulk of the halogen in the 2-position mitigating the approach of the zinc in order to form a complex with the pyridine substrate, even when a small halogen such as fluorine was used (Entry 4, Table 21).

A test for this hypothesis was carried out by using 2,4-dichloropyridine; as the chlorine in the 4-position has successfully been substituted by the amine. If the chlorine in the 2-position is indeed hindering the approach of the zinc for coordination, no reaction should be observed. This is indeed the case (Entry 5, Table 21): the reaction proceeded with quantitative return of starting materials. This result also eliminates the possibility of the reaction proceeding *via* a cross-coupling reaction, which would have proceeded at either site. To elucidate further the mechanism and eliminate the possibility of this transformation being achieved *via* a cross-coupling mechanism the reactions were run with 3-chloropyridine (Entry 1, Table 21) which is unreactive towards substitution reactions as the *N*-oxide analogue.⁷ With the chlorine further from the nitrogen on the pyridine ring, it should not interfere

with the approach of the catalyst; and indeed if a coupling mechanism was taking place then conversion into the product should be observed. However the reaction gave complete return of starting materials which further supports the idea of activation of the pyridine (through coordination with the zinc Lewis acid) to facilitate a nucleophilic aromatic substitution mechanism.

An alternative explanation for the lack of activity of the 2-chloropyridine is by virtue of the reduced electron density on the nitrogen as the result of an electron withdrawing substituent on an adjacent carbon. The reaction was therefore carried out using 2-chloro-4-methoxypyridine (Entry 6, Table 21), which also showed no activity towards nucleophilic substitution. This further confirms the steric hindrance of the chlorine in the 2-position as even with an electron enriched pyridine-nitrogen, no reaction had taken place.

Interestingly 4-bromopyridine exhibited a much higher reactivity than 4-chloropyridine, yielding the aromatic substitution product in a much shorter reaction time of only 2 hours (Entry 7, Table 21). Smaller groups such as the C-H unit of an adjacent fused ring in the case of 4-chloroquinoline (Entry 8, Table 21) are also tolerated and allow for the approach of the zinc Lewis acid to the nitrogen of the pyridine unit, allowing the reaction to proceed in high yield (93%).

Halodiazenes are also structural motifs of interest and importance in synthetic chemistry, and as such two halodiazenes were investigated as potential substrates for the methodology. This class of substrates is more reactive than halopyridines, with their relative reactivities shown in Figure 19.

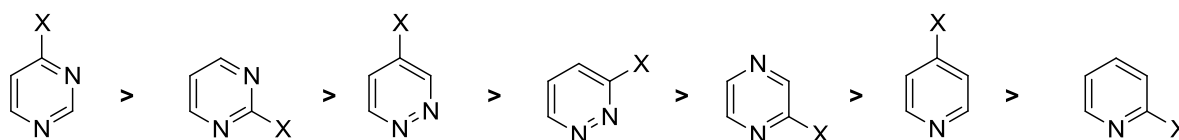


Figure 19: General reactivity of halogenated diazenes and pyridines towards nucleophilic substitution (X= halogen) [7]

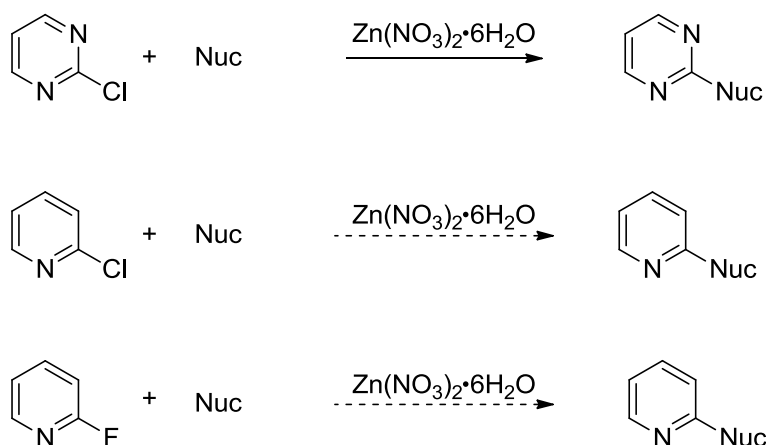
Given the results from the 2-halopyridines, it is unsurprising that the 2-chloropyridazine (Entry 12, Table 21) gave no conversion as the chlorine was

at the 2-position relative to one of the nitrogen atoms, thus hindering coordination of the zinc catalyst.

The 2-chloropyrimidine did show good conversions for the methodology, which is unexpected given the position of the chlorine relative to the two nitrogen atoms, however as Figure 19 suggests, it is one of the more reactive diazenes towards nucleophilic substitution. As a prominent diazene in synthetic organic chemistry, some of the amines from the nucleophile screen were also run for 2-chloropyrimidine in good yields (Entries 9-11, Table 21), the increased reactivity of 2-chloropyrimidine was indeed observed given that high yields for the nucleophilic substitution reactions of 2-chloropyrimidine were achieved in only 8 h, in comparison to the 4-chloropyridine which required 24 h for the same nucleophiles.

2.2.8.1 2-Chloropyridine

Despite the evidence that the lack of reactivity for the 2-chloropyridine is a direct result of the steric hindrance of the chlorine at the 2-position; the reactions of 2-chloropyrimidine and 2-fluoropyridine did bring our conclusions on steric hindrance into question (Scheme 88). 2-Chloropyrimidine requires the zinc catalyst in order to achieve the conversions reported, yet the reaction requires the zinc to bind to a pyrimidine nitrogen that is adjacent to a chlorine atom. Equally, fluorine atoms have rather small covalent radii, yet their lack of reactivity would imply steric bulk beyond that tolerated by our methodology. The conclusion to this observation is that the pyrimidine is far more reactive than the 2-fluoropyridine.



Scheme 88: Reactions of 2-chloropyrimidine, 2-chloro and 2-fluoropyridine with incoming nucleophile under zinc Lewis acid catalysed conditions

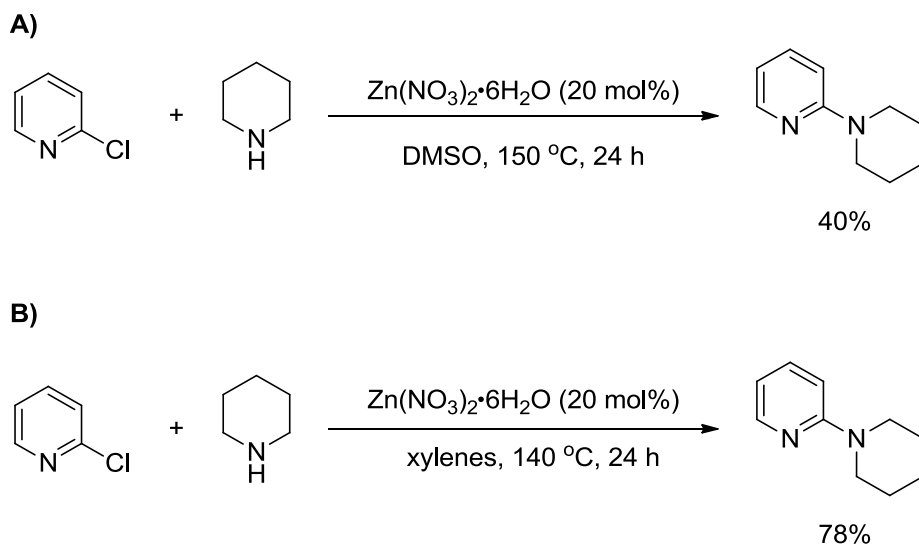
To address this lack of reactivity, a variety of Lewis acids that proved promising for the S_NAr reaction of *N*-methyl aniline with 4-chloropyridine were (20 mol%, 80 °C, 8 h) were screened for 2-chloropyridine however, no conversion to the product was observed (Table 22), even for the zirconium acetoacetate (Entry 6) which displayed higher reactivity than the zinc nitrate in the initial screen, did not show any catalytic action for this reaction.

Table 22 Lewis acid screen for nucleophilic aromatic substitution reaction of *N*-methylaniline with 2-chloropyridine

Entry	Lewis acid	Conversion% ^[a]
1	LiBr	0
2	Mg(NO ₃) ₂ •6H ₂ O	0
3	AlCl ₃	0
4	KPF ₆	0
5	Sc(OTf) ₃	0
6	Zr(acac) ₄	0
7	FeBr ₂	0
8	Fe ₂ O ₃	0
9	CuBr	0
10	Cu(OAc) ₂	0
11	ZnCl ₂	0
12	AgNO ₃	0
13	AgOTf	0

^[a] Conversions were determined through analysis of the ¹H NMR spectra of the crude reaction mixture (the integral for the protons at the α-position on the pyridine in the product were compared to the integral of the protons at the α-position on the pyridine in 4-chloropyridine (dd, 8.36 ppm)).

Given the issue of reactivity that was highlighted between 2-chloropyrimidine and 2-fluoropyridine, we considered that the system required more energy (higher temperature) than the 4-Cl-pyr. Consequently the reaction of 2-Cl-pyr with piperidine (a stronger nucleophile) was run with 20 mol% catalyst loading of zinc nitrate in dimethyl sulfoxide (DMSO) at 150 °C for 24 h (**A**, Scheme 89) forming the product in 40% conversion (the control yielding complete return of starting materials). In an attempt to optimise the process, the reaction was also run in xylenes (**B**, Scheme 89) at 140 °C for 24 h to give the product in 78% conversion (control - 15%).



Scheme 89: Reaction of 2-chloropyridine with piperidine catalysed by zinc nitrate; percentages reported are conversions

DMSO was chosen, as a polar aprotic solvent with a high boiling point, which would allow the reaction to be run at 150 °C, however the reaction profile was not clean and gave a low conversion. Xylenes offered a cleaner reaction profile and higher conversion at a slightly lower temperature. Nonetheless a small solvent screen was run in an effort to achieve higher conversions to the product (Table 23).

Table 23 Solvent screen for zinc nitrate catalysed reaction of piperidine with 2-chloropyridine

Entry	Solvent	Conversion (%) ^[a]
1	Toluene	64
	Control	43
2	Xylenes	76
	Control	12
3	DMF	61
	Control	48
4	Water	16
	Control	2
5	Nonanol	0
	Control	0
6	Neat	44
	Control	6

^[a]Conversions were determined through analysis of the ¹H NMR spectra of the crude reaction mixture (the integral for the proton at the α-position on the pyridine in the product were compared to the integral of the proton at the α-position on the pyridine in 2-chloropyridine (app. dd 8.39 ppm))

N-methylpyrrolidone would not have been considered for reaction design even if they had yielded excellent conversions and was chosen to aid in a better understanding of which solvents served best for the transformation. From the results shown in Table 23, none of the solvents, or even in the absence of a solvent, provided better conversions than xylenes. Thus xylenes was decided upon as the reaction solvent. Further optimisation studies are required, however due to time constraints, an optimised process and reaction scope could not be realised.

2.3. Conclusions

A method for the Lewis acid activation of pyridines for nucleophilic substitution has been developed that utilises a cheap, naturally abundant metal based catalyst. The conditions under which the reaction occurs are comparatively mild and simpler than current methods for the functionalisation of pyridines.

Preliminary kinetic investigations indicate that a 4-Cl-pyr/zinc complex is involved in the rate limiting step for the process, lending some support to our hypothesis for activation of the pyridine through coordination to the zinc Lewis acid. Scope in pyridine analogue further supports the idea of the zinc activating the pyridine ring in a similar manner to the oxygen in pyridine *N*-oxides and that the reaction proceeds *via* nucleophilic aromatic substitution.

The method has shown some scope for various pyridine substrates, although preliminary results show that the reaction can be applied to 2-chloropyridine further investigations are required. Nonetheless the methodology does show excellent reactivity for 2-chloropyrimidines. The system has shown a broad scope in nucleophiles with good to excellent conversions reported for anilines, cyclic amines and alcohols.

2.4. Future work

This methodology shows promise as a simpler alternative to current literature techniques. However, it is limited by its lack of activity towards primary amines, oxygen nucleophiles (in 1:1 ratio) and carbon nucleophiles. The further work section will address two challenges in this methodology; firstly broadening scope in nucleophiles and secondly looking into alternative methods for activating pyridines.

2.4.1. Broader scope of nucleophile

Further investigations need to be carried out to broaden the scope in nucleophile for this process. For carbon nucleophiles, a binding study for the affinity of activated esters should be investigated; this would confirm or rule out association of the activated esters to the zinc catalyst. The result would highlight the need for an alternative catalyst for the process, or a better base for the deprotonation of the activated ester.

A screen for alternative Lewis acid catalysts should be investigated for the reaction of alcohol nucleophiles with 4-Cl-pyr. The optimum base investigated for this methodology prevents degradation of the 4-chloropyridine without impeding the reaction, however a stronger Lewis acid catalyst may have an increased activating effect on the pyridine ring making it more susceptible to nucleophilic substitution by weaker nucleophiles.

Attempts to optimise the methodology towards the reaction with primary amines (specifically benzylamine) were investigated (Table 24). The results of which show early promise, with a conversion of 50% observed with indium nitrate (Entry 5, Table 24), however further investigation is required.

Table 24 Lewis acid screen for the reaction of 4-chloropyridine with benzylamine

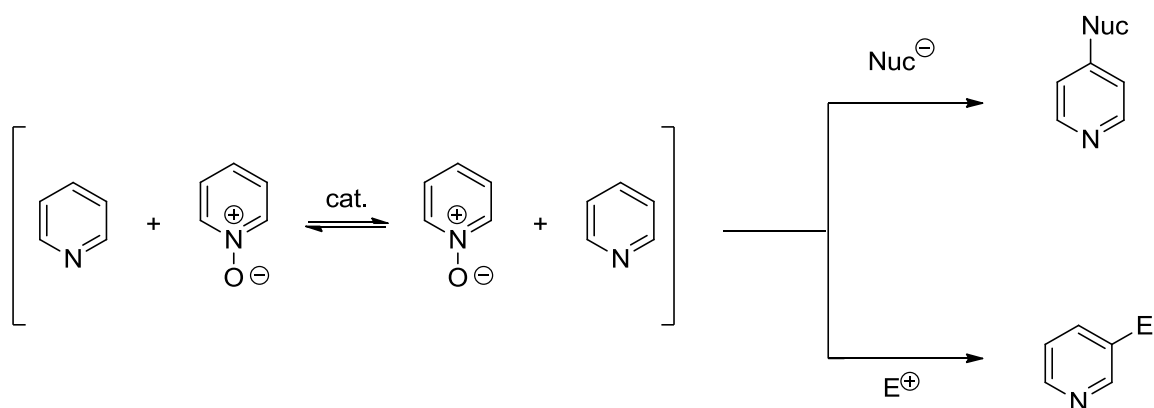
Reaction scheme: 4-chloropyridine + benzylamine $\xrightarrow[\text{MeCN, 80 } ^\circ\text{C, 24 h}]{\text{Lewis Acid (20 mol\%)}}$ N-benzylpyridine

Entry	Lewis Acid	Conversion (%)
1	LiBF ₄	0
2	NaBF ₄	2
3	KPF ₆	5
4	AlCl ₃	8
5	In(NO ₃) ₃	50
6	Mg(NO ₃) ₂ •6H ₂ O	10
7	Sc(OTf) ₃	8
8	Cp ₂ ZrCl ₂	0
9	CuBr	0
10	CuOAc	0
11	AgNO ₃	15
12	Control	0

^[a]Conversions were determined through analysis of the ¹H NMR spectra of the crude reaction mixture (the integral for the protons at the α-position on the pyridine in the product were compared to the integral of the protons at the α-position on the pyridine in 4-chloropyridine (dd, 8.36 ppm)).

2.4.3. Oxygen transfer catalysis in pyridines

The design of this methodology was to achieve pyridine *N*-oxide reactivity in pyridines without the need for a stoichiometric oxidant. An alternative strategy, which would overcome the shortcomings of the zinc Lewis acid catalysed methodology, would be to develop a catalyst that could transfer the oxygen of a pyridine *N*-oxide present in catalytic amounts to the pyridine core requiring functionalisation (Scheme 90). In this way, electrophilic as well as nucleophilic aromatic substitution reactions could take place at the pyridine ring.



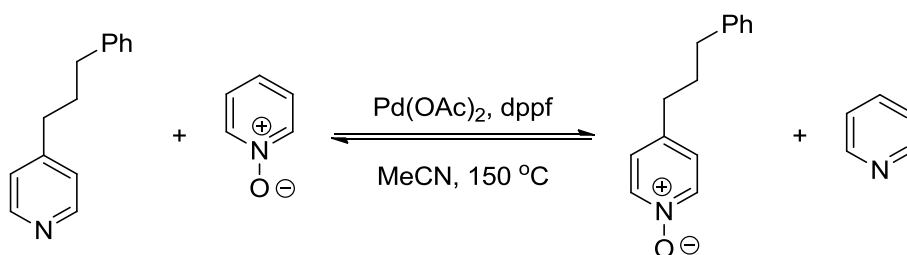
Scheme 90: Proposed oxygen transfer catalysis method for nucleophilic and electrophilic aromatic substitution

Clark *et al*¹¹⁰ employed a method for the deoxygenation of pyridine *N*-oxide by transfer oxidation of trialkylamines. The method was successfully applied using palladium acetate ($\text{Pd}(\text{OAc})_2$) as the catalyst in combination with a bis(diphenylphosphino)ferrocene (dppf) ligand, for the deoxygenation of a variety of pyridine *N*-oxides, by transfer oxidation to trimethylamine. The authors did not offer a hypothesised mechanism by which the reaction was proceeding, but investigations into the process would be of great import.

Table 25 Pyridine *N*-oxide deoxygenation by transfer oxidation to trimethylamine [110]

Entry	R=	Yield(%)
1	3-NHCOCH ₃	64
2	2-Me	94
3	Quinoline	88
4	3-COOMe	91
5	2-CH ₂ OH	66
6	COCH ₃	64

This methodology was adapted to investigate its applicability for oxygen transfer between pyridine *N*-oxides and pyridines. The use of $\text{Pd}(\text{OAc})_2$ in the presence of a dppf ligand, achieved successful oxygen transfer between pyridine *N*-oxide and 4-(3-phenylpropyl)pyridine (Scheme 91).



Scheme 91: Oxygen transfer between pyridine *N*-oxide and 4-(3-phenylpropyl)pyridine catalysed by palladium acetate

The limited attempts to apply this to substitution reactions of pyridine were ineffective as the palladium mediated some of the reactions through cross-coupling mechanisms. However, an investigation into other more naturally abundant and cheaper metals for mediating this oxygen transfer could be investigated, thus a new universal method for functionalising pyridines could be realised. This is currently being investigated by another student within the Williams group, further elaboration on this methodology can be found in future publications by Jones and Williams *et al.*

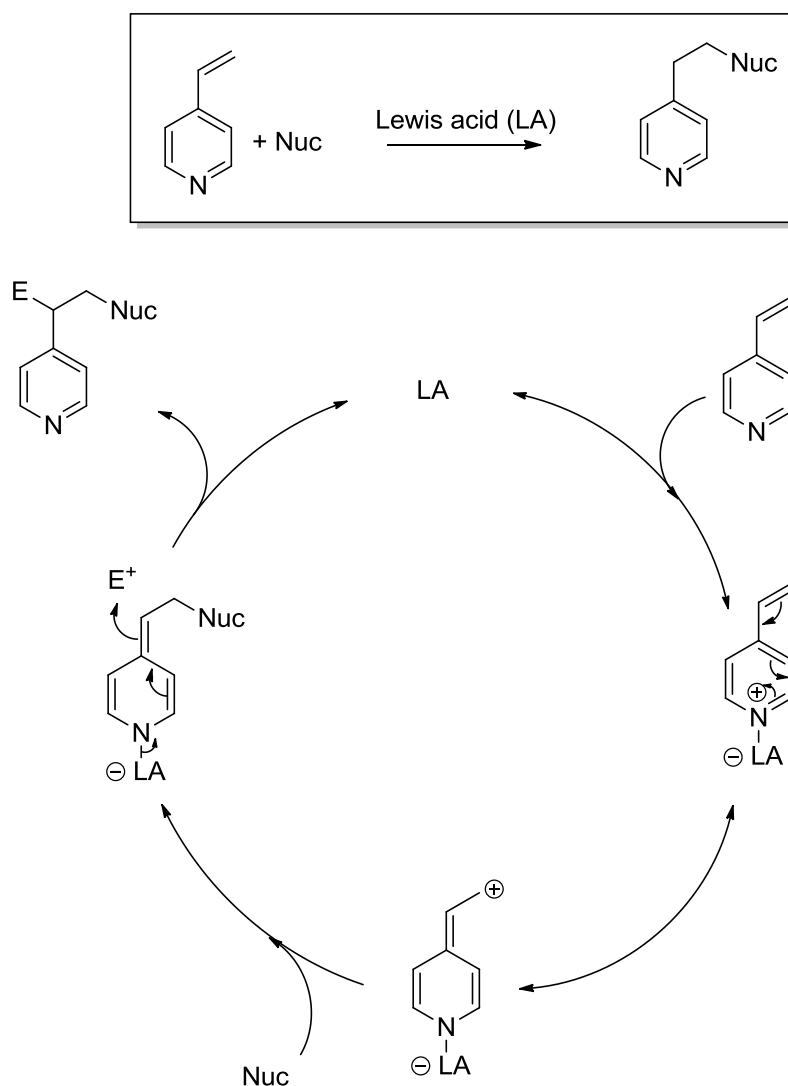
Chapter 3: Lewis acids for the activation of vinylpyridines towards conjugate addition and cyclisation reactions

*I kept a diary after I was born. Day
1: tired from the move. Day 2:
everyone thinks I'm an idiot"*

-Steven Wright

3.1. Aims

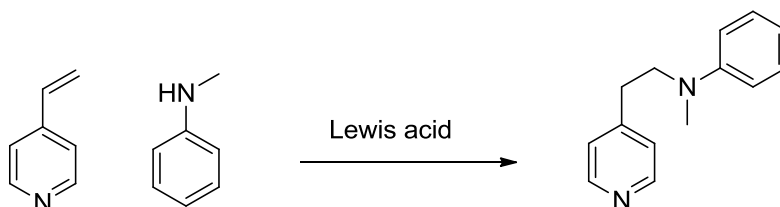
Given the success of the zinc Lewis acid methodology for activating pyridines towards nucleophilic aromatic substitution (Chapter 2), we considered that use of Lewis acids in this manner could be extended to activate vinylpyridines towards conjugate addition and cyclisation reactions. Given that the electron-withdrawing nature of pyridine activates vinyl groups bound at the α - and γ -position on the pyridine; we hypothesised that in the same manner a Lewis acid could exaggerate the electron-withdrawing quality of the pyridine nitrogen and allow conjugate addition reactions of vinylpyridine to proceed under less forcing conditions (Scheme 92).



Scheme 92: Proposed catalytic cycle for activation of vinylpyridines for conjugate addition

3.2. Results and Discussion

Building on the previous work with 4-chloropyridine, the conjugate addition reaction of *N*-methylaniline to 2- and 4-vinylpyridines was investigated for Lewis acid activation (Scheme 93).



Scheme 93: Parent reaction for investigation of Lewis acid activation of vinylpyridines

3.2.1. Lewis acid catalyst screen

A screen of a variety of Lewis acids was run, shown in Table 26. As a starting point, the solvent and temperature selected were those obtained from optimising for the aromatic substitution of 4-chloropyridine.

Table 26 Lewis acid screen for the activation of 4-vinylpyridine towards conjugate addition (carried out by Matthew Teasdale)

Entry	Lewis Acid	Conversion (%) ^[a]
1	LiBF ₄	46
2	KPF ₆	0
3	Mg(NO ₃) ₂ •6H ₂ O	79
4	MgBr ₂	73
5	Sc(OTf) ₃	24
6	Ti(Cp) ₂ (Cl) ₂	01
7	Zr(Cp) ₂ (Cl) ₂	67
8	Zr(acac) ₄	0
9	FeSO ₄ •7H ₂ O	19
10	Co(OAc) ₂	0
11	Pd(OAc) ₂	8
12	CuBr•SMe ₂	0
13	Cu(OAc) ₂	0
14	AgBF ₄	61
15	Zn(OTf) ₂	0
16	Zn(NO ₃) ₂ •6H ₂ O	55
17	AlCl ₃	63
18	Al(O ⁱ Pr) ₃	0
19	In(OTf) ₃	67
20	Control	0

^[a] Conversions were determined through analysis of the ¹H NMR spectra of the crude reaction mixture (the integral for the protons at the β-position on the pyridine in the product were compared to the integral of the protons at the β-position on the pyridine in 4-vinylpyridine (dd, 7.15 ppm)).

The results from Table 26 indicate that magnesium based Lewis acids are the best at activating vinylpyridines towards conjugate addition reactions. The results from the control (Entry 20, Table 26) show that under these

conditions the reaction cannot proceed without catalytic activity of the Lewis acids. Interestingly, the zinc nitrate (Entry 16, Table 26), which had proved a good catalyst for activating 4-halopyridines towards nucleophilic aromatic substitution reactions, only gave a 55% conversion into the conjugate addition product.

This screen is the result of work carried out by an undergraduate Masters student within the group, who further investigated the use of magnesium nitrate as a Lewis acid for the activation of vinylpyridines for conjugate addition. Some of his preliminary results are discussed in the following subsections.

3.2.2. Solvent screen

In an attempt to improve the conversion into the product from 79% to 100% for the magnesium nitrate catalysed system, the reaction time was extended from 8 h to 24 h, for which no improvement in conversion was obtained. The reaction temperature was increased from 75 °C to 80 °C, however this had little effect on the conversion. As a result an investigation into the reaction solvent was carried out, the results for which are shown in Table 27.

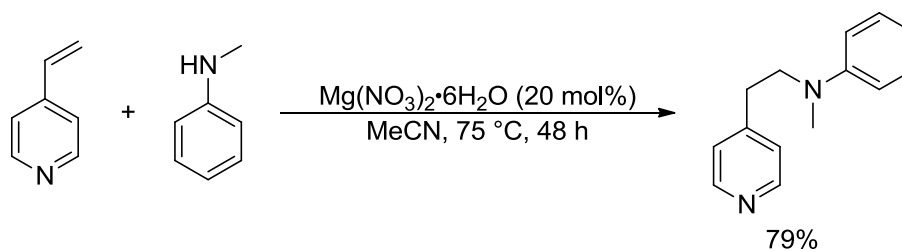
Table 27 Solvent screen for magnesium nitrate catalysed activation of 4-vinylpyridine for conjugate addition reaction with *N*-methylaniline (carried out by Matthew Teasdale)

Entry	Solvent	Conversion (%) ^[a]
1	Toluene	16
2	Dichloromethane	42
3	Tetrahydrofuran	60
4	Ethyl acetate	24
5	Acetone	74
6	Acetonitrile	88
7	Isopropyl alcohol	86
8	Water	54

^[a] Conversions were determined through analysis of the ¹H NMR spectra of the crude reaction mixture (the integral for the protons at the β-position on the pyridine in the product were compared to the integral of the protons at the β-position on the pyridine in 4-vinylpyridine (dd, 7.15 ppm)).

As can be seen from Table 27, acetonitrile (Entry 6, Table 27) was the best solvent for mediating the reaction. Isopropyl alcohol (Entry 7, Table 27) gave a similar result, although the reaction profile was not as clean as that of acetonitrile, showing formation of biproducts.

The student went on to run the reaction under the same conditions but for 48 h in acetonitrile and reported no increase in the conversion (Scheme 94).



Scheme 94: Conjugate addition reaction of 4-vinylpyridine with *N*-methylaniline mediated by magnesium nitrate at 75 °C for 48 h

3.2.3. Alternative Lewis acid catalyst screen

Given the weak nucleophilicity of *N*-methylaniline, an alternative nucleophile was considered for the investigation. The reaction of morpholine with 4-vinylpyridine was investigated and screened using the best performing Lewis acids for mediating the reaction with *N*-methylaniline (Table 28).

Table 28 Lewis acid screen for the reaction of 4-vinylpyridine with morpholine (carried out by Matthew Teasdale)

Entry	Lewis acid	Conversion (%) ^[a]
1	LiBF ₄	96
2	KPF ₆	71
3	Mg(NO ₃) ₂ •6H ₂ O	95
4	Zn(NO ₃) ₂ •6H ₂ O	96
5	Control	35

^[a] Conversions were determined through analysis of the ¹H NMR spectra of the crude reaction mixture (the integral for the protons at the β-position on the pyridine in the product were compared to the integral of the protons at the β-position on the pyridine in 4-vinylpyridine (dd, 7.15 ppm)).

The results from Table 28 displayed superior conversions for all Lewis acids selected, owing to the higher nucleophilicity of the morpholine. The best Lewis acid catalysts proved to be lithium tetrafluoroborate, magnesium and zinc nitrates (Entries 1, 3-4, Table 28); the control however (Entry 5, Table 28) did show some product formation under these conditions (35%), albeit far less than those catalysed by the Lewis acids. Therefore, a subsequent screen was run at 40 °C, where the catalyst loadings for the three best Lewis acids were varied (Table 29).

Table 29 Catalyst loading screen of Lewis acids for the reaction of 4-vinylpyridine with morpholine at 40 °C (carried out by Matthew Teasdale- all but Entries 3-4)

Entry	Lewis acid	Catalyst loading (mol%)	Conversion (%) ^[a]
1	Mg(NO ₃) ₂ •6H ₂ O	20	100
2	Mg(NO ₃) ₂ •6H ₂ O	10	93
3	Zn(NO ₃) ₂ •6H ₂ O	20	94
4	Zn(NO ₃) ₂ •6H ₂ O	10	100
5	LiBF ₄	20	88
6	LiBF ₄	10	74
7	Control	0	6

^[a] Conversions were determined through analysis of the ¹H NMR spectra of the crude reaction mixture (the integral for the protons at the β-position on the pyridine in the product were compared to the integral of the protons at the β-position on the pyridine in 4-vinylpyridine (dd, 7.15 ppm)).

All Lewis acids provided good to excellent conversions for both catalyst loadings; however the zinc and magnesium nitrates gave superior conversions over the lithium tetrafluoroborate. Interestingly, though the magnesium nitrate gave a higher conversion with increased catalyst loading (Entries 1 and 2, Table 29), the zinc displayed the opposite trend (Entries 3 and 4, Table 29) with the 10 mol% catalyst loading giving the product in 100% conversion and the 20 mol% giving a 94% conversion.

At this point Teasdale went on to optimise the process for magnesium nitrate, however the reaction when applied to other nucleophiles, did not yield the products in high conversion. Thus the investigations into the development of zinc nitrate mediated conjugate addition reaction of vinylpyridines reported from this point onwards, are my own.

3.2.4. Reaction optimisation

Given the previous success of the zinc catalyst with the more demanding reaction of the aromatic substitution of 4-chloropyridine, and its efficacy at lower catalyst loadings for the conjugate addition reaction, we chose to focus

our investigations on the use of zinc nitrate. Initially a screen of the catalyst loading at various temperatures was run (Table 30).

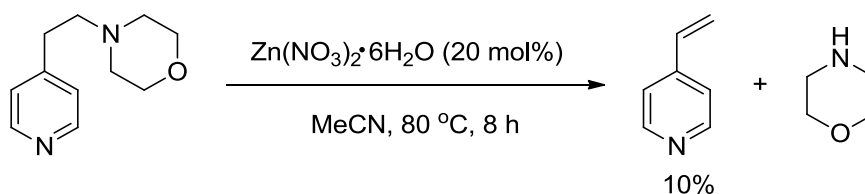
Table 30 Temperature and catalyst loading screen for the conjugate addition of morpholine to 4-vinylpyridine mediated by zinc nitrate

Entry	Temp (°C)	Catalyst loading (mol%)	Conversion (%) ^[a]
1	80	5	94
2	80	10	84
3	80	15	78
4	80	20	71
5	80	0	26
6	60	5	100
7	60	10	100
8	60	15	100
9	60	20	85
10	60	0	15
11	40	5	100
12	40	10	100
13	40	15	100
14	40	20	87
15	40	0	5
16	25	5	94
17	25	10	93
18	25	15	93
19	25	20	89
20	25	0	2

^[a] Conversions were determined through analysis of the ¹H NMR spectra of the crude reaction mixture (the integral for the protons at the β-position on the pyridine in the product were compared to the integral of the protons at the β-position on the pyridine in 4-vinylpyridine (dd, 7.15 ppm)).

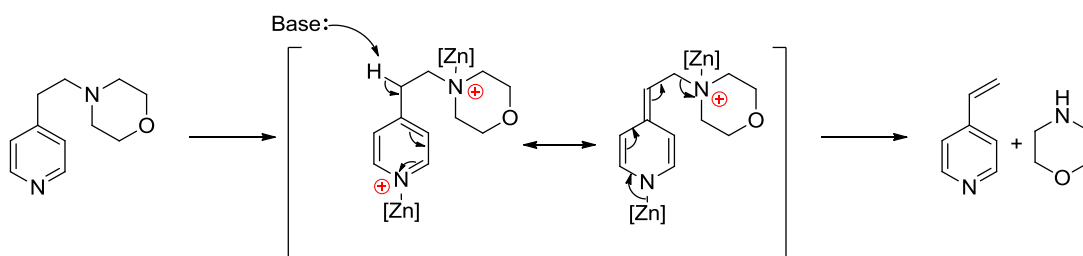
As the catalyst loading approaches 20 mol% the conversion decreases relative to the lower catalyst loadings (Table 30). This mitigation in conversion is also observed as the system acquires more energy; 20 mol% catalyst loading at 25 °C giving an 89% conversion into the product (5 mol% displaying 94% conversion) versus the same catalyst loading at 80 °C giving a conversion of 71% whilst the 5 mol% catalyst loading at the same temperature yielded a conversion of 94% (Entries 19, 16, 4 and 1 respectively, Table 30).

As addressed in section 1.4 in Chapter 1 (Scheme 47), some conjugate addition reactions of vinylpyridines can be reversible; we considered that this maybe the cause for the decrease in conversion at higher temperatures and catalyst loadings. To test this hypothesis, the product was subjected to the reaction conditions in entry 4 (Table 30): 80 °C, 20 mol% catalyst loading for 8 h (Scheme 95).



Scheme 95: Reversibility of conjugate addition of morpholine to vinylpyridine mediated by high catalyst loading in zinc nitrate and higher reaction temperature

The reaction yielded a 10% conversion into the 4-vinylpyridine starting material; the reason for this observed reversion to the starting materials is due to the acidity of the protons on the aliphatic carbon closest to the pyridine, which is exaggerated by coordination of the zinc at the pyridine nitrogen and morpholine nitrogen. Effectively the molecule is being pulled apart through polarisation by the Lewis acid, providing an opening for a base (morpholine, product) to deprotonate at the acidic position, which is followed by elimination of the morpholine (Scheme 96).



Scheme 96: Hypothesised mechanism by which the conjugate addition product reverts to its starting materials

From the range of temperatures screened, 40 °C seemed the optimum temperature for mediating the reaction; giving a 100% conversion into the product at a 5 mol% catalyst loading over 8 hours. Having stated this, reactions at 25 °C did perform well, albeit with a slightly lower conversion into the product. Given the observed results from Table 30, the following temperature and catalyst loading screens were run (Table 31).

Table 31 Temperature, time and catalyst loading screen for the reaction of 4-vinylpyridine with morpholine mediated by zinc nitrate

Entry	Temp (°C)	Catalyst loading (mol%)	Time (h)	Conversion (%) ^[a]
1	25	5	12	100
2	25	0	12	0
3	30	2.5	8	85
4	30	5	8	95
5	30	0	8	5
6	40	2.5	8	100
7	40	0	8	4
8	40	2.5	4	90
9	40	5	4	100
10	40	0	4	5

^[a]Conversions were determined through analysis of the ¹H NMR spectra of the crude reaction mixture (the integral for the protons at the β-position on the pyridine in the product were compared to the integral of the protons at the β-position on the pyridine in 4-vinylpyridine (dd, 7.15 ppm)).

From Table 31, the systems that give 100% conversion are 5 mol% catalyst loading at 40 °C for 4 h (Entry 9, Table 31), or at room temperature (25 °C) for 12 h (Entry 1, Table 31), alternatively a catalyst loading of 2.5 mol% at 40 °C for 8 h (Entry 6, Table 31). All systems are viable considering that 40 °C is not a particularly high temperature. However, as the control for the room temperature reaction (Entry 2, Table 31) showed no product formation under these conditions, this system was selected as the optimised reaction conditions for this transformation.

3.2.4.1. Reaction optimisation for 2-vinylpyridine

With an optimised system developed for the 4-vinylpyridine system, 2-vinylpyridine was investigated as a substrate for this methodology. Given that the zinc nitrate system has worked with the 4-chloroquinoline substrate in Chapter 2, the relative bulk of the vinyl system would be analogous to that of the fused aromatic ring in the quinoline. Indeed, a preliminary test reaction showed that the zinc nitrate Lewis acid mediated the conjugate addition of morpholine to 2-vinylpyridine. Initially, the optimised system for the 4-vinylpyridine was run for the conjugate addition of morpholine to 2-vinylpyridine (Table 32).

Table 32 Temperature, time and catalyst loading screen for the reaction of 2-vinylpyridine with morpholine mediated by zinc nitrate

Reaction scheme: 2-vinylpyridine + morpholine $\xrightarrow[\text{MeCN}]{\text{Zn(NO}_3)_2 \cdot 6\text{H}_2\text{O}}$ 2-(2-morpholinoethyl)pyridine

Entry	Temp (°C)	Catalyst loading (mol%)	Time (h)	Conversion (%) ^[a]
1	25	5	12	71
2	25	2.5	12	56
3	25	0	12	0
4	25	5	24	94
5	25	2.5	24	74
6	25	0	24	0
7	40	5	8	80
8	40	2.5	8	55
9	40	0	8	0
10	40	5	12	78
11	40	2.5	12	76
12	40	0	12	23

^[a]Conversions were determined through analysis of the ¹H NMR spectra of the crude reaction mixture (the integral for the proton at the α-position on the pyridine in the product were compared to the integral of the proton at the α-position on the pyridine in 2-vinylpyridine (app. dd, 8.58 ppm)).

The 2-vinylpyridine seemed a less reactive system than that of the 4-vinylpyridine, given that the optimised system for the latter gave high conversions into the product. The reaction time was extended to 24 h which showed a near quantitative conversion into the product (Entry 4, Table 32). In an effort to increase the conversion, the system was run at a higher temperature at different reaction times and various catalyst loadings (Entries 6-12, Table 32). The temperature increase showed the same adverse effect on the conversion as seen with the 4-vinylpyridine, and did not yield better conversions at this temperature despite extensions in reaction times. Thus the reaction conditions of 5 mol% zinc nitrate for 24 h at 25 °C were chosen

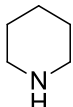
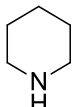
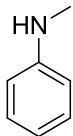
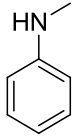
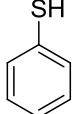
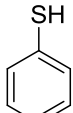
as the optimum for the conjugate addition reaction of 2-vinylpyridine with morpholine.

3.2.5. Scope in incoming group for conjugate addition

3.2.5.1. 4-Vinylpyridine

A series of nucleophiles was screened under the optimised reaction conditions developed in the previous section (Table 33).

Table 33 Screen of a variety of incoming groups for conjugate addition to 4-vinylpyridine catalysed by zinc nitrate

Entry	Nucleophile	Catalyst loading (mol%)	Conversion (%) ^[a]
1		5	60
2		0	5
3		5	0
4		0	0
5		5	100
6		0	76

^[a]Conversions were determined through analysis of the ¹H NMR spectra of the crude reaction mixture (the integral for the protons at the β-position on the pyridine in the product were compared to the integral of the protons at the β-position on the pyridine in 4-vinylpyridine (dd, 7.15 ppm)).

The catalysed system gave good to excellent conversions for piperidine and thiophenol (Entries 1 and 5, Table 33) with very little conversion seen in the case of piperidine, and a high conversion for the thiophenol control reactions (Entries 2 and 6, Table 33). The high reactivity of the thiophenol is perhaps unsurprising, given its high nucleophilicity. Predictably, no conversion was observed for the *N*-methylaniline reaction, given that in the initial screen when the reaction was run at 75 °C for 8 h with a catalyst loading of 20 mol% only a 55% conversion was observed. The system was optimised for each of the incoming groups.

3.2.5.1.1. Piperidine

As shown in the previous section the reaction with piperidine under the optimised conditions gave a 60% conversion with the control showing a minimal conversion of 5% (Entries 1 and 2, Table 33).

Table 34 Optimisation for reaction of 4-vinylpyridine with piperidine mediated by zinc nitrate Lewis acid

Entry	Temp (°C)	Catalyst loading (mol%)	Time (h)	Conversion (%) ^[a]
1	25	5	24	68
2	25	2.5	24	63
3	25	0	24	6
4	40	5	4	90
5	40	0	4	10
6	40	5	6	78
7	40	2.5	6	68
8	40	0	6	9

^[a]Conversions were determined through analysis of the ¹H NMR spectra of the crude reaction mixture (the integral for the protons at the β-position on the pyridine in the product were compared to the integral of the protons at the β-position on the pyridine in 4-vinylpyridine (dd, 7.15 ppm)).

An increase in the reaction time as well as lowering the catalyst loading did not provide a great increase in conversion (Entries 1-3, Table 34), with conversions of 68% and 63% observed for the 5 mol% and 2.5 mol% catalyst loadings respectively. The temperature of the reaction was increased to 40 °C and reaction times were shortened to 4 h; given the relatively high reactivity at 25 °C, it was considered that with an increase of energy input into the system, the reaction would not require as much time to reach a higher conversion. This system provided a 90% conversion into the product after 4 h at 40 °C with a catalyst loading of 5 mol% (Entry 4, Table 34), the control provided the product in 10% conversion. The reaction time was extended to 6 h and run for both 2.5 and 5 mol% catalyst loading, however the extension in time resulted in mitigation in conversions, which could indicate that at 40 °C the reverse reaction may begin to take effect. Given the results for the increased reaction time at 40 °C, the optimised reaction conditions selected were 5 mol% Zn(NO₃)₂·6H₂O, at 40 °C for 4 h.

3.2.5.1.2. *N*-Methylaniline

As a weak nucleophile, *N*-methylaniline required more forcing reaction conditions than the other nucleophiles. As the reaction did not proceed at 25 °C for 12 h with a 5 mol% catalyst loading, the reaction was screened at a variety of temperatures and catalyst loadings, the results for which are shown in Table 35.

Table 35 Temperature, time and catalyst loading screens for the conjugate addition of *N*-methylaniline to 4-vinylpyridine

Entry	Temp (°C)	Catalyst loading (mol%)	Time (h)	Conversion (%) ^[a]
1	40	5	12	0
2	40	0	12	0
3	60	5	12	12
4	60	0	12	0
5	70	5	12	16
6	70	0	12	0
7	80	5	24	21
8	80	10	24	30
9	80	15	24	56
10	80	20	24	71
11	80	0	24	0
12	90	5	24	48
13	90	10	24	86
14	90	0	24	6

^[a]Conversions were determined through analysis of the ¹H NMR spectra of the crude reaction mixture (the integral for the protons at the β-position on the pyridine in the product were compared to the integral of the protons at the β-position on the pyridine in 4-vinylpyridine (dd, 7.15 ppm)).

Initially, reaction temperatures of 40-70 °C were run for 12 h for the 5 mol% catalyst loading (Entries 1-6, Table 35), with control reactions yielding no conversion into the product in all cases. The catalysed reactions at 40, 60 and 70 °C achieved the product in 0%, 12% and 16% respectively. Given the observed low reactivity at these temperatures, coupled with the aim of avoiding high reaction temperatures; a catalyst loading screen was run at 80 °C for 24 h (Entries 7-11, Table 35).

Catalyst loadings of 10, 15 and 20 mol% obtained the product, in 30%, 56% and 71% conversion respectively, with the control displaying no formation of product. Although a 71% conversion can be considered sufficient, the catalyst loading of 20 mol% was high, albeit of a cheap catalyst. Nonetheless, a screen for the 5 and 10 mol% catalyst loading at 90 °C for 24 h was run, for which the product was obtained in 48% and 86% conversion respectively (control – 6%). Given the higher yield and lower catalyst loading, the optimised reaction conditions selected were: 10 mol% $\text{Zn}(\text{NO}_3)_2 \cdot 6\text{H}_2\text{O}$, 90 °C for 24 h.

3.2.5.1.3. Thiophenol

The conjugate addition of thiophenol to 4-vinylpyridine at 25 °C for 12 h gave the product in 100% conversion for both the 2.5 and 5 mol% catalyst loadings, with the control achieving the product in 76% conversion (Entries 5 and 6, Table 33). The option of lowering the temperature of the reaction is a viable one, however decreasing the reaction temperature below room temperature can be as energy intensive as increasing it, so we opted to maintain the temperature at 25 °C and look to screen for reaction times instead (Table 36).

Table 36 Time and catalyst loading screen for the conjugate addition of thiophenol to 4-vinylpyridine

Entry	Temp (°C)	Catalyst loading (mol%)	Time (min)	Conversion (%) ^[a]
1	25	5	60	100
2	25	2.5	60	100
3	25	0	60	36
4	25	5	30	100
5	25	2.5	30	100
6	25	0	30	32
7	25	5	10	99
8	25	2.5	10	99
9	25	0	10	29

^[a]Conversions were determined through analysis of the ¹H NMR spectra of the crude reaction mixture (the integral for the protons at the β-position on the pyridine in the product were compared to the integral of the protons at the β-position on the pyridine in 4-vinylpyridine (dd, 7.15 ppm)).

To gauge how rapidly the reaction took effect both in the catalysed reactions and control, the reaction time was limited to 60 min (Entries 1-3, Table 36). Again both catalyst loadings yielded the product in 100% conversion; the control however, still demonstrated a high conversion into the product (36%). The reaction time was shortened to 30 min (Entries 4-6, Table 36), the catalysed reaction proceeded to quantitative conversion into the product, the control again showed some conversion (32%).

From here the reaction time was limited to 10 min (Entries 7-9, Table 36) and a conversion of 99% was observed for both catalyst loadings, and a small mitigation in the conversion of the control was observed (29%).

Granted this reaction does not require a catalyst for conjugate addition to occur, as an extension of the reaction time for the control at 25 °C to 18 h

would most likely have achieved the product in near quantitative conversions. However, our method does offer a faster alternative; quick transformations such as these, using an immobilised catalysts can be useful when considering their application in flow. Such a catalysed reaction would require minimum residence times and would provide the product in quantitative yield.

Given that the reaction for 10 min yielded the product in high conversion, the control for which exhibited the minimum conversion; these conditions coupled with 2.5 mol% $\text{Zn}(\text{NO}_3)_2 \cdot 6\text{H}_2\text{O}$, were chosen as the optimum for this nucleophile.

3.2.5.2. 2-Vinylpyridine

In a similar manner to the 4-vinylpyridine substrate, the same nucleophiles were screened for conjugate addition to the 2-vinylpyridine analogue. These reactions were performed under the optimised reaction conditions developed for the conjugate addition of morpholine to 4-vinylpyridine (Table 37).

Table 37 Screen of a variety of incoming groups for conjugate addition to 2-vinylpyridine catalysed by zinc nitrate

Entry	Nucleophile	Catalyst loading (mol%)	Conversion (%) ^[a]
1		5	0
2		0	0
3		5	0
4		0	0
5		5	100
6		0	61

^[a]Conversions were determined through analysis of the ¹H NMR spectra of the crude reaction mixture (the integral for the proton at the α-position on the pyridine in the product were compared to the integral of the proton at the α-position on the pyridine in 2-vinylpyridine (app. dd, 8.58 ppm)).

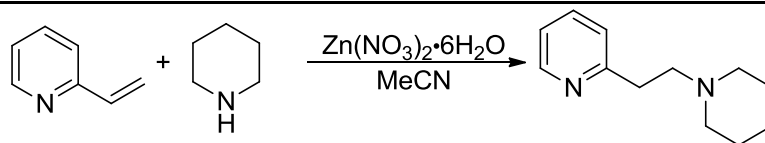
The 2-vinylpyridine system is clearly less reactive than the 4-vinyl analogue; with no conversion in either the catalysed or control reactions observed for the piperidine and *N*-methylaniline (Entries 1-4, Table 37). However, as with the 4-vinylpyridine the thiophenol yielded the product in 100% conversion with the control yielding the product in 61% conversion (Entry 5 and 6, Table 37). As a weak nucleophile, *N*-methylaniline gave no conversion in either catalysed or control reactions (Entries 3 and 4, Table 37). The system was optimised for each of the incoming groups. The lower reactivity of the 2-vinyl substrate in comparison to the 4-vinyl analogue is a result of the greater

electron-deficiency of the 4-position relative to the 2-position, which results in the higher reactivity observed for the 4-vinylpyridines. Thus, 2-vinylpyridines are likely to require more forcing conditions for the variety of incoming groups investigated.

3.2.5.2.1. Piperidine

The reaction of piperidine with 2-vinylpyridine under the optimised conditions for the parent reaction (5 mol% catalyst loading, 25 °C, 12 h) showed no conversion into the product. The subsequent optimisation studies for this nucleophile are shown in Table 38.

Table 38 Optimisation for reaction of 2-vinylpyridine with piperidine mediated by zinc nitrate Lewis acid



Entry	Temp (°C)	Catalyst loading (mol%)	Time (h)	Conversion (%) ^[a]
1	25	5	24	15
2	25	0	24	4
3	40	5	4	22
4	40	2.5	4	20
5	40	0	4	0
6	40	5	12	23
7	40	2.5	12	17
8	40	0	12	0
9	60	5	12	100
10	60	2.5	12	95
11	60	0	12	26
12	60	5	4	40
13	60	2.5	4	24
14	60	0	4	0

^[a]Conversions were determined through analysis of the ¹H NMR spectra of the crude reaction mixture (the integral for the proton at the α -position on the pyridine in the product were compared to the integral of the proton at the α -position on the pyridine in 2-vinylpyridine (app. dd, 8.58 ppm)).

The reaction time was extended to 24 h at 25 °C with a catalyst loading of 5 mol% (Entries 1-2, Table 38). A conversion of 15% was observed for the catalysed reaction and 4% for the control, clearly the reaction requires higher energy input. Accordingly the reaction was run with 2.5 and 5 mol% catalyst loadings at 40 °C for 4 h (Entries 3-5, Table 38), the result for which yielded a conversion of 20% and 22% respectively with the control showing no formation of product.

An increase in reaction time to 12 h under the same conditions did not achieve a substantial increase in conversion for either catalyst loading

(Entries 6-8, Table 38). At this point the reaction temperature was increased to 60 °C for 12 h for both catalyst loadings (Entries 9-11, Table 38); conversions of 100% and 95% were observed for the 5 and 2.5 mol% catalyst loading respectively, with the control yielding formation of product in 26%. In an attempt to mitigate the conversion in the control reaction, the 60 °C reaction was run for 4 h (Entries 12-14, Table 38) although the control reaction yielded no formation of product, the conversions for the catalysed reaction were also much lower.

Given that the reaction at 60 °C for 12 h for the 5 mol% catalyst loading achieved the product in 100% conversion; the optimum reaction conditions for the conjugate addition of piperidine to 2-vinylpyridine were chosen as follows: 5 mol% in $\text{Zn}(\text{NO}_3)_2 \cdot 6\text{H}_2\text{O}$, 60 °C for 12 h.

3.2.5.2.2. *N*-Methylaniline

Given the lack of reactivity observed for the reaction of 4-vinylpyridine with *N*-methylaniline, the investigation into optimising the reaction for the 2-vinylpyridine began with a catalyst loading screen at 80 °C for 24 h (Entries 1-5, Table 39). Conversions of 12%, 21%, 48% and 59% were observed for 5, 10, 15 and 20 mol% respectively; the control showed no conversion. A catalyst loading screen was run at 90 °C (Entries 6-9, Table 39) which achieved the product in 38%, 61% and 89% for 5, 10 and 15 mol% respectively. Thus, the optimised conditions for the conjugate addition of *N*-methylaniline to 2-vinylpyridine were chosen as: 15 mol% in $\text{Zn}(\text{NO}_3)_2 \cdot 6\text{H}_2\text{O}$ at 90 °C for 24 h.

Table 39 Optimisation of reaction of *N*-methylaniline with 2-vinylpyridine

Entry	Temp (°C)	Catalyst loading (mol%)	Time (h)	Conversion (%) ^[a]
1	80	5	24	12
2	80	10	24	21
3	80	15	24	48
4	80	20	24	59
5	80	0	24	0
6	90	5	24	38
7	90	10	24	61
8	90	15	24	89
9	90	0	24	-

^[a] Conversions were determined through analysis of the ¹H NMR spectra of the crude reaction mixture (the integral for the proton at the α-position on the pyridine in the product were compared to the integral of the proton at the α-position on the pyridine in 2-vinylpyridine (app. dd, 8.58 ppm)).

3.2.5.2.3. Thiophenol

The conjugate addition to 2-vinylpyridine at 25 °C for 12 h gave the product in 100% conversion for the catalysed reaction, with the control achieving the product in 61% (Entries 5 and 6, Table 37). As with the 4-vinylpyridine substrate, we opted to maintain the reaction temperature at 25 °C and look to screen for reaction time only (Table 40). Reduction of the reaction time to 60 min also yielded the product in 100% conversion for both catalyst loadings with the control giving a 45% conversion (Entries 1-3, Table 40), a reaction time of 30 min also yielded the product in 100% conversion, with a mitigation in the conversion for the control reactions providing a conversion of 23% (Entries 4-6, Table 40). The reaction time was further limited to 10 min for both catalyst loadings (Entries 7-9, Table 40), conversions of 90% and 95% were observed for the 5 and 2.5 mol% catalyst loadings respectively; the

control for this reaction also showed a conversion of 9%. The decrease in conversion of the 5 mol% catalyst loading relative to the 2.5 mol% loading could be due to reversion of the product to the starting materials, as observed with the high catalyst loading for the conjugate addition of morpholine to 4-vinylpyridine. The optimum reaction conditions selected were: 2.5 mol% in $\text{Zn}(\text{NO}_3)_2 \cdot 6\text{H}_2\text{O}$, 25 °C for 10 min, as the control gave minimal conversion into the product under these conditions.

Table 40 Reaction optimisation for the conjugate addition of thiophenol to 2-vinylpyridine

Entry	Temp (°C)	Catalyst loading (mol%)	Time (min)	Conversion (%) ^[a]
1	25	5	60	100
2	25	2.5	60	100
3	25	0	60	45
4	25	5	30	100
5	25	2.5	30	100
6	25	0	30	23
7	25	5	10	90
8	25	2.5	10	95
9	25	0	10	9

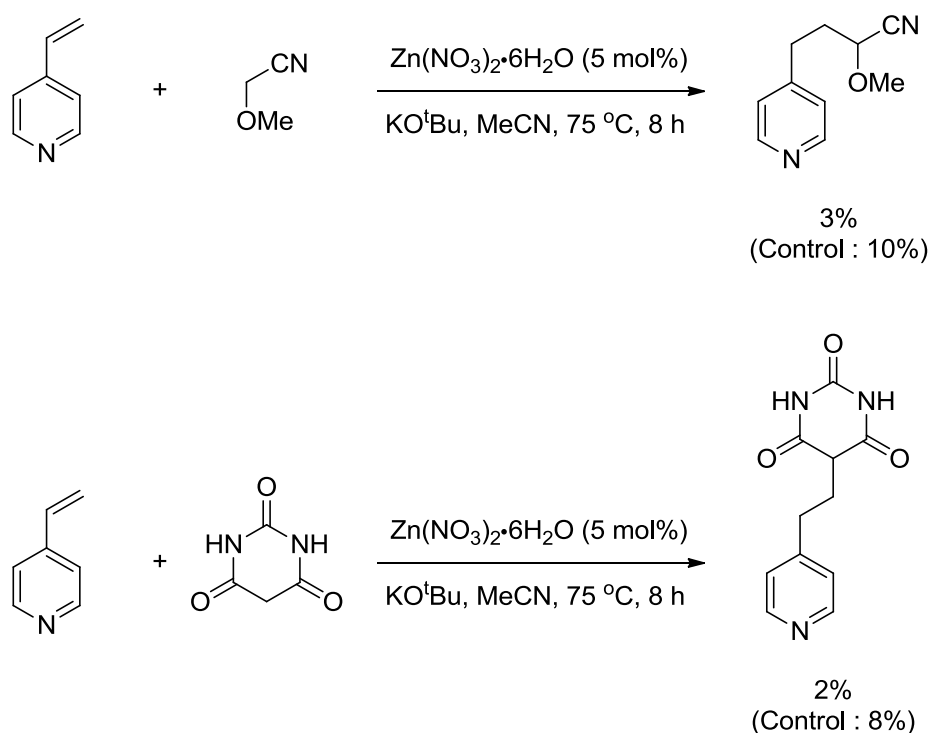
^[a]Conversions were determined through analysis of the ¹H NMR spectra of the crude reaction mixture (the integral for the proton at the α-position on the pyridine in the product were compared to the integral of the proton at the α-position on the pyridine in 2-vinylpyridine (app. dd, 8.58 ppm)).

3.2.5.3 Oxygen and carbon based nucleophiles

Oxygen and carbon based nucleophiles were investigated for conjugate addition to the 4-vinylpyridine substrate, however these showed little reactivity. In the case of activated esters, a variety of substrates was run for

reaction with 4-vinylpyridine under zinc Lewis acid catalysed conditions, however these similarly showed little conversion into the product.

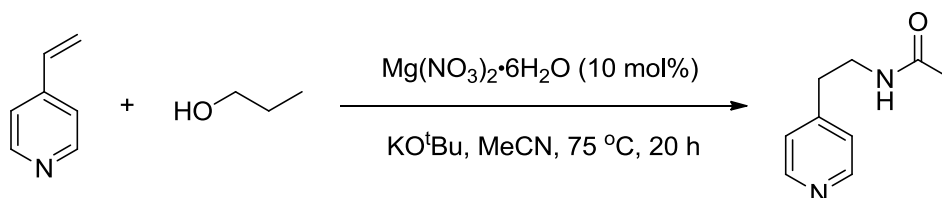
If we consider the reactions of methoxyacetonitrile and barbituric acid with 4-vinylpyridine (Scheme 97), the conversions for the catalysed reaction are quite low when the reaction is run with a catalyst loading of 5 mol% at 75 °C for 8 h. Clearly, optimisation might enhance the reaction conversions however a closer look at the control reactions, which display higher conversions than the catalysed system for both substrates, indicate that the Lewis acid in fact hinders the reaction.



Scheme 97: Conjugate addition of methoxyacetonitrile and barbituric acid to 4-vinylpyridine under zinc Lewis acid mediated conditions

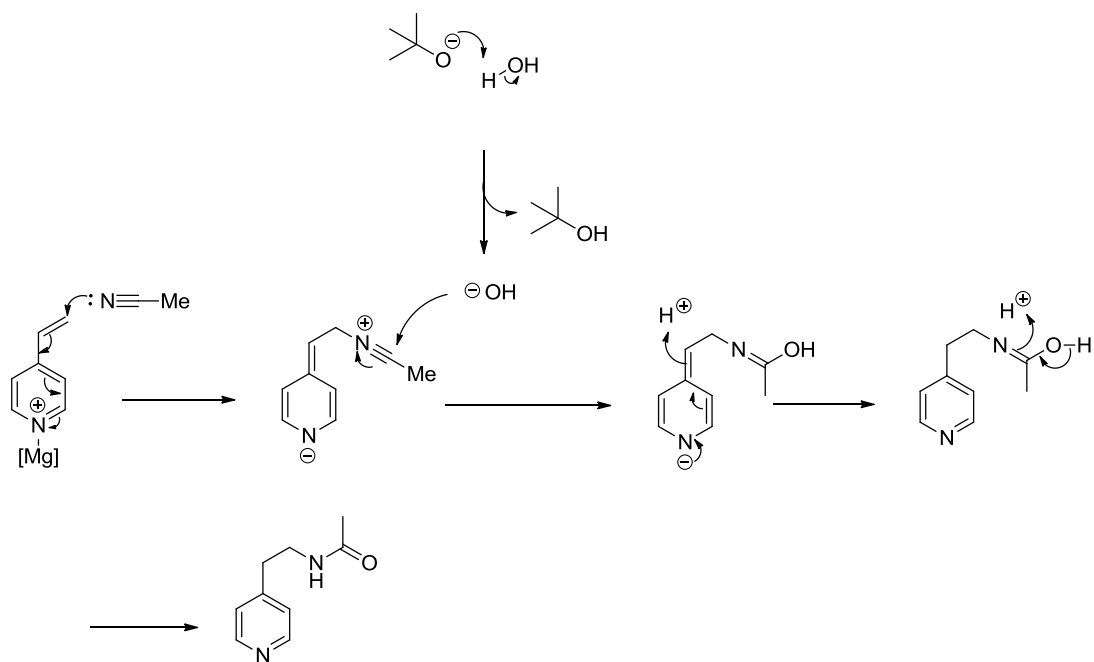
This mitigation in conversion as a result of addition of the catalyst can be attributed to coordination of these nucleophiles to the zinc catalyst, thus preventing the catalyst from mediating the reaction as well as preventing the nucleophile from carrying out the conjugate addition reaction.

Oxygen based nucleophiles such as alcohols performed well in the S_NAr reactions when the incoming group was used as a solvent in the presence of a base. The vinylpyridines are far more stable than 4-chloropyridine at high temperatures and with no source of acid in this methodology, the presence of a base was not required. However, investigations into the use of alcohol incoming groups for conjugate addition to the 4-vinyl group were carried out by the project student who investigated the use of magnesium nitrate as a Lewis acid for the activation of vinylpyridines for conjugate addition. The results of his investigations showed that the use of an alcohol incoming group in equimolar amounts to the vinylpyridine in acetonitrile (in the presence of a magnesium Lewis acid) led to the formation of an amide (Scheme 98).



Scheme 98: Reaction carried out by Teasdale for the reaction of propanol with 4-vinylpyridine under magnesium nitrate catalysed conditions

Given the reagents present in the reaction mixture (Scheme 98), it is likely that the formation of the amide proceeded by the Ritter reaction mechanism, known for the formation of *N*-alkyl carboxamides from aliphatic and aromatic nitriles (Scheme 99).⁷⁴ With this observed amide formation under these reaction conditions, it was hypothesised that the same transformation would be observed with the use of the zinc Lewis acid catalyst, thus investigations into oxygen nucleophiles were not pursued.



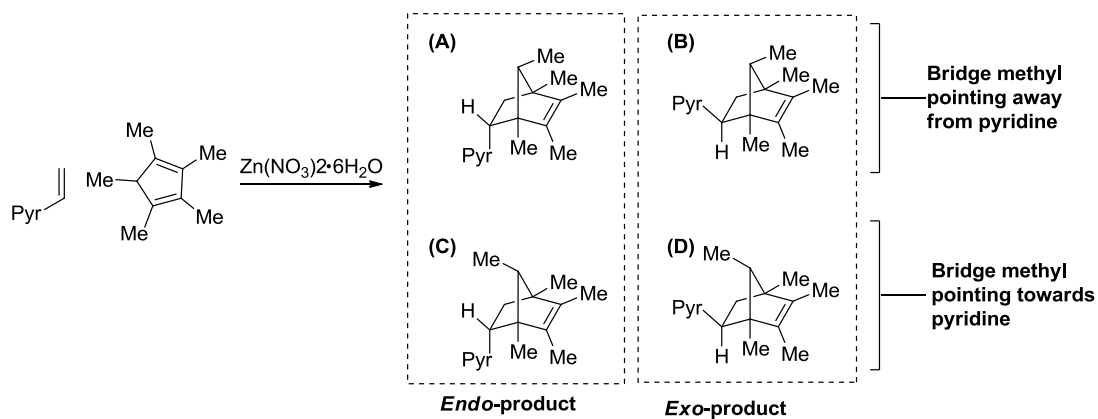
Scheme 99: Ritter reaction mechanism for the formation of an amide *in situ*, by the reaction of propanol with 4-vinylpyridine in acetonitrile in the presence of magnesium nitrate and potassium *t*-butoxide

3.3. Lewis acid catalysed Diels–Alder reactions of vinylpyridines

Given that the vinylpyridine substrates carried out conjugate addition reactions under zinc Lewis acid catalysis we hypothesised that our catalyst could also be used to mediate a Diels–Alder cyclisation of vinylpyridine with a diene such as 1,2,3,4,5-pentamethyl cyclopentadiene (Cp*H). Given the electron poor nature of the vinyl group and the electron-rich nature of the diene, we would expect the DA reaction to proceed as a normal electron-demand.

There are four possible products that could be achieved from the DA reaction of vinylpyridine with Cp*H; in the first instance considerations as to the *endo* or *exo* product need to be taken into account. In the *endo* product, the pyridine functionality points away from the bridge group, whereas in the *exo* it would be pointing towards it ((**A**) and (**B**), Scheme 100). The *endo*-rule predicts that the *endo*-product is favoured over the *exo*-product as a result of the favourable bonding interactions between the dienophile and the developing π -bond at the back of the diene.

Equally, a question of which face of the Cp*H reacts with the vinylpyridine needs to be appraised; the one in which the methyl group at the saturated carbon would be pointing towards the vinyl group (hindered), or on the face in which it points away ((**A**) and (**C**), Scheme 100). The face that is less hindered in which the methyl group of the bridge carbon is pointing away from the incoming vinylpyridine would be favoured. Thus, the expected product of the reaction of a vinylpyridine with Cp*H is the *endo*-product with the bridge methyl pointing towards the alkene and away from the pyridine: (**A**) in Scheme 100.



Scheme 100: Possible Diels-Alder cyclisation products of reaction of vinylpyridine with Cp^*H

As with the nucleophiles for the conjugate addition reactions; the system was optimised for the Diels-Alder cyclisation reaction of 2- and 4-vinylpyridine with Cp^*H .

3.3.1. 4-Vinylpyridine

The results of temperature, time and catalyst loading optimisation for the Diels–Alder reaction of Cp*H with 4-vinylpyridine are shown in Table 41.

Table 41 Temperature, time and catalyst loading screen for the optimisation of the Diels–Alder reaction of 4-vinylpyridine with Cp*H catalysed by zinc nitrate Lewis acid

Entry	Temp. (°C)	Catalyst loading (mol%)	Time (h)	Conversion (%) ^[a]	Diastereomeric ratio
1	25	5	12	69	87:13
2	25	2.5	12	63	87:13
3	25	0	12	10	81:19
4	25	5	24	72	86:14
5	25	2.5	24	65	85:15
6	25	0	24	10	81:19
7	40	5	4	79	89:11
8	40	2.5	4	75	88:12
9	40	0	4	22	79:21

^[a] Conversions were determined through analysis of the ¹H NMR spectra of the crude reaction mixture (the integral for the protons at the β-position on the pyridine in the product were compared to the integral of the protons at the β-position on the pyridine in 4-vinylpyridine (dd, 7.15 ppm)).

Initially, the reaction was screened for two catalyst loadings and was run under the optimised time and temperature conditions developed for the conjugate addition of morpholine to 4-vinylpyridine (25 °C, 12 h). Good conversions were observed under these conditions with 5 mol% catalyst loading giving the product in 69% conversion (Entry 1, Table 41) and the reaction run with 2.5 mol% catalyst loading proceeding in 63% conversion

(Entry 2, Table 41); and control giving the product in 10% conversion. In a drive to improve the conversion the reaction was run at 25 °C for both catalyst loadings for 24 h (Entries 4-6, Table 41). The conversion improved marginally for both catalyst loadings with 72% and 65% conversion observed for the 5 and 2.5 mol% catalyst loading respectively; the control yielded the product in 10% conversion. The reaction was then run at 40 °C for 4 h for both catalyst loadings (Entries 7-9, Table 41): conversions of 79%, 75% and 22% were observed for the 5 and 2.5 mol% catalyst loadings and the control respectively. Given the small increase in reaction conversion in going to from 25 °C to 40 °C for the catalysed reactions and the greater increase in conversion observed for the control reaction at 40 °C, optimised reaction conditions of: 5 mol% in $\text{Zn}(\text{NO}_3)_2 \cdot 6\text{H}_2\text{O}$, 40 °C, 4 h were selected.

Worthy of note, from the results shown in Table 41, the zinc catalysed reactions versus the control, show an improvement in selectivity for the catalysed reaction. With the control reactions at 25 °C (Entries 3 and 6, Table 41) giving an 81:19 dr for the two stereoisomers present in the crude reaction mixture. The zinc catalysed reactions at the same temperature and times showed an improvement of 87:13 dr for the reactions run at 25 °C for 12 h (Entries 1-2, Table 41), and a dr of 86:14 and 85:15 for the catalysed reactions run at 25 °C for 24 h (Entries 4-5, Table 41). As would be expected, running the reaction at a higher temperature, shows a marginal decrease in selectivity in the control reaction 78:22 (Entry 9, Table 41), owed to the increase in energy gained by the reaction mixture allowing for more occurrences of the reaction that forms the minor isomer to occur. Conversely, the catalysed mixture shows a marginal improvement in selectivity for the reactions at this temperature.

Isolation gave the product in 78% yield; with a diastereomeric ratio of 89:11 calculated from the integrals of the bridge methyl groups of both stereoisomers observed in the ^1H NMR spectrum.

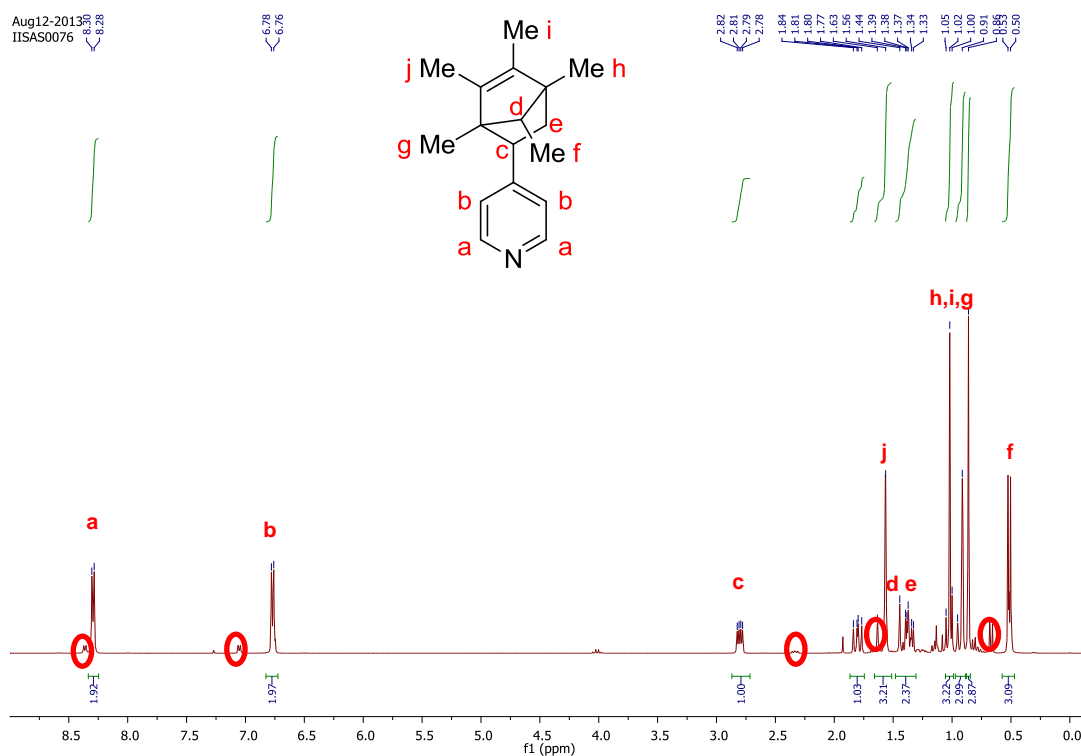


Figure 20: ^1H NMR spectrum of 4-(1,4,5,6,7-pentamethylbicyclo[2.2.1]hept-5-en-2-yl)pyridine (circled signals are attributed to minor isomer)

The major and minor products were determined to be both *endo*-isomers; with the difference between the isomers being the orientation of the bridge methyl group. In the major product, the bridge methyl group is pointing away from the pyridine and in the minor product it is pointing towards the pyridine (Figure 21).

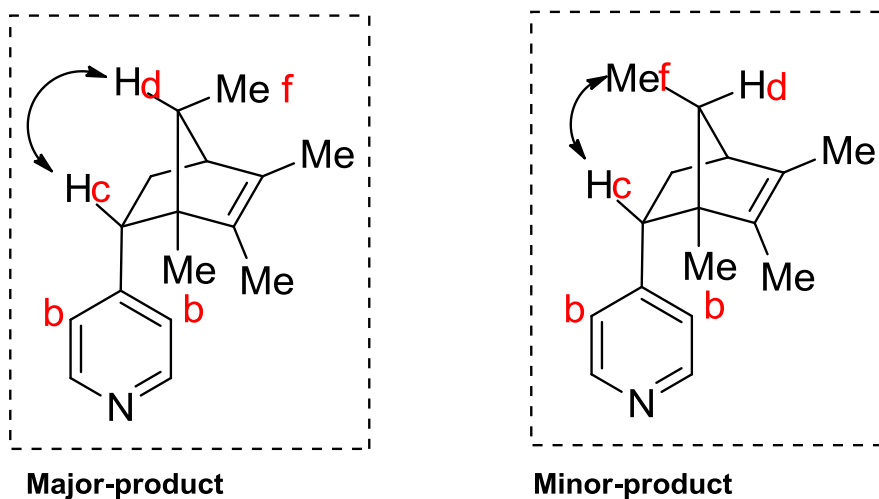
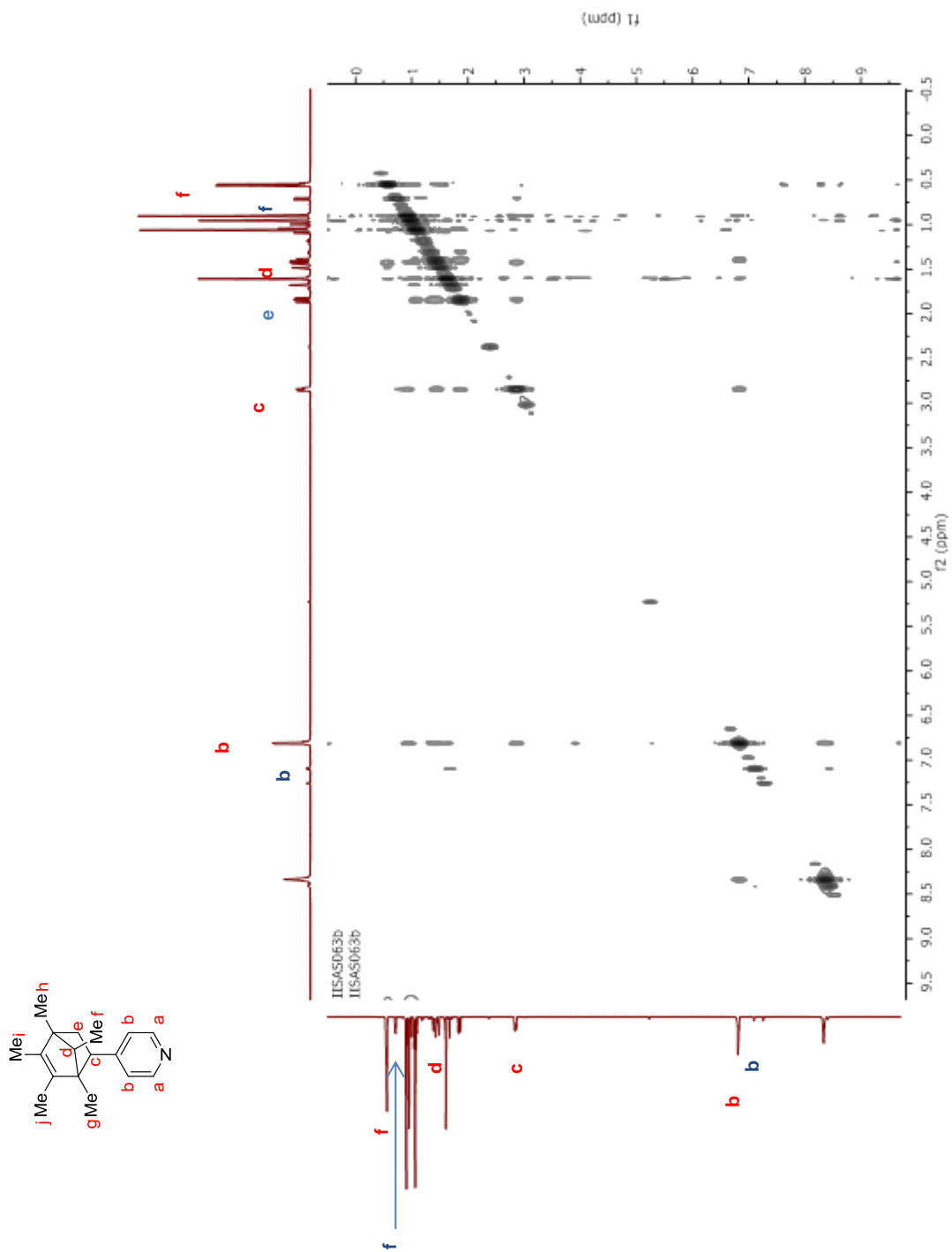


Figure 21: Major and minor isomers of 4-(1,4,5,6,7-pentamethylbicyclo[2.2.1]hept-5-en-2-yl)pyridine

The structures of the isomers were determined through examination of the NOESY Spectrum of the isolated product mixture (Figure 22).

Figure 22: NOESY Spectrum of 4-(1,4,5,6,7-pentamethylbicyclo[2.2.1]hept-5-en-2-yl)pyridine



The chemical shift of proton “d” sits very closely to that of one of the “e” protons. Closer inspection shows that the chemical shift of “d” is a little more downfield and shows an apparent quartet expected for a proton adjacent only to methyl protons, overlapping with the signal for one of the “e” protons. In the major isomer a cross peak can be seen between the bridge proton “d” and proton “c”, indicating interaction between the two protons as a result of the pyridine pointing away from the bridge group in the *endo*-isomer, thus supporting the argument for the *endo*-configuration (Figure 23).

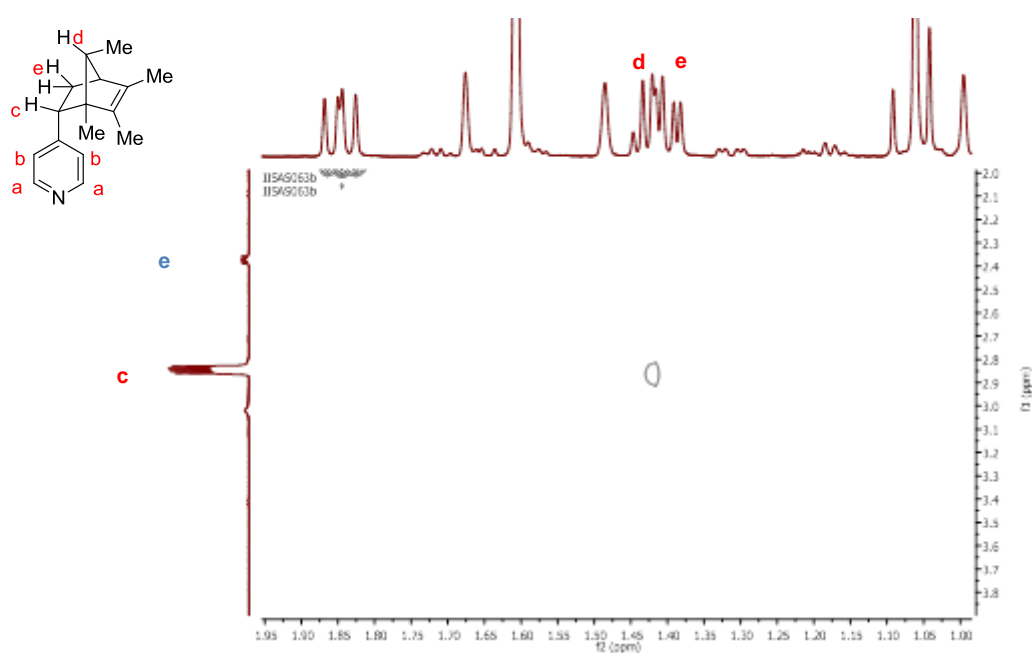


Figure 23: Cross peak between bridge proton “d” and proton “c” in major isomer

The minor isomer shows a cross peak between the bridge methyl protons “f” and proton “c” that is not observed in the major isomer (Figure 24), this is indicative of two things: that the bridge methyl group is pointing towards proton “c”, which is implicit to the pyridine pointing away from the bridge group in an *endo*-conformation; and that the bridge methyl group is pointing away from the alkene.

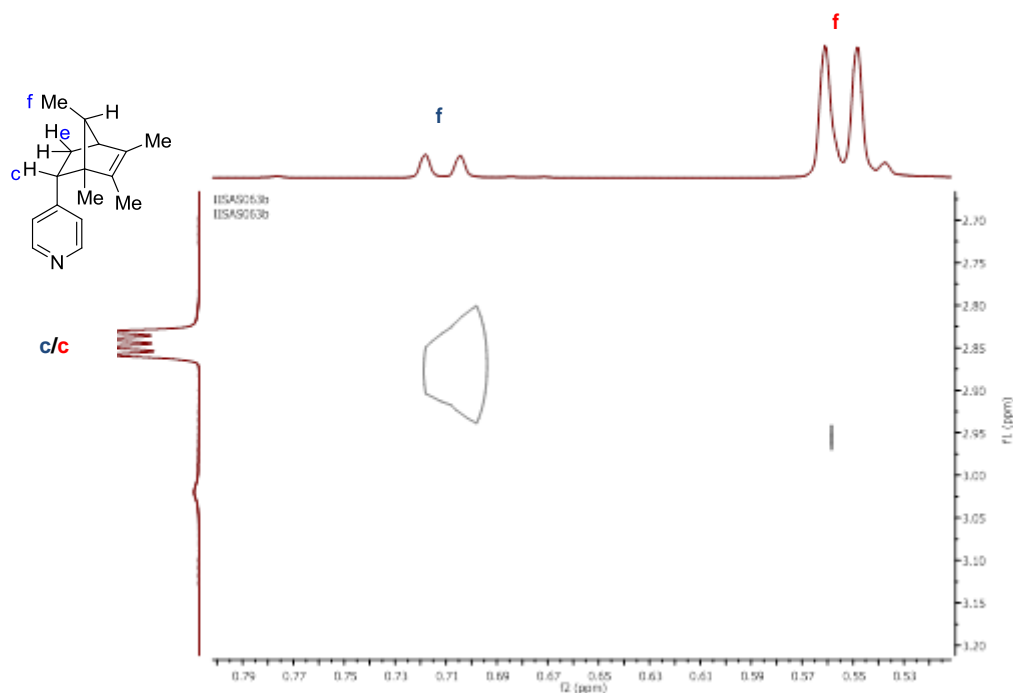
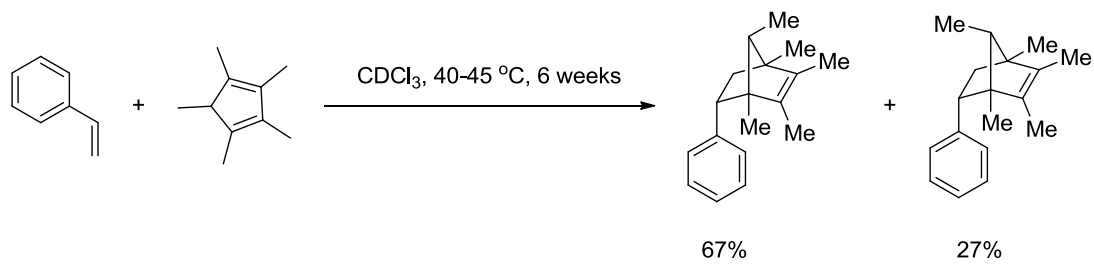


Figure 24: Cross peak between bridge methyl protons “f” and proton “c” in the minor isomer

It can be concluded that the two isomers are indeed *endo*-isomers; the major isomer is the result of the reaction of the vinylpyridine with the less hindered face of the Cp*H in which the methyl group on the bridge carbon is pointing away from the incoming group. The minor isomer is the product of the reaction of vinylpyridine with the Cp*H face in which the methyl group is pointing towards it.

This conclusion is further supported by the work carried out by Maitlis and co-workers,⁷⁶ who reacted styrene with Cp*H to give the same *endo*-isomer products, with the major product containing the bridge methyl group pointing away from the phenyl ring and the minor product containing the bridge methyl group pointing towards the phenyl ring and away from the alkene group (Scheme 101).



Scheme 101: Reaction of styrene with Cp*H to give the same isomers achieved with reaction of vinylpyridine with Cp*H [76]

3.3.2. 2-Vinylpyridine

The results of temperature, time and catalyst loading optimisation for the Diels–Alder reaction of Cp*H with 2-vinylpyridine are shown in Table 42.

Table 42 Temperature, time and catalyst loading screen for the optimisation of the Diels–Alder reaction of 2-vinylpyridine with Cp*H catalysed by zinc nitrate Lewis acid

Entry	Temp. (°C)	Catalyst loading (mol%)	Time (h)	Conversion (%) ^[a]	Diastereomeric ratio
1	25	5	12	70	89:11
2	25	2.5	12	65	89:11
3	25	0	12	4	79:21
4	25	5	24	71	88:12
5	25	2.5	24	66	87:13
6	25	0	24	4	78:22
7	40	5	4	67	90:10
8	40	2.5	4	79	90:10
9	40	0	4	9	75:25

^[a] Conversions were determined through analysis of the ¹H NMR spectra of the crude reaction mixture (the integral for the proton at the α-position on the pyridine in the product were compared to the integral of the proton at the α-position on the pyridine in 2-vinylpyridine (app. dd, 8.58 ppm)).

In a similar manner to the 4-vinylpyridine analogue, the reaction was initially screened for catalyst loadings at 25 °C for 12 h (Entries 1-3, Table 42). Good conversions were observed under these conditions with 5 mol% catalyst loading giving the product in 70% conversion (Entry 1, Table 42) and the reaction run with 2.5 mol% catalyst loading proceeding in 65% conversion (Entry 2, Table 42); with the control giving the product in 4% conversion (Entry 3, Table 42).

Increasing the reaction time for all catalyst loadings to 24 h (Entries 4-6, Table 42) generated little improvement in conversion for both catalyst loadings with 71% and 66% conversions observed for the 5 and 2.5 mol% catalyst loadings respectively. Thus, the reaction was run at 40 °C for 4 h (Entries 7-9, Table 42): conversions of 67%, 79% and 9% were observed for the 5 and 2.5 mol% catalyst loadings and control respectively.

Given the small conversion into the product seen with the control at 40 °C, and the improved conversion at a lower catalyst loading of 2.5 mol%; the optimised reaction conditions were thus chosen as: 2.5 mol% in $\text{Zn}(\text{NO}_3)_2 \cdot 6\text{H}_2\text{O}$ at 40 °C for 4 h. Similar trends in selectivity were observed for the 2-vinylpyridine as with the 4-vinylpyridine.

Isolation gave the product in 76% yield; with a diastereomeric ratio of 90:10 calculated from the integrals if the bridge methyl groups of both stereoisomers observed in the ^1H NMR spectrum.

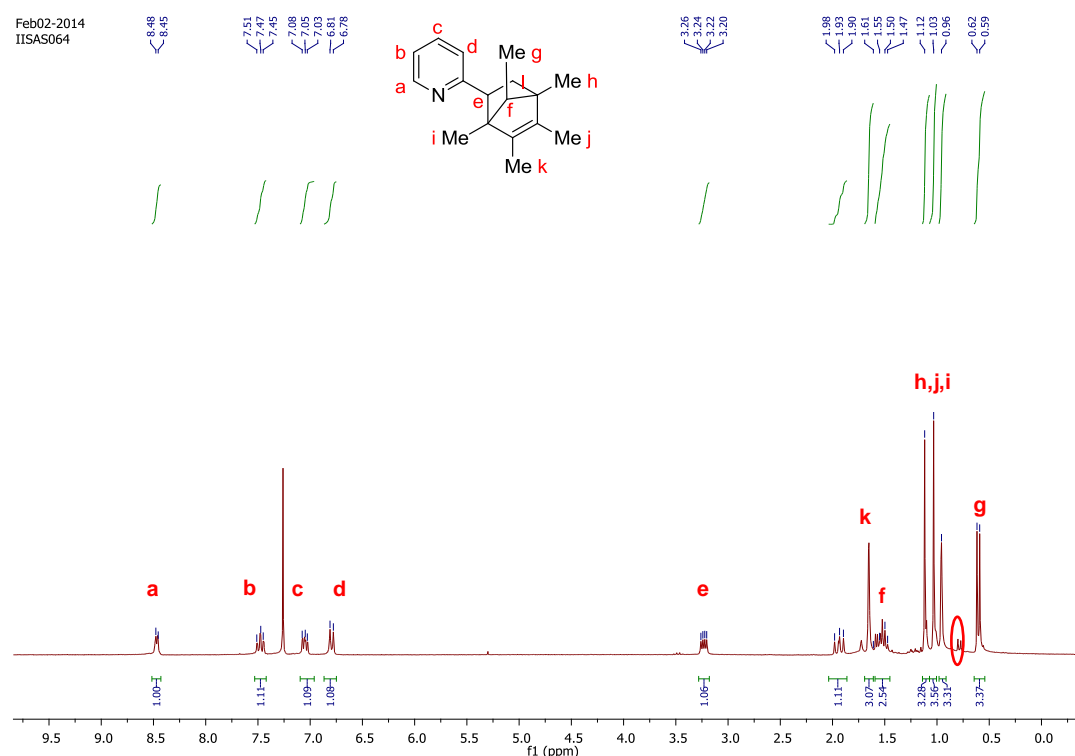


Figure 25: ^1H NMR spectrum of 2-(1,4,5,6,7-pentamethylbicyclo[2.2.1]hept-5-en-2-yl)pyridine

As with the 4-vinylpyridine cycloadduct, the product isomers were determined to be two *endo*-isomers, the major isomer being the product of

the reaction of the 2-vinylpyridine with the less hindered Cp*H face, in which the bridge methyl group points away from the pyridine. The minor isomer contains the bridge methyl group pointing towards the pyridine and away from the alkene bond (Figure 26).

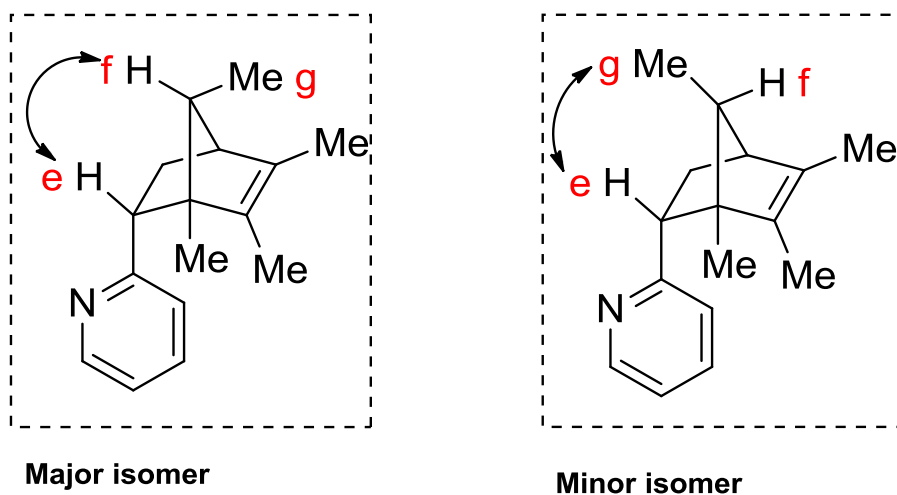
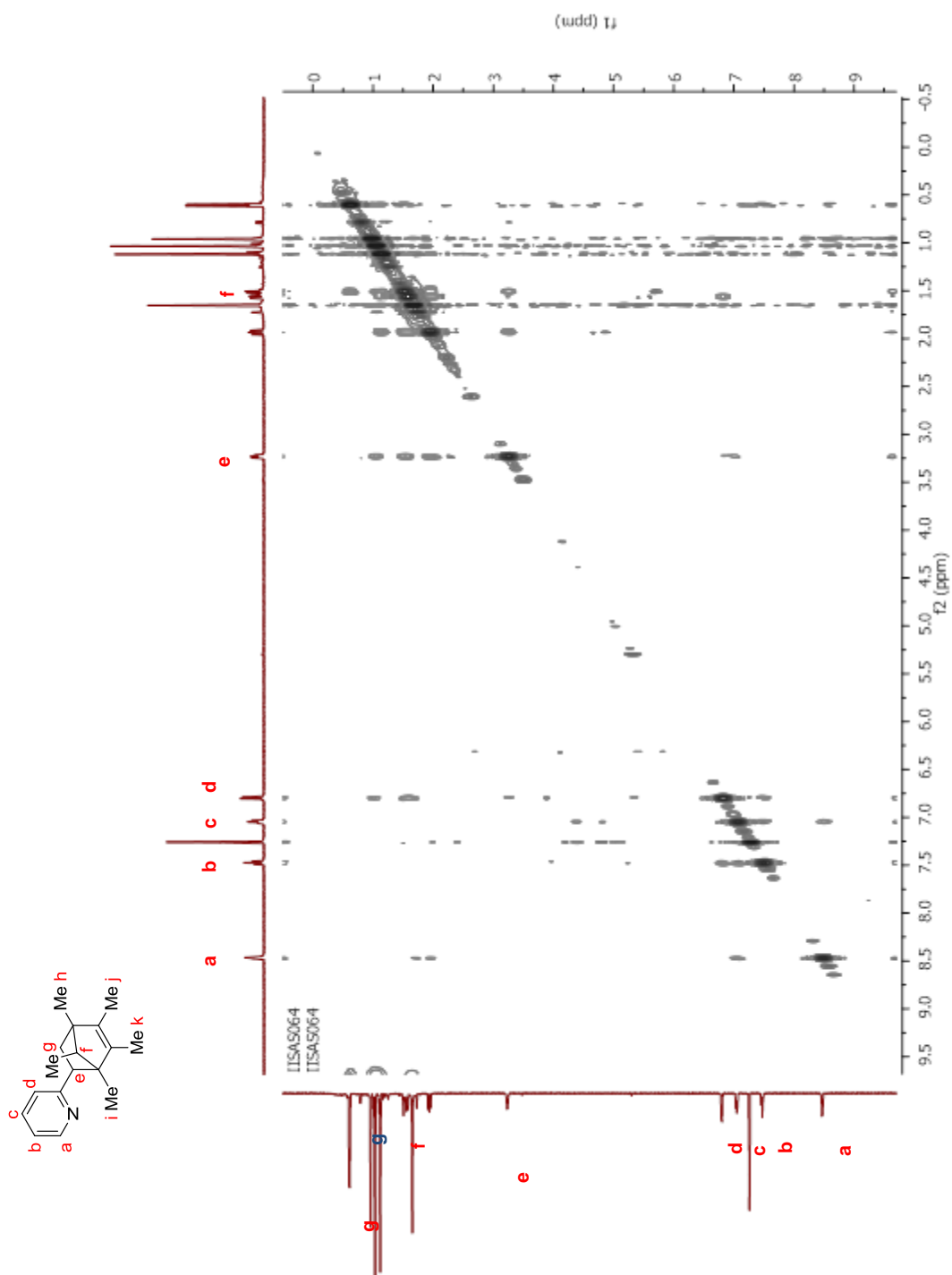


Figure 26: Expected structures of major and minor isomers of 2-(1,4,5,6,7-pentamethylbicyclo[2.2.1]hept-5-en-2-yl)pyridine

A NOESY Spectrum of the isolated product was also run to confirm the predicted isomers of the reaction (Figure 27). For the major isomer, cross peaks should be observed between the proton “e” and the bridge proton “f”. In the case of the minor isomer, cross peaks between the “e” protons and the bridge methyl “g” protons should be observed.

Figure 27: NOESY Spectrum of 2-(1,4,5,6,7-pentamethylbicyclo[2.2.1]hept-5-en-2-yl)pyridine



The major isomer showed a cross peak between the bridge "f" proton and proton "e" indicating interaction between the two protons, thus the major isomer is indeed the *endo*-product (Figure 28).

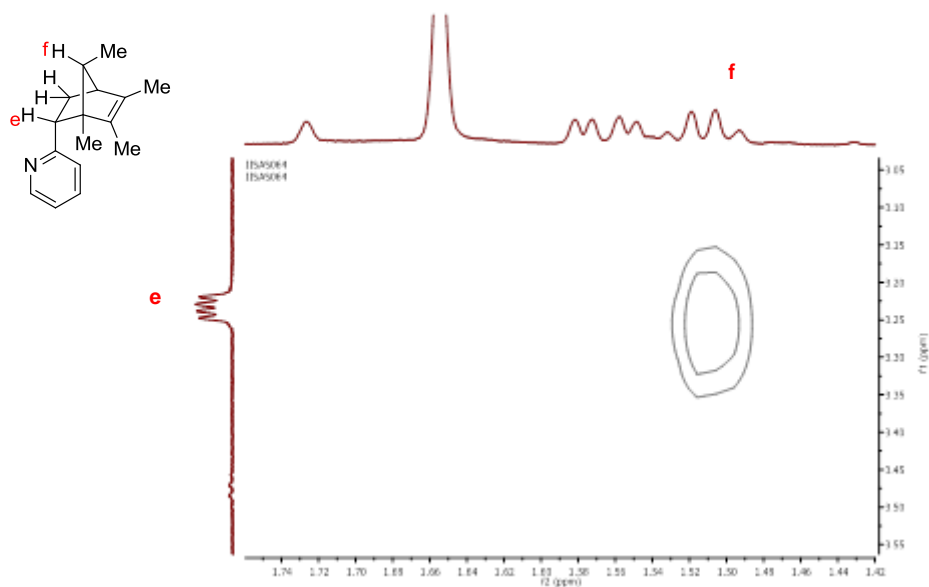


Figure 28: Cross peak between bridge proton "f" and proton "e" in major isomer

This conclusion is further supported by the observed interaction of the bridge methyl group protons "g" with proton "e" in the minor isomer (i.e. the methyl group is pointing away from the alkene, towards the pyridine) and its absence in the major isomer (Figure 29).

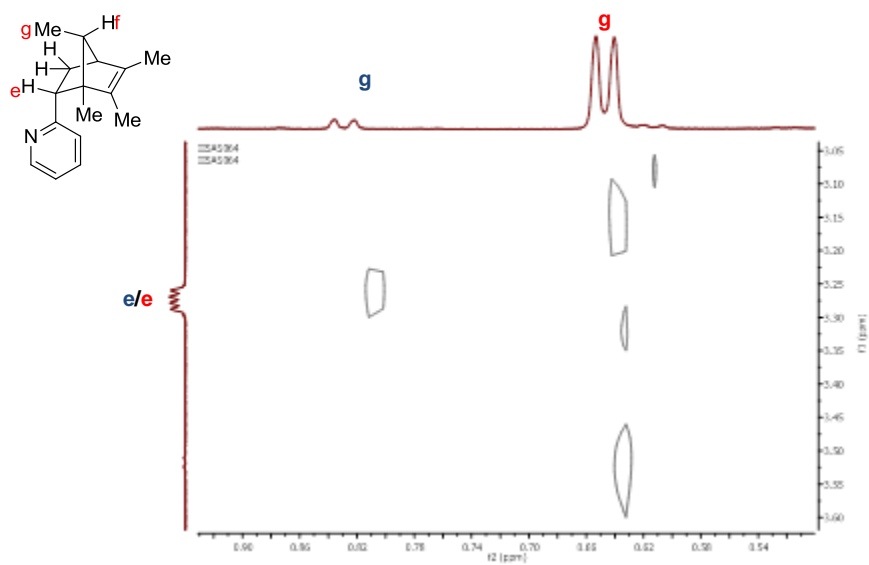


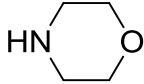
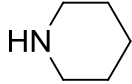
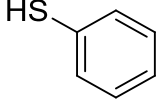
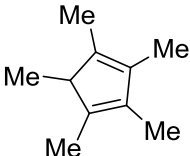
Figure 29: Cross peak observed between bridge methyl protons "g" and proton "e" in minor isomer

3.4. Scope in nucleophile – Summary

The selected optimised conditions for each substrate and nucleophile were run and the products isolated; reaction conditions and yields are shown in Table 43.

Table 43 Optimised conditions and isolated yields for conjugate addition reactions of successful nucleophiles with 2-/4-vinylpyridine using zinc nitrate as the Lewis acid catalyst

Entry	Substrate	Nucleophile	t (h)	T (°C)	Catalyst loading (mol%)	Conv. (%) ^[a]	Yield (%)
1			24	90	10	86	85
2			12	25	5	100	99
3			4	40	5	90	87
4			10 min	25	2.5	99	96
5		<i>Diels–Alder</i> 	4	40	5	79	78 (89:11 dr)
6			24	90	15	89	87

7		24	25	5	94	90
8		12	60	5	100	95
9		10 mi n	25	2.5	95	92
10	<i>Diels–Alder</i> 	4	40	2.5	79	76 (90:10 dr)

^[a]Conversions were determined through analysis of ¹H NMR spectra of the crude reaction mixture; 4-vinylpyridine derivatives: the integral for the protons at the β -position on the pyridine in the product were compared to the integral of the protons at the β -position on the pyridine in 4-vinylpyridine (dd, 7.15 ppm); 2-vinylpyridine derivatives: the integral for the proton at the α -position on the pyridine in the product were compared to the integral of the proton at the α -position on the pyridine in 2-vinylpyridine (app. dd, 8.58 ppm)

3.5. Conclusions

A novel methodology of activating vinylpyridines towards conjugate addition from nitrogen and sulfur based nucleophiles as well as Diels–Alder cyclisations has been developed. The zinc nitrate Lewis acid catalyst operates through binding to the pyridine nitrogen, which polarises the vinyl group and activates it towards conjugate addition and Diels–Alder cyclisations. This protocol offers a simple, mild and expedient method for achieving conjugate addition products compared with current literature methods.

The methodology developed is limited by its inability to carry out conjugate additions with oxygen and activated esters, as a result of coordination of the esters to the zinc Lewis acid and formation of an amide bond *in situ* in the case of incoming alcohol groups.

3.6. Future work

3.5.1. Oxygen nucleophiles

Further work could be carried out to optimise the system for reaction with oxygen nucleophiles. The current methodology utilises acetonitrile in the reaction conditions which resulted in the formation of amide functionality. A solvent screen for the reaction of oxygen-based nucleophiles could be carried out to circumvent this formation and extend the scope in incoming group to include this class.

3.5.2. Broader substrate scope

Fused ring systems are important motifs in synthetic chemistry and an extension in the scope in substrate would further expand the utility of the process. Given that this methodology was successful for 2- and 4-vinylpyridines, fused aliphatic ring analogues could also be explored for this process such as 5,6-dihydroquinoline and 7,8-dihydroisoquinoline (**A** and **B**, Figure 30). Moreover, building on both the work carried out for the aromatic substitution and this electron relay observed in the vinylpyridine, functionalised quinoline and isoquinoline derivatives could be achieved through remote activation of the C-X bonds in **C**, **D**, **E** and **F** (Figure 30) through Lewis acid activation of the pyridine ring. Furthermore, a transformation that would be of great interest would be nucleophilic substitution at the alkene that preserves the alkene moiety in the product (**G** and **H**, Figure 30), the use of Lewis acids could be explored for this transformation.

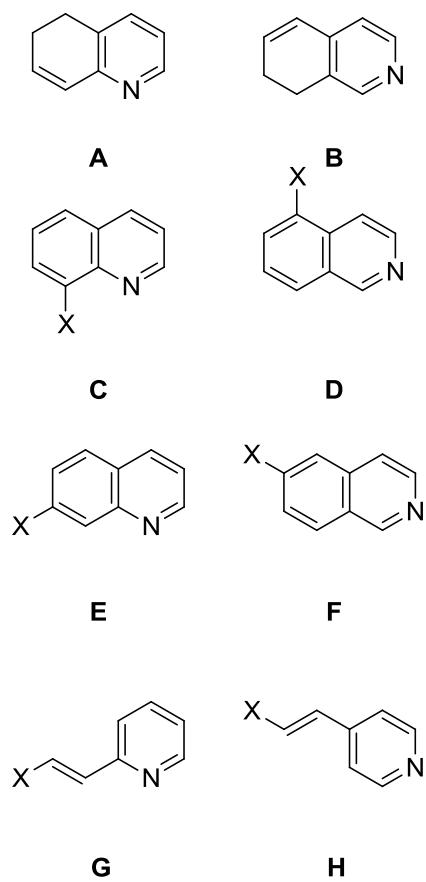


Figure 30: Potential substrates for conjugate addition reaction catalysed by zinc nitrate

Chapter 4: Experimental

“To call in the statistician after the experiment is done may be no more than asking him to perform a post-mortem examination: he may be able to say what the experiment died of”

-Ronald Fischer

4.1. Materials and Methods

Starting materials and solvents were obtained from commercial sources without further purification. Chemicals were purchased from Acros Organics, Sigma-Aldrich, Alfa Aesar, Fluka, Lancaster, Maybridge, Strem or TCI UK and used without further purification. Thin layer chromatography was carried out on aluminium or plastic backed silica plates (Aldrich). Plates were visualised under UV (254 nm) light, followed by staining with phosphomolybdic acid dip or potassium permanganate and gentle heating. Compound separations were carried out using column chromatography on 60 micron dry silica (Aldrich), solvents were concentrated using a Büchi rotary evaporator.

^1H NMR / ^{13}C NMR spectra were run in deuterated (>99.5%) solvent (Aldrich, Fluorochem) and recorded on a Bruker Avance 250 (250 MHz, 62.5 MHz) or a Bruker Avance (300 MHz, 75 MHz) spectrometer at 303 K. Chemical shifts are reported as parts per million (ppm) with reference to residual solvent signals. Coupling constants are reported in Hz and signal multiplicities are reported as singlet (s), doublet (d), triplet (t), quartet (q), doublet of doublets (dd), triplet of doublets (td), multiplet (m) or a broad singlet (brs).

Mass spectra were recorded using an electrospray Time-of-Flight MicroTOFTM (ESI-TOF) mass spectrometer (Bruker Daltonik, GmbH, Bremen, Germany), coupled with an Agilent 1200 LC system (Agilent Technologies, Waldbronn, Germany). The observed isotope pattern matched the corresponding theoretical values as calculated from the expected elemental formula. Masses were recorded in either positive or negative mode. Samples were introduced as either flow injection or syringe pump. Samples were diluted with HPLC grade methanol.

Infra-red spectra were recorded on a PerkinElmer 100 FT-IR spectrometer, using a Universal ATR accessory for sampling; relevant absorbance quoted as $\tilde{\nu}$ in cm^{-1} . Melting points were determined using Stuart SMP10 melting point equipment using closed end capillary tubes and are uncorrected.

4.2. Chapter 2 Experimental Procedures

Procedure I: 4-Halopyridine freebase

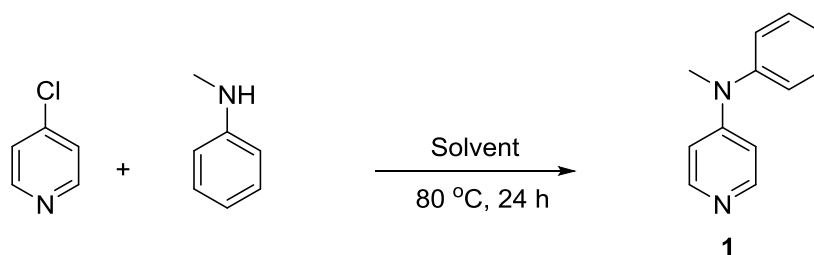
4-Halopyridine hydrochloride (88.5 mmol) was added to 100 mL of cold saturated sodium hydrogen carbonate solution. Once the mixture ceased to effervesce, the mixture was washed with 2 × 100 mL cold CH₂Cl₂, the organic extracts were washed with 2 × 40 mL cold brine solution and were dried over MgSO₄. Solvent was removed *in vacuo* using a cold water bath. Compound was analysed by ¹H and ¹³C NMR spectroscopy and used without further purification.

General note on handling 4-chloropyridine freebase:

4-Chloropyridine freebase is unstable at room temperature and should be stored in a freezer (~ -20 °C). Addition of 4-chloropyridine occurred once all other reactants had been added to the reaction vessel and directly from a -20 °C freezer.

Solvent screen: Control Reaction

(Table 3, Chapter 2)

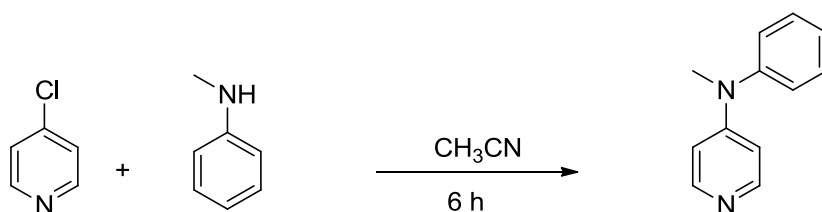


To a solution of *N*-methylaniline (2 mmol, 0.21 g, 0.22 mL) in the appropriate solvent, 4-chloropyridine (2 mmol, 0.23 g, 0.19 mL) was added. The reaction mixture was allowed to stir at 80 °C for 24 h. On completion the reaction was allowed to cool to room temperature and solvent removed *in vacuo*, using a water bath temperature of 40 °C. Conversions were determined by analysis of the ¹H NMR spectra of the crude reaction mixtures.

N-Methyl-*N*-phenylpyridin-4-amine (**1**): ¹H NMR (300 MHz, CDCl₃): δ_H= 8.29 (2H, dd, *J*= 5.2, 1.3 Hz, -CH=N-CH-), 7.50-7.45 (2H, m, aromatic), 7.35-7.30 (1H, m, aromatic), 7.30-7.24 (2H, m, aromatic), 6.62 (2H, dd, *J*= 5.2, 1.3 Hz, -CH=C(N)-CH), 3.34 (3H, s, N-CH₃)

Temperature Screen: Control Reaction

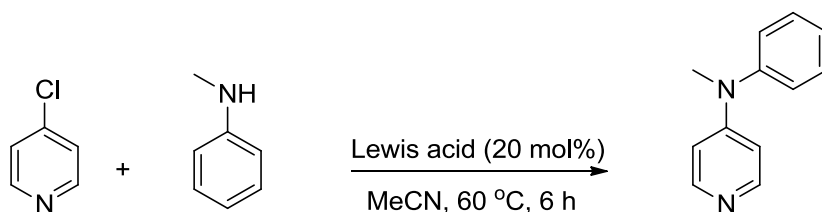
(Table 4, Chapter 2)



To a solution of *N*-methylaniline (2 mmol, 0.21 g, 0.22 mL) dissolved in CH₃CN (2 mL), 4-chloropyridine (2 mmol, 0.23 g, 0.19 mL) was added and the reaction mixture was allowed to stir at the appropriate temperature for 6 h. On completion the reaction was allowed to cool to room temperature and solvent removed *in vacuo*, using a water bath temperature of 40 °C. Conversions were determined by analysis of the ¹H NMR spectra of the crude reaction mixtures.

Lewis acid catalyst screen

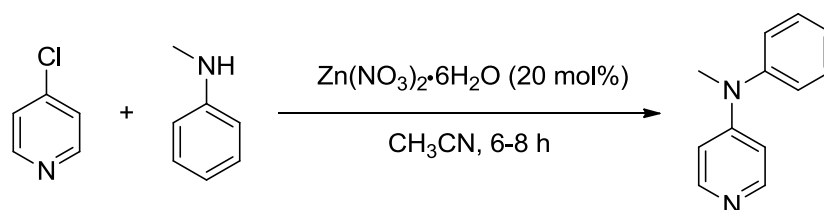
(Tables 5-6, Chapter 2)



The appropriate Lewis acid (20 mol%) was dissolved in CH₃CN (2 mL), to which *N*-methylaniline (2 mmol, 0.21 g, 0.22 mL) was added followed by 4-chloropyridine (2 mmol, 0.23 g, 0.19 mL). The reaction mixture was allowed to stir at 60 °C for 6 h. On completion the reaction was allowed to cool to room temperature and solvent removed *in vacuo*, using a water bath temperature at 40 °C. Conversions were determined by analysis of the ¹H NMR spectra of the crude reaction mixtures.

Temperature screen

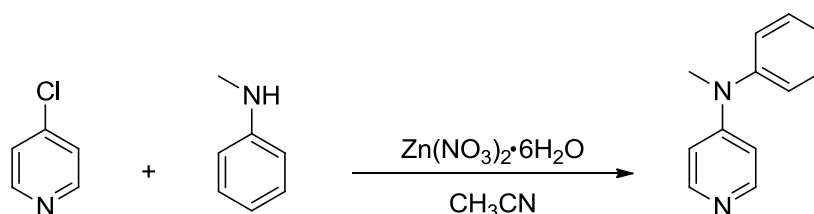
(Table 8, Chapter 2)



Zn(NO₃)₂·6H₂O (20 mol%, 0.4 mmol, 0.12 g) was dissolved in CH₃CN (2 mL), to this *N*-methylaniline (2 mmol, 0.21 g, 0.22 mL) was added followed by 4-chloropyridine (2 mmol, 0.23 g, 0.19 mL). The reaction mixture was allowed to stir at the appropriate temperature for 6 or 8 h as required. On completion the reaction was allowed to cool to room temperature and solvent removed *in vacuo*, using a water bath temperature at 40 °C. Conversions were determined by analysis of the ¹H NMR spectra of the crude reaction mixtures.

Catalyst loading and temperature screen

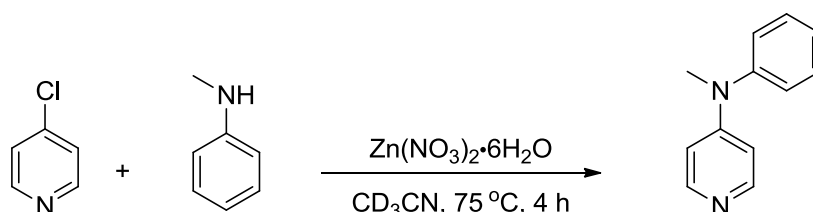
(Table 9, Chapter 2)



The appropriate catalyst loading in Zn(NO₃)₂·6H₂O was added to the reaction vessel and dissolved in CH₃CN (2 mL), to which *N*-methyl aniline (2 mmol, 0.2 g, 0.22 mL) was added. This was followed by addition of 4-chloropyridine (2 mmol, 0.23 g, 0.19 mL), the reaction mixture was allowed to stir under the appropriate conditions. On completion the reaction was allowed to cool to room temperature and solvent removed *in vacuo*, using a water bath at 40 °C. Conversions were determined by analysis of the ¹H NMR spectra of the crude reaction mixtures.

Procedure for kinetic study

(Tables 10-12, Chapter 2)



- Determining order of reaction with respect to 4-chloropyridine
(Table 9, Chapter 2)

0.5 mmol in 4-Chloropyridine

To an oven dried NMR tube, $\text{Zn}(\text{NO}_3)_2 \cdot 6\text{H}_2\text{O}$ (0.025 mmol, 0.006 g) was added, followed by *N*-methylaniline (1 mmol, 0.11 g, 0.11 mL) and dissolved in CD_3CN (1 mL). To this 4-chloropyridine was added (0.5 mmol, 0.06 g, 0.05 mL) and the NMR tube shaken rigorously. The NMR instrument (500 MHz, Bruker Avance II+) was pre-heated to 348 K and maintained at this temperature for the duration of the experiment. The NMR tube inserted, and after obtaining an initial spectrum, ^1H NMR spectra were recorded every 10 minutes for at least 250 minutes. Conversions over time were determined through analysis of the resultant ^1H NMR spectra.

0.7 mmol in 4-Chloropyridine

To an oven dried NMR tube, $\text{Zn}(\text{NO}_3)_2 \cdot 6\text{H}_2\text{O}$ (0.025 mmol, 0.006 g) was added, followed by *N*-methylaniline (1 mmol, 0.11 g, 0.11 mL) and dissolved in CD_3CN (1 mL). To this 4-chloropyridine was added (0.7 mmol, 0.08 g, 0.07 mL) and the NMR tube shaken rigorously. The NMR instrument (500 MHz, Bruker Avance II+) was pre-heated to 348 K and maintained at this temperature for the duration of the experiment. The NMR tube inserted, and after obtaining an initial spectrum, ^1H NMR spectra were recorded every 10 minutes for at least 250 minutes. Conversions over time were determined through analysis of the resultant ^1H NMR spectra.

0.9 mmol in 4-Chloropyridine

To an oven dried NMR tube, $\text{Zn}(\text{NO}_3)_2 \cdot 6\text{H}_2\text{O}$ (0.025 mmol, 0.006 g) was added, followed by *N*-methylaniline (1 mmol, 0.11 g, 0.11 mL) and dissolved in CD_3CN (1 mL). To this 4-chloropyridine was added (0.9 mmol, 0.10 g, 0.09 mL) and the NMR tube shaken rigorously. The NMR instrument (500 MHz, Bruker Avance II+) was pre-heated to 348 K and maintained at this temperature for the duration of the experiment. The NMR tube inserted, and after obtaining an initial spectrum, ^1H NMR spectra were recorded every 10 minutes for at least 250 minutes. Conversions over time were determined through analysis of the resultant ^1H NMR spectra.

1.1 mmol in 4-Chloropyridine

To an oven dried NMR tube, $\text{Zn}(\text{NO}_3)_2 \cdot 6\text{H}_2\text{O}$ (0.025 mmol, 0.006 g) was added, followed by *N*-methylaniline (1 mmol, 0.11 g, 0.11 mL) and dissolved in CD_3CN (1 mL). To this 4-chloropyridine was added (1.1 mmol, 0.12 g, 0.10 mL) and the NMR tube shaken rigorously. The NMR instrument (500 MHz, Bruker Avance II+) was pre-heated to 348 K and maintained at this temperature for the duration of the experiment. The NMR tube inserted, and after obtaining an initial spectrum, ^1H NMR spectra were recorded every 10 minutes for at least 250 minutes. Conversions over time were determined through analysis of the resultant ^1H NMR spectra.

- Determining order of reaction with respect to *N*-methylaniline
(Table 10, Chapter 2)

0.5 mmol in *N*-methylaniline

To an oven dried NMR tube, $\text{Zn}(\text{NO}_3)_2 \cdot 6\text{H}_2\text{O}$ (0.025 mmol, 0.006 g) was added, followed by *N*-methylaniline (0.5 mmol, 0.053 g, 0.054 mL) and dissolved in CD_3CN (1 mL). To this 4-chloropyridine was added (1.0 mmol, 0.11 g, 0.09 mL) and the NMR tube shaken rigorously. The NMR instrument (500 MHz, Bruker Avance II+) was pre-heated to 348 K and maintained at this temperature for the duration of the experiment. The NMR tube inserted, and after obtaining an initial spectrum, ^1H NMR spectra were recorded every 10 minutes for at least 250 minutes. Conversions over time were determined through analysis of the resultant ^1H NMR spectra.

0.7 mmol in *N*-methylaniline

To an oven dried NMR tube, $\text{Zn}(\text{NO}_3)_2 \cdot 6\text{H}_2\text{O}$ (0.025 mmol, 0.006 g) was added, followed by *N*-methylaniline (0.7 mmol, 0.075 g, 0.076 mL) and dissolved in CD_3CN (1 mL). To this 4-chloropyridine was added (1.0 mmol, 0.11 g, 0.09 mL) and the NMR tube shaken rigorously. The NMR instrument (500 MHz, Bruker Avance II+) was pre-heated to 348 K and maintained at this temperature for the duration of the experiment. The NMR tube inserted, and after obtaining an initial spectrum, ^1H NMR spectra were recorded every 10 minutes for at least 250 minutes. Conversions over time were determined through analysis of the resultant ^1H NMR spectra.

0.9 mmol in *N*-methylaniline

To an oven dried NMR tube, $\text{Zn}(\text{NO}_3)_2 \cdot 6\text{H}_2\text{O}$ (0.025 mmol, 0.006 g) was added, followed by *N*-methylaniline (0.9 mmol, 0.096 g, 0.10 mL) and dissolved in CD_3CN (1 mL). To this 4-chloropyridine was added (1.0 mmol, 0.11 g, 0.09 mL) and the NMR tube shaken rigorously. The NMR instrument (500 MHz, Bruker Avance II+) was pre-heated to 348 K and maintained at this temperature for the duration of the experiment. The NMR tube inserted, and after obtaining an initial spectrum, ^1H NMR spectra were recorded every 10 minutes for at least 250 minutes. Conversions over time were determined through analysis of the resultant ^1H NMR spectra.

1.1 mmol in *N*-methylaniline

To an oven dried NMR tube, $\text{Zn}(\text{NO}_3)_2 \cdot 6\text{H}_2\text{O}$ (0.025 mmol, 0.006 g) was added, followed by *N*-methylaniline (1.1 mmol, 0.120 g, 0.12 mL) and dissolved in CD_3CN (1 mL). To this 4-chloropyridine was added (1.0 mmol, 0.11 g, 0.09 mL) and the NMR tube shaken rigorously. The NMR instrument (500 MHz, Bruker Avance II+) was pre-heated to 348 K and maintained at this temperature for the duration of the experiment. The NMR tube inserted, and after obtaining an initial spectrum, ^1H NMR spectra were recorded every 10 minutes for at least 250 minutes. Conversions over time were determined through analysis of the resultant ^1H NMR spectra.

- Determining order of reaction with respect to $\text{Zn}(\text{NO}_3)_2 \cdot 6\text{H}_2\text{O}$
(Table 11, Chapter 2)

0.014 mmol in $\text{Zn}(\text{NO}_3)_2 \cdot 6\text{H}_2\text{O}$

To an oven dried NMR tube, $\text{Zn}(\text{NO}_3)_2 \cdot 6\text{H}_2\text{O}$ (0.014 mmol, 0.004 g) was added, followed by *N*-methylaniline (0.5 mmol, 0.053 g, 0.054 mL) and dissolved in CD_3CN (1 mL). To this 4-chloropyridine was added (0.5 mmol, 0.06 g, 0.05 mL) and the NMR tube shaken rigorously. The NMR instrument (500 MHz, Bruker Avance II+) was pre-heated to 348 K and maintained at this temperature for the duration of the experiment. The NMR tube inserted, and after obtaining an initial spectrum, ^1H NMR spectra were recorded every 10 minutes for at least 250 minutes. Conversions over time were determined through analysis of the resultant ^1H NMR spectra.

0.025 mmol in $\text{Zn}(\text{NO}_3)_2 \cdot 6\text{H}_2\text{O}$

To an oven dried NMR tube, $\text{Zn}(\text{NO}_3)_2 \cdot 6\text{H}_2\text{O}$ (0.025 mmol, 0.006 g) was added, followed by *N*-methylaniline (0.5 mmol, 0.053 g, 0.054 mL) and dissolved in CD_3CN (1 mL). To this 4-chloropyridine was added (0.5 mmol, 0.06 g, 0.05 mL) and the NMR tube shaken rigorously. The NMR instrument (500 MHz, Bruker Avance II+) was pre-heated to 348 K and maintained at this temperature for the duration of the experiment. The NMR tube inserted, and after obtaining an initial spectrum, ^1H NMR spectra were recorded every 10 minutes for at least 250 minutes. Conversions over time were determined through analysis of the resultant ^1H NMR spectra.

0.042 mmol in Zn(NO₃)₂•6H₂O

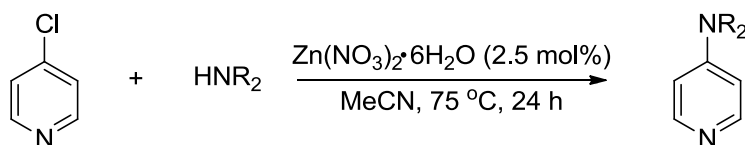
To an oven dried NMR tube, Zn(NO₃)₂•6H₂O (0.025 mmol, 0.012 g) was added, followed by *N*-methylaniline (0.5 mmol, 0.053 g, 0.054 mL) and dissolved in CD₃CN (1 mL). To this 4-chloropyridine was added (0.5 mmol, 0.06 g, 0.05 mL) and the NMR tube shaken rigorously. The NMR instrument (500 MHz, Bruker Avance II+) was pre-heated to 348 K and maintained at this temperature for the duration of the experiment. The NMR tube inserted, and after obtaining an initial spectrum, ¹H NMR spectra were recorded every 10 minutes for at least 250 minutes. Conversions over time were determined through analysis of the resultant ¹H NMR spectra.

0.051 mmol in Zn(NO₃)₂•6H₂O

To an oven dried NMR tube, Zn(NO₃)₂•6H₂O (0.051 mmol, 0.015 g) was added, followed by *N*-methylaniline (0.5 mmol, 0.053 g, 0.054 mL) and dissolved in CD₃CN (1 mL). To this 4-chloropyridine was added (0.5 mmol, 0.06 g, 0.05 mL) and the NMR tube shaken rigorously. The NMR instrument (500 MHz, Bruker Avance II+) was pre-heated to 348 K and maintained at this temperature for the duration of the experiment. The NMR tube inserted, and after obtaining an initial spectrum, ¹H NMR spectra were recorded every 10 minutes for at least 250 minutes. Conversions over time were determined through analysis of the resultant ¹H NMR spectra.

Amine nucleophile screen

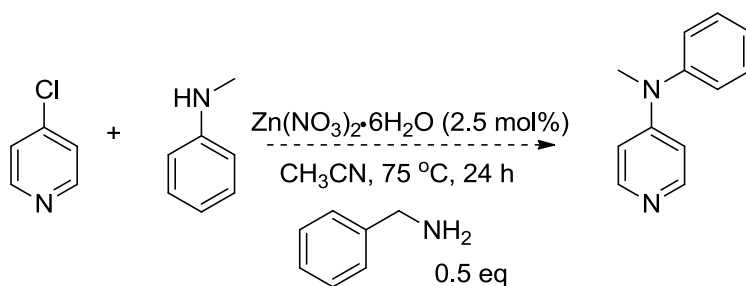
(Table 13, Chapter 2)



$\text{Zn}(\text{NO}_3)_2 \cdot 6\text{H}_2\text{O}$ (2.5 mol%, 0.05 mmol, 0.015 g) was added to the reaction vessel and dissolved in CH_3CN (2 mL), to which the appropriate nucleophile (2 mmol) was added followed by 4-chloropyridine (2 mmol, 0.23 g, 0.19 mL). The reaction mixture was allowed to stir at $75\text{ }^\circ\text{C}$ for 24 h. On completion the reaction was allowed to cool to room temperature and the solvent removed *in vacuo*, using a water bath at $40\text{ }^\circ\text{C}$. Conversions were determined by analysis of the ^1H NMR spectra of the crude reaction mixture.

Reaction on *N*-methylaniline with 4-chloropyridine in the presence of benzylamine

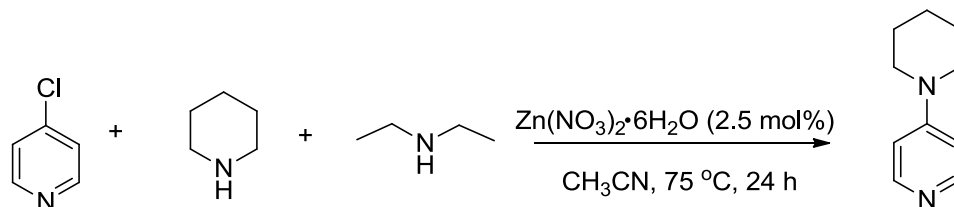
(Section 2.2.6.1, Chapter 2)



$\text{Zn}(\text{NO}_3)_2 \cdot 6\text{H}_2\text{O}$ (2.5 mol%, 0.05 mmol, 0.015 g) was dissolved in CH_3CN (2 mL), to which *N*-methylaniline (2 mmol, 0.21 g, 0.22 mL), benzylamine (1 mmol, 0.11 g, 0.11 mL) were added, followed by the addition of 4-chloropyridine (2 mmol, 0.23 g, 0.19 mL). The reaction mixture was allowed to stir at $75\text{ }^\circ\text{C}$ for 24 h. On completion, the reaction mixture was allowed to cool to room temperature and solvent removed *in vacuo*, using a water bath at $40\text{ }^\circ\text{C}$. Conversions were determined through analysis of the ^1H NMR spectra of the crude reaction mixture.

Reaction of 4-chloropyridine with piperidine in the presence of diethylamine

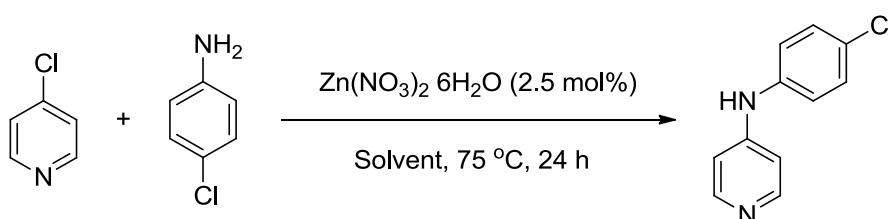
(Section 2.2.6.1, Chapter 2)



$\text{Zn}(\text{NO}_3)_2 \cdot 6\text{H}_2\text{O}$ (2.5 mol%, 0.05 mmol, 0.015 g), was added to the reaction vessel and dissolved in CH_3CN (2 mL), to this solution piperidine (2 mmol, 0.17 g, 0.20 mL), diethylamine (2 mmol, 0.15 g, 0.21 mL) were followed by the addition of 4-chloropyridine (2 mmol, 0.23 g, 0.19 mL). The reaction mixture was allowed to stir at $75\text{ }^\circ\text{C}$ for 24 h. On completion the reaction mixture was allowed to cool to room temperature and solvent removed *in vacuo*, using a water bath at $40\text{ }^\circ\text{C}$ and yielded 4-(piperidin-1-yl)pyridine in 95% conversion. Conversions were determined by analysis of the ^1H NMR spectra of the crude reaction mixture.

Solvent screen for reaction of 4-chloropyridine with 4-chloroaniline

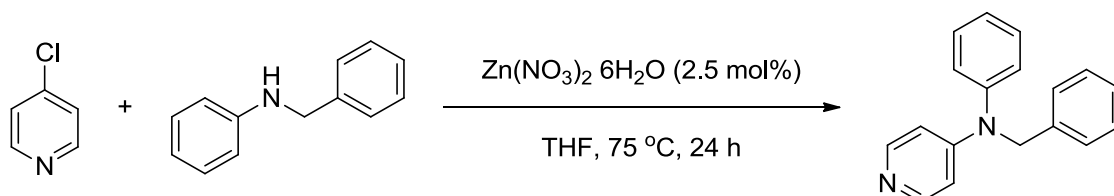
(Table 14, Entries 1-4, Chapter 2)



$\text{Zn}(\text{NO}_3)_2 \cdot 6\text{H}_2\text{O}$ (2.5 mol%, 0.05 mmol, 0.15 g) and 4-chloroaniline (2 mmol, 0.26 g) were dissolved in the appropriate solvent (2 mL), to this 4-chloropyridine (2 mmol, 0.23 g, 0.19 mL) was added. The reaction was allowed to stir at $75\text{ }^\circ\text{C}$ for 24 h. On completion, the reaction mixture was allowed to cool to room temperature and solvent removed *in vacuo*, using a water bath at $40\text{ }^\circ\text{C}$. Conversions were determined by analysis of the ^1H NMR spectra of the crude reaction mixture.

Solvent screen for reaction of 4-chloropyridine with 4-chloroaniline

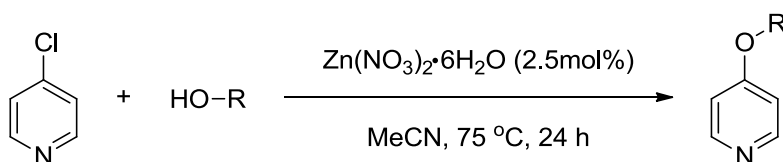
(Table 14, Entry 5, Chapter 2)



$\text{Zn}(\text{NO}_3)_2 \cdot 6\text{H}_2\text{O}$ (2.5 mol%, 0.05 mmol, 0.15 g) and *N*-benzylaniline (2 mmol, 0.37 g) were dissolved in THF (2 mL), to this 4-chloropyridine (2 mmol, 0.23 g, 0.19 mL) was added. The reaction was allowed to stir at 75 °C for 24 h. On completion, the reaction mixture was allowed to cool to room temperature and solvent removed *in vacuo*, using a water bath at 40 °C, giving the product in 75% conversion. Conversions were determined by analysis of the ^1H NMR spectra of the crude reaction mixture.

Initial alcohol screen

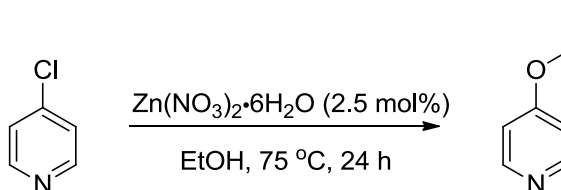
(Table 15, Chapter 2)



$\text{Zn}(\text{NO}_3)_2 \cdot 6\text{H}_2\text{O}$ (2.5 mol%, 0.05 mmol, 0.015 g) was added to the reaction vessel and dissolved in CH_3CN (2 mL), to which the appropriate alcohol nucleophile (2 mmol) was added followed by 4-chloropyridine (2 mmol, 0.23 g, 0.19 mL). The reaction mixture was allowed to stir at 75 °C for 24 h. On completion the reaction was allowed to cool to room temperature and the solvent removed *in vacuo*, using a water bath at 40 °C. Conversions were determined by analysis of the ^1H NMR spectra of the crude reaction mixture.

Base screen for alcohol nucleophiles

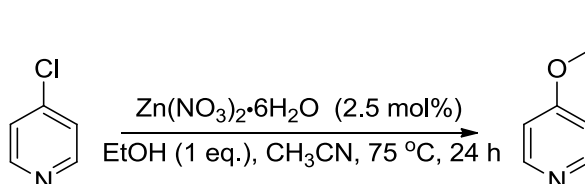
(Table 16, Chapter 2)



Zn(NO₃)₂·6H₂O (2.5 mol%, 0.05 mmol, 0.15 g) was dissolved in EtOH (2 mL), to this the appropriate base (4 mmol) was added followed by 4-chloropyridine (2 mmol, 0.23 g, 0.19 mL). The reaction was allowed to stir at 75 °C for 24 h. On completion, the reaction mixture was allowed to cool to room temperature and solvent removed *in vacuo*, using a water bath at 40 °C. Conversions were determined by analysis of the ¹H NMR spectra of the crude reaction mixture.

Base screen for incoming alcohol groups- 1:1 4-chloropyridine to ethanol

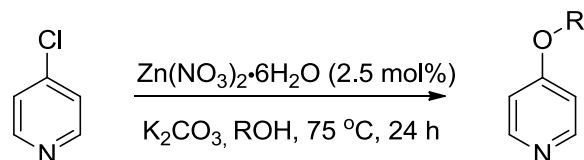
(Table 17, Chapter 2)



Zn(NO₃)₂·6H₂O (2.5 mol%, 0.05 mmol, 0.15 g) was added to the reaction vessel and dissolved in CH₃CN (2 mL). EtOH (2 mmol, 0.095 g) and the appropriate base (4 mmol) base were added to the solution followed by 4-chloropyridine (2 mmol, 0.23 g, 0.19 mL). The reaction mixture was allowed to stir at 75 °C for 24 h. On completion, the reaction mixture was allowed to cool to room temperature and solvent removed *in vacuo*, using a water bath at 40 °C. Conversions were determined by analysis of the ¹H NMR spectra of the crude reaction mixture.

Optimised methodology for reaction of 4-chloropyridine with alcohol nucleophiles

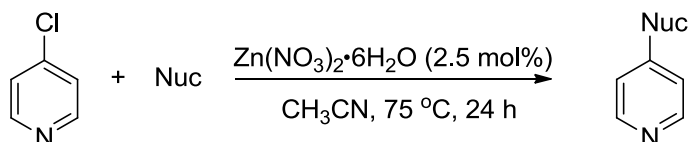
(Table 18, Chapter 2)



Zn(NO₃)₂·6H₂O (2.5 mol%, 0.05 mmol, 0.15 g) was dissolved in the appropriate alcohol (2 mL), to this K₂CO₃ (4 mmol, 0.28 g) was added followed by addition of 4-chloropyridine (2 mmol, 0.23 g, 0.19 mL). The reaction was allowed to stir at 75 °C for 24 h. On completion, the reaction mixture was allowed to cool to room temperature and solvent removed *in vacuo*, using a water bath at 40 °C. Conversions were determined by analysis of the ¹H NMR spectra of the crude reaction mixture.

Miscellaneous nucleophile screen

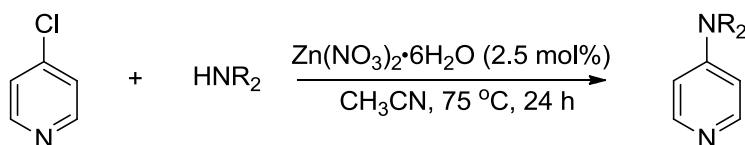
(Table 19, Chapter 2)



Zn(NO₃)₂·6H₂O (2.5 mol%, 0.05 mmol, 0.15 g) was dissolved in CH₃CN (2 mL) and the appropriate nucleophile (2 mmol) was added followed by addition of 4-chloropyridine (2 mmol, 0.23 g, 0.19 mL). The reaction mixture was allowed to stir at 75 °C for 24 h. Where required, potassium *t*-butoxide was also added (4 mmol, 0.45 g). On completion, the reaction mixture was allowed to cool to room temperature and solvent removed *in vacuo*, using a water bath at 40 °C. Conversions were determined by analysis of the ¹H NMR spectra of the crude reaction mixture.

Procedure II: Nitrogen-based nucleophiles

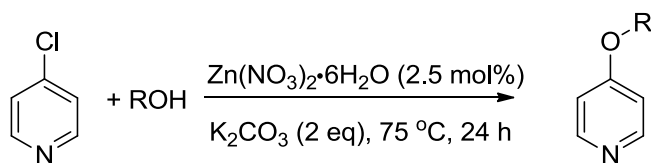
(Table 20, Chapter 2)



Zn(NO₃)₂·6H₂O (2.5 mol%, 0.05 mmol, 0.015 g) was dissolved in the appropriate solvent (2 mL), to this the appropriate nucleophile (2 mmol) was added followed by addition of 4-chloropyridine (2 mmol, 0.23 g, 0.19 mL). The reaction mixture was allowed to stir at 75 °C for 24 h (unless otherwise indicated). On completion, the reaction mixture was allowed to cool to room temperature and solvent removed *in vacuo*, using a water bath at 40 °C. Products were purified by silica gel chromatography (eluent: 5% methanolic ammonia in CH₂Cl₂). Compounds were analysed by their ¹H and ¹³C NMR and mass spectrometry data.

Procedure III: Alcohol incoming group

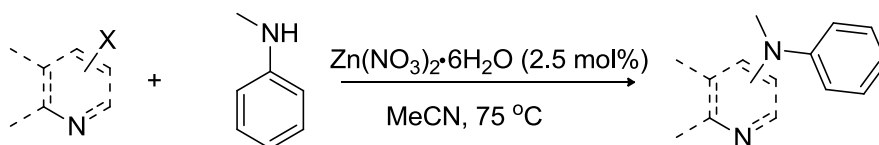
(Entries 17-19, Table 20, Chapter 2)



Zn(NO₃)₂·6H₂O (2.5 mol%, 0.05 mmol, 0.15 g) and K₂CO₃ (4 mmol, 0.55 g) were dissolved in 2 mL of the appropriate alcohol, followed by the addition of 4-chloropyridine (2 mmol, 0.23 g, 0.19 mL). The reaction mixture was allowed to stir at 75 °C for 24 h. On completion, the reaction mixture was allowed to cool to room temperature and solvent removed *in vacuo*, using a water bath at 40 °C. Products were purified by silica gel chromatography (eluent: 5% methanolic ammonia in CH₂Cl₂). Compounds were analysed by their ¹H and ¹³C NMR spectroscopy and mass spectrometry data.

Representative Procedure IV: Substrate screen

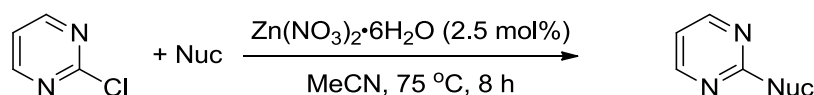
(Table 21, Chapter 2)



Zn(NO₃)₂·6H₂O (2.5 mol%, 0.05 mmol, 0.015 g) was added to the reaction vessel and dissolved in CH₃CN (2 mL), to this *N*-methylaniline (2 mmol, 0.21 g, 0.22 mL) was added followed by the appropriate substrate (2 mmol). The reaction mixture was allowed to stir at the appropriate temperature for the indicated reaction time. On completion, the reaction mixture was allowed to cool to room temperature and solvent removed *in vacuo*, using a water bath at 40 °C. Products were purified by silica gel chromatography (eluent: 5% methanolic ammonia in CH₂Cl₂). Compounds were analysed by their ¹H and ¹³C NMR spectroscopy and mass spectrometry data.

Procedure V: Scope in nucleophile for 2-chloropyrimidine

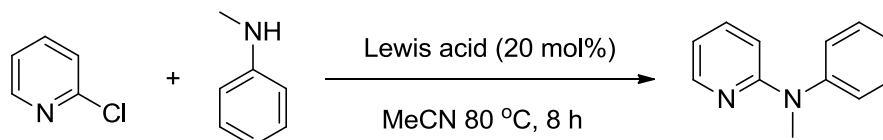
(Entries 10-12, Table 21, Chapter 2)



2-Chloropyrimidine (2 mmol, 0.23 g), Zn(NO₃)₂·6H₂O (2.5 mol%, 0.05 mmol, 0.015 g) were added to the reaction vessel and dissolved in 2 mL CH₃CN, to this the appropriate nucleophile (2 mmol) was added. The reaction mixture was allowed to stir at 75 °C for 8 h. On completion, the reaction mixture was allowed to cool to room temperature and solvent removed *in vacuo*, using a water bath at 40 °C. Products were purified by silica gel chromatography (eluent: 5% methanolic ammonia in CH₂Cl₂). Compounds were analysed by their ¹H and ¹³C NMR spectroscopy and mass spectrometry data.

Lewis acid catalyst screen for S_NAr reaction of 2-chloropyridine with piperidine

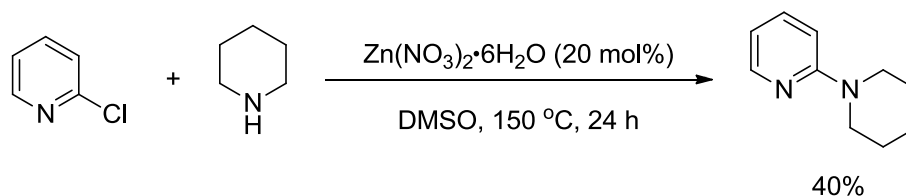
(Table 22., Chapter 2)



The appropriate Lewis acid (20 mol%) was dissolved in CH₃CN (2 mL), to which *N*-methylaniline (2 mmol, 0.21 g, 0.22 mL) was added followed by 2-chloropyridine (2 mmol, 0.23 g, 0.19 mL). The reaction mixture was allowed to stir at 80 °C for 8 h. On completion the reaction was allowed to cool to room temperature and solvent removed *in vacuo*, using a water bath temperature at 40 °C. Conversions were determined by analysis of the ¹H NMR spectra of the crude reaction mixtures

Reaction of 2-chloropyridine with piperidine in DMSO

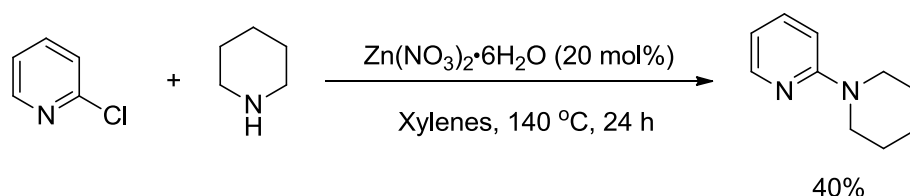
(Section 2.2.8., Chapter 2)



Zn(NO₃)₂·6H₂O (20 mol%, 0.4 mmol, 0.12 g) was dissolved in 2 mL DMSO, to this 2-chloropyridine (2 mmol, 0.23 g, 0.19 mL) was added followed by piperidine (2 mmol, 0.17 g, 0.20 mL), the resultant reaction mixture was allowed to stir at 150 °C for 24 h. On completion, the reaction mixture was allowed to cool to rt and was diluted in water (10 mL) and washed with 3 × 15 mL DCM, the organic layer was dried over MgSO₄ and the solvents removed *in vacuo*, using a water bath at 40 °C. The conversion (40%) was determined by analysis of the ¹H NMR spectrum of the crude reaction mixture.

Reaction of 2-chloropyridine with piperidine in xylenes

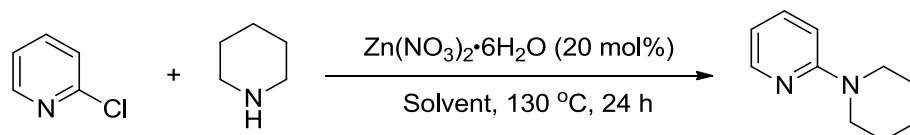
(Section 2.2.8., Chapter 2)



$\text{Zn}(\text{NO}_3)_2 \cdot 6\text{H}_2\text{O}$ (20 mol%, 0.4 mmol, 0.12 g) was dissolved in 2 mL xylenes, to this 2-chloropyridine (2 mmol, 0.23 g, 0.19 mL) was added followed by piperidine (0.17 g, 0.20 mL), the resultant reaction mixture was allowed to stir at 150 °C for 24 h. The solvent removed *in vacuo*, using a water bath at 50 °C. The conversion (70%) was determined by analysis of the ^1H NMR spectrum of the crude reaction mixture.

Solvent Screen for reaction of 2-chloropyridine with piperidine catalysed by $\text{Zn}(\text{NO}_3)_2 \cdot 6\text{H}_2\text{O}$

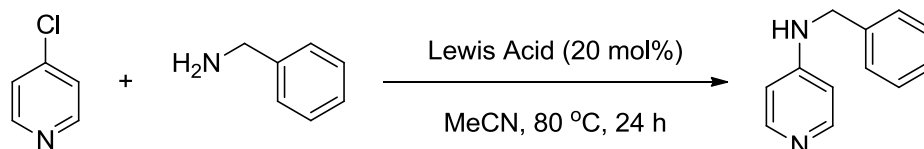
(Table 23, Chapter 2)



$\text{Zn}(\text{NO}_3)_2 \cdot 6\text{H}_2\text{O}$ (20 mol%, 0.4 mmol, 0.12 g) was dissolved in 2 mL of the appropriate solvent, to this 2-chloropyridine (2 mmol, 0.23 g, 0.19 mL) was added followed by piperidine (0.17 g, 0.20 mL), the resultant reaction mixture was allowed to stir at 130 °C for 24 h. The solvent removed *in vacuo*, using a water bath at 50 °C. The conversion (70%) was determined by analysis of the ^1H NMR Spectrum of the crude reaction mixture.

Lewis acid Screen for the reaction of 4-chloropyridine with benzylamine

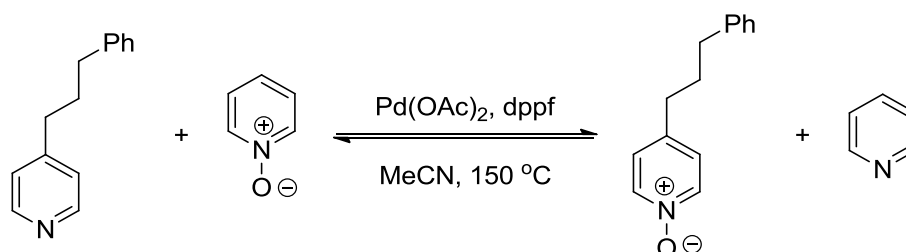
(Table 24, Chapter 2)



The appropriate Lewis acid (20 mol%) was dissolved in CH_3CN (2 mL), to this *N*-methylaniline (2 mmol, 0.21 g, 0.22 mL) was added followed by 4-chloropyridine (2 mmol, 0.23 g, 0.19 mL), the resultant reaction mixture was allowed to stir at 80 °C for 24 h. On completion, the reaction was allowed to cool to room temperature and solvent removed *in vacuo*, using a water bath temperature at 40 °C. Conversions were determined by analysis of the ^1H NMR spectra of the crude reaction mixtures.

Oxygen transfer between 4-(3-phenylpropyl)pyridine and pyridine *N*-oxide

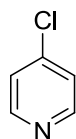
(Section 2.4.3., Chapter 2)



$\text{Pd}(\text{OAc})_2$ (3 mol%, 0.006 mmol, 0.0013 g), dppf (3 mol%, 0.006 mmol, 0.003 g) and pyridine *N*-oxide (2 mmol, 0.19 g) were added to the reaction vessel and diluted in CD_3CN (2 mL), to this 4-(3-phenylpropyl)pyridine was added. The reaction vessel was sealed and the reaction was left to stir at 150 °C for 18 h. On completion a sample of the reaction mixture was submitted for ^1H NMR analysis.

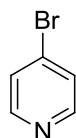
4.2.3. Characterisation of starting materials

4-Chloropyridine⁷⁷



Following procedure I, 4-chloropyridine was recovered as a glassy oil (5.8 g, 58%); ¹H NMR (300 MHz, CDCl₃): δ_H= 8.36 (2H, dd, *J*= 4.6, 1.5 Hz, N=CH-CH=CCl), 7.12 (2H, dd, *J*= 4.6, 1.5 Hz, N=CH-CH=CCl); ¹³C NMR (75 MHz, CDCl₃): δ_C= 150.4, 143.7, 123.8. Data is in agreement with the literature.⁷⁷

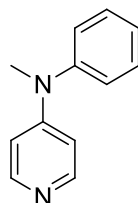
4-Bromopyridine freebase⁷⁸



Following procedure I, 4-bromopyridine was recovered as a glassy oil (5.69 g, 41%); ¹H NMR (300 MHz, (CD₃)₂SO): δ_H= 8.42 (2H, dd, *J*= 5.1, 1.8 Hz, N=CH-CH=CBr), 7.71 (2H, dd, *J*= 5.1, 1.8 Hz, N=CH-CH=CBr); ¹³C NMR (75 MHz, (CD₃)₂SO): δ_C= 149.1, 133.2, 125.6. Data is in agreement with published work.⁷⁸

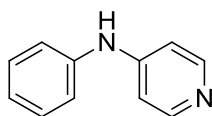
4.2.1. Characterisation of nucleophilic aromatic substitution products

N-Methyl-N-phenylpyridin-4-amine¹¹¹

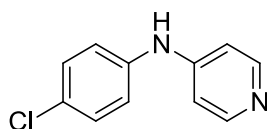


Following procedure II, *N*-methylaniline was used as the nucleophile (0.21 g, 0.22 mL). The product was recovered as a pale yellow oil (0.37 g, 99%); ¹H NMR (300 MHz, CDCl₃): δ_H= 8.29 (2H, app. dd, *J*= 5.2, 1.3 Hz, -CH=N-CH-), 7.50-7.45 (2H, m, aromatic), 7.35-7.30 (1H, m, aromatic), 7.30-7.24 (2H, m, aromatic), 6.62 (2H, app. dd, *J*= 5.2, 1.3 Hz, -CH=C(N)-CH), 3.34 (3H, s, N-CH₃); ¹³C NMR (75 MHz, CDCl₃): δ_C= 153.3, 149.5, 145.7, 129.6, 126.3, 126.0, 107.9, 39.0; HRMS *m/z* (ES+) 185.1079 C₁₂H₁₃N₂ [M+H]⁺ requires 185.1073.

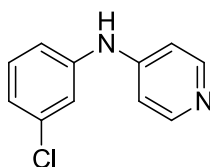
N-Phenylpyridin-4-amine¹¹²



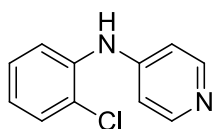
Following procedure II, aniline was used as the nucleophile (0.18 g, 0.18 mL). The product was recovered as a pale yellow solid (0.22 g, 65%); *mp* 176-177 °C [lit¹¹² *m.p.* 173.5-175 °C]; ¹H NMR (300 MHz, (CD₃)₂SO): δ_H= 8.80 (1H, s, pyr-NH), 8.18 (2H, app. dd, *J*= 5.0, 2.5 Hz, -CH=N-CH-), 7.35 (2H, t, *J*= 8.2 Hz, aromatic), 7.21-7.17 (2H, m, aromatic), 7.03 (1H, t, *J*= 8.2 Hz, aromatic), 6.89 (2H, app. dd, *J*= 5.0, 2.5 Hz, -CH=C(N)-CH); ¹³C NMR (75 MHz, (CD₃)₂SO): δ_C= 155.3, 145.7, 139.6, 134.6, 127.8, 125.3, 114.4; HRMS *m/z* (ES+) 171.0921 C₁₁H₁₁N₂ [M+H]⁺ requires 171.0917.

N-(4-Chlorophenyl)pyridin-4-amine¹¹³

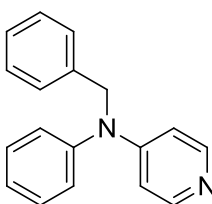
Following procedure II, 4-chloroaniline was used as the nucleophile (0.26 g). The product was recovered as a crystalline white solid (0.37 g, 91%); *mp* 251-252 °C [lit.¹¹³ *m.p.* 250–252 °C]; ¹H NMR (300 MHz, (CD₃)₂SO): δ_H= 8.99 (1H, s, pyr-NH), 8.21 (2H, d, *J*= 5.6 Hz, -CH=N-CH-), 7.53-7.37 (2H, m, aromatic), 7.32-7.22 (2H, m, aromatic), 6.91 (2H, d, *J*= 5.6 Hz, -CH=C(N)-CH); ¹³C NMR (75 MHz, (CD₃)₂SO): δ_C= 150.8, 150.7, 140.4, 130.3, 126.9, 122.4, 110.4.; HRMS *m/z* (ES+) 205.0520 C₁₁H₁₀N₂Cl³⁵ [M+H]⁺ requires 205.0528.

N-(3-Chlorophenyl)pyridin-4-amine¹¹⁴

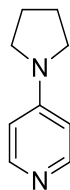
Following procedure II, 3-chloroaniline was used as the nucleophile (0.26 g). The product was recovered as a crystalline white solid (0.39 g, 95%); *mp* 181-183 °C; ¹H NMR (300 MHz, (CD₃)₂SO): δ_H= 8.96 (1H, s, pyr-NH), 8.24 (2H, app. dd, *J*= 4.8, 1.5 Hz, -CH=N-CH-), 7.42-7.33 (1H, m, aromatic), 7.26-7.16 (2H, m, aromatic), 7.04 (1H, app. ddd, *J*= 7.9, 2.0, 0.9 Hz, aromatic), 6.94 (2H, app. dd, *J*= 4.8, 1.5 Hz, -CH=C(N)-CH); ¹³C NMR (75 MHz, (CD₃)₂SO): δ_C= 150.3, 149.2, 142.4, 133.7, 131.0, 121.8, 118.8, 117.8, 109.8; HRMS *m/z* (ES+) C₁₁H₉N₂Cl³⁵Na 227.0346 [M+Na]⁺ requires 227.0347.

N-(2-Chlorophenyl)pyridin-4-amine¹¹⁵

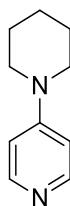
Following procedure II, 2-chloroaniline was used as the nucleophile (0.26 g). The product was recovered as a crystalline yellow solid (0.36 g, 87%); *mp* 120-122 °C [lit¹¹⁵ 123 °C]; ¹H NMR; (300 MHz, (CD₃)₂SO): δ_H= 8.53 (1H, s, pyr-NH), 8.17 (2H, app. dd, *J*= 4.9, 1.5 Hz, -CH=N-CH-), 7.54 (1H, dd, *J*= 8.0, 1.3 Hz, aromatic), 7.44 (1H, dd, *J*= 8.0, 1.5 Hz, aromatic), 7.34 (1H, td, *J*= 7.7, 1.4 Hz, aromatic), 7.19 (1H, td, *J*= 7.9, 1.6 Hz, aromatic), 6.75 (2H, app. dd, *J*= 4.9, 1.5 Hz, -CH=C(N)-CH); ¹³C NMR (75 MHz, (CD₃)₂SO): δ_C= 150.6, 150.0, 137.1, 130.4, 128.1, 127.6, 125.7, 124.9, 109.3; HRMS *m/z* (ES+) C₁₁H₁₀N₂Cl³⁵ 205.0524 [M+H]⁺ requires 205.0528.

N-Benzyl-N-phenylpyridin-4-amine

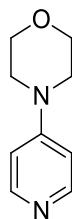
Following procedure II, *N*-benzylaniline was used as the nucleophile (0.37 g). The product was recovered as a yellow solid (0.40 g, 75%); *mp* 58-60 °C; ¹H NMR (300 MHz, CDCl₃): δ_H= 8.12 (2H, app. dd, *J*= 5.2, 1.2 Hz, -CH=N-CH-), 7.39-7.34 (5H, m, aromatic), 7.29-7.21 (5H, m, aromatic), 6.52 (2H, app. dd, *J*= 5.2, 1.2 Hz, -CH=C(N)-CH-), 4.92 (2H, s, ph-CH₂-N); ¹³C NMR (75 MHz, CDCl₃): δ_C= 153.3, 149.8, 145.4, 137.3, 130.0, 128.7, 127.2, 126.8, 126.5, 126.3, 108.8, 55.8; IR cm⁻¹ $\tilde{\nu}$ = 3028 (C-H), 1600(C=C), 1270 (C-N); HRMS *m/z* (ES+) 283.1192 C₁₈H₁₇N₂ [M+H]⁺ requires 283.1211.

4-(Pyrrolidin-1-yl)pyridine¹¹⁶

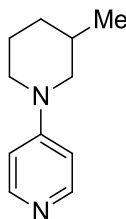
Following procedure II, pyrrolidine was used as the nucleophile (0.14 g, 0.17 mL). The product was recovered as yellow crystalline solid (0.26 g, 89%); *mp* 57-58 °C [lit¹¹⁷ *m.p.* 57 °C]; ¹H NMR (300 MHz, CDCl₃): δ_H= 8.11 (2H, app. dd, *J*= 4.9, 1.5 Hz, -CH=N-CH-), 6.29 (2H, app. dd, *J*= 4.9, 1.5 Hz, -CH=C(N)-CH-), 3.22-3.20 (4H, m, pyr-N-CH₂-CH₂), 1.95-1.93 (4H, m, pyr-N-CH₂-CH₂); ¹³C NMR (75 MHz, CDCl₃): δ_C= 151.7, 149.5, 106.9, 46.9, 25.3; HRMS *m/z* (ES+) 149.1079 C₉H₁₃N₂ [M+Na]⁺ requires 149.1074.

4-(Piperidin-1-yl)pyridine¹¹⁸

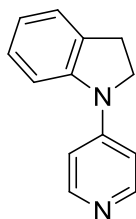
Following procedure II, piperidine was used as the nucleophile (0.17 g, 0.20 mL). The product was recovered as yellow crystalline solid (0.23 g, 71%); *mp* 79-80 °C [lit¹¹⁹ 78-79 °C]; ¹H NMR (300 MHz, CDCl₃): δ_H= 8.13 (2H, d, *J*= 5.1 Hz, -CH=N-CH-), 6.54 (2H, d, *J*= 5.1 Hz, -CH=C(N)-CH-), 3.25-3.19 (4H, m, pyr-N-CH₂-CH₂-CH₂), 1.56-1.51 (6H, m, pyr-N-CH₂-CH₂-CH₂); ¹³C NMR (75 MHz, CDCl₃): δ_C= 154.6, 149.9, 107.9, 46.8, 24.8, 24.0; HRMS *m/z* (ES+) 163.1233 C₁₀H₁₅N₂ [M+H]⁺ requires 163.1230.

4-(Pyridin-4-yl)morpholine¹²⁰

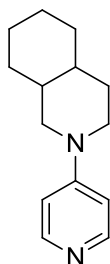
Following procedure II, morpholine was used as the nucleophile (0.17 g, 0.17 mL). The product was recovered as a white disc-like crystalline solid (0.18 g, 56%); *mp* 106-107 °C [lit¹²⁰ 105-107 °C]; ¹H NMR (300 MHz, (CD₃)₂SO): δ_H= 8.23 (2H, app. dd, *J*= 5.1, 1.5 Hz, -CH=N-CH-), 6.61 (2H, app. dd, *J*= 5.1, 1.5 Hz, -CH=C(N)-CH-), 3.78 (4H, t, *J*= 6.0 Hz, pyr-N-CH₂-CH₂-O), 3.24 (4H, t, *J*= 6.0 Hz, pyr-N-CH₂-CH₂-O); ¹³C NMR (75 MHz, (CD₃)₂SO): δ_C= 154.9, 149.9, 107.9, 66.0, 45.7; HRMS *m/z* (ES+) 165.1027 C₉H₁₃N₂O [M+H]⁺ requires 165.1023.

4-(3-Methylpiperidin-1-yl)pyridine

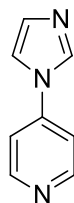
Following procedure II, 3-methylpiperidine was used as the nucleophile (0.20 g). The product was recovered a yellow oil (0.31 g, 89%); ¹H NMR (300 MHz, CDCl₃): δ_H= 8.09 (2H, app. brs, -CH=N-CH-), 6.54 (2H, app. brs, -CH=C(N)-CH), 3.69-3.58 (2H, m, 2.8 Hz, pyr-N-CH₂-CH₂-), 2.77 (1H, app. td, *J*= 12.7, pyr-N-CH₂-CH(CH₃)-CH₂), 2.37 (1H, app. t, *J*= 12.5 Hz, pyr-N-CH₂-CH₂-), 1.75-1.38 (4H, m, pyr-N-CH₂-CH₂-CH₂-CH(CH₃)), 1.15-0.95 (1H, m, pyr-N-CH₂-CH(CH₃)-CH₂), 0.83 (3H, d, *J*= 6.6 Hz, pyr-N-CH₂-CH(CH₃)-CH₂); ¹³C NMR (75 MHz, CDCl₃): δ_C= 154.4, 149.2, 142.9, 53.6, 46.3, 32.6, 30.0, 24.20, 18.9; IR cm⁻¹ $\tilde{\nu}$ = 3031 (C-H), 1615 (C=C), 1254 (C-N); HRMS *m/z* (ES+) 177.1483 C₉H₁₆N₃ [M+H]⁺ requires 177.1487.

1-(Pyridin-4-yl)indoline¹²¹

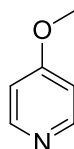
Following procedure II, indoline was used as the nucleophile (0.24 g, 0.22 mL). The product was recovered as a brown crystalline solid (0.37 g, 95%); *mp* 81-82 °C [lit¹²¹ 81-82 °C]; ¹H NMR (300 MHz, CDCl₃): δ_H= 8.42 (2H, app. d, *J*= 6.3 Hz, -CH=N-CH-), 7.35 (1H, d, *J*= 9.0 Hz, aromatic), 7.21-7.15 (2H, m, aromatic), 7.04 (2H, app. d, *J*= 6.3 Hz, -CH=C(N)-CH-), 6.92 (1H, t, *J*= 9.0 Hz, aromatic), 3.96 (2H, t, *J*= 8.4 Hz, pyr-N-CH₂-), 3.16 (2H, t, *J*= 8.4 Hz, pyr-N-CH₂-CH₂-); ¹³C NMR (75 MHz, CDCl₃): δ_C= 150.1, 149.1, 144.1, 132.0, 127.0, 125.2, 120.9, 110.4, 109.9, 50.7, 27.6; HRMS *m/z* (ES+) 197.1071 C₁₃H₁₃N₂ [M+Na]⁺ requires 197.1074.

2-(Pyridin-4-yl)decahydroisoquinoline

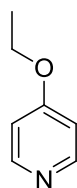
Following procedure II, perhydroisoquinoline was used as the nucleophile (0.28 g, 0.30 mL). The product was recovered as a pale yellow oil (0.41 g, 95%); ¹H NMR (300 MHz, CDCl₃): δ_H= 8.20 (2H, d, *J*= 4.9 Hz, -CH=N-CH-), 6.62 (2H, d, *J*= 4.9 Hz, CH=C(N)-CH-), 3.88 (1H, d, *J*= 12.5, Hz, pyr-N-CH₂-CH<), 3.69 (1H, d, *J*= 12.5 Hz, pyr-N-CH₂-CH₂-CH<), 2.80 (1H, app. td, *J*= 12.5, 3.0 Hz, pyr-N-CH₂-CH<), 2.44 (1H, app. td, *J*= 12.5, 3.0 Hz, pyr-N-CH₂-CH₂-CH<), 1.74-1.58 (5H, m, aliphatic ring), 1.17-0.97 (7H, m, aliphatic ring); ¹³C NMR (75 MHz, CDCl₃): δ_C= 154.6, 149.9, 108.0, 52.6, 46.9, 41.7, 40.9, 32.7, 31.9, 30.0, 26.0, 25.7; IR cm⁻¹ ν= 3027 (C-H), 1596 (C=C) 1236 (C-N); HRMS *m/z* (ES+) 217.1703 C₁₄H₂₁N₂ [M+H]⁺ requires 217.1700

4-(1H-Imidazol-1-yl)pyridine¹²²

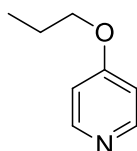
Following procedure II, imidazole was used as the nucleophile (0.14 g). The product was recovered as a white solid (0.16 g, 56%); *mp* 114-116 °C [lit¹²² 114-115 °C]; ¹H NMR (300 MHz, CDCl₃): δ_H= 8.72 (2H, d, *J*= 5.9 Hz, -CH=N-CH-), 8.03 (1H, s, pyr-N-CH=N), 7.40-7.34 (3H, m, pyr-N-CH=CH-N and -CH=C(N)-CH-); ¹³C NMR (75 MHz, CDCl₃): δ_C=151.8, 134.9, 131.6, 116.7, 115.9, 114.4; HRMS *m/z* (ES+) 147.0743 [M+Na+H]²⁺ requires 147.0747

4-Methoxypyridine¹²³

Following procedure III, methanol was used as the solvent. The product was recovered as a colourless oil (0.16 g, 75%) after column chromatography; ¹H NMR (300 MHz, CDCl₃): δ_H= 8.39 (2H, app. dd, *J*= 4.7, 1.5 Hz, -CH=N-CH-), 6.77 (2H, app. dd, *J*= 4.7, 1.5 Hz, -CH=C(O)-CH-), 3.80 (3H, s, O-CH₃); ¹³C NMR (75 MHz, CDCl₃): δ_C= 165.5, 150.9, 109.8, 54.9; HRMS *m/z* (ES+) 132.0399 C₆H₇NNaO[M+Na]⁺ requires 132.0420

4-Ethoxypyridine¹²⁴

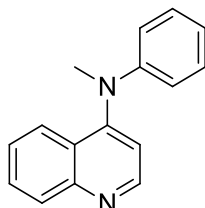
Following procedure III, ethanol was used as the solvent. The product was recovered as a pale yellow oil (0.20 g, 81%); ¹H NMR (300 MHz, CDCl₃): δ_H= 8.40 (2H, app. dd, *J*= 4.8, 1.5 Hz, -CH=N-CH-), 6.68 (2H, app. dd, *J*= 4.8, 1.5 Hz, -CH=C(O)-CH-), 4.08 (2H, q, *J*= 7.0 Hz, O-CH₂-CH₃), 1.43 (3H, t, *J*= 7.0 Hz, O-CH₂-CH₃); ¹³C NMR (75 MHz, CDCl₃): δ_C= 164.9, 151.0, 110.1, 63.4, 14.4; HRMS *m/z* (ES+) 146.0574 C₇H₉NNaO [M+Na]⁺ requires 146.0577.

4-Propoxypyridine

Following procedure III, propanol was used as the solvent. The product was recovered as a yellow oil (0.23 g, 84%); ¹H NMR (300 MHz, CDCl₃): δ_H= 8.36 (2H, app. brs, -CH=N-CH-), 6.75 (2H, app. brs, -CH=C(O)-CH-), 3.90 (2H, t, *J*= 6.5 Hz, O-CH₂-CH₂-), 1.81-1.73 (2H, m, O-CH₂-CH₂-), 0.98 (3H, t, *J*= 7.4 Hz, -CH₂-CH₃); ¹³C NMR (75 MHz, CDCl₃): δ_C= 164.2, 150.6, 110.2, 69.2, 22.1, 10.3; IR cm⁻¹ $\tilde{\nu}$ = 2980 (C-H), 1644 (C=C); HRMS *m/z* (ES+) 160.0707 C₈H₁₁NNaO [M+Na]⁺ requires 160.0701.

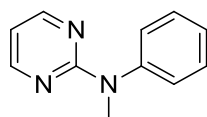
4.2.2. Characterisation of substrate screen for nucleophilic aromatic substitution

N-Methyl-N-phenylquinolin-4-amine¹²⁵

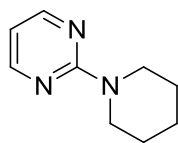


Following procedure IV, 4-chloroquinoline was used as the substrate (0.33 g). The product was recovered as a yellow crystalline solid (0.44 g, 93%); *mp* 56-59 °C; ¹H NMR (300 MHz, CDCl₃): δ_H= 8.49 (1H, d, *J*= 4.9 Hz, >C=N-CH-), 7.79-7.68 (1H, m, aromatic), 7.37 (1H, dd, *J*= 9.5, 1.0 Hz, aromatic), 7.28 (1H, ddd, *J*= 8.4, 5.4, 1.4 Hz, aromatic), 7.00-6.84 (3H, m, aromatic), 6.77 (1H, d, *J*= 4.9 Hz, aromatic), 6.61-6.57 (1H, m, aromatic), 6.53-6.50 (3H, m, aromatic), 3.10 (3H, s, N-CH₃); ¹³C NMR (75 MHz, CDCl₃): δ_C= 153.5, 151.0, 149.9, 149.5, 129.8, 129.1, 129.0, 125.5, 124.5, 124.4, 121.4, 119.2, 114.2, 41.7; HRMS *m/z* (ES+) 235.1231 C₁₆H₁₅N₂ [M+H]⁺ requires 235.1230.

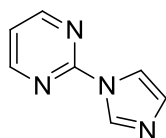
N-Methyl-N-phenylpyrimidin-2-amine¹⁰⁴



Following procedure V, 2-chloropyrimidine was used as the substrate (0.23 g). The product was recovered as orange needles (0.26 g, 71%); *mp* 49-51 °C; ¹H NMR (300 MHz, CDCl₃): δ_H= 8.35 (2H, d, *J*= 4.3 Hz, -CH-N-C(N)=N-CH-), 7.44-7.40 (2H, m, aromatic), 7.35-7.32 (2H, m, aromatic), 7.27-7.22 (1H, m, aromatic), 6.57 (1H, t, *J*= 4.3 Hz, N-C(N)=N-CH-CH-), 3.55 (3H, s, N-CH₃); ¹³C NMR (75 MHz, CDCl₃): δ_C= 161.2, 157.5, 145.4, 129.1, 126.5, 125.7, 110.6, 38.6; HRMS *m/z* (ES+) 186.1023 C₁₁H₁₂N₃ [M+H]⁺ requires 186.1026.

2-(Piperidin-1-yl)pyrimidine¹²⁶

Following procedure V, 2-chloropyrimidine was used as the substrate (0.23 g) and piperidine as the nucleophile (0.17 g, 0.20 mL). The product was recovered as a yellow oil (0.21 g, 63%); ¹H NMR (300 MHz, CDCl₃): δ_H= 8.28 (2H, d, *J*= 4.7 Hz, -CH-N-C(N)=N-CH-), 6.41 (1H, t, *J*= 4.7 Hz, N-C(N)=N-CH-CH-), 3.77 (4H, t, *J*= 7.6 Hz, pyrim-N-CH₂), 1.64-1.60 (6H, m, pyrim-N-CH₂-CH₂-CH₂); ¹³C NMR (75 MHz, CDCl₃): δ_C= 162.4, 157.7, 109.0, 44.7, 25.7, 24.8; HRMS *m/z* (ES+) 164.1190 C₁₁H₁₂N₃ [M+H]⁺ requires 164.1188.

2-(1H-Imidazol-1-yl)pyrimidine¹²⁷

Following procedure V, 2-chloropyrimidine was used as the substrate (0.23 g) and imidazole was as the nucleophile (0.14 g). The product was recovered as a white solid (0.18 g, 61%); *m.p* 122-124 °C [lit⁹⁵ 120-122 °C]; ¹H NMR (300 MHz, CDCl₃): δ_H= 8.67 (2H, d, *J*= 4.8 Hz, -CH-N-C(N)=N-CH-), 8.60 (1H, s, pyrim-N-CH=N), 7.87-7.86 (1H, m, pyrim-N-CH=CH-N), 7.19 (1H, t, *J*= 4.8 Hz, N-C(N)=N-CH=CH), 7.16 (1H, app. t, *J*= 1.4 Hz, pyrim-N-CH=CH-N); ¹³C NMR (75 MHz, CDCl₃): δ_C=158.7, 154.7, 136.1, 130.7, 118.8, 116.4; HRMS *m/z* (ES+) 164.0487 C₇H₆N₄Na [M+Na]⁺ requires 164.0490.

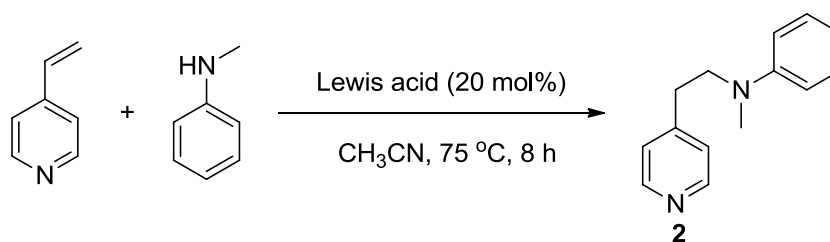
4.3. Chapter 3 Experimental Procedures

General note on handling 2- and 4-vinylpyridine:

2- and 4-vinylpyridine are unstable at room temperature and should be stored in a freezer (~ -20 °C). Addition of 2- or 4- vinylpyridine occurred once all other reactants had been added to the reaction vessel and directly from a -20 °C freezer.

Lewis acid catalyst screen

(Table 26, Chapter 3)

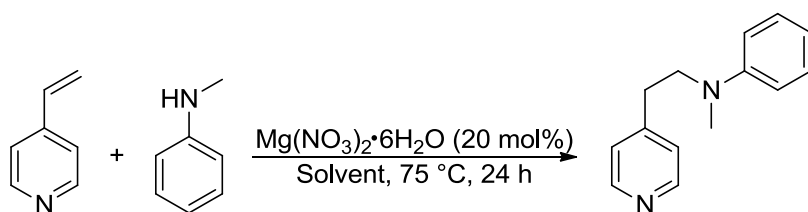


The appropriate Lewis acid (20 mol%) was dissolved in CH₃CN (2 mL), *N*-methylaniline (2 mmol, 0.21 g, 0.22 mL) was added to this solution followed by addition of 4-vinylpyridine (2 mmol, 0.21 g, 0.22 mL). The reaction mixture was left to stir at 75 °C for 8 h. On completion, the reaction mixture was allowed to cool to room temperature and solvent removed *in vacuo*, using a water bath at 40 °C. Conversions were determined by analysis of the ¹H NMR spectra of the crude reaction mixture.

N-Methyl-*N*-(2-(pyridin-2-yl)ethyl)aniline (**2**): ¹H NMR (300 MHz, CDCl₃): δ_H= 8.51 (2H, d, *J*= 4.5 Hz, -CH=N-CH-), 7.29-7.23 (3H, m, aromatic), 7.13 (2H, d, *J*= 5.9 Hz, aromatic), 6.73 (2H, d, *J*= 4.5 Hz, -CH-C(CH₂)=CH), 3.59 (2H, t, *J*= 6.0 Hz, pyr-CH₂-CH₂-N-), 2.87 (3H, s, N-CH₃), 2.87-2.82 (2H, m, pyr-CH₂-CH₂-N-).

Solvent screen

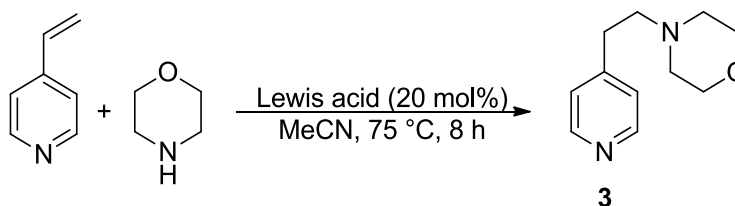
(Table 27, Chapter 3)



Mg(NO₃)₂·6H₂O (20 mol%, 0.4 mmol, 0.103 g) was dissolved in 2 mL of the appropriate solvent, to this *N*-methylaniline (2 mmol, 0.21 g, 0.22 mL) was added followed by addition of 4-vinylpyridine (2 mmol, 0.21 g, 0.22 mL). The reaction mixture was left to stir at 75 °C for 24 h. On completion, the reaction mixture was allowed to cool to room temperature and solvent removed *in vacuo*, using a water bath at 40 °C. Conversions were determined by analysis of the ¹H NMR spectra of the crude reaction mixture.

Second Lewis acid catalyst screen- Morpholine nucleophile

(Table 28, Chapter 3)

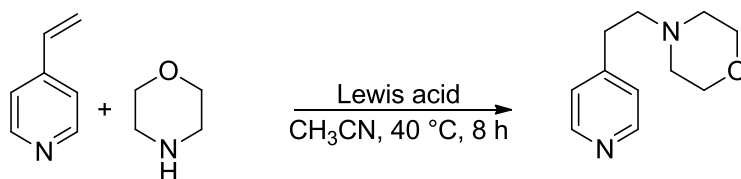


The appropriate Lewis acid (20 mol%) was dissolved in CH₃CN (2 mL), to which morpholine (2 mmol, 0.17 g, 0.17 mL) was added followed by addition of 4-vinylpyridine (2 mmol, 0.21 g, 0.22 mL). The reaction mixture was allowed to stir at 75 °C for 8 h. On completion, the reaction mixture was allowed to cool to room temperature and solvent removed *in vacuo*, using a water bath at 40 °C. Conversions were determined by analysis of the ¹H NMR spectra of the crude reaction mixture.

4-(2-(Pyridin-4-yl)ethyl)morpholine (**3**): ¹H NMR (300 MHz, CDCl₃): δ_H= 8.28 (2H, app. dd, *J*= 4.4, 1.6 Hz, -CH=N-CH-), 6.93 (2H, app. dd, *J*= 4.4, 1.6 Hz, -CH-C(CH₂)=CH-), 3.51-3.48 (4H, m, -CH₂-O-CH₂-), 2.60-2.55 (2H, m, pyr-CH₂-CH₂-N-), 2.42-2.36 (2H, m, pyr-CH₂-CH₂-N-), 2.30-2.27 (4H, m, CH₂-N(CH₂)-CH₂-).

Catalyst loading screen for the best performing Lewis acids

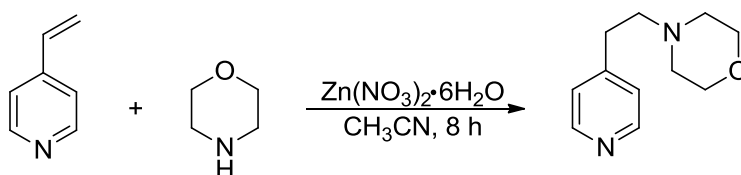
(Table 29, Chapter 3)



The appropriate Lewis acid catalyst at the appropriate catalyst loading was dissolved in CH₃CN (2 mL), to this morpholine (2 mmol, 0.17 g, 0.17 mL) was added followed by addition of 4-vinylpyridine (2 mmol, 0.21 g, 0.22 mL). The reaction mixture was allowed to stir at 40 °C for 8 h. On completion, the reaction mixture was allowed to cool to room temperature and solvent removed *in vacuo*, using a water bath at 40 °C. Conversions were determined by analysis of the ¹H NMR spectra of the crude reaction mixture.

Temperature and catalyst loading screen- 8 h

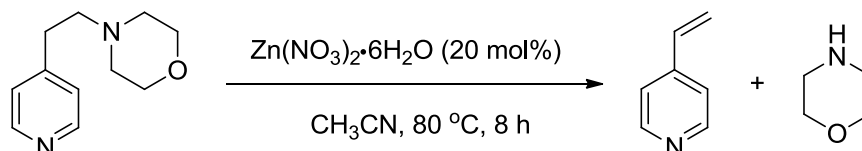
(Table 30, Chapter 3)



The appropriate loading in Zn(NO₃)₂·6H₂O was dissolved in CH₃CN (2 mL), to this morpholine (2 mmol, 0.17 g, 0.17 mL) was added followed by addition of 4-vinylpyridine (2 mmol, 0.21 g, 0.22 mL). The reaction mixture was allowed to stir at the indicated temperature for 8 h. On completion, the reaction mixture was allowed to cool to room temperature and solvent removed *in vacuo*, using a water bath at 40 °C. Conversions were determined by analysis of the ¹H NMR spectra of the crude reaction mixture.

Representative procedure for degradation of conjugate addition product at 80 °C in the presence of 20 mol% $Zn(NO_3)_2 \cdot 6H_2O$

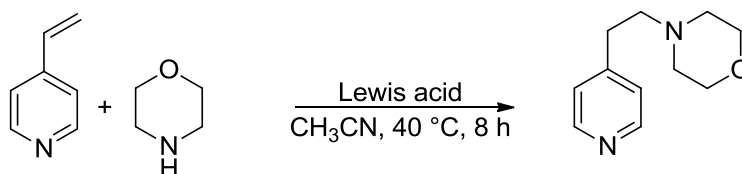
(Section 3.2.4, Chapter 3)



4-(2-(Pyridin-4-yl)ethyl)morpholine (1 mmol, 0.19 g) and $Zn(NO_3)_2 \cdot 6H_2O$ (20 mol%, 0.2 mmol, 0.06 g) were dissolved in 2 mL CH_3CN and allowed to stir at 80 °C for 8 h. On completion the reaction mixture was allowed to cool to room temperature and solvent removed *in vacuo*, using a water bath at 40 °C. The reaction yielded 4-vinylpyridine in 10% conversion, determined by analysis of the 1H NMR spectra of the crude reaction mixture.

Temperature, time and catalyst loading screen

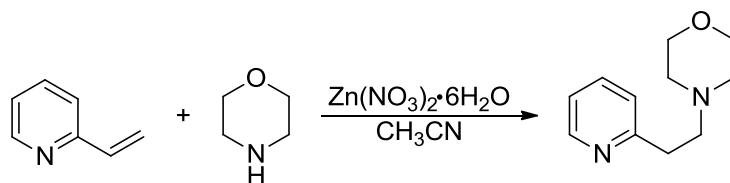
(Table 30, Chapter 3)



The appropriate loading in $Zn(NO_3)_2 \cdot 6H_2O$ was dissolved in CH_3CN (2 mL), to this morpholine (2 mmol, 0.17 g, 0.17 mL) was added followed by addition of 4-vinylpyridine (2 mmol, 0.21 g, 0.22 mL). The reaction mixture was allowed to stir under the appropriate conditions. On completion, the reaction mixture was allowed to cool to room temperature and solvent removed *in vacuo*, using a water bath at 40 °C. Conversions were determined by analysis of the 1H NMR spectra of the crude reaction mixture.

Reaction optimisation for 2-vinylpyridine

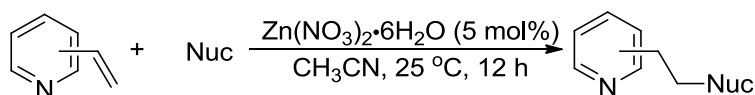
(Table 32, Chapter 3)



The appropriate loading in Zn(NO₃)₂·6H₂O was dissolved in CH₃CN (2 mL), to this morpholine (2 mmol, 0.17 g, 0.17 mL) was added, followed by addition of 2-vinylpyridine (2 mmol, 0.21 g, 0.22 mL). The reaction mixture was allowed to stir at 25 °C for the indicated reaction time. On completion, the reaction mixture was allowed to cool to room temperature and solvent removed *in vacuo*, using a water bath at 40 °C. Conversions were determined by analysis of the ¹H NMR spectra of the crude reaction mixtures.

Initial nucleophile screen for 2- and 4-vinylpyridine

(Table 33 and 35, Chapter 3)

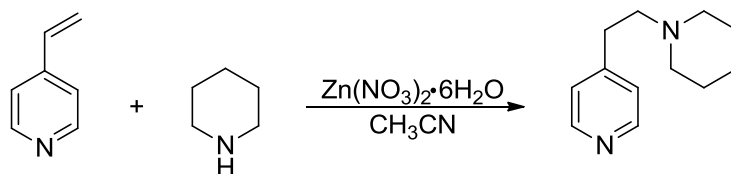


Zn(NO₃)₂·6H₂O (5 mol%, 0.1 mmol, 0.03 g) was dissolved in CH₃CN (2 mL), to this the appropriate nucleophile (2 mmol) was added, followed by the addition of 2-/4-Vinylpyridine (2 mmol, 0.21 g, 0.22 mL). The reaction mixture was allowed to stir at 25 °C for 12 h. On completion, the reaction mixture was allowed to cool to room temperature and solvent removed *in vacuo*, using a water bath at 40 °C. Conversions were determined by analysis of the ¹H NMR spectra of the crude reaction mixture.

Optimising reaction conditions for piperidine incoming group

4-Vinylpyridine - Temperature and catalyst loading screen (25-40 °C, 2.5 and 5 mol% catalyst loading)

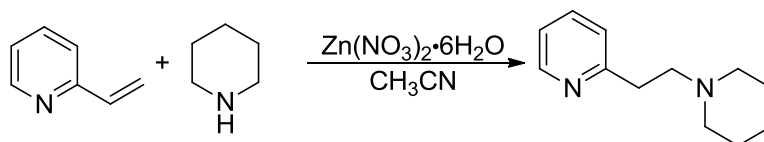
(Table 34, Chapter 3)



The appropriate loading in $\text{Zn}(\text{NO}_3)_2 \cdot 6\text{H}_2\text{O}$ was dissolved in CH_3CN (2 mL), to this piperidine (2 mmol, 0.17 g, 0.20 mL) was added followed by the addition of 4-vinylpyridine (2 mmol, 0.21 g, 0.22 mL). The reaction mixture was allowed to stir at the appropriate conditions. On completion, the reaction mixture was allowed to cool to room temperature and solvent removed *in vacuo*, using a water bath at 40° C. Conversions were determined by analysis of the ^1H NMR spectra of the crude reaction mixture.

2-Vinylpyridine - Temperature and catalyst loading screen (25-40 °C, 2.5 and 5 mol% catalyst loading)

(Table 38, Chapter 3)

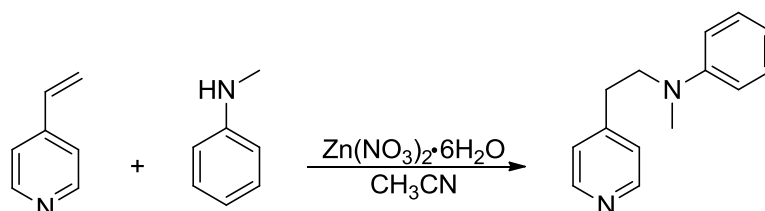


The appropriate loading in $\text{Zn}(\text{NO}_3)_2 \cdot 6\text{H}_2\text{O}$ was dissolved in CH_3CN (2 mL), to this piperidine (2 mmol, 0.17 g, 0.20 mL) was added followed by the addition of 2-vinylpyridine (2 mmol, 0.21 g, 0.22 mL). The reaction mixture was allowed to stir at the appropriate conditions. On completion, the reaction mixture was allowed to cool to room temperature and solvent removed *in vacuo*, using a water bath at 40 °C. Conversions were determined by analysis of the ^1H NMR spectra of the crude reaction mixture.

Optimising reaction conditions for *N*-methylaniline incoming group

4-Vinylpyridine - Temperature and catalyst loading screen (25-90 °C, 5-20 mol% catalyst loading)

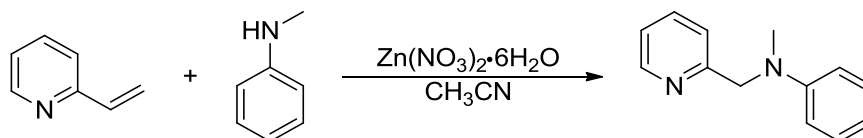
(Table 35, Chapter 3)



The appropriate loading in $\text{Zn}(\text{NO}_3)_2 \cdot 6\text{H}_2\text{O}$ was dissolved in CH_3CN (2 mL), to this *N*-methylaniline (2 mmol, 0.21 g, 0.22 mL) was added followed by the addition of 4-vinylpyridine (2 mmol, 0.21 g, 0.22 mL). The reaction mixture was left to stir at the appropriate conditions. On completion, the reaction mixture was allowed to cool to room temperature and solvent removed *in vacuo*, using a water bath at 40 °C. Conversions were determined by analysis of the ^1H NMR spectra of the crude reaction mixture.

2-Vinylpyridine - Temperature and catalyst loading screen (25-90 °C, 5-20 mol% catalyst loading)

(Table 39, Chapter 3)

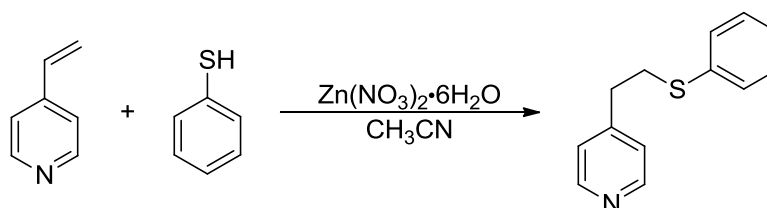


The appropriate loading in Zn(NO₃)₂·6H₂O was dissolved in CH₃CN (2 mL), to this *N*-methylaniline (2 mmol, 0.21 g, 0.22 mL) was added followed by the addition of 2-vinylpyridine (2 mmol, 0.21 g, 0.22 mL). The reaction mixture was allowed to stir at the appropriate conditions. On completion, the reaction mixture was allowed to cool to room temperature and solvent removed *in vacuo*, using a water bath at 40 °C. Conversions were determined by analysis of the ¹H NMR spectra of the crude reaction mixture.

Optimising reaction conditions for thiophenol incoming group

4-Vinylpyridine - Temperature and catalyst loading screen (25 °C, 2.5 and 5 mol% catalyst loading)

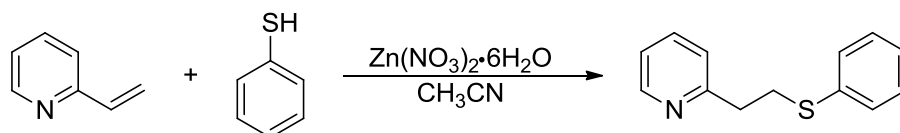
(Table 36, Chapter 3)



The appropriate loading in Zn(NO₃)₂·6H₂O was dissolved in CH₃CN (2 mL), to this thiophenol (2 mmol, 0.22 g, 0.21 mL) was added followed by the addition of 4-vinylpyridine (2 mmol, 0.21 g, 0.22 mL). The reaction mixture was allowed to stir at the appropriate conditions. On completion, the solvent was removed *in vacuo*, using a water bath at 40 °C. Conversions were determined by analysis of the ¹H NMR spectra of the crude reaction mixture.

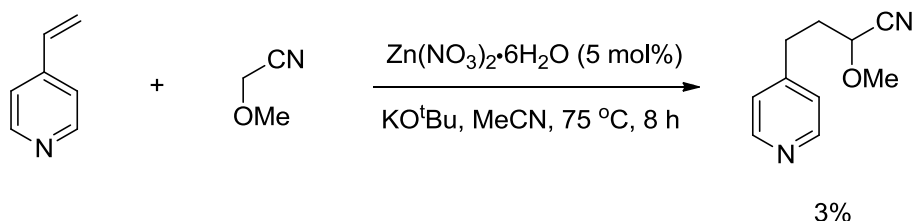
2-Vinylpyridine - Temperature and catalyst loading screen (25-40 °C, 2.5 and 5 mol% catalyst loading)

(Table 40, Chapter 3)

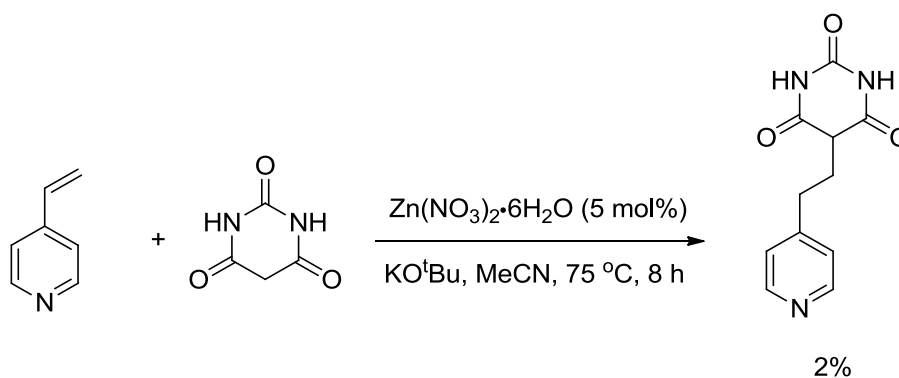


The appropriate loading in $\text{Zn}(\text{NO}_3)_2 \cdot 6\text{H}_2\text{O}$ was dissolved in CH_3CN (2 mL), to this thiophenol (2 mmol, 0.22 g, 0.21 mL) was added followed by the addition of 2-vinylpyridine (2 mmol, 0.21 g, 0.22 mL). The reaction mixture was allowed to stir at the appropriate conditions. On completion, the solvent was removed *in vacuo*, using a water bath at 40 °C. Conversions were determined by analysis of the ^1H NMR spectra of the crude reaction mixture.

Reaction of methoxyacetonitrile with 4-vinylpyridine



$\text{Zn}(\text{NO}_3)_2 \cdot 6\text{H}_2\text{O}$ (5mol%, 0.1 mmol, 0.03 g) and KO^tBu (2 mmol, 0.22 g) were dissolved in CH_3CN (2 mL), to this methoxyacetonitrile (2 mmol, 0.14 g, 0.15 mL) was added followed by 4-vinylpyridine (2 mmol, 0.21 g, 0.22 mL). The reaction mixture was left to stir at 75 °C for 8 h. On completion, the reaction solvent was removed *in vacuo*, using a water bath at 40 °C. The conversion (3% to the product) was determined by analysis of the ^1H NMR spectra of the crude reaction mixture.

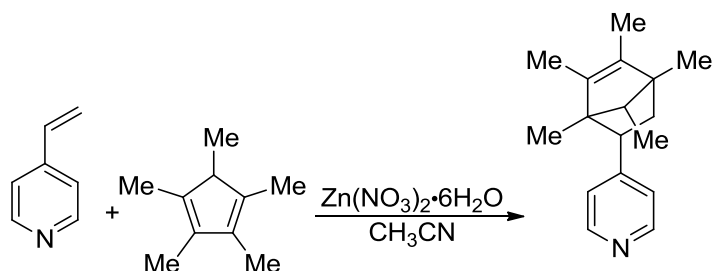
Reaction of methoxyacetonitrile with 4-vinylpyridine

$\text{Zn}(\text{NO}_3)_2 \cdot 6\text{H}_2\text{O}$ (5mol%, 0.1 mmol, 0.03 g) and KO^tBu (2 mmol, 0.22 g) were dissolved in CH_3CN (2 mL), to this barbituric acid (2 mmol, 0.26 g) was added followed by 4-vinylpyridine (2 mmol, 0.21 g, 0.22 mL). The reaction mixture was left to stir at 75 °C for 8 h. On completion, the reaction solvent was removed *in vacuo*, using a water bath at 40 °C. The conversion (2% to the product) was determined by analysis of the ^1H NMR spectra of the crude reaction mixture.

Optimising reaction conditions for Diels–Alder cyclisation of 1,2,3,4,5-pentamethylcyclopentadiene with 2-/4-vinylpyridine

4-Vinylpyridine - Temperature and catalyst loading screen (25-40 °C, 2.5 and 5 mol% catalyst loading)

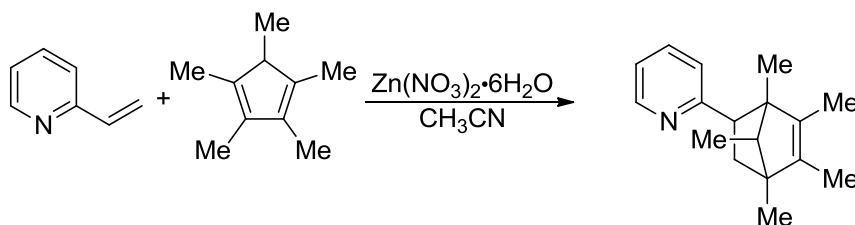
(Table 41, Chapter 3)



The appropriate loading in $\text{Zn}(\text{NO}_3)_2 \cdot 6\text{H}_2\text{O}$ was dissolved in CH_3CN (2 mL), to this 1,2,3,4,5-pentamethylcyclopentadiene (2 mmol, 0.27 g, 0.31 mL) was added followed by the addition of 4-vinylpyridine (2 mmol, 0.21 g, 0.22 mL). The reaction mixture was allowed to stir at the appropriate conditions. On completion, the reaction mixture was allowed to cool to room temperature and solvent removed *in vacuo*, using a water bath at 40 °C. Conversions were determined by analysis of the ^1H NMR spectra of the crude reaction mixture.

2-Vinylpyridine - Temperature and catalyst loading screen (25-40 °C, 2.5 and 5 mol% catalyst loading)

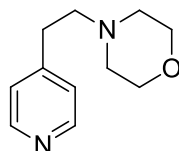
(Table 42, Chapter 3)



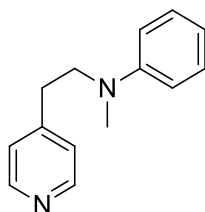
The appropriate loading in $\text{Zn}(\text{NO}_3)_2 \cdot 6\text{H}_2\text{O}$ was dissolved in CH_3CN (2 mL), to this 1,2,3,4,5-pentamethylcyclopentadiene (2 mmol, 0.27 g, 0.31 mL) was added followed by the addition of 2-vinylpyridine (2 mmol, 0.21 g, 0.22 mL). The reaction mixture was allowed to stir at the appropriate conditions. On completion, the reaction mixture was allowed to cool to room temperature and solvent removed *in vacuo*, using a water bath at 40 °C. Conversions were determined by analysis of the ^1H NMR spectra of the crude reaction mixture.

4.3.1. Characterisation of conjugate addition products

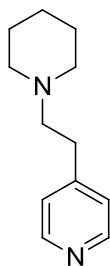
4-(2-(Pyridin-4-yl)ethyl)morpholine¹²⁸



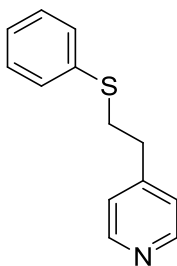
Zn(NO₃)₂•6H₂O (5 mol%, 0.1 mmol, 0.03 g) was dissolved in CH₃CN (2 mL), to this morpholine (2 mmol, 0.17 g, 0.17 mL) was added followed by 4-vinylpyridine (2 mmol, 0.21 g, 0.22 mL). The reaction mixture was left to stir at 25 °C for 12 h. On completion, the reaction mixture was allowed to cool to room temperature and solvent removed *in vacuo*, using a water bath at 40 °C. The crude reaction mixture was purified by silica gel chromatography (eluent: 5% methanolic ammonia in CH₂Cl₂) yielding a pale yellow oil (0.38 g, 99%); ¹H NMR (300 MHz, CDCl₃): δ_H= 8.28 (2H, app. dd, *J*= 4.4, 1.6 Hz, -CH=N-CH-), 6.93 (2H, app. dd, *J*= 4.4, 1.6 Hz, -CH-C(CH₂)=CH-), 3.51-3.48 (4H, m, -CH₂-O-CH₂-), 2.60-2.55 (2H, m, pyr-CH₂-CH₂-N-), 2.42-2.36 (2H, m, pyr-CH₂-CH₂-N-), 2.30-2.27 (4H, m, CH₂-N(CH₂)-CH₂-); ¹³C NMR (75 MHz, CDCl₃): δ_C= 149.3, 148.8, 123.7, 66.5, 58.8, 53.2, 32.1; HRMS *m/z* (ES+) 193.1343 C₁₂H₁₇N₂O [M+H]⁺ requires 193.1341.

N-Methyl-N-(2-(pyridin-4-yl)ethyl)aniline

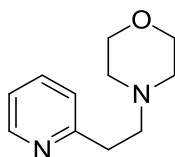
Zn(NO₃)₂•6H₂O (10 mol%, 0.2 mmol, 0.06 g) was dissolved in CH₃CN (2 mL), to this *N*-methylaniline (2 mmol, 0.22 g, 0.22 mL) was added followed by 4-vinylpyridine (2 mmol, 0.21 g, 0.22 mL). The reaction mixture was left to stir at 90 °C for 24 h. On completion, the reaction mixture was allowed to cool to room temperature and solvent removed *in vacuo*, using a water bath at 40 °C. The crude reaction mixture was purified by silica gel chromatography (eluent: 5% methanolic ammonia in CH₂Cl₂), the product was recovered as pale yellow oil (0.36 g, 85%); ¹H NMR (300 MHz, CDCl₃): δ_H= 8.51 (2H, app. dd, *J*= 4.5, 1.4 Hz, -CH=N-CH-), 7.29-7.23 (3H, m, aromatic), 7.13 (2H, d, *J*= 5.9 Hz, aromatic), 6.73 (2H, app. dd, *J*= 4.5, 1.4 Hz, -CH-C(CH₂)=CH), 3.59 (2H, t, *J*= 6.0 Hz, pyr-CH₂-CH₂-N-), 2.87 (3H, s, N-CH₃), 2.87-2.82 (2H, m, pyr-CH₂-CH₂-N-); ¹³C NMR (75 MHz, CDCl₃): δ_C= 149.7, 148.9, 148.5, 129.3, 124.2, 116.6, 112.2, 53.7, 38.6, 32.3; HRMS *m/z* (ES+) 213.1396 C₁₄H₁₇N₂ [M+H]⁺ requires 213.1387.

4-(2-(Piperidin-1-yl)ethyl)pyridine¹²⁸

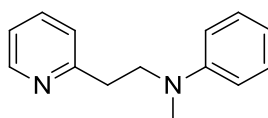
Zn(NO₃)₂•6H₂O (5 mol%, 0.1 mmol, 0.03 g) was dissolved in CH₃CN (2 mL), to this piperidine (2 mmol, 0.17 g, 0.19 mL) was added followed by 4-vinylpyridine (2 mmol, 0.21 g, 0.22 mL). The reaction mixture was left to stir at 40 °C for 4 h. On completion, the reaction mixture was allowed to cool to room temperature and solvent removed *in vacuo*, using a water bath at 40 °C. The crude reaction mixture was purified by silica gel chromatography (eluent: 5% methanolic ammonia in CH₂Cl₂) yielding a dark brown oil (0.33 g, 87%); ¹H NMR (300 MHz, CDCl₃): δ_H= 8.43 (2H, d, *J*= 5.8 Hz, -CH=N-CH-) 7.08 (2H, d, *J*= 5.8 Hz, -CH-C(CH₂)=CH), 2.78-2.71 (2H, m, pyr-CH₂-CH₂-N-), 2.54-2.38 (6H, m, N-CH₂-CH₂-CH₂-CH₂), 1.60-1.51 (4H, m, -CH₂-N(CH₂)-CH₂), 1.44-1.37 (2H, m, pyr-CH₂-CH₂-N-); ¹³C NMR (75 MHz, CDCl₃): δ_C= 149.7, 149.6, 124.2, 60.0, 54.5, 32.9, 25.9, 24.3; HRMS *m/z* (ES+) 191.1541 C₁₂H₁₉N₂ [M+H]⁺ requires 191.1543.

4-(2-(Phenylthio)ethyl)pyridine¹²⁹

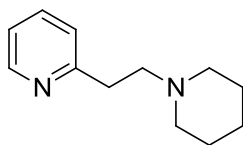
Zn(NO₃)₂•6H₂O (2.5mol%, 0.05 mmol, 0.015 g) was dissolved in CH₃CN (2 mL), to this thiophenol (2 mmol, 0.22 g, 0.21 mL) was added followed by 4-vinylpyridine (2 mmol, 0.21 g, 0.22 mL). The reaction mixture was allowed to stir at 25 °C for 10 min. On completion, the solvent was removed *in vacuo*, using a water bath at 40 °C. The crude reaction mixture was purified by silica gel chromatography (eluent: 5% methanolic ammonia in CH₂Cl₂) yielding a pale yellow oil (0.41 g, 96%); ¹H NMR (300 MHz, CDCl₃): δ_H= 8.47 (2H, d, *J*= 4.8 Hz, -CH=N-CH-), 7.33-7.15 (5H, m, aromatic), 7.08 (2H, d, *J*= 4.8 Hz, -CH-C(CH₂)=CH), 3.16-3.13 (2H, m, pyridine-CH₂-CH₂-S), 2.90-2.85 (2H, m, pyr-CH₂-CH₂-S-); ¹³C NMR (75 MHz, CDCl₃): δ_C= 149.6, 149.1, 135.5, 129.7, 129.0, 126.4, 123.9, 34.8, 34.1; HRMS *m/z* (ES+) 216.0856 C₁₃H₁₃NS [M+H]⁺ requires 216.0842

4-(2-(Pyridin-2-yl)ethyl)morpholin¹²⁸

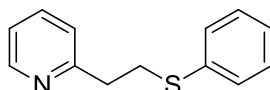
Zn(NO₃)₂•6H₂O (5mol%, 0.1 mmol, 0.03 g) was dissolved in CH₃CN (2 mL), to this morpholine (2 mmol, 0.17 g, 0.17 mL) was added followed by 2-vinylpyridine (2 mmol, 0.21 g, 0.22 mL). The reaction mixture was allowed to stir at 25 °C for 24 h. On completion, the reaction mixture was allowed to cool to room temperature and solvent removed *in vacuo*, using a water bath at 40 °C. The crude reaction mixture was purified by silica gel chromatography (eluent: 5% methanolic ammonia in CH₂Cl₂) yielding a clear yellow oil (0.35 g, 90%); ¹H NMR (300 MHz, CDCl₃): δ_H= 8.39 (1H, d, *J*= 7.7 Hz, =CH-CH=N-C(CH₂-), 7.46 (1H, app. td, *J*= 7.7, 0.9 Hz, N-C(CH₂-CH=CH-CH), 7.05 (1H, d, *J*= 7.7 Hz, N(CH₂-CH=CH-), 6.98 (1H, t, *J*= 7.7, 4.9 Hz, =CH-CH=N-C(CH₂)), 3.59 (4H, t, *J*= 4.9 Hz, -CH₂-O-CH₂-), 2.88-2.23 (2H, m, pyr-CH₂-CH₂-N-), 2.85 (2H, m, pyr-CH₂-CH₂-N-), 2.41-2.38 (4H, m, CH₂-N(CH₂)-CH₂-); ¹³C NMR (75 MHz, CDCl₃): δ_C= 165.9, 149.0, 136.1, 122.9, 121.00, 66.7, 58.5, 53.4, 35.3; HRMS *m/z* (ES+) 193.1340 C₁₂H₁₇N₂O [M+H]⁺ requires 193.1341.

N-Methyl-N-(2-(pyridin-2-yl)ethyl)aniline¹³⁰

Zn(NO₃)₂•6H₂O (15mol%, 0.3 mmol, 0.09 g) was dissolved in CH₃CN (2 mL), to this *N*-methylaniline (2 mmol, 0.21 g, 0.22 mL) was added followed by 2-vinylpyridine (2 mmol, 0.21 g, 0.22 mL). The reaction mixture was allowed to stir at 90 °C for 24 h. On completion, the reaction mixture was allowed to cool to room temperature and solvent removed *in vacuo*, using a water bath at 40 °C. The crude reaction mixture was purified by silica gel chromatography (eluent: 5% methanolic ammonia in CH₂Cl₂), the product was recovered as a pale yellow oil (0.36 g, 87%); ¹H NMR (300 MHz, CDCl₃): δ_H= 8.60 (1H, d, *J*= 6.0, Hz, =CH-CH=N-C(CH₂)-), 7.56 (1H, t, *J*= 6.0 Hz, N-C(CH₂)₂-CH=CH-CH), 7.27 (2H, t, *J*= 6.0 Hz, aromatic), 7.12-7.10 (2H, m, N(CH₂)₂-CH=CH-CH-), 6.85-6.67 (3H, m, aromatic), 3.78 (2H, t, *J*= 7.4 Hz, pyr-CH₂-CH₂-N-), 3.06 (2H, t, *J*= 7.4 Hz, pyr-CH₂-CH₂-N), 2.90 (3H, s, N-CH₃); ¹³C NMR (75 MHz, CDCl₃): δ_C= 159.1, 149.0, 148.4, 136.0, 138.9, 123.2, 120.9, 115.8, 111.8, 52.5, 37.91, 34.8; HRMS *m/z* (ES+) 213.1389 C₁₄H₁₇N₂ [M+H]⁺ requires 213.1387.

2-(2-(Piperidin-1-yl)ethyl)pyridine¹²⁸

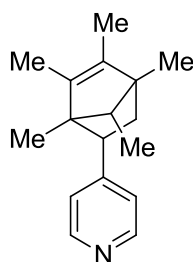
Zn(NO₃)₂•6H₂O (5mol%, 0.1 mmol, 0.03 g) was dissolved in CH₃CN (2 mL), to this piperidine (2 mmol, 0.17 g, 0.19 mL) was added followed by 2-vinylpyridine (2 mmol, 0.21 g, 0.22 mL). The reaction mixture was left to stir at 60 °C for 12 h. On completion, the solvent was removed *in vacuo*, using a water bath at 40 °C. The crude reaction mixture was purified by silica gel chromatography (eluent: 5% methanolic ammonia in CH₂Cl₂) yielding a dark brown oil (0.36 g, 95%); ¹H NMR (300 MHz, CDCl₃): δ_H= 8.39 (1H, d, *J*= 7.7 Hz, =CH-CH=N-C(CH₂-), 7.45 (1H, app. td, *J*= 7.7, 1.8 Hz, N-C(CH₂)₂-CH=CH-CH), 7.06 (1H, d, *J*= 7.7 Hz, N(CH₂)₂-CH=CH-), 6.97 (1H, t, *J*= 7.7 Hz, =CH-CH=N-C(CH₂-), 2.91-2.85 (2H, m, pyr-CH₂-CH₂-N-), 2.63-2.57 (2H, m, pyr-CH₂-CH₂-N-), 2.38-2.34 (4H, m, -CH₂-N(CH₂)-CH₂), 1.50-1.44 (4H, m, N-CH₂-CH₂-CH₂-CH₂), 1.31 (2H, m, N-CH₂-CH₂-CH₂-); ¹³C NMR (75 MHz, CDCl₃): δ_C= 160.4, 148.9, 136.0, 122.9, 120.8, 59.0, 54.2, 35.6, 25.8, 24.1; HRMS *m/z* (ES+) 191.1550 C₁₄H₁₇N₂ [M+H]⁺ requires 191.1548.

2-(2-(Phenylthio)ethyl)pyridine¹³¹

Zn(NO₃)₂•6H₂O (2.5 mol%, 0.05 mmol, 0.015 g) was dissolved in CH₃CN (2 mL), to this thiophenol (2 mmol, 0.22 g, 0.21 mL) was added followed by 2-vinylpyridine (2 mmol, 0.21 g, 0.22 mL). The reaction mixture was left to stir at 25 °C for 10 min. On completion, the reaction mixture was allowed to cool to room temperature and solvent removed *in vacuo*, using a water bath at 40 °C. The crude reaction mixture was purified by silica gel chromatography (eluent: 5% methanolic ammonia in CH₂Cl₂) yielding a pale yellow oil (0.40, 92%); ¹H NMR (300 MHz, CDCl₃): δ_H= 8.56 (1H, d, *J*= 5.2 Hz, =CH-CH=N-C(CH₂-), 7.61 (1H, app. td, *J*= 5.2, 2.6 Hz, N-C(CH)₂-CH=CH-CH), 7.40-7.36 (2H, m, N-C(CH)₂-CH=CH-CH=CH), 7.32-7.27 (2H, m, aromatic) 7.22-7.17 (3H, m, aromatic), 3.39-3.34 (2H, m, pyr-CH₂-CH₂-S-), 3.15-3.10 (2H, m, pyr-CH₂-CH₂-S); ¹³C NMR (75 MHz, CDCl₃): δ_C= 159.6, 149.3, 136.3, 136.1, 129.3, 128.8, 125.9, 123.2, 121.5, 37.7, 33.1; HRMS *m/z* (ES+) 217.0924 C₁₄H₁₇N₂ [M+H]⁺ requires 217.0925.

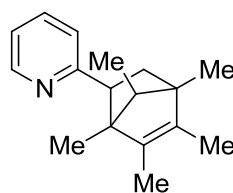
4.3.2. Characterisation of Diels–Alder cyclisation products

4-(1,4,5,6,7-Pentamethylbicyclo[2.2.1]hept-5-en-2-yl)pyridine



Zn(NO₃)₂•6H₂O (5mol%, 0.1 mmol, 0.03 g) was dissolved in CH₃CN (2 mL), to this 1,2,3,4,5-pentamethylcyclopentadiene (2 mmol, 0.27 g, 0.31 mL) was added followed by 4-vinylpyridine (2 mmol, 0.21 g, 0.22 mL). The reaction mixture was allowed to stir at 40 °C for 4 h. On completion, the reaction mixture was allowed to cool to room temperature and solvent removed *in vacuo*, using a water bath at 40 °C. The crude reaction mixture was purified by silica gel chromatography (eluent: 7:3 Et₂O:CH₂Cl₂) yielding a yellow oil (0.38 g, 78%); Major Isomer: ¹H NMR (300 MHz, CDCl₃): δ_H= 8.29 (2H, app. dd, *J*= 4.5, 1.5 Hz, -CH=N-CH-), 6.77 (2H, app. dd, *J*= 4.5, 1.5 Hz, -CH-C(CH₂)=CH), 2.83-2.80 (1H, m, pyr-CH-CH₂), 1.84-1.80 (1H, m, pyr-CH-CH₂), 1.58 (3H, s, pyr-CH-C(CH₃)-C(CH₃)=C), 1.42-1.39 (1H, m, bridge-CH(CH₃)), 1.38-1.35 (1H, m, pyr-CH-CH₂), 1.03 (3H, s, pyr-CH-CH₂-C(CH₃)), 0.92 (3H, s, pyr-CH-C(CH₃)-C(CH₃)=C(CH₃-), 0.87 (3H, s, pyr-CH-C(CH₃)-), 0.52 (3H, d, *J*= 9.0 Hz, bridge-CH(CH₃)); ¹³C NMR (75 MHz, CDCl₃): δ_C= 149.1, 148.65, 134.9, 131.5, 123.8, 62.34, 60.0, 53.4, 53.0, 41.5, 15.1, 13.8, 12.1, 9.7, 8.1; IR cm⁻¹ $\tilde{\nu}$ = 3057 (C-H), 1669 (C=C, alkene), 1569 (C=C, pyridine); HRMS *m/z* (ES+) 242.1902 C₁₇H₂₃N₁Na [M+Na]⁺ requires 242.1908.

2-(1,4,5,6,7-Pentamethylbicyclo[2.2.1]hept-5-en-2-yl)pyridine)



Zn(NO₃)₂•6H₂O (2.5mol%, 0.05 mmol, 0.015 g) was dissolved in CH₃CN (2 mL), to this 1,2,3,4,5-pentamethylcyclopentadiene (2 mmol, 0.27 g, 0.31 mL) was added followed by 2-vinylpyridine (2 mmol, 0.21 g, 0.22 mL). The reaction mixture was allowed to stir at 40 °C for 4 h. On completion, the reaction mixture was allowed to cool to room temperature and solvent removed *in vacuo*, using a water bath at 40 °C. The crude reaction mixture was purified by silica gel chromatography (eluent: 7:3 Et₂O:CH₂Cl₂) yielding a yellow oil (0.37 g, 76%); Major Isomer: ¹H NMR (300 MHz, CDCl₃): δ_H= 8.43 (1H, d, *J*= 7.7 Hz, =CH-CH=N-C(CH₂-), 7.47 (1H, app. td, *J*= 7.7, 1.9 Hz, N(CH)₂-CH=CH-CH), 7.05 (1H, d, *J*= 7.7 Hz, N(CH)₂-CH=CH-), 6.80 (2H, t, *J*= 8.0, 4.8 Hz, =CH-CH=N-C(CH₂-), 3.22-3.19 (1H, m, pyr-CH-CH₂), 1.93-1.89 (1H, m, pyr-CH-CH₂), 1.62 (3H, s, pyr-CH-C(CH₃)-C(CH₃)=C), 1.55-1.52 (1H, m, pyr-CH-CH₂), 1.50-1.46 (1H, m, bridge-CH(CH₃)), 1.09 (3H, s, pyr-CH-CH₂-C(CH₃)), 1.03 (3H, s, pyr-CH-C(CH₃)-C(CH₃)=C(CH₃-), 0.96 (3H, s, pyr-CH-C(CH₃-), 0.61 (3H, d, *J*= 9.0 Hz, bridge-CH(CH₃)); ¹³C NMR (75 MHz, CDCl₃): δ_c= 163.3, 147.9, 135.1, 134.6, 131.5, 121.3, 120.5, 62.3, 60.0, 55.7, 52.9, 41.3, 15.2, 11.0, 11.7, 9.7, 8.01.; IR cm⁻¹ $\tilde{\nu}$ = 3031 (C-H), 1640 (C=C, alkene), 1586 (C=C, pyridine); HRMS *m/z* (ES+) 242.1900 C₁₇H₂₄N₁ [M+H]⁺ requires 242.1908; HRMS *m/z* (ES+) 264.1709 C₁₇H₂₃N₁Na [M+Na]⁺ requires 264.1728.

References

1. G. D. Henry, *Tetrahedron*, 2004, **60**, 6043-6061.
2. J. S. Carey, D. Laffan, C. Thomson and M. T. Williams, *Org. Biomol. Chem.*, 2006, **4**, 2337-2347.
3. S. D. Roughley and A. M. Jordan, *J. Med. Chem.*, 2011, **54**, 3451-3479.
4. S. Y. Chou and S. F. Chen, *Heterocycles*, 1997, **45**, 77-85.
5. Y. Nakao, *Synthesis-Stuttgart*, 2011, 3209-3219.
6. J. A. Varela and C. Saá, *Chem. Rev.*, 2003, **103**, 3787-3802.
7. J. A. Joule and K. Mills, 5 edn., 2010, ch. 8, pp. 125-175.
8. J. A. Joule and K. Mills, Wiley 5th edn., 2010, ch. 8, pp. 19-33.
9. R. B. Woodward and W. E. Doering, *J. Am. Chem. Soc.*, 1945, **67**, 860-874.
10. G. Pfister-Guillouzo, C. Guimon, J. Frank, J. Ellison and A. R. Katritzky, *Liebigs Ann. Chem.*, 1981, 366-375.
11. Y. Kawazoe and Y. Yoshioka, *Chem. Pharm. Bull.*, 1968, **16**, 715-720.
12. J. M. Bakke and I. Sletvold, *Org. Biomol. Chem.*, 2003, **1**, 2710-2715.
13. B. Jamart-Gregoire, C. Leger and P. Caubere, *Tetrahedron Lett.*, 1990, **31**, 7599-7602.
14. K. Konishi, Y. Onari, S. Goto and K. Takahashi, *Chem. Lett.*, 1975, 717-720.
15. Y. Ogata, A. Kawasaki and H. Hirata, *J. Chem. Soc., Perkin Trans. 2*, 1972, 1120-1124.
16. M. Schlosser and F. Cottet, *Eur. J. Org. Chem.*, 2002, 4181-4184.
17. A. Klapars, J. H. Waldman, K. R. Campos, M. S. Jensen, M. McLaughlin, J. Y. L. Chung, R. J. Cvetovich and C.-y. Chen, *J. Org. Chem.*, 2005, **70**, 10186-10189.
18. S. Dumouchel, F. Mongin, F. Trécourt and G. Quéguiner, *Tetrahedron Lett.*, 2003, **44**, 2033-2035.
19. J. N. Collie and N. T. M. Wilsmore, *J. Chem. Soc., Trans.*, 1896, **69**, 293-304.
20. J. C. Jung, Y. J. Jung and O. S. Park, *Synth. Commun.*, 2001, **31**, 2507-2511.
21. W. K. Fife, *J. Org. Chem.*, 1983, **48**, 1375-1377.
22. J. Yin, B. Xiang, M. A. Huffman, C. E. Raab and I. W. Davies, *J. Org. Chem.*, 2007, **72**, 4554-4557.
23. P. J. Manley and M. T. Bilodeau, *Org. Lett.*, 2002, **4**, 3127-3129.
24. T. Koenig, *J. Am. Chem. Soc.*, 1966, **88**, 4045-4049.
25. M.-L. Louillat and F. W. Patureau, *Chem. Soc. Rev.*, 2014, **43**, 901-910.
26. J. F. Hartwig, *Angew. Chem., Int. Ed.*, 1998, **37**, 2046-2067.
27. J. F. Hartwig, *Acc. Chem. Res.*, 2008, **41**, 1534-1544.
28. F. Ullmann and J. Bielecki, *Ber. Dtsch. Chem. Ges.*, 1901, **34**, 2174-2185.

29. E. Colacino, L. Villebrun, J. Martinez and F. Lamaty, *Tetrahedron*, 2010, **66**, 3730-3735.
30. R. S. Yaunner, J. C. Barros and J. F. M. da Silva, *Appl. Organomet. Chem.*, 2012, **26**, 273-276.
31. R. Rossi, F. Bellina, M. Lessi and C. Manzini, *Adv. Synth. Catal.*, 2014, **356**, 17-117.
32. R. F. Jordan and D. F. Taylor, *J. Am. Chem. Soc.*, 1989, **111**, 778-779.
33. S. Rodewald and R. F. Jordan, *J. Am. Chem. Soc.*, 1994, **116**, 4491-4492.
34. J. C. Lewis, R. G. Bergman and J. A. Ellman, *J. Am. Chem. Soc.*, 2007, **129**, 5332-5333.
35. S. H. Wiedemann, J. C. Lewis, J. A. Ellman and R. G. Bergman, *J. Am. Chem. Soc.*, 2006, **128**, 2452-2462.
36. A. M. Berman, J. C. Lewis, R. G. Bergman and J. A. Ellman, *J. Am. Chem. Soc.*, 2008, **130**, 14926-14927.
37. E. J. Moore, W. R. Pretzer, T. J. O'Connell, J. Harris, L. LaBounty, L. Chou and S. S. Grimmer, *J. Am. Chem. Soc.*, 1992, **114**, 5888-5890.
38. M. Li and R. Hua, *Tetrahedron Lett.*, 2009, **50**, 1478-1481.
39. I. B. Seiple, S. Su, R. A. Rodriguez, R. Gianatassio, Y. Fujiwara, A. L. Sobel and P. S. Baran, *J. Am. Chem. Soc.*, 2010, **132**, 13194-13196.
40. J. Wen, S. Qin, L.-F. Ma, L. Dong, J. Zhang, S.-S. Liu, Y.-S. Duan, S.-Y. Chen, C.-W. Hu and X.-Q. Yu, *Org. Lett.*, 2010, **12**, 2694-2697.
41. M. Tobisu, I. Hyodo and N. Chatani, *J. Am. Chem. Soc.*, 2009, **131**, 12070-12071.
42. R. Grigg and V. Savic, *Tetrahedron Lett.*, 1997, **38**, 5737-5740.
43. M. Wasa, B. T. Worrell and J.-Q. Yu, *Angew. Chem., Int. Ed.*, 2010, **49**, 1275-1277.
44. J. Takagi, K. Sato, J. F. Hartwig, T. Ishiyama and N. Miyaoura, *Tetrahedron Lett.*, 2002, **43**, 5649-5651.
45. D. F. Fischer and R. Sarpong, *J. Am. Chem. Soc.*, 2010, **132**, 5926-5927.
46. B.-J. Li and Z.-J. Shi, *Chemical Science*, 2011, **2**, 488-493.
47. M. Ye, G.-L. Gao and J.-Q. Yu, *J. Am. Chem. Soc.*, 2011, **133**, 6964-6967.
48. C.-C. Tsai, W.-C. Shih, C.-H. Fang, C.-Y. Li, T.-G. Ong and G. P. A. Yap, *J. Am. Chem. Soc.*, 2010, **132**, 11887-11889.
49. Y. Nakao, Y. Yamada, N. Kashihara and T. Hiyama, *J. Am. Chem. Soc.*, 2010, **132**, 13666-13668.
50. L. Kurti and B. Czako, *Strategic Applications of Named Reactions in Organic Synthesis*, Elsevier Academic Press, San Diego, California, 2005.
51. T. Komnenos, *Justus Liebigs Ann. Chem.*, 1883, **218**, 145-167.
52. A. Michael, *J. Prakt. Chem./Chem.-Ztg*, 1887, 349.
53. W. E. Doering and R. A. N. Weil, *J. Am. Chem. Soc.*, 1947, **69**, 2461-2466.
54. D. A. Klumpp, *Synlett*, 2012, 1590-1604.
55. Y. Zhang, J. Briski, Y. Zhang, Rendy and D. A. Klumpp, *Org. Lett.*, 2005, **7**, 2505-2508.

56. Y. Zhang, M. R. Sheets, E. K. Raja, K. N. Boblak and D. A. Klumpp, *J. Am. Chem. Soc.*, 2011, **133**, 8467-8469.
57. A. P. Gray and W. L. Archer, *J. Am. Chem. Soc.*, 1957, **79**, 3554-3559.
58. Y. Zhang, A. McElrea, G. V. Sanchez, D. Do, A. Gomez, S. L. Aguirre, Rendy and D. A. Klumpp, *J. Org. Chem.*, 2003, **68**, 5119-5122.
59. A. R. Katritzky, G. R. Khan and O. A. Schwarz, *Tetrahedron Lett.*, 1984, **25**, 1223-1226.
60. A. R. Katritzky, I. Takahashi and C. M. Marson, *J. Org. Chem.*, 1986, **51**, 4914-4920.
61. E. Kim, J. Shearer, S. Lu, P. Moënne-Loccoz, M. E. Helton, S. Kaderli, A. D. Zuberbühler and K. D. Karlin, *J. Am. Chem. Soc.*, 2004, **126**, 12716-12717.
62. D. Krishnamurthy, A. N. Sarjeant, D. P. Goldberg, A. Caneschi, F. Totti, L. N. Zakharov and A. L. Rheingold, *Chem. Eur. J.*, 2005, **11**, 7328-7341.
63. A. L. Logothetis, *J. Org. Chem.*, 1964, **29**, 1834-1837.
64. J. Y. L. Chung, D. L. Hughes, D. Zhao, Z. Song, D. J. Mathre, G.-J. Ho, J. M. McNamara, A. W. Douglas, R. A. Reamer, F.-R. Tsay, R. Varsolona, J. McCauley, E. J. J. Grabowski and P. J. Reider, *J. Org. Chem.*, 1996, **61**, 215-222.
65. S. Danishefsky and R. Cavanaugh, *J. Am. Chem. Soc.*, 1968, **90**, 520-521.
66. S. Danishefsky, P. Cain and A. Nagel, *J. Am. Chem. Soc.*, 1975, **97**, 380-387.
67. M. A. Ciufolini and F. Roschangar, *J. Am. Chem. Soc.*, 1996, **118**, 12082-12089.
68. J. L. Archibald, *J. Heterocycl. Chem.*, 1966, **3**, 409-412.
69. X. Han, R. L. Civiello, S. E. Mercer, J. E. Macor and G. M. Dubowchik, *Tetrahedron Lett.*, 2009, **50**, 386-388.
70. F. C. Tucci, Y.-F. Zhu, Z. Guo, T. D. Gross, P. J. Connors Jr, R. S. Struthers, G. J. Reinhart, J. Saunders and C. Chen, *Bioorg. Med. Chem. Lett.*, 2003, **13**, 3317-3322.
71. I. A. Cliffe, A. D. Ifill, H. L. Mansell, R. S. Todd and A. C. White, *Tetrahedron Lett.*, 1991, **32**, 6789-6792.
72. C. Safak, H. Erdogan, E. Palaska, R. Sunal and S. Duru, *J. Med. Chem.*, 1992, **35**, 1296-1299.
73. E. C. Taylor and S. F. Martin, *J. Am. Chem. Soc.*, 1972, **94**, 6218-6220.
74. J. E. Macor, T. Ordway, R. L. Smith, P. R. Verhoest and R. A. Mack, *J. Org. Chem.*, 1996, **61**, 3228-3229.
75. A. Ishida, T. Uesugi and S. Takamuku, *Bull. Chem. Soc. Jpn.*, 1993, **66**, 1580-1582.
76. S. Alunni, F. De Angelis, L. Ottavi, M. Papavasileiou and F. Tarantelli, *J. Am. Chem. Soc.*, 2005, **127**, 15151-15160.
77. X. H. Bi, Q. Liu, S. G. Sun, J. Liu, W. Pan, L. Zhao and D. W. Dong, *Synlett*, 2005, 49-54.
78. L. Bauer and L. A. Gardella, *J. Org. Chem.*, 1961, **26**, 82-85.
79. G. M. Schaaf, S. Mukherjee and A. G. Waterson, *Tetrahedron Lett.*, 2009, **50**, 1928-1933.

80. M. Lautens, A. Roy, K. Fukuoka, K. Fagnou and B. Martín-Matute, *J. Am. Chem. Soc.*, 2001, **123**, 5358-5359.
81. I. N. Houpis, J. Lee, I. Dorziotis, A. Molina, B. Reamer, R. P. Volante and P. J. Reider, *Tetrahedron*, 1998, **54**, 1185-1195.
82. J. H. Nelson, P. N. Howells, G. C. DeLullo, G. L. Landen and R. A. Henry, *J. Org. Chem.*, 1980, **45**, 1246-1249.
83. L. Routaboul, C. Buch, H. Klein, R. Jackstell and M. Beller, *Tetrahedron Lett.*, 2005, **46**, 7401-7405.
84. M. Utsunomiya, R. Kuwano, M. Kawatsura and J. F. Hartwig, *J. Am. Chem. Soc.*, 2003, **125**, 5608-5609.
85. C. Michon, F. Medina, F. Capet, P. Roussel and F. Agbossou-Niedercorn, *Adv. Synth. Catal.*, 2010, **352**, 3293-3305.
86. J. S. Meek, R. T. Merrow and S. J. Cristol, *J. Am. Chem. Soc.*, 1952, **74**, 2667-2668.
87. W. v. E. Doering and S. J. Rhoads, *J. Am. Chem. Soc.*, 1953, **75**, 4738-4740.
88. J. Bourguignon, G. L. Nard and G. Queguiner, *Can. J. Chem.*, 1985, **63**, 2354-2361.
89. Y. Yamashita, T. Hanaoka, Y. Takeda, T. Mukai and T. Miyashi, *Bull. Chem. Soc. Jpn.*, 1988, **61**, 2451-2458.
90. F. A. Selimov, O. A. Ptashko, A. A. Fatykhov, N. R. Khalikova and U. M. Dzhemilev, *Russ. Chem. B+*, 1993, **42**, 872-878.
91. K. D. Redwine and J. H. Nelson, *J. Organomet. Chem.*, 2000, **613**, 177-199.
92. P. A. Gugger, A. C. Willis, S. B. Wild, G. A. Heath, R. D. Webster and J. H. Nelson, *J. Organomet. Chem.*, 2002, **643**, 136-153.
93. D. C. Wilson and J. H. Nelson, *J. Organomet. Chem.*, 2003, **682**, 272-289.
94. K. Y. Ghebreyessus, N. Gul and J. H. Nelson, *Organometallics*, 2003, **22**, 2977-2989.
95. K. Y. Ghebreyessus and J. H. Nelson, *J. Organomet. Chem.*, 2003, **669**, 48-56.
96. D. Duraczynska and J. H. Nelson, *Dalton Trans.*, 2005, 92-103.
97. R. A. Sheldon, *Chem. Commun.*, 2008, 3352-3365.
98. R. A. Sheldon, I. Arends and U. Hanefeld, *Green Chemistry and Catalysis*, WILEY-VCH, Weinheim 2007.
99. C. M. Richardson, R. J. Gillespie, D. S. Williamson, A. M. Jordan, A. Fink, A. R. Knight, D. M. Sellwood and A. Misra, *Bioorg. Med. Chem. Lett.*, 2006, **16**, 5993-5997.
100. S. L. Buchwald, C. Mauger, G. Mignani and U. Scholz, *Adv. Synth. Catal.*, 2006, **348**, 23-39.
101. F. Monnier and M. Taillefer, *Angew. Chem., Int. Ed.*, 2009, **48**, 6954-6971.
102. Q. Yang, Y. Wang, L. Yang and M. Zhang, *Tetrahedron*, 2013, **69**, 6230-6233.
103. S. Ge, R. A. Green and J. F. Hartwig, *J. Am. Chem. Soc.*, 2014, **136**, 1617-1627.
104. L. B. Delvos, J.-M. Begouin and C. Gosmini, *Synlett*, 2011, 2325-2328.

105. Z.-J. Liu, J.-P. Vors, E. R. F. Gesing and C. Bolm, *Adv. Synth. Catal.*, 2010, **352**, 3158-3162.
106. Z.-J. Liu, J.-P. Vors, E. R. F. Gesing and C. Bolm, *Green Chem.*, 2011, **13**, 42-45.
107. K. Walsh, H. F. Sneddon and C. J. Moody, *ChemSusChem*, 2013, **6**, 1455-1460.
108. P. S. Fier and J. F. Hartwig, *J. Am. Chem. Soc.*, 2014, **136**, 10139-10147.
109. J. n. M. Campos, M. a. C. Núñez, R. M. Sánchez, J. A. Gómez-Vidal, A. n. Rodríguez-González, M. Báñez, M. A. Gallo, J. C. Lacal and A. Espinosa, *Bioorg. Med. Chem.*, 2002, **10**, 2215-2231.
110. J. A. Fuentes and M. L. Clarke, *Synlett*, 2008, 2579-2582.
111. B. Mu, J. Li and Y. Wu, *Appl. Organomet. Chem.*, 2013, **27**, 537-541.
112. D. J. Keddie, C. Guerrero-Sanchez, G. Moad, R. J. Mulder, E. Rizzardo and S. H. Thang, *Macromolecules*, 2012, **45**, 4205-4215.
113. D. M. Bailey, C. G. DeGrazia, S. J. Hoff, P. L. Schulenberg, J. R. O'Connor, D. A. Paris and A. M. Slee, *J. Med. Chem.*, 1984, **27**, 1457-1464.
114. M. P. Sammes, K.-W. Ho, M.-L. Tam and A. R. Katritzky, *J. Chem. Soc., Perkin Trans. 1*, 1983, 973-978.
115. G. Van Baelen, S. Hostyn, L. Dhooghe, P. Tapolcsányi, P. Mátyus, G. Lemièrre, R. Dommissie, M. Kaiser, R. Brun, P. Cos, L. Maes, G. Hajós, Z. Riedl, I. Nagy, B. U. W. Maes and L. Pieters, *Bioorg. Med. Chem.*, 2009, **17**, 7209-7217.
116. A. Sakakura, M. Katsukawa and K. Ishihara, *Org. Lett.*, 2005, **7**, 1999-2002.
117. H. Vorbrüggen, *Angew. Chem.*, 1972, **84**, 348-349.
118. T. Hatakeyama, Y. Yoshimoto, S. K. Ghorai and M. Nakamura, *Org. Lett.*, 2010, **12**, 1516-1519.
119. S. Hashimoto, S. Otani, T. Okamoto and K. Matsumoto, *Heterocycles*, 1988, **27**, 319-322.
120. G. Podolan, D. Lentz and H.-U. Reissig, *Angew. Chem., Int. Ed.*, 2013, **52**, 9491-9494.
121. A. K. Sheinkman, A. N. Kost, I. V. Komisarov, A. O. Ginzburg, K. A. Arnol'dova and L. P. Makhno, *Pharm. Chem. J.*, 1968, **2**, 501-505.
122. N. V. Shevchuk, K. Liubchak, K. G. Nazarenko, A. A. Yurchenko, D. M. Volochnyuk, O. O. Grygorenko and A. A. Tolmachev, *Synthesis-Stuttgart*, 2012, **44**, 2041-2048.
123. R. Ma, A.-H. Liu, C.-B. Huang, X.-D. Li and L.-N. He, *Green Chem.*, 2013, **15**, 1274-1279.
124. E. C. Taylor, J. L. LaMattina and C. P. Tseng, *J. Org. Chem.*, 1982, **47**, 2043-2047.
125. D. Galanakis, J. A. D. Calder, C. R. Ganellin, C. S. Owen and P. M. Dunn, *J. Med. Chem.*, 1995, **38**, 3536-3546.
126. Z. Abdullah, N. Tahir, M. Abas, Z. Aiyub and B. Low, *Molecules*, 2004, **9**, 520-526.
127. Y.-X. Xie, S.-F. Pi, J. Wang, D.-L. Yin and J.-H. Li, *J. Org. Chem.*, 2006, **71**, 8324-8327.
128. M. Beller, H. Trauthwein, M. Eichberger, C. Breindl and T. E. Müller, *Eur. J. Inorg. Chem.*, 1999, 1121-1132.

129. T. Itoh and T. Mase, *Org. Lett.*, 2004, **6**, 4587-4590.
130. F. A. Selimov, V. R. Khafizov and U. M. Dzhemilev, *Chem. Heterocycl. Compd.*, 1984, **20**, 290-295.
131. M. Watanabe, S. Suga and J.-i. Yoshida, *Bull. Chem. Soc. Jpn.*, 2000, **73**, 243-247.